5-1-2014

Characterization and Optimization of Extraction Chromatography Resins for Rapid Separations for Safeguard and Nuclear Forensics Purposes

Audrey Roman
University of Nevada, Las Vegas, romana8@unlv.nevada.edu

CHARACTERIZATION AND OPTIMIZATION OF EXTRACTION CHROMATOGRAPHY RESINS FOR RAPID SEPARATIONS FOR SAFEGUARD AND NUCLEAR FORENSICS PURPOSES

By

Audrey Rae Roman

Bachelor of Science in Chemistry
University of Idaho
2009

A dissertation submitted in partial fulfillment
of the requirements for the

Doctor of Philosophy – Radiochemistry

Department of Chemistry
College of Sciences
The Graduate College

University of Nevada, Las Vegas
May 2014

UNIVERSITY OF NEVADA LAS VEGAS

THE GRADUATE COLLEGE

We recommend the dissertation prepared under our supervision by

Audrey Roman

entitled

Characterization and Optimization of Extraction Chromatography Resins for Rapid Separations for Safeguard and Nuclear Forensics Purposes

is approved in partial fulfillment of the requirements for the degree of

Doctor of Philosophy - Radiochemistry

Department of Chemistry

Ralf Sudowe, Ph.D., Committee Chair

Kenneth Czerwinski, Ph.D., Committee Member

Gary Cerefice, Ph.D., Committee Member

Evelyn Bond, Ph.D., Committee Member

William Culbreth, Ph.D., Graduate College Representative

Kathryn Hausbeck Korgan, Ph.D., Interim Dean of the Graduate College

May 2014

ABSTRACT

Characterization and Optimization of Extraction Chromatography Resins for Rapid Separations for Safeguard and Nuclear Forensic Purposes

By
Audrey Roman

Dr. Ralf Sudowe, Examination Committee Chair
Professor of Health Physics and Radiochemistry
University of Nevada, Las Vegas

In this work, extraction chromatography resins, DGA and UTEVA, were characterized under various conditions in order to identify novel rapid separations for safeguards and nuclear forensic purposes. For safeguards purposes, mixed matrices containing some of the largest components found in used fuel and either Am, Pu, or U were characterized on DGA and UTEVA resins in order to determine any effects from the addition of these constituents. Results indicated that 5 M HNO_3 would be an optimal loading condition due to the consistent actinide adsorption in the presence of the additional used fuel components. Investigations of varying the anion in the system were also performed. Trends were seen based on charge density and hydration energies. The trends of actinide adsorption in various reducing agents were studied. A novel separation scheme was determined and applied to a vacuum box.

For nuclear forensic based separations, DGA and UTEVA were characterized with some of the most common metals found in soil. Overall, the resins were still selective with samples of complex matrices. A separation of a glass/cement bead was performed and separation of some of the analytes was achieved.

ACKNOWLEDGMENTS

I want start my acknowledgements by thanking everyone that has helped me along this sometimes treacherous but yet rewarding path. Most of all, I would like to thank with the deepest gratitude my advisor, Ralf Sudowe, for his continued guidance and support through this process. Even though his guidance was always there, he's allowed me to find my own way which has given me confidence in myself and my work. I would also like to show my gratitude towards Evelyn Bond, my LANL mentor, the summers that I've spent with her have been some of the most rewarding; not only due to the greatly enjoyable times but also the huge learning experiences and growth that came with them. I would also like to thank my thesis committee for their patience and support throughout my research and writing. Gary Cerefice and Ken Czerwinski have been very influential in my professional growth. I also would like to thank Patricia Paviet for getting me started in the Radiochemistry program at UNLV. The direction of my professional life could be very different without her influence and help.

The path that I took to get here would not have been nearly as wonderful without the amazing friends that have surrounded me. I would also like to thank my fiancé, Brian Jennings, for being so supportive even from across the country throughout the last four years. I would like to dedicate this work to my parents who have given me unconditional support throughout the long path to completing my PhD. You have inspired me through your own trials, tribulations and taught me that to prove the skeptics wrong often all it takes is some hard work.

TABLE OF CONTENTS

Contents

LIST OF TABLES

LIST OF FIGURES

LIST OF EQUATIONS

Chapter 1. INTRODUCTION

Section 1.1 Motivation for Research

In the nuclear field, safety is very important not only during the day-to-day activities, but often as a main driving force behind research. For this reason, our nation has focused largely on safeguards and nuclear forensics in order to improve and continue to guarantee our ability to ensure our nation's safety. Safeguards keep our special nuclear material (SNM) protected in order to hinder the ability of people to gain access to make radiological devices for ill intent. Nuclear forensic analysis gathers information from pre- and post-detonation samples; as well as interdicted samples in order to identify the transgressors as quickly as possible.

The composition of safeguard and nuclear forensic samples will both be based on the original SNM utilized, the sampling location and method. Even though the possible complexity of all the samples could vary widely, similar analysis techniques could potentially be used on both types of samples. For instance, the same chromatography methods have been used to separate identical elements of interest in soil, vegetation, food, concrete and brick samples.[1, 2, 3, 4] Unfortunately many of these radioanalytical chemistry techniques currently in use for both safeguard and nuclear forensic samples, are cumbersome and labor as well as time intensive and therefore not able to deliver the necessary amount of data in an acceptable timeframe.[5]

Since the analysis of both nuclear forensics and safeguard related samples place very high demands on time, reliability, and accuracy, it is advantageous to explore possible techniques that can be optimized to achieve rapid and reliable assay of the material. As defined in Title I of the Atomic Energy Act of 1954, SNM is defined as any substance with U-233 or U-235 or any of the Pu isotopes.[6, 7] It would therefore be ideal to analyze these isotopes individually for the best detection capabilities.[7] The application of rapid radioanalytical techniques, especially separations, could also allow utilization of instruments and detectors which were previously not an option due to the complexity of the sample. e.g. by removing potentially interfering isotopes from mass spectrometric analysis. Finding a very selective separation technique, such as extraction chromatography, would be necessary in order to simplify the matrix of samples prior to analysis. For this reason, this thesis covers the characterization and optimization of extraction chromatography separations in regards to safeguards and nuclear forensics applications with the intent to shorten analysis time, improve reliability and increase detection capabilities.

Actinide Separations for Safeguards

Safeguards became important once congress enacted Title I of the Atomic Energy Act of 1954.[6] In general, a common way to safeguard SNM is to maintain material accountancy. The International Atomic Energy Agency (IAEA) stated that a material accountancy system should sample near-real-time, homogenously, and the data acquired would need to provide extensive details for

the SNM, such as concentration, isotopic ratios, and the relationship between Pu produced and power generated.[8] Finding safeguards techniques that can be implemented in a nuclear waste reprocessing facility will alleviate the proliferation concerns and stimulate the closing of the US fuel cycle.[9] It would also be beneficial to determine the Am/Pu isotopic ratios in order to gain more information on the composition of the fuel.[10]

Industrially reprocessing facilities throughout the world are typically using the PUREX (Plutonium Uranium Extraction) process in order to separate Pu and U from the used fuel. Material accountancy is typically needed for transferring, receiving, and adjustments to the special nuclear material.[11] In the used fuel cycle there are multiple locations which could benefit from a sampling system but for this thesis we will focus on a system for sampling the dissolver prior to introduction into the PUREX process and after Pu/U separation, these positions are denoted in the below figure.

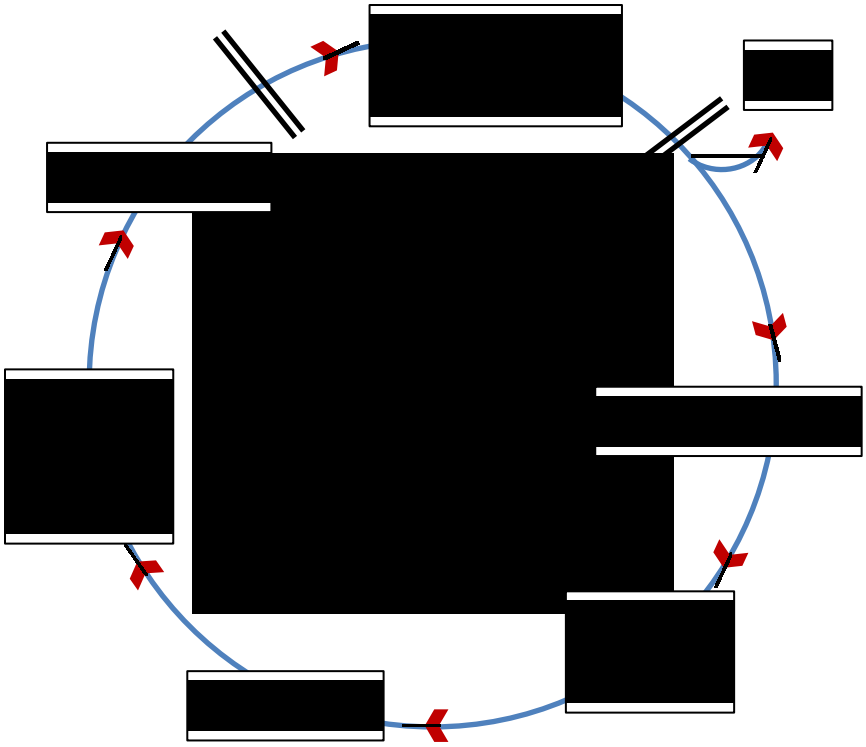

Figure 1. Material Accountancy in the Nuclear Fuel Cycle

Current verification techniques for used fuel receipt rely on neutron detection, gamma ray, x-ray, and Cherenkov radiation detection. More specifically for onsite measurements of U and Pu, hybrid K-edge densitometry (HKED) is used for measuring the U and Pu concentrations in mixed solutions by combining x-ray fluorescence (XRF) and k-absorption edge spectrometry (KED) technologies.[10, 11] Even though this technique is very accurate, it only detects concentration and not the isotopic ratios of U and Pu. The best technique to determine isotope concentrations for long lived radioisotopes is mass spectroscopy.[12, 13] Since there are numerous isobaric overlaps for the actinides, due to beta-decay and neutron capture in used fuel, the detection of fission products and actinide isotopes by mass spectrometry (ICP-MS) is not an

option without prior chemical separation.[14] To avoid isobaric or polyatomic interferences and reduce abundance sensitivity that may appear in the mass range 230-245, extremely high decontamination factors are required to remove the interferences. Therefore a separation technique that is very selective to Am, Pu, and U will be necessary for coupling with an ICP-MS.

Since actinide separations have been of interest since the start of the civil and military use of nuclear power, there have been many procedures developed in order to achieve them. N. Vajda et al. have comprehensively compiled the analytical techniques and procedures developed, as of 2011, for the separation of Pu, Np, and Am from a wide variety of sample matrixes.[15] The use of extraction chromatography resin separations accomplish good quality, high recoveries, high decontamination factors for many nuclides, and online mass spectrometric analysis.[15] Although there are many techniques for the separation of actinides, none have been reported for the separation of Am, Pu, and U from used fuel based only on the use of extraction chromatography (EXC) resins. Due to the complexity of the used fuel it is necessary to also consider the effects on Am, Pu, and U loading, eluting, and stripping characteristics in the presence of the additional components, which are listed in

Table 1. The list and ranking of the components in Table 1 were determined based on ORIGIN calculations for used fuel which had a 2.9 % initial U-235 enrichment with 30,000 MWd/MT after a 10 year cool down period.[16]

Table 1. Used Fuel Components [16]

Ranked by Mass		
Rank	Element	Percent
1	U	98.43
2	Pu	0.85
3	Nd	0.13
4	Cs	0.13
5	Ce	0.1
6	Tc	0.07
7	Zr	0.07
8	Am	0.06
9	Np	0.04
10	Sr	0.04
11	Rb	0.02
12	Sm	0.02
13	I	0.02
14	Cm	0.01
15	Sn	<0.00

There are multiple EXC resins that can obtain similar separations of Am, U, and Pu, such as TRU, DGA, and UTEVA resin. Eikenberg et al. compared three different procedures each using UTEVA, TRU, Dowex AG 1-X2 anion exchange, and DGA resins for U, Th, Am, and Pu separations.[17] The procedure using DGA and the Dowex AG 1-X2 resins were determined to have

the highest chemical recoveries due to the extraordinarily high Am adsorption coefficients provided by DGA.[17] In a study to simplify the sample preparation for TIMS analysis, by Grate et al., the separation of Pu-242 was compared on TEVA and DGA where DGA was found to have better recovery.[18] Due to the high Am and Pu affinity and the resins' rapid kinetics it makes this extraction chromatography separation technique a strong contender for rapid actinide separations. The extraction chromatography resin DGA, is supplied either in bulk form or in pre-packed column and cartridges by Eichrom Technologies Inc. and is often used in pressurized, sequential or flow injection and vacuum box applications.

There have been multiple studies in which used fuel pellets have been analyzed for various actinides.[19, 20, 21] Most of these studies were performed with complex separation and analytical techniques. K.A. Venkatesan, et al. characterized high activity waste from reprocessed fast reactor fuel using a wide variety of analytical techniques, such as but not limited to solvent extraction, liquid chromatography, spectrophotometry, inductively coupled plasma-mass spectrometer, and high performance liquid chromatography.[20] They employed various individual techniques for Np, Pu, U, Am, and Cm analysis which made the characterization time lengthy and the approach therefore not suitable for rapid material accountancy application. S. Asai, et al. developed a single separation scheme using an anion exchange resin which could precisely separate the actinides and fission products while including the potential to be coupled to an ICP-MS.[21] However the loading solution used was 10 M HCl –

0.1 M HNO_3. This means the reprocessing process streams would need to be dried to completeness and reconstituted into the loading matrix which will slow the analysis down considerably.[21] Therefore, a suitable separation scheme for material accountancy in the fuel cycle should have the same loading matrix as found in the PUREX process, ~5 M HNO_3.

There is no single universal procedure developed thus far for rapid actinide separation and characterization of used fuel in a reprocessing facility. For this reason, this thesis was performed with the intent to create a single accurate radioanalytical separation technique for a rapid material accountancy system applicable to used fuel reprocessing material streams.

Optimization of Nuclear Forensic Separations

When considering a post-detonation scenario, there are three main methods used to conduct nuclear forensic analysis. One way is to identify the isotopic ratios of the actinides, which will provide information on the fuel and neutron spectrum. Another way is to identify the concentrations of the activation products, which can provide additional information about the neutron spectrum and design of the weapon. Lastly, measuring fission product yields can also provide information about the fuel and neutron spectrum.[22] Depending on the event, either radiological dispersal or fission device, the nuclides of interest vary, as seen in Tables 1 and 2. In this thesis, the actinides of interest for separation and analysis are Am, Pu, and U. Their respective isotopic ratios can be used to obtain information about the fuel and neutron spectrum. The activation products

of interest are from the first row transition metals which are selectively produced by the capture of fast neutrons emitted during a fission or fusion which reaction provides information about the design of the weapon. For instance, a 14 MeV neutron is only produced from a two stage thermonuclear device. These fast neutrons can provide a range of n,xn or n,p reactions that yield definitive signatures seen in the activation products.[7]

Table 2. Possible Radionuclides Resulting from a Radiological Dispersal Device [23]

Alpha Emitters		Beta/Gamma Emitters	
Am-241	Ra-226	Ac-227	Ir-192
Cm-242	Th-228	Bi-210	P-32
Cm-243	Th-230	Bi-212	Pd-103
Cm-244	Th-232	Bi-214	Pb-210
Np-237	U-234	Co-57	Pb-212
Po-210	U-235	Co-60	Pb-214
Pu-238	U-238	Cs-137	Pu-241
Pu-239	U-Nat	I-125	Ra-228
Pu-240		I-129	Se-75

Table 3. Possible Radionuclides Resulting from a Fission Event [23]

Alpha Emitters	Beta/Gamma Emitters		
Am-241	Ba-140/La-140	Nd-147/Pm-147	Ru-106/Rh-106
U-234	Ce-141	Eu-155	Sb-125
U-235	Ce-143/Pr-143	H-3	Sr-89
U-238	Ce-144/Pr-144	I-131/Xe-131	Sr-90/Y-90
Pu-238	Cs-134	I-133	Tc-99
Pu-239	Cs-137	Np-239	Te-132/I-132
Pu-240	Eu-154	Pm-151/Sm151	Zr-95/Nb-95
Pu-241	Mo-99/Tc-99m	Ru-103/Rh-103	Zr-97/Nb-97
Activation Products			
Co-58	Ag-110m	Cr-51	Mn-54
Np-239	Co-60	Fe-59	Na-24

Many radioanalytical chemistry techniques currently in use are not able to deliver sufficient results in a timeframe acceptable for the quick interpretation and analysis needed in attribution and response to a radiological event.[99.] To achieve efficient detection of many isotopes and their ratios, individual separations of the actinides and activation products from a sample are often necessary. This necessity is typically due to the limits of the detectors' resolution. There have been extraction chromatography procedures developed to separate actinides from a variety of samples[24]: food [1], sea water [25], soil [3, 26], and plants [4] but few have been applied to melt glass and urban rubble.[2] Lately there has been an increase in efforts to develop optimized rapid actinide separation methods [27, 28] but none of the methods published have been developed for the analysis of samples with complex matrices such as melt glass and urban rubble.

Extraction chromatography resins have been of interest for the separation of actinides due to their affinity and high selectivity in various matrices. More specifically, DGA and UTEVA resins show great potential for the separation of actinides from melt glass and urban rubble samples based on previously published trends and their selectivity for tri- and tetravalent metals.[29, 30, 31, 32, 33] There appears to be little to no affinity for the natural elements on these resins, whereas, there is high affinity and selectivity for the actinides and activation products of interest.[31, 32, 33] Due to the established need for rapid actinide separations in regards to post detonation scenarios, separation techniques which have previously shown potential were further investigated and characterized in this thesis.

Section 1.2 Extraction Chromatography

Extraction chromatography is a form of liquid-liquid column chromatography.[34] This term is generally used when the stationary phase is an organic liquid and the mobile phase is an aqueous solution. There are three main components of an EXC system: the inert support, the stationary phase, and the mobile phase, as depicted in Figure 2.[35] The inert support is usually porous silica or an organic polymer which ranges in size from 50 to 150 μm. The stationary phase consists of liquid extractants, which are adsorbed onto the inert support and are either single compounds or mixtures. Often times the liquid extractants adsorbed onto the stationary phase were chosen based on previous studies of their selectivity in solvent extraction systems. The mobile phase is

typically a mineral acid, which may include complexants to enhance selectivity or stripping of ions from the column. The selectivity of these resins is based on exploiting the differences in the resin's affinity for a metal and counter ion complexes, in charge density and steric effects.[35] This technique combines the selectivity of solvent extraction with the multi-stage character and the ease of operation of ion exchange chromatography.[34]

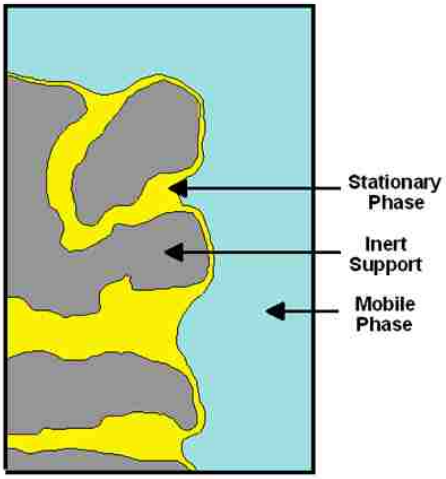

Figure 2. Surface of Extraction Chromatography Bead [36]

The advantages of EXC in comparison to solvent extraction (SX) and ion exchange (IEC) are:

- Less reagents and chemicals are used
- Less hazardous waste is produced
- More economical than SX
- Smaller footprint than SX
- Faster exchange kinetics than IEC [37]

Due to the EXC resin's faster exchange kinetics, it allows for more rapidly moving mobile phases while still maintaining sufficient separation efficiencies. For this reason, it should be possible to apply a pressure difference to an EXC separation system in order to decrease the elution time for a separation.

Many of the same system parameters are needed for a resin to be considered for separations of samples from the fuel cycle for material accountancy or for nuclear forensics samples. Since matrix conversions would not be well suited for rapid separations, the possible matrices and sample conditions are restrained for the Am, Pu, and U separation from a PUREX stream. Due to the more restrained conditions necessary for the material accountancy in-stream implementation for a reprocessing facility, this discussion will be heavily geared towards addressing those concerns. Similar considerations are however applicable to many issues in nuclear forensics. In order to develop a reliably rapid material accountancy separation scheme a resin would need to:

- At a minimum separate out the special nuclear material of interest
- Provide a separation scheme which would have easy implementation into the PUREX process
- Deliver high efficiencies preferably independent of the used fuel composition
- Run at elevated flow rates in order to provide rapid separations
- Be coupled to an instrument that allows detection of the separated elements/isotopes

In the following sections these requirements will be discussed in regards to two commercially available extraction chromatographic resins, DGA and UTEVA.

DGA Resin

DGA resin's extractant N,N,N',N'-tetraoctyl diglycolamide (TODGA), in Figure 3, was initially studied via solvent extraction and was found to have very high selectivity for tri- and tetravalent metals with an ionic radius between ~80-120 pm.[38] For these reasons, DGA resin is of interest to separate Am(III), Pu(IV) and possibly U(VI). Even though solvent extraction studies can not necessarily be directly translated to trends in extraction chromatography, they still provide a general idea of extraction and chemical characteristics.

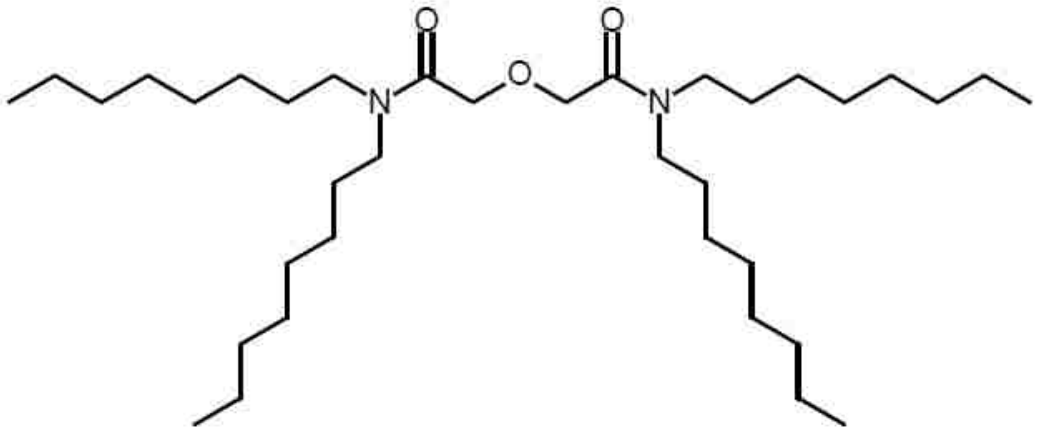

Figure 3. DGA Resin's Extractant

A very comprehensive review of diglycolamide chemistry was compiled by Ansari et al., in which most of the literature for the TODGA extractant published

to date was summarized.[39] In solvent extraction techniques, TODGA was found to be ampiphilic and form reverse micelles where its aggregation depends on the aqueous acidity.[40] In these reverse micelles, it was determined that 3-4 ligands complexed with tri- and tetravalent metals in the inner and outer sphere depending on acid matrices.[41, 42] In a TRLFS (Time-Resolved Laser-induced Fluorescence Spectroscopy) study on the complexation of Eu^{3+} with TODGA in n-dodecane, only TOGDA complexing europium in the inner coordination sphere was observed. Once varying nitrate concentrations were added, the complex was devoid of water molecules in the inner coordination sphere of the metal ion and either occupied by TODGA and/or NO_3^-.[43, 44] Since the anion is in the inner coordination sphere with TODGA, the variation of the anion and its concentration in a sample could greatly affect the stability of the ligand/neutral-metal complex. Overall, the micelle formation was found to be strongly influenced by the acidity of the aqueous solution and the nature of the counter anion. Sasaki et al. reported that the ion-pair extraction mechanism is strongly dependent on the ionic strength.[41] For these reasons, it will be very important to investigate various counter anions, various acid matrices and concentrations, and their potential effects on actinide adsorption to DGA resin; since, the various matrix components could enhance the selectivity or stripping of an ion.

Initially, TODGA was of interest due to its specific selectivity in solvent extraction and its potential for partitioning out the actinides from the PUREX process in order to reduce heat loading in the recycled waste. These interests lead to the thorough investigation of this extractant in a variety of solvents and to

an assessment of its stability in high radiation fields. TODGA was found to have relatively high alpha radiation stability but is fairly sensitive to gamma radiation in certain solvents which is thought to be due to the localization of the irradiation products and their ability to recombine. It was determined that the concentration of TODGA decreases exponentially with the γ-dose but with the addition of n-dodecane less degradation was observed.[45, 46] Even though TODGA was seen to have noticeable degradation from γ-radiation, it is still studied due to its great potential for actinide removal from used fuel.[47] The stability of the resin is essential for its implementation into the fuel cycle. It can be assumed that TODGA would act similarly in resin form as found in solvent extraction, but a detailed study of the effects of radiation on the resin was outside the scope of this thesis.

These studies sparked further interest in the utilization of this extractant as an extraction chromatography resin and its potential application to the fuel cycle.[48, 49, 50, 51, 52, 53] Some of these techniques use several different extractants in order to achieve the separation they desire. For instance, Zhang et al. used two columns implementing TODGA and CMPO (octylphenyl-N,N-di-isobutyl carbamoylphosphine oxide) extractants to separate Pd(III), Zr(IV), Sr(II), Fe(III), and Mo(VI) from simulated high level liquid waste.[50] Zhang, A. et al. used TODGA impregnated SiO_2-P material to investigate the potential to extract Sr(II) from a PUREX raffinate in the MAREC (Minor Actinides Recovery from HLW by Extraction Chromatography) process which uses multiple columns with varying extractants.[51] In this study no actinides or lanthanides were studied

and mainly mono- and divalent metals were studied. Modolo et al. performed a separation of spent fuel using TODGA and TBP impregnated resins.[48] This study does not separate Am, Pu and U from one another but does separate actinides and the lanthanides from the rest of the used fuel constituents. Hoshi et al. performed a study on two pressurized TODGA chromatographic columns for the group separation of trivalent actinides and lanthanides. In this procedure Pd, U, Np, and Pu were removed from the spent fuel prior to contact with the TODGA columns. Even though this experiment addresses the use of TODGA resin in the fuel cycle, it does not supply the information needed for material accountancy since it does not take into account the presence of other fission products, or rapid flow rates necessary for near real time measurements. Shaibu et al. investigated TODGA impregnated magnetic particles for the uptake of lanthanides and actinides from nuclear waste.[52] The distribution ratios of these magnetic particles were determined and compared to TODGA on a silica-based support. No column separation was performed. Although, these studies investigate the separations of actinides from used fuel there is not one consistent study which could be applied to the PUREX process conditions. Therefore, further work is needed investigating the possibility for Am, Pu, and U separation in the presence of other fission products under PUREX conditions and rapid flow rates to determine its application for spent fuel material accountancy in a reprocessing facility.

As stated above, the chemical trends seen for TODGA in solvent extraction aren’t always a direct correlation to the performance of the extractant

on a resin. Therefore it was necessary to investigate the resin's characteristics in detail to determine its affinities. DGA resin has shown a high selectivity for tri- and tetra- valent actinides.[29, 30, 31] DGA was previously characterized in nitric and hydrochloric acids by Horwitz et al., as seen in Figure 4.[29] Looking at Figure 4, the assumption can be made that with a k' values ~10^3 or greater for Am and Pu and k' ~100 for U for 5 M HNO_3, they would all sorb onto DGA. This is of importance since the used fuel is dissolved in ~5 M HNO_3 and would allow for simple implementation because Am, Pu and U would sorb onto DGA at that concentration. Therefore, the used fuel feed could be directly loaded onto the column without further treatment.

In order to obtain efficient separations it is necessary to achieve clean elutions of each metal of interest. The ratio of k' values of two metals can be used to estimate the potential for efficient separations of these two elements the larger the number, the more likely the elements can be separated. Based on the large ratios for k' for Am/U and Pu/U 1 M HNO_3, three orders of magnitude, the k' values the separation of Am/Pu from U should be easily obtained. However, a separation of Am/Pu from U on a simple column is unlikely due to the magnitude of the k' values. Such a high free column volume to peak maximum would require a large amount of mobile phase in order to completely elute U from a column. Therefore, another alternative was considered in this thesis using a sequential extraction with UTEVA resin to separate U from Am and Pu prior to using a DGA column. To obtain high accuracy and precision the separation procedure

performance would need to be fairly independent of the sample matrix and flow rates.

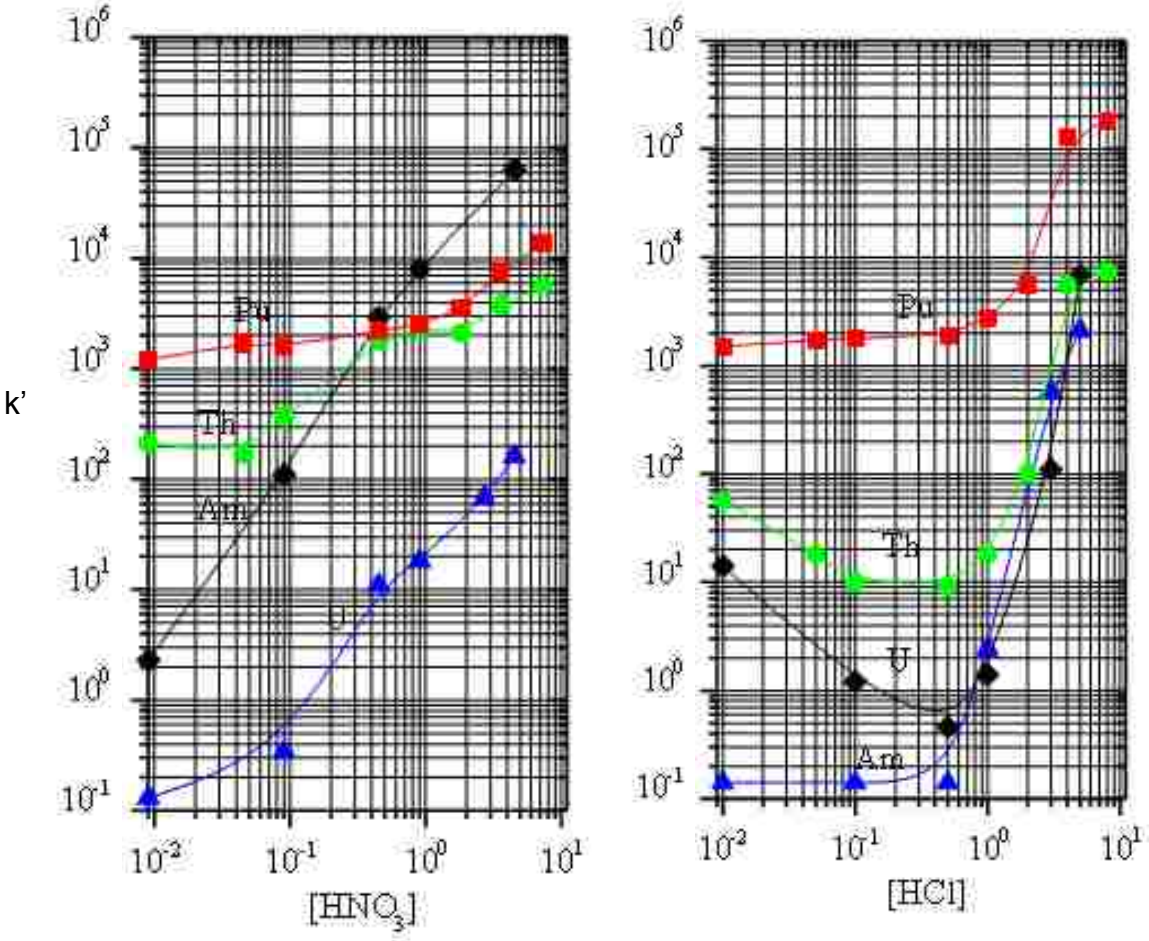

Figure 4. Preliminary k' values for actinide adsorption on DGA resin in varying nitric and hydrochloric acid concentrations, at 23-25 °C [29]

Even though other studies use samples with a different matrix, useful information can be gleaned from further literature review, such as separation

schemes or effects of common ions. DGA resin has been used for separating actinides, especially Am, from many different sample matrices, such as soil, air filters, animal tissue and water.[17, 30, 31, 54, 55, 56, 57] Thakur et al. used Eichrom's TEVA, TRU and DGA resin in tandem to separate Pu, Th, Am and U from air filters and drinking water around the Waste Isolation Pilot Plant (WIPP) site.[54] In this procedure DGA was used to separate Am from Fe which yielded >90% recovery with high iron content. Horwitz et al. performed a study to investigate the effects on trivalent actinides and lanthanides from the presence of Fe, Ga, In, Tl, or Bi in hydrochloric media. In this study, synergistic effects were found in hydrochloric matrices due to the presence of these trivalent metals; where the increased of metal(III) chloride concentration increases the adsorption of trivalent actinides and lanthanide chloride complex.[30] Since the synergistic effect persisted even when the capacity for the resin was exceeded, these data most likely suggest the formation of a co-complex. For example the mechanism reported for iron(III) chloride was:

$$Am^{3+} + 3Cl^{-} + 3FeCl_3 + \overline{3DGA} \leftrightarrow \overline{Am(DGA)_3(FeCl_4)_3} \qquad \textbf{(1-1)}$$

These data suggest that DGA's adsorption of certain metals may be easily affected by the other components in a sample. Therefore, it is important to either analyze a true sample or to investigate the possibility for interference or synergistic effects from the components individually. Pourmand et al. investigated 60 elements' adsorption on DGA resin in varying concentrations of hydrochloric, hydrofluoric, and nitric acid media.[31] These elements were

combined into one multi-element sample and were then contacted with the resin for equilibrium studies; the resulting solutions were analyzed by ICP-MS. Even though the results generally correlate well with some of those already published by Horwitz et al.[29] these results are not good representations of how the elements may interact with DGA individually or in a differently composed sample since only multi-element samples were analyzed.[31] Therefore, more equilibrium studies will need to be carried out in order to determine the effects on separation efficiency that will specifically come from components in a reprocessing facility waste stream.

As previously discussed, there have been a considerable number of studies of DGA for the separation of actinides from many different matrices very few have been performed for its implementation into the fuel cycle. Resins impregnated with TODGA were assessed by Van Hecke et al. for their ability to separate minor actinides and lanthanides from low level liquid waste related to PUREX raffinate.[58] Based on the weight distribution of actinides and lanthanides in the raffinate solutions the partitioning of the actinides and lanthanides from low-level liquid waste seem viable.[58] Since only weight distributions were determined in various acid matrices, viable accelerate flow rates and separation conditions would be needed to be determined in order to assess the implementation of DGA resin as an achievable rapid separation technique for the fuel cycle. One study by Esbelin, et al. separated Am, Cm, and Nd from an ECRIX-H irradiated pellet, which consists of MgO-$AmO_{1.62}$, in order to evaluate the potential to transmutate Am in a Phenix sodium cooled fast

reactor.[59, 60] An ion exchange resin, Biorad AG 1X8, was coupled with DGA resin in order to separate U, Pu, and Am/Cm/Nd into separate streams and then further AG 1X8 separations were performed in a glove box to further separate Am, Cm, and Nd for Thermal Ionization Mass Spectrometry (TIMS) measurements. In this experiment a peristaltic pump was used on DGA column in a shielded hot cell. This separation provided good accuracy and the concentrations recovered matched well with the estimates calculated by the evolution code used.[59] Even though this study did look at the irradiated pellets they were ECRIX-H specific pellets with an inert magnesia/Am matrix and are not a good representation of the fuel recycled in the PUREX process.[60] Since this experiment was able to use higher flow rates for a complex matrix and still achieve relatively low standard deviations using DGA the same should be possible for separation of Am from other fuel pellets, as would be found in the PUREX process. Another study was performed using TODGA and CMPO impregnated resins by Zhang et al. in their MAREC process (Minor Actinide Recovery from HLLW by Extraction Chromatography) where some minor actinides and rare earths, Sr, Pd, and Zr were separated from simulated HLW.[61] In this study, the simulated high-level waste (HWL) was made to represent waste from a nuclear reactor after PUREX reprocessing therefore Pu, U was not investigated.[61] Even though this system was pressurized, basically automated, and had the same composition as used fuel it did not cover all the information needed, such as high flow rates and the effects on Am, Pu, and U adsorption. Overall, the studies performed for DGA resin implementation confirm

its potential since higher flow rates and similar samples matrices obtained sufficient separations but these two parameters are not performed in the same study. Therefore, it is important to determine how high the flow rate can increase for a sample with a composition similar to PUREX process waste streams.

Since a rapid separation will be necessary to achieve near real time material accountancy, separations using DGA must be able to function under increased flow rates. DGA was used in an automated pressurized injections system implementing flow rates up to 30 mL min^{-1}. Using average flow rates of 24 ± 2 mL min^{-1}, Th(IV), Pu(III) and Am(III) were adsorbed onto DGA and were separated with relative yields of ~97%.[27] These fast flow rates and high yields show DGA's great potential for very rapid separation and analysis.

In order to evaluate the composition of the used fuel it is essential that the separation can be directly coupled with an instrument which could identify the isotope ratios of the elements of interest. Another rapid and automatic sequential separation of actinides by using DGA, TEVA, and UTEVA was performed by Lariviere et al. which was directly coupled with ICP-MS analysis.[28] The direct coupling of the separation and instrument will not only allow complete automation but quicker sample turnaround times. Li et al., using the same methodology as Lariviere et al. to separate Am-241 from a urine sample, was able to obtain an average turnaround time (including ICP-MS analysis) of about 15 minutes with flow rates of 2.5 mL min^{-1}.[62] Since the composition of a reprocessing waste stream will tend to be more complex than a urine sample slower flow rates may be needed to obtain the same separation efficiencies. Fast flow rates may still be

achievable depending on the possible matrix effects on the adsorption and elution of actinides. Since there are little to no results published on these potential component effects on actinide adsorption to DGA from used fuel this thesis explores the effects from the main components and assess the employment of a DGA separation on a vacuum box.

In summary, although there has been a lot of research performed with DGA in relation to actinide separations some significant gaps still need to be filled. Some of these gaps include the effects of used fuel components on actinide adsorption in PUREX like mobile phases; as well as, the possibility and the effects of accelerating the flow rates of a used fuel sample through a DGA column.

UTEVA Resin

Since ~96% of the used fuel is composed of U, finding a resin that has a high affinity and capacity for U is highly desirable for a reprocessing facility material accountancy system. In order to efficiently separate a less abundant fission product such as Am, the capacity of the resin becomes very important. If the capacity of a resin is exceeded, meaning the adsorption sites are all full, the elution characteristics will change and often decrease the separation efficiency. Therefore, finding a resin which has a high capacity for U is necessary in order to allow unhindered separation of the less abundant fission products. UTEVA resin, commercially available through Eichrom Technologies Inc., shows a high

selectivity for tetra- and hexavalent actinides and has little to no selectivity for trivalent actinides. Since UTEVA has little to no affinitiy for many of the fission products, its application appears very advantageous. In addition a high capacity for U (37 mg/mL UTEVA) has been reported for this resin.[32]

Figure 5. UTEVA resins' extractant, Dipentyl pentyl phosphonate

UTEVA resin uses diamyl amylphosphonate (DAAP), seen in Figure 5, as its extractant in its stationary phase. Horwitz et al. had initially characterized this resin for the acid dependency of the capacity factor, the elution behavior of three dozen elements, and its column stability.[32] It was found that DAAP extracts tetra- and hexavalent metals for U and thorium according to the following equations.

$$UO_2^{2+}{}_{(aq)} + 2NO_3^-{}_{(aq)} + \overline{2E_{(org)}} \leftrightarrow \overline{UO_2(NO_3)_2 \cdot E_{2_{(org)}}} \qquad \textbf{(1-2)}$$

$$Th^{4+}{}_{(aq)} + 4NO_3^-{}_{(aq)} + \overline{3E_{(org)}} \leftrightarrow \overline{Th(NO_3)_4 \cdot E_{3_{(org)}}} \qquad \textbf{(1-3)}$$

Where E represents DAAP and a neutrally extracted U or Th nitrate complex.[33] It was found that as nitric acid concentration increased, the U capacity factor

increased until 4 M nitric acid. At 4 M nitric acid, the capacity factor decreases, as seen in Figure 3, which is thought to be due to the formation of nitrato complexes in the aqueous phase and the free extractant concentration lowering in the organic phase following nitric acid extraction.[63] The variances seen in the U and Pu adsorption trends based on acid concentration suggest the possibility to easily load and strip a UTEVA column selectively. Also, since UTEVA resin does not have an affinity for trivalent metals, it would allow for separation of Pu(IV) from Am(III).

Typically to effectively separate an element, it is retained on a resin while the other components in a matrix flow through and then the element of interest is eluted off individually. Considering this, Pu and U can be separated from one another by UTEVA.[64] Therefore, UTEVA alone cannot be used for the separation of Am, Pu, and U from used fuel but could be an advantageous addition in tandem to DGA.

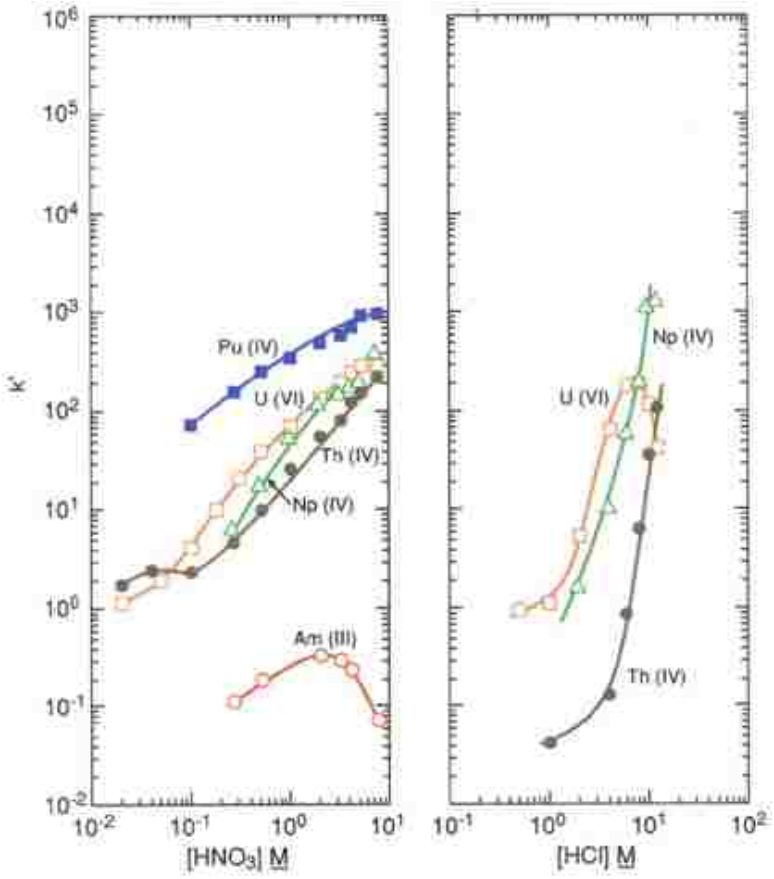

Figure 6. Preliminary k' values for Actinide Adsorption on UTEVA resin in varying nitric and hydrochloric acid concentrations, 23 - 25 ^{o}C [65]

UTEVA resin has been used widely for the preconcentration and separation of actinides from many different sample compositions such as soil, sediment, vegetation, water, and food.[67, 68, 69, 70, 71, 72, 73] Lee et al. has investigated the separation of Pu, U, Am and Sr isotopes from environmental samples with UTEVA and compared extraction chromatography techniques to the highest recovery anion exchange technique. It was found that extraction chromatography has better recoveries for U and Pu on UTEVA resin than anion exchange.[74] Kim et al. was able to separate Am, Pu, U, and Th with high and

consistent recoveries (85%) from 10 g soil and sediment samples sequentially using UTEVA and TRU resins in tandem.[75] Even though they were able to obtain consistent and high recoveries near what would be needed this study did not take into account the effects seen from the composition of the nuclear fuel cycle and did not try to decrease the process time.

Although extraction chromatography itself is not an instrument for concentration or isotope identification it can aid in improving detection limits and the capabilities of those instruments and detectors which are already well characterized but may not be currently in use due to complexity of the matrix. Krachler et al. separated Am-241 from Pu-239 in order to improve the limit of detection (by two orders of magnitude) on their inductively coupled plasma optical emission spectroscopy (ICP-OES).[76] Perna et al. coupled a UTEVA column online to an ICP-MS detector for the determination of actinides. They demonstrated that UTEVA can lower the detection limit to a few pg/g.[77] Coleman et al. used UTEVA resin in order to purify the solution being electrodeposited for alpha spectroscopy analysis for U-232.[78] These improved samples made it possible to take advantage of the low detection limit possible on an alpha spectroscopy detector.[79] These studies show how this technique could be applied to already known and developed instruments to improve the limit of detection and therefore increase the instrument's potential application in monitoring the reprocessing waste streams in the fuel cycle. A few procedures using UTEVA have advantageously directly injected the eluent from an extraction

chromatography column to an ICP-MS which helps to keep the analysis time as short as possible as well as keeping it automated.[77, 79, 80, 81]

Taguchi et al. looked at the difference between Pu(VI) and Pu(IV) adsorption and elution characteristics on UTEVA resin for low level liquid wastes.[82] It was found that the elution profile curve for Pu(VI) with 0.01mol L^{-1} HNO_3 gave the sharper and more symmetrical peak than Pu(VI) in 0.1 mol L^{-1} HNO_3 and Pu(IV) with 0.1 mol L^{-1} HNO_3. In particular, Pu(IV) had considerably broader elution peaks and tailing than in other matrices studied.[82] This means that Pu(VI) in low nitric acid concentration may be the optimal elution conditions for UTEVA resin. Goodall and Lythgoe separated U and Pu using UTEVA from solutions of spent fuel for analysis on thermal ionization mass spectrometry where they investigated the potential to use oxalic acid and ascorbic acid as a stripping agent.[83] In this study it was determined that the most useful separation employed the ascorbic acid to reduce Pu(IV) to Pu(III) since it gave a sharper elution curve. This gives another possible elution matrix for the U and Pu separation. This study was also performed using a vacuum box in order to expedite the analysis of samples. At least 50% reduction in time per separation of U and Pu was achieved while precision was maintained.[84] This trait is very important to its implementation into the fuel cycle as near real time analysis is necessary.

High flow rates will be essential to achieving rapid separations necessary for fuel material accountancy. There have been many studies with UTEVA used on a vacuum box with flow rates up to 3-4 mL/min.[85, 86] One study performed

by Maxell used TEVA, UTEVA and TRU resin to separate Am, Cm, Pu, U, and Np with higher flow rates of 2-3 mL/min (where gravity typically has 0.5 mL/min flow rates) in order to minimize sample turnaround time.[87] The UTEVA was investigated for its potential to separate U from nuclear wastes and environmental samples and even though it was at a higher flow rate still achieved >98% recovery.[87] The ability to still achieve high recovery under rapid flow rates is essential to maintaining a near real time material accountancy. Osvath et al. have looked at the application of UTEVA in nuclear power plant wastes but only in the recovery of Zr and Np.[88] Thakkar performed a rapid separation of U, Pu, and Am from soil using UTEVA and TRU in tandem on a vacuum box system.[84] Consistent, reliable and fast separations were able to be maintained; therefore, UTEVA separation characteristics should stay consistent unless unforeseen complications arise from the matrix of the sample.

There are many extraction chromatography techniques using UTEVA in order to separate actinides from various matrices but few techniques were used for solutions from the nuclear fuel cycle.[87, 88, 89, 90] Osvath et al. developed a method for the separation of U, Np, Pu, Am and Cm. One of the key parameters in this method is controlling the oxidation states of the actinides with $(NH_4)_2S_2O_8$ before contact with UTEVA.[88] After analyzing 10 evaporation concentrates of a nuclear power plant chemical yields of 65% U, 82% Pu, between 66-93% Np, and 55% Am/Cm were obtained.[88] Even though this method fundamentally separated Am, Pu, and U from nuclear reactor samples, it has room for improvement as it was not rapid and had highly variable results for some of the

actinides. Solatie et al. developed a procedure using TOPO in cyclohexane loaded on silica gel, Dowex anion exchanger and UTEVA resin for determining U-232 and Pu-236 in spent nuclear fuel by alpha spectrometry.[89] The recovery for U was 70% and for Pu was 80-90%. This procedure determined concentrations of U and Pu fairly close to those calculated by ORIGIN for each fuel pellets specific burn-up.[89] Even though this procedure was fairly simple and proved to be efficient in separation for alpha spectrometry applications it was not a rapid analysis and recovery efficiency could be improved.

It would be ideal to separate out Am, Pu, and U individually from used fuel. Morgenstern et al. separated U, Pu, Np and Am from one another from a gravity fed UTEVA column.[90] Even though recoveries were high, >87%, no other metals were included in the sample. Also, in the separation scheme they have developed, Am would elute off with all of the other fission products found in used fuel.[90] This could cause difficulties when it comes to detection of Am. In order to achieve the Am separation needed, UTEVA and a column with high Am affinity and recoveries would be needed, such a DGA resin. The combination of these two resins provide a sufficient separation scheme of Am, Pu, and U. To truly verify the ability of this scheme to separate these actinides in mixed sample matrices, all the possible components in a sample must been analyzed for the effects on the analytes' adsorption.

Section 1.3 Goals

The purpose of this work was to develop new radioanalytical methods for the separation of actinide elements and first row transition metals to assist rapid material accountancy and nuclear forensic analysis. This work thoroughly characterizes two extraction chromatography resins, DGA and UTEVA, by batch contact studies in order to identify any effects on actinide adsorption due to the presence of some of the components of used fuel, as listed in Table 1. Initially these resins were studied with the intent to use them individually and/or in combination. Once the effects of the additional components were identified, a separation scheme for actinides and/or transition metals from used fuel, melt glass, and urban rubble was applied to a gravity fed column(s) in order to optimize the separation. The characterized extraction chromatography separations were then transitioned to a vacuum box to be further optimized and to characterize the reliability and accuracy of the separations. The main goal of this thesis was to supply new rapid and reliable separation procedures that show a potential for automation.

Section 1.4 Thesis Organization

In this thesis, initially, resins were characterized for separations, and rapid actinide separations were then developed, characterized, and optimized for safeguard and nuclear forensic purposes. A general background regarding the primary methods used is provided in Chapter 2. There are two main parts to this thesis, the first is Chapters 3, 4, 5, 7, and 8 which are focused on separations for safeguards in the fuel cycle and the second is Chapter 6, which is focused on separations for nuclear forensic purposes related to glass and urban rubble. Each data chapter is in a manuscript format and includes a detailed materials and methods section.

Preliminary investigations of DGA and UTEVA's adsorption for Am, Cm, Pu, and U were performed. DGA resin characterization for Am, Cm, Pu in the presence of used fuel components and UTEVA resin characterization for Am, Pu, and U in the presence of used fuel components were performed and discussed in Chapters 3 and 4. The potential for these resins application to Am, Pu, and U separation from other fission products in a material accountancy system for used nuclear fuel are discussed as well. These studies were performed with the assumption that UTEVA and DGA columns would most likely need to be stacked in order to achieve the separation needed. These studies allowed the ideal conditions to be identified in which to set up the column separation of the used fuel. After the separation of Am, Pu, and U was proven to be possible for used

nuclear fuel, optimization of the separation for a rapid sequentially stacked prepacked cartridges of UTEVA and DGA was performed.

More specifically, Chapter 3 summarizes the effects seen from some of the larger constituents in the dissolved used fuel on Am and Pu adsorption to DGA. In Chapter 4, Am, Pu, and U adsorption to UTEVA resin in the presence of used fuel components in nitric and hydrochloric acid matrices are presented and discussed. In order to see the effects of the components in used fuel, it was necessary to perform these studies at an acid concentration which did not get near the analyte's limit of detection. The synergistic, antagonistic, and competitive effects on Am and Pu are presented and discussed in these chapters. To find the ideal conditions of a stripping phase for UTEVA and DGA, the matrix of the mobile phase was varied; these results are discussed in Chapter 4.

Since DGA and UTEVA were well characterized in Chapters 3 and 4, Chapter 5 investigated the effects from varying the anion in the matrix. Various acids, reducing agents, and complexing agents were studied. Comparison of all studies is performed and discussed in order identify optimal loading, eluting, and stripping matrices.

The sixth chapter of this thesis is directed at rapid separations for nuclear forensic purposes, more specifically glass and urban rubble samples in a post-detonation situation. Preliminary batch contact studies of various metal adsorptions on DGA and UTEVA resins pertaining to soil, glass, and urban rubble were performed and are found in Chapter 6. Some interference effects

were studied, as well, but were not a main focus of this study. Also, a flowsheet was developed for the separation of activated transition metals out of a man-made hybrid glass/cement button based off of preliminary data and previously reported trends. This flowsheet also hypothesized the elution of Am and Pu even though there was none in the glass button. Dissolution of the glass button was achieved and separated on a gravity fed DGA column.

In chapters 7 and 8, the individual actinide elution profiles were analyzed on DGA and UTEVA columns to ensure the possibility of separation. The ideal loading, eluting, and stripping phases and necessary volumes were identified for a gravity fed column. Once the transition to a vacuum box was performed, where the same conditions were applied, the changes of the performance due to application to a vacuum box were identified. A mock used fuel was separated in order to substantiate the viability of applying this separation technique for a used fuel material accountancy system.

Chapter 2. BACKGROUND

Section 2.1 Introduction

In this chapter, a more detailed background and literature review of the methods performed and instruments used in this thesis is provided. There are detailed descriptions of the methods' specifics as they apply to each experiment performed in this work present in the introduction of each experimental chapter, Chapters 3 through 7.

Section 2.2 Extraction Chromatography

Extraction chromatography combines the selectivity of solvent extraction and the ease of use of column chromatography.[91] The chemical and physical characteristics of the metal analyte, counter ion of the analyte, and the matrix components can all affect the efficiency of extraction.[92] Therefore, an extraction chromatography system can be selectively tuned to extract a specific analyte to a certain degree based off of the composition of the mobile phase. This ability makes extraction chromatography very useful for selectively separating a specific analyte but also means full characterization of the component's cations and anions in a sample's matrix must be determined.

In this thesis, the effects seen from additional components in the matrix are called synergistic, antagonistic, and competitive effects. Synergistic effects are seen when an addition of another metal to the system increases the adsorption of the analyte either by creating a co-complex or combined species,

such as $M_x^+M_y^{3+}A_4^-$, which is extracted by the resin. A synergistic effect can also be possible by creating a salting out effect. This salting out effect is a phenomena were the solubility of a non-electrolyte in water is decreased by the addition of an electrolyte.[93] The decreased solubility would therefore an increase in an electrolyte concentration can drive the extraction of another species. Antagonistic effects are possible when the addition of another metal creates a co-complex or combined species which is not favorable and has a lower affinity than the individual analyte. Competition effects may be present in a system where the additional component competes for the binding sites on the resin; therefore, lowering the available sites for the analyte. For these reasons, it is essential to fully investigate the effects of the components in a sample prior to column separation and automation. In this thesis batch contact studies are used in order to quantify these effects, the method is described later in this section.

The oxidation states of the actinides can be very useful in the separation and have been employed in the work of this thesis. The differences between various oxidation states of a single actinide are larger than those of different actinides in the same oxidation states.[93] The ability of the various species to form complexes is dependent on the charge density. For example, the complexation strength tendency of Pu decreases in the order:[93]

$$M^{4+}(IV) > M^{3+}(III) \approx M(VI)O_2^+ > M(V)O_2^+$$

And the stability series of the inorganic complexes of tri-, tetra- and hexavalent actinides are generally the same:[93]

$$OH^- > carbonate > oxalate > F^- \approx acetate^- > SO_4^{2-} > NO_3^- > Cl^- > ClO_4^-$$

except for Am(III) where nitrates and chlorides are more similar in stability. These characteristics of Am, Pu, and U can be exploited in order to achieve a more efficient separation.

For a column separation, there are additional effects which can change a separation's efficiency. The efficiency of a chromatography column depends on the number of plates in a column.[94] These theoretical plates are defined as a surface within the column where the ratio between the average concentrations of the solute in the stationary phase and in the solution flowing out of the region corresponds to the ratio attained in true equilibrium.[94] A plate, therefore, can be thought to represent one stage of a solvent extraction multi-stage process. Since there are a number of plates in one column it allows for a more simplified and compact setup in order to achieve the same separation efficiency. The number of plates in a column depends on the height equivalent to one theoretical plate (HETP). The HETP is calculated by dividing the height of the column by N, the number of plates. The number of plates for a column is calculated by:[94]

$$N = 8\left(\frac{V_R}{w}\right)^2 \qquad (2\text{-}1)$$

where, V_R is the elution volume at which the maximum concentration of analyte is achieved, and w is the peak width at 1/e of the peak height. There are many different parameters in a column separation which could affect the HETP.

Particle size of the supporting material, loading of the extractant, temperature, column cross section area, bed length, and rate of elution have been studied for their effects on a column separation by Horwitz and Bloomquist.[95] To reduce HETP, it was shown that the best packing method was by a slurry method, using small resin particle size with lower extraction loading, and slower flow rates at elevated temperatures. The reduction in HETP, giving more plates, will give a longer retention time and a larger elution volume. Some other factors affecting the width of peak and tailing of elution curve for an extraction system, include but are not limited to, diffusion effects, the amount of eluted elements, the capacity of the column, rate of formation of the extractable species, and rate at which equilibrium is reached.[95] It is therefore important to be aware and minimize as many of the potential negative effects during a separation as possible.

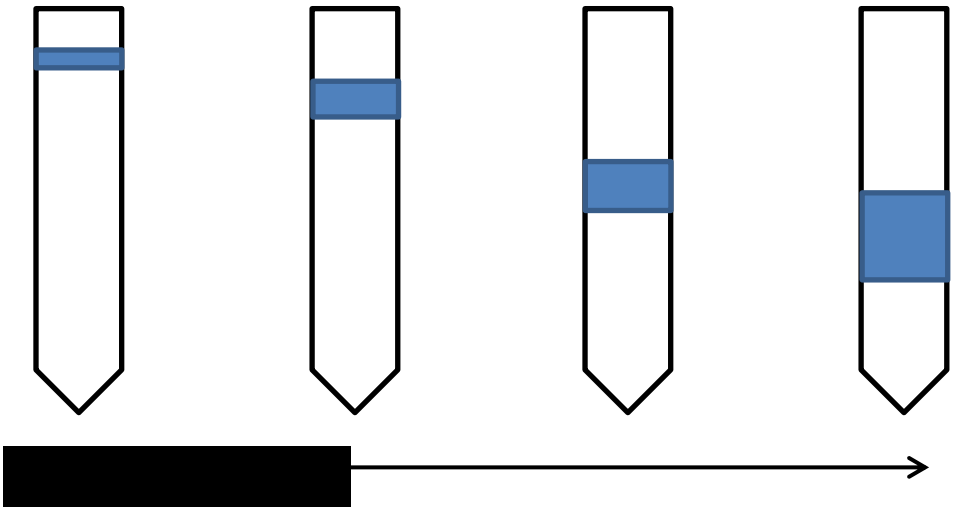

Figure 7. Band Broadening Due to Increased Flow Rate

One of the most important factors on band broadening for an extraction chromatography column is the mobile phase flow pattern.[94] This includes the mobile phase flow rate $\left({}^{mL}/_{Cm^2 \cdot min}\right)$ which with its increase there is a reduction in the number of theoretical plates; therefore, giving a broadened band, as seen in Figure 7. This is a parameter that will need to be optimized to achieve a more rapid separation but still achieve a sufficient separation of the analytes. Many extraction chromatography columns are performed with an excess of theoretical plates.[96]

Separation of a mixture can be obtained by a variety of techniques but generally, it is achieved by taking advantage of the degrees of retention for different components in a sample.[94] The degrees of retention are caused by differences in partition equilibrium and/or mass transfer kinetics. Ideally, as the sample is traveling down the column each component will separate enough into its own band which eventually elutes off individually.[94] The use of additional components whether they be reducing/oxidizing agents or complexing agents, can affect the degree of retention for a specific component. Therefore, these agents are also investigated for their potential in optimizing the separation.

In this thesis, due to the complexity of the sample composition, the sample was loaded onto the column where the components of interest were retained and those of no interest were eluted off. The retained components, with the variation of mobile phase matrices, were eluted off into separate fractions. The changes in the mobile phase were studied for an increase or decrease in the acid

concentration, as well as, the addition of salting out, redox, and complexing reagents. These reagents change partition ratios changing mobile phase bulk properties. Some of the reagents high affinity for the resin and are extracted into the stationary phase; therefore, lowering the number of available extraction sites, giving a competition reaction. Redox and complexing reagents directly reacts with the species either in the mobile or stationary phase to form a new species with a different distribution ratio which allows further separation. Introduction of various mobile phases to a chromatography separation can be performed with a stepwise or gradient elution. When a large number of steps are used in an elution results are similar between stepwise and gradient elution.

Batch Contact Studies Method

The purpose of this method was to determine the magnitude of adsorption for individual metals and mixed metal matrices to varying extraction chromatography resins. This research is necessary in order to develop optimized separation schemes prior to column studies. Even though batch contact studies do not include the columnar effects seen in a column separation, the free column volume to peak maximum, k' (or the resin capacity factor), for a slurry packed column can be determined by applying a k' conversion factor. The k' values, as determined in equation 2-5 and 2-6, quantifies the affinity and selectivity a resin has for a specific metal under varying conditions.

$$k'(DGA) = D_w \cdot 0.57 \quad \text{(2-2)[29]}$$

$$k'(UTEVA) = D_w \cdot 0.257 \quad \text{(2-3)[32]}$$

Determining the free column volume to peak maximum, k', in this manner allows for simple procedures, such as batch contact studies, to be conducted in order to determine a metal's adsorption to the resin under various conditions in a column separation. The specifics to each batch study experiment performed will be presented within the introduction for each chapter.

The experimental method was based on a previously developed procedure by Gharibyan.[97] A known amount of dry free EXC resin was placed in a polypropylene microcentrifuge tube. This resin was preconditioned using a certain concentration of a desired acid and mixed by placing the microcentrifuge tube on a Labquake Rotisserie shaking table for an hour. After the resin was wet, equal parts of an acid solution containing a component's metal salt and of the same acid solution containing Am-241, Cm-244, or Pu-239 were added. These samples were mixed again on the shaking table for one hour. Separation of the liquid and resin beads were achieved by transferring and expelling the liquid from a 0.45 μm PTFE filtered polypropylene syringe. Volume, radioisotope and nitric acid concentrations were kept constant while the metal analyte concentrations were varied in order to determine the effects from the added metal salt. All batch studies were performed in five replicates. All samples with a stable metal and a radioisotope were analyzed by taking an aliquot for analysis by ICP-AES (inductively coupled plasma – atomic emission spectroscopy) or ICP-MS, for the

stable metal concentration, and LSC (liquid scintillation counting), for the radioisotope activity. The procedures for these instruments are presented in section 2.3, 2.4 and 2.5 respectively.

Volume Correction

In the past to determine the volume correction factor for the amount of volume retained on the resin, scientists have used the weight of the acid retained on the resin and the density of the original acid in contact with the resin. This method does not take into account the fact that the resin may have an affinity for the acid which can then change the density of the acid after contact. Therefore, the volume corrections applied by this method may have substantial error depending on the resin's adsorption of the acid.

To determine the volume correction for the batch contact studies in this thesis, 1.5 mL of an acid of a desired concentration was mixed with 50 mg of resin, same conditions were maintained as in batch contact studies. The 1 mL adjustable pipet used was calibrated by mass to deliver 0.75 mL and 0.3 mL, based on the density of water at the room temperature (0.9982 g/mL), with the least amount of deviation. This was achieved by changing the set pipet volume until 0.7513 g or 0.3005 g of water was delivered.

The error for the pipet was determined by taking 6 - 7 replicates of 0.75 mL of water and pipetting into a tared vial on a mass balance. Based on waters density at room temperature the volume was determined and error was then

calculated. Then the acid was filtered off the resin into a preweighed vial and reweighed to determine the mass of the entire volume eluted. Then a 0.3 mL aliquot of the eluted acid was placed into another previously weighed vial which was reweighed and titrated. Titration was performed by using of 0.1 M NaOH, and 0.1% phenolphthalein and a 25 mL buret. The error of the buret was determined by eluting and weighing 1mL fractions in seven replicates and based on this weight the volume and error was calculated. The solutions were added slowly and continually mixed with 0.1 M NaOH until a pink end point was reached and the volume used was recorded. For each sample, three titrations were performed. Then using the molarity of the acid, and its density, the amount of volume which was not eluted off the resin was determined and a correction factor was used on all batch contact studies k' values. All concentrations of nitric and hydrochloric acid used in characterization studies were analyzed for the volume lost.

Column Chromatography

In this procedure, 2 mL Biospin columns were used to determine elution profiles for Am, Pu, and U individually on DGA and UTEVA resins. A slurry pack technique was used to prepare the columns. A known amount of resin was preconditioned in DI water and resin was allowed to settle by gravity. Great care was taken to ensure no bubbles or channels were formed in packing. After filling the columns, the free column volume (FCV) was determined by litmus paper and elution of loading phase acid matrix. Once this was determined, additional acid, 5

FCVs (free column volumes), were passed through the column in order to rinse and condition the resin. A solution of ~100 Bq/mL Am-241, Pu-239 or U-233 was loaded onto the columns. Aliquots of 1mL were sampled from the load, elution, and strip phases. In order to analyze these aliquots by LSC, a fraction was combined with 15 mL of cocktail in 20 mL LSC vials. Further detail of the LSC analysis procedure is in section 2.5.

Vacuum Box Separations

In order to decrease the processing time to analyze a sample increased flow rates are necessary. The vacuum box system used, shown in Figure 8, was an in-house design which was thoroughly characterized by Gostic.[98] The vacuum box held cartridges in a 3 x 5 configuration. The internal pressure of the vacuum box was controlled by a vacuum pump (Edwards) coupled to a digital vacuum regulator (J-Kem Scientific).

Figure 8. In-house Designed Vacuum Box System

Prepacked 2 mL EXC resin cartridges, available through Eichrom Technologies, were placed on the vacuum extraction unit. These prepacked

cartridges can be stacked providing a method which would simplify the separation process, reduce possible sample loss, and minimize creation of waste. Increased flow rates achieved by this system can affect the efficiency of a separation but there are other parameters which can be used to influence a separation as well, such as the matrix constituents, the extractant loading, the column length, and the operating temperature. To control the flow rate as well as possible, a digital vacuum regulator controlled the internal pressure of the box.

DGA resin was previously characterized on this vacuum box system, by Gostic, for Am-241's flow rate reproducibility, and its efficiency for a sequential extraction.[98] It was determined that the kinetics of the resin was sufficiently high to achieve efficient separations over a wide range of flow rates, up to 10 ml min^{-1}. Since it was determined that fine control was not necessary for consistent recoveries, the separations performed in this thesis were performed with flow rates between 1-5 mL min^{-1}. The rinse and loading phases were performed at ~1 mL min^{-1} and the elution and stripping phases were set to ~4 mL min^{-1}.

Initially the separation schemes were characterized for Am, Pu, and U recoveries on DGA and UTEVA resins, individually, for various loading, elution, and stripping phases. Each phase volume was collected in whole and characterized on the LSC by mixing an aliquot with LSC cocktail in a 20 mL vial. Once the optimal separation conditions were determined, the cartridges were stacked, UTEVA on top of DGA, and characterized for a mixed actinide sample separation and recovery. For this separation, 5 mL fractions were collected and a 1 mL aliquot was taken for LSC analysis in order to determine the amount of

activity in each fraction. For the mixed actinide samples, an aliquot was taken based on the activity of each fraction, where the aliquot did not exceed 10 Bq for electrodeposition. The electrodeposition parameters are described in more detail later. These aliquots were electrodeposited using a sulfate based system and analyzed on the alpha spectrometer, further description of these procedures are described in Section 2.8 and 2.7, respectively.

Section 2.3 Inductively Coupled Plasma – Atomic Emission Spectrometry

Inductively Coupled Plasma – Atomic Emission Spectrometry is an analytical technique which uses an inductively coupled plasma to excite an element's or ion's electrons to an excited state and in its de-excitation it emits a characteristic photon spectrum. The sensitivity of the ICP-AES is typically in the 1-100 ppm range for most elements. Analysis is typically performed on aqueous samples which are pumped through a nebulizer chamber where it is aerosolized with argon gas. This aerosolized sample is then carried into the argon plasma torch where it is atomized and excited by the extreme heat (6000-10,000K). As the atoms travel through the torch chamber they return to ground state and emit a photon which is detected by an array of charge-injection devices which are solid state silicon detectors. A signal is produced by the photon being absorbed in the detector and being converted to a charge that is proportional to the intensity of the photon at that wavelength. Therefore a given a calibration plot for a specific analyte(s), the quantity could be identified. A more in-depth explanation of ICP-AES can be found in literature.[99]

In this thesis, for most stable element analysis an iCAP 6500 series (Thermo Scientific, Inc., Cambridge, UK) ICP-AES was coupled with an ASX520 Autosampler was used, Figure 9. This spectrometer has a higher performance detector, CID86, which covers the wavelengths 166-847 nm. The iCAP 6500 series software, iTEVA, was used for all data acquisition and analysis. More information is available from Thermo Scientific.[100]

Figure 9. iCAP 6500 and ASX520 Autosampler

For sample analysis the instrument settings, described in Table 4, which were optimized by the manufacturer, were used for the experiment. All samples had three measurements per sample.

Table 4. Operating Parameters for iCAP 6500

Parameter	Setting
Radio Frequency Power	1150 W
Analysis Pump Rate	50 rpm
Purge Pump Rate	50 rpm
Flush Time	30 sec
Auxiliary Gas Flow	0.5 L/min
Nebulizer Gas Flow	0.5 L/min
Coolant Gas Flow	12 L/min

The wavelengths used for analysis of analytes, Table 5, were chosen carefully to ensure as little interference as possible. Prior to sample analysis, 1-100 ppm M+ standards were created in each matrices used order to make a calibration curve with $R^2 \geq .98$ where R^2 is a statistical measure of how close the data are to the fitted line. All samples were viewed using the auto mode which switches between radial and axial positions depending on the intensity of the emission.

Table 5. Wavelength and Relative Intensities used on iCAP 6500 for analysis

Element	Wavelength	Intensity	Wavelength	Intensity
Calcium	184	180000	317.9	300000
Erbium	350	600,000	367.6	15000
Molybdenum	202	500000	281.6	400000
Strontium	216.5	300000	228.2	12000
Zirconium	3391	3500000		
Neodymium	4061	60000		
Aluminum	3092	600000		

Samples were analyzed of the solution pre- and post- batch contact studies. The calibration curve was used to determine the concentration of the

samples. The amount of the analyte sorbed onto the EXC resin was determined using the following equation:

$$[M^+]_{adsorbed} = \left(PPM_{pre} - PPM_{post}\right)\left(\frac{V_{pre}}{V_{post}}\right) \qquad (2\text{-}4)$$

Where PPM_{pre} and PPM_{post} are reported concentrations of metal determined by ICP-AES analysis, V_{pre} is the total volume of the aliquot prior to chemistry and V_{post} is the volume taken from aliquot contacted with the resin for analysis.

Section 2.4 Inductively Coupled Plasma – Mass Spectrometry

Inductively coupled plasma – mass spectrometer is an analytical technique which is often used to determine elemental isotopic composition in a sample by taking advantage of the differences in the mass-to-charge ratios, m/z, of each isotope of an element. The mass-to-charge ratio of each isotope is based on the fact that the isotopes of a given element will have the same number of protons, therefore the same ionic charge, but have a different number of neutrons changing the atomic mass. The ICP-MS has low detection limits, of low ppb (µg/L) to ppt(ng/L) levels, compared to the ICP-AES. In this thesis, the ICP-MS was used for elemental quantification where detection was not possible on the ICP-AES.

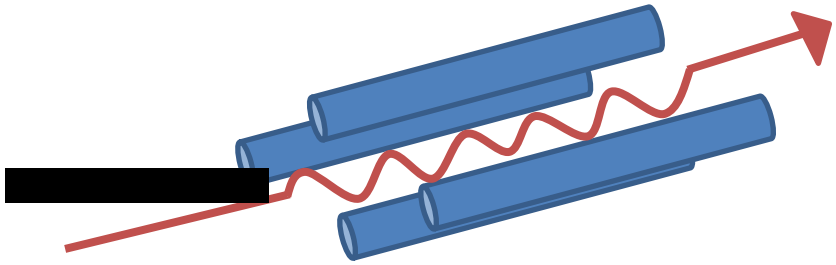

Figure 10. Quadrouple Mass Filter

There are two parts to the ICP-MS: the ICP and the mass spectrometer. The sample introduction for the ICP-MS is the same as in the ICP-AES where an aqueous sample is pumped into a nebulizer chamber and aerosolized. The aerosolized sample is then carried by argon into an argon torch held around 10,000K. This torch atomizes the samples into charged particles which passes through two cones in order to sample just the inner portion of the ion beam. This beam is focused by electrostatic lenses into the entrance of the mass spectrometer, which is a quadrupole mass filter, where they are separated by their mass-to-charge ratio. In the quadrupole mass filter there are four rods where quickly alternating AC and DC voltages are applied along with an RF (radio frequency) field where the ions travel in the spaces between the electric fields as seen in Figure 10. The applied voltage to the rods will selectively allow only an ion with a specific mass-to-charge ratio reach the detector. Therefore, you can either scan for a range of m/z values or select detection at a specific m/z.

Figure 11. ELAN DRC II ICP-MS coupled with S-10 Autosampler

An ELAN DRC II ICP-MS (Perkin Elmer, Inc., Shelton, CT, USA) coupled with a CETAC autosampler (CETAC Technologies, Omaha, NE, USA), Figure 11, was used in this thesis for Cs adsorption in batch contact studies summarized in Chapters 3 and 4. The manufacture provided software was used for data acquisition and analysis. The operating parameters used, in Table 6, were optimized by the manufacturer upon installation. A daily performance system check was performed with a multi-elemental solution which ensured that instrument sensitivity, precision, doubly charged, and oxide ratios were at acceptable levels. More detailed description and information for an ICP-MS is available in the literature.[101]

Table 6. Operating Parameters for ELAN DRC II

Parameter	Setting
RF Power	1100 W
Nebulizer Gas Flow	0.90 L/min
Auxiliary Gas Flow	1.20 L/min
Plasma Gas Flow	15 L/min
Vacuum Pressure	< $7x10^{-6}$ torr

Samples were diluted in 5% nitric acid to compatible metal concentrations. Prior to sample analysis, 1-50 ppb M+ standards were created in order to make a calibration curve with $R^2 \geq .98$. Samples were analyzed for mobile phases pre- and post- batch contact studies. The calibration curve was used to determine the concentration of the samples. Equation 6 was used to determine amount of metal adsorbed onto the resin.

Section 2.5 Liquid Scintillation Counter

Liquid Scintillation Counter is a commonly used radioanalytical technique for determining the activity in a sample. In this thesis, all samples containing radioactive material were characterized using this technique to determine either radionuclide concentrations or gross activity. This technique cannot be used to identify an unknown radionuclide but only determine the amount of activity.

Detection by scintillation depends on the radioactive material being located close to a molecule which can scintillate. Therefore, the radioactive materially is typically dissolved in LSC cocktail which is composed of three components: a solvent, a wavelength shifter and an aromatic hydrocarbon.

While the solvent used in the LSC cocktail must dissolve the wavelength shifter and the aromatic hydrocarbon it must also be compatible with the matrix of sample to be dissolved. The scintillating component is the aromatic hydrocarbon containing π-bonds in which an electron is excited upon interaction with radiation of sufficient energy. As these scintillators de-excite, photons are emitted. These photons are at energies which are not efficiently detected by the photomultiplier tubes (PMTs). Therefore another organic molecule, the wavelength shifter, are used to absorb the initial photons emitted by the scintillator and re-emits another photon at more efficiently detected wavelength.[102]

Since the radioactive material needs to be in close proximity to the scintillators in order to maximize the energy transferred, the sample is directly dissolved in the LSC cocktail and placed in a LSC vial. Mixing the sample in the LSC cocktail gives 4π geometry which creates 100% detection efficiency for alphas. As the photons are emitted from these vials, they reach the two PMTs on opposite sides of the vial where the PMTs multiply the current produced by the light. There are two PMTs in such an arrangement in order to reduce the environmental background by using a coincidence technique. The signal intensity is proportional to the energy of the radiation and the number of pulses is recorded for that specific energy. The energy is not defined enough to use for radionuclide identification. Since there are differences in alpha and beta pulse decays they can be discriminated from one another in the same sample giving gross alpha and gross beta activity.

Limitations of the LSCs stem from the poor resolution and quenching effects. Quenching effects reduce the number of photons which make it to the detector. This can occur due to the chemical quenching which is when other molecules present within the cocktail provide alternate paths for de-excitation and no light is emitted. Thus, it can decrease not only the number of pulses but the intensity as well. This often happens with colored solutions and peak shifting is typically seen. More information is available on scintillators and detectors in literature.[102]

Two LSCs in Figure 12 were used for activity measurements. The Tri-Carb 3100TR (Perkin Elmer, Boston, MA, USA) was used for general measurements and the Tri-Carb 2900TR (Perkin Elmer, Boston, MA) was used for alpha/beta discrimination. The QuantaSmart software was used for data acquisition and analysis. Regions of interest were set to define areas of background versus analyte counts. More detailed product description is provided by Perkin Elmer.[103, 104]

Figure 12. Tri-Carb 3100TR (top) and Tri-Carb 2900TR (bottom) Liquid Scintillation Counters

For analysis of samples, a 0.1 to 1.0 mL aliquot was taken and mixed with 15 mL of Ultima Gold AB cocktail (Perkin Elmer, Waltham, MA, USA) in a 20 mL high-density polyethylene (HDPE) vial. These HDPE vials provide lower background and high counting efficiency than glass vials and reduce the possibility of breaking. Ultima Gold AB was selected due to its durability with mineral acids ranging from 0 to concentrated molarity.[105] Although this cocktail

is more durable than most, above 2 M there are chemical quenching effects. These effects were taken into account during data analysis. Blanks were prepared by adding in equal volume of the same acid concentration as the samples but without any radioactive material. Multiple blanks were used in each batch of samples analyzed. Each sample was counted for an hour or until 10,000 total counts (1% error) was reached. Once the count rates for blanks, standards and unknown samples were determined the blank count rates were subtracted from the standards and unknowns; these background corrected count rates were used for k' value determination.

Section 2.6 Gamma Spectroscopy

Gamma spectroscopy is a technique which detects the gamma rays emitted from a decaying nucleus and is often used for radionuclide identification and activity determination in a wide variety of samples.[102] The detection of gamma rays occur when the photon emitted interacts with the active volume of the scintillation detector. These detectors are crystals that emit light when gamma rays interact with the atoms similarly to the scintillators in the LSC. These scintillation crystals are joined to a photomultiplier tube. A characteristic spectrum of a radionuclide's gamma rays is produced making identification possible.[102]

Not all gamma rays that pass through the detector will be detected. The detector efficiency is the probability that an emitted gamma ray will interact with

the detector and produce a count. The efficiency for gamma spectrometers can vary widely depending on the size of the detector and its geometry.

Figure 13. PerkinElmer 2840 Wizard^2 Automatic Gamma Counter

A PerkinElmer 2480 WIZARD^2 automatic gamma counter, Figure 13, was used for Am/Pu mixed samples. This detector incorporates end-well NaI(Tl) detectors into the design of a high throughput automatic gamma counter. This detector has almost 4π geometry which gives high counting efficiency. More detailed information on this detector is available through the manufacturer.[106] Another NaI well detector was used for single component analysis after batch contact studies. This was set up as seen in Figure 10.

Figure 14. NaI well detector setup

For column separations of Am and Pu, mixed Am-241/Pu-239 fractions were analyzed on the automatic gamma detector. All samples were counted for an hour or up to 1% error. A portion of these aqueous samples were first analyzed on the LSC for total activity and then analyzed on the gamma spectrometer for the Am-241 samples. After taking into account the detector efficiency and branching ratio, the Am-241 activity was subtracted from the gross alpha activity determined on the LSC to calculate the Pu-239 activity.

Section 2.7 Alpha Spectrometry

Alpha Spectroscopy is a method which can identify and distinguish between various alpha emitting radionuclides.[102] Alpha spectrometers are comprised of a series of vacuum chambers that have solid-state semiconductor

detectors in each one. A vacuum is necessary to have the emitted alpha travel from the sample to the detector. Once the alpha reaches the active region of the detector, the energy deposited is converted to a charge creating free electron-hole pairs.[102] As higher energy is deposited there are proportionally more free electrons and holes created. Under an electric field, the electrons and holes move to the electrodes where a pulse is generated. Since the number of electron hole pairs is proportional to the alpha energy, the intensity of the deposited alpha radiation can be determined.

In order to avoid contamination of the detectors all samples to be analyzed on the alpha spectrometer were first analyzed for overall activity on the LSC. Once the overall, activity was known an appropriate aliquot was taken in order to achieve an activity of ~1 Bq in the alpha samples. Typically the samples are either electrodeposited or microprecipitated on a planchet or filter prior to analysis on the alpha spectrometer. Since alphas are easily attenuated, thin samples are necessary so that the alphas will not be attenuated in the sample. All alpha samples were electrodeposited and this process is described in the next section.

Figure 15. Alpha Analyst System

In this thesis, a 12 chamber Alpha Analyst system (Canberra Industries, Inc, Meriden, CT, USA), seen in Figure 10, was used for all alpha spectrometer analyses. The solid state detectors in this system were passivated implanted planar silicon (PIPS) detectors and had an active area of 450 mm^2. The electrodeposited disks were placed in planchets which were then placed in the manufacture's sample trays in the fourth position from the detector.

All samples analyzed on the alpha spectrometer were counted for 12 hour time periods. The background for each chamber was counted for 12 hours weekly as well and subtracted from the spectra. The manufacture's software, Genie 2000 (Canberra Industries, Inc) was used to view and analyze the spectrum.

Section 2.8 Electrodeposition

Electrodeposition is a technique that uses electric current to deposit metal cations on an electrode, or planchet. This technique is often used to make alpha spectroscopy samples because it makes a very fine, even source which helps to decrease self-attenuation and improve the resolution of the peaks. Actinides are more difficult to deposit because the decomposition of water will create interfering reactions at the electrode.[107] Glover et al.'s electrodeposition procedure was used since it provides sources with excellent spectral resolution and high recoveries for Am, Pu, and U.[108]

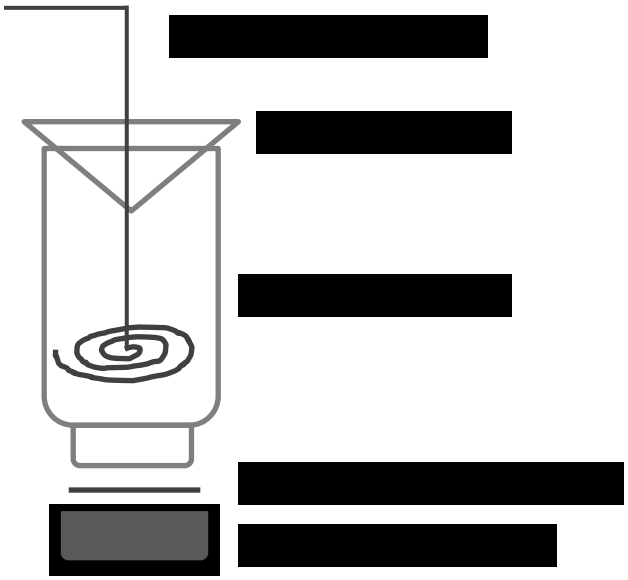

Figure 16. Electrodeposition Cell

The electrodeposition was performed in a cell as seen above in Figure 16. The HDPE LSC vial has the bottom cut off which in the above arrangement is the top

of the electrodeposition cell. The splatter shield is the bottom of a 50 mL plastic centrifuge tube with a hole cut in the center to allow the electrode to go through it. The electrodeposition was performed on an in-house developed electrodeposition apparatus, Figure 17.

Figure 17. Electrodeposition System

Prior to electrodepostion, the planchet, planchet cap, and LSC vial are assembled and tested for leaks with DI water. Mixed actinide samples were electrodeposited for the vacuum box separations. Since the activities in the samples are unknown, an aliquot of each fraction was analyzed on the LSC for total activity. The size of the aliquot was based on the activity determined which ranges from 0.1 µL to 2 mL. This aliquot and 1 mL of 20% $NaHSO_4$ was added into a glass LSC vial and brought to complete dryness. Before removing the vial from the hotplate to cool, 0.3 mL of concentrated H_2SO_4 was added in order to

speed up the dissolution of the sample. Once the samples are completely dissolved, 4 mL of DI water was added, 4 mL of 1% H_2SO_4 and 2 drops of 0.1% thymol blue indicator were added. The pH was adjusted to 2.0-2.3 by adding concentrated NH_4. Then the solution was poured into the electrodeposition cell and the glass LSC vial was rinsed three times using a solution with a pH of 2.0-2.3. This solution is then electrolyzed for 1 hour at 0.8 A. One minute before it is finished, ~1mL of concentrated NH_4 is added into the cell to ensure the deposit doesn't dissolve when the electrodeposition is ended. After this, the solution is disposed and the planchet is rinsed with weak NH_4 solution and finally with acetone. Prior to analysis, the planchets are baked on a hotplate at 500^{o}C for 2-3 minutes.

Chapter 3. EFFECTS OF USED FUEL COMPONENTS ON ACTINIDE ADSORPTION TO DGA RESIN

Section 3.1 Abstract

Material accountancy for used fuel is an important and essential part of developing strong safeguards for a reprocessing facility. For this purpose, the properties of extraction chromatography resins are being characterized in order to develop rapid separations of Am, Cm, and Pu from used fuel in reprocessing waste streams. In this chapter, first the methodology used to ensure reliable and reproducible adsorption studies for Am, Cm, and Pu is reviewed. Then the adsorption characteristics of Tc-99 on DGA resin were investigated in varying concentrations of nitric and hydrochloric acid since there is no published data available. All of these studies are discussed in the following sections.

Due to the complexity of the matrices found in reprocessing waste streams, the adsorption characteristics of the elements may not stay the same as those previously determined in pure acid matrices. Thus, the main part of this chapter describes the effects that result from the addition of the most abundant spent fuel constituents, seen in, on Am, Cm, and Pu adsorption to an extraction chromatography resin, DGA, in nitric and hydrochloric acid. Interference and synergistic effects are seen in in the presence of mg/L quantities of various metals in 1 M HNO_3 and HCl. The effects of Cs, Sr, Nd, Er, Tc, and Zr on Am, Cm and Pu adsorption and separation will be discussed in detail.

Section 3.2 Materials and Methods

Batch Contact Method

Batch contact studies were performed in separate M^+-Am, M^+-Cm, and M^+-Pu batches with five replicates to individually analyze the spent fuel components' interference on Am, Cm, and Pu uptake. To wet the resin, 50 mg of DGA resin was contacted with 0.5 mL of 1.45 M HNO_3 or HCl and placed on a shaking table for 1 hour and allowed to sit overnight. After the resin was wetted, 0.5 mL of 1.45 M HNO_3 solution containing either 3, 15, 30, 45 or 60 mM Metal (Cs, Sr, Nd, Er, and Zr), and 0.5 mL of a standard consisting of 0.1 M HNO_3 or HCl with 75-100 Bq/mL of Am-241, Cm-244, or Pu-239 were added. For Tc-99 interference studies, the resin was pretreated in the same manner but then 0.5 mL of 1.45 M HNO_3 or HCl solution with 70, 80, 90, 100 or 130 Bq/mL of NH_4TcO_4 were added to the same standards. The samples were agitated for 1 hour to ensure equilibrium was reached. Separation of the liquid from the resin beads was achieved by transferring the liquid and pushing it through a PTFE filtered 3 mL syringe. Volume, radioisotope and acid concentrations were kept constant for each set of data points and only the metal analyte (M^+) concentrations were varied.

Reagents

The extraction chromatography resin DGA was obtained from Eichrom Technologies, Inc. Nitric and hydrochloric acid stock solutions, listed in Table 7, were prepared from ACS reagent grade acid (Sigma-Aldrich) using deionized

water with a resistivity of 18.2 Megaohms from a Cascada system manufactured by Pall Corporation. These stock solution concentrations were chosen based off of the desired final concentrations, seen in Table 7, after the addition of the 0.5 mL of 0.1 M acid radionuclide standard.

Table 7. Stock and Final Acid Concentrations

Stock Solution		Final Concentrations	
Nitric Acid (M)	Hydrochloric Acid (M)	Nitric Acid (M)	Hydrochloric Acid (M)
0.0025	0.0025	0.035	0.035
0.025	0.025	0.05	0.05
0.7	0.1	0.5	0.1
1.45	0.7	1	0.5
7.45	1.45	5	1
14.95	2.95	10	2
15.805	7.45	10.57	5
	11.95		8.1

The Am-241, Cm-244, and Pu-239 stock solutions of activities between 75 – 100 Bq/mL in 0.1 M nitric or hydrochloric acid were obtained from Isotope Products Laboratories. Metal solutions of 3 – 60 mM and 1 – 100 ppm ICPAES standards were prepared from $Sr(NO_3)_2$ (Alfa Aesar, ACS, 99%), $CsNO_3$ (Sigma-Aldrich, 99%), $Nd(NO_3)_3$ (Sigma-Aldrich, trace metal basis, 99.9%), $Er(NO_3)_3{\cdot}6H_2O$ (Sigma-Aldrich, 99.9%), $Zr(NO_3)_4$ was prepared by dissolving $ZrCl_4$ (Alpha Aesar, 98%) in concentrated nitric and reconstituting it in concentrated HNO_3 three times. The 130 Bq/mL Tc stock solution was prepared from an ammonium pertechnetate standard.

Measurements

Samples of Am-241, Cm-244, and Pu-239 were measured either on a Tri-Carb 2800TR or a Tri-Carb 3100TR scintillation counter in polypropylene vials by taking a 0.9 mL aliquot of the filtrate and added 15 mL of Ultima Gold AB cocktail. The radiotracers were measured for up to an hour or until the one sigma counting error (10,000 counts) was reached. For alpha-beta discrimination, standards with varying concentrations of Am and Tc were measured to determine the amount of cross-talk as a function of amount of activity and the pulse shape analysis value was selected based on the point of most minimal overlap. Non-radioactive metal concentrations were determined on an iCAP 6500 ICP-AES Spectrometer (Thermo Scientific). The Elan DRC II Inductively Coupled Plasma-Mass Spectroscopy was used to analyze for Cs and any metals or replicates with concentrations were below the ICP-AES detectable limit or where its detection was not compatible.

Section 3.3 Methodology

In order to ensure that the batch contact study method is offering an accurate representation of the k' values, the amount of liquid adsorbed by the resin needs to be taken into account to give the proper volume correction factor. Certain resins have a specific affinity for acid which can result in a preferential adsorption of the acid in comparison to the water. Therefore, it was essential to investigate the amount of nitric and hydrochloric acid adsorbing to DGA in varying acid concentrations. Once the amount adsorbed is determined, the

correct density for volume correction factors can be identified. Initially, to determine the amount of acid adsorbed by the resin, 50 mg of DGA resin was contacted with 1.5 mL of various acid concentrations. The eluted acid, after contact, was then titrated and the wet resin was rinsed with DI water and titrated again to confirm the amount of acid adsorbed.

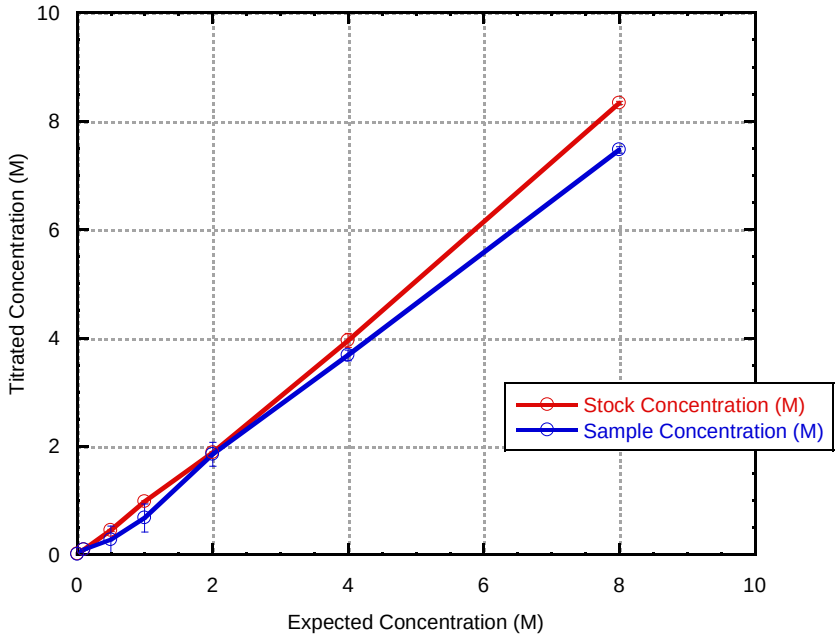

Figure 18. Nitric Acid Stock vs Eluent Concentrations

In Figure 14, the concentration of the titrated acid stock solution is graphed in comparison with the sample's acid concentration after contact with DGA resin. Above 2 M HNO_3, there is a decrease in the eluted acid concentration, after mixing with DGA resin, which means nitric acid is adsorbing to the resin disproportionately compared to water which therefore decreases the

changes the nitric acid concentration. In order to confirm this decrease in concentration the following graph, Figure 19, illustrates the change in the nitric concentration in the rinses of DGA.

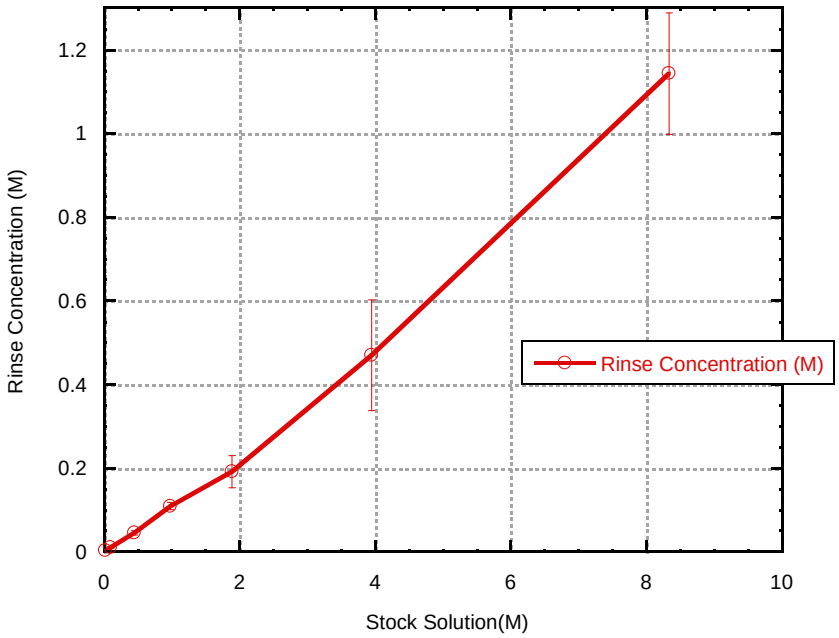

Figure 19. Nitric Acid Concentrations in DGA Rinses

Even though there was no detection of preferential nitric acid adsorption below 2 M HNO_3, there was nitric acid detected in all rinses independent of nitric acid stock solution concentrations. The amount of acid determined in the rinse is below the error for nitric acid concentrations of the samples from 0.01 M to 1 M, seen in Figure 18; so, it is possible that a small amount of acid is adsorbing at those concentrations as well. For this reason, the batch studies' eluent volume

was determined using the densities at room temperature of the acid concentrations, shown in Figure 18, and the weights of the eluent.

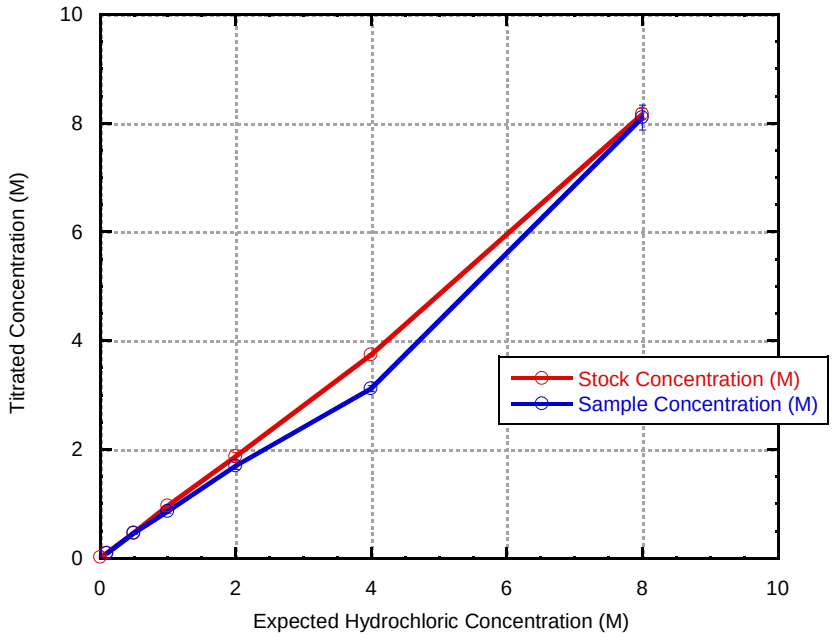

Figure 20. Hydrochloric Acid Stock Solution vs Eluent Concentration

In Figure 20, the hydrochloric stock and sample concentrations are graphed in relation to the expected hydrochloric acid concentration. There is little to no change between the stock and sample concentrations for hydrochloric acid mixing with DGA resin, except for 4 M HCl. The rinses were tested as well and no acid was found to be present. The discrepancy at 4 M HCl could point to the possibility that the actual error of the measurement is larger than the error graphed. Since there was no change in the hydrochloric acid concentration, the

density of the stock acid solution at room temperature was used to determine the volume eluted from the batch studies.

The adsorption of Am, Cm, and Pu in varying concentrations of nitric and hydrochloric acid was determined using the batch contact study methodology. Over the entire range of nitric acid studied, Figure 21, as the nitric concentration increases, the k' values of Am and Cm increase three orders of magnitude (20 to 60,000). The Pu k' values gradually increase until 5 M HNO_3, and then as the nitric acid concentration increases the k'_{Pu} increases ~1.5 orders of magnitude (900 to 20,000). The high affinity of Am, Cm, and Pu in > 5 M HNO_3 will allow an aliquot of dissolved spent fuel to be directly loaded onto the column without needing to reconstitute the spent fuel into a different mobile phase. This will decrease the separation time in comparison to other separations previously investigated for used fuel separations and may allow in-stream implementation.

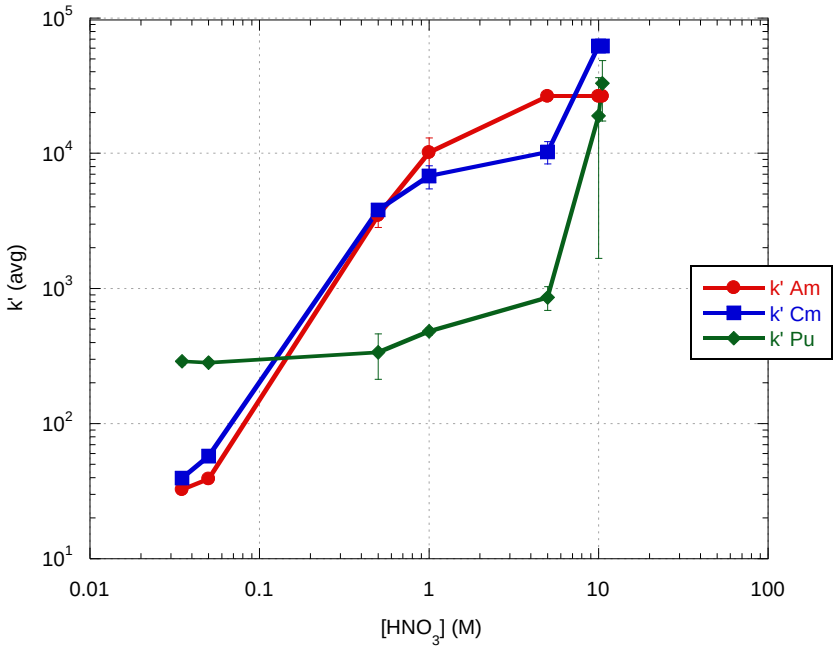

Figure 21. Adsorption of Americium, Curium, and Plutonium to DGA in Varying Concentrations of Nitric Acid

As the concentration of HCl increased, the k' values of Am and Cm increased up to four orders of magnitude, Figure 22. The k' values appear to plateau above 5 M HCl. At low concentrations of HCl (below 1 M), the Am and Cm adsorption drops near or below 0.1. This trend shows the importance of Cl^- concentrations on trivalent metal adsorption. For Pu, as the concentration of HCl was increased, the k' values increased as well, but only up to two orders of magnitude. The adsorption for Pu does not drop below a k' value of 10. Since this is considerably high, elution from DGA may prove difficult. In later chapters, additional reagents were therefore investigated to determine the optimal mobile phase for stripping of Pu.

The adsorption of Cm to DGA resin in varying concentrations of nitric or hydrochloric acid has been reported previously by Gharibyan.[97] The results found in Figure 22, have similar Am and Cm trends to those previously reported. Due to its similarity in charge and size to Am it shows, as expected, a similar adsorption trend. In the following sections discussing the interference effects, Cm was studied under the same conditions as Am and Pu. The data is however not presented in the graphs to avoid crowding, since Am represents Cm chemistry well.

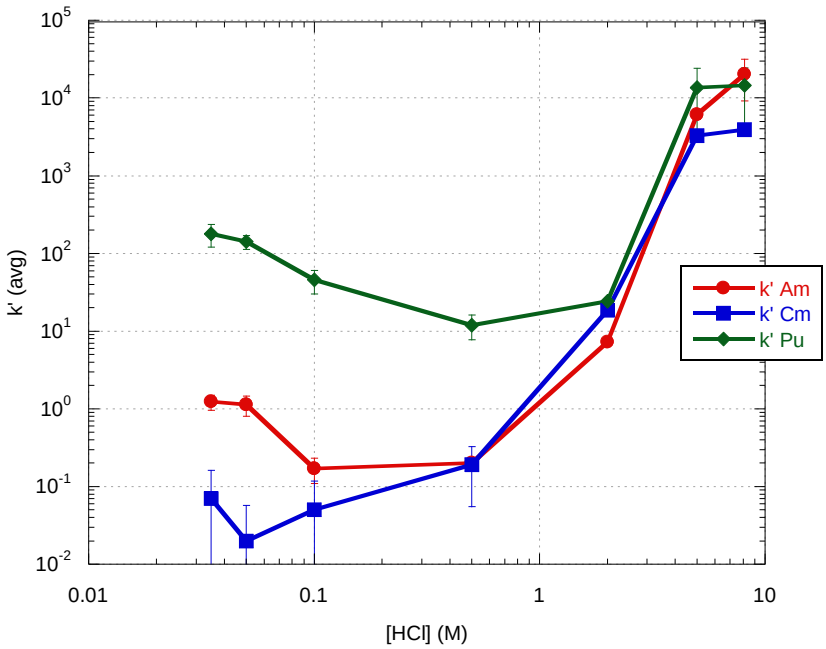

Figure 22. Adsorption of Americium, Curium, and Plutonium to DGA resin in Varying Concentrations of Hydrochloric Acid

The mass transfer kinetics of DGA and the effect of varying DGA mass were also probed using the batch contact study methodology. The results match well with the data reported by Horwitz et al., reaching equilibrium in 30 minutes. It

can therefore be assumed that the batch contact study's methodology is reliable and reproducible.[29]

Section 3.4 Adsorption Characteristics of Tc-99

No adsorption characterization for Tc on DGA has been previously reported in the literature. The uptake of Tc by the resin was therefore analyzed for varying concentrations of nitric acid or hydrochloric acid for its affinity to DGA resin. Results for both systems are presented in this section. As seen in Figure 23, in low concentrations of nitric acid the Tc adsorption shows high k' values and in high nitric acid concentrations Tc has low k' values. DGA is known to complex a cation in a tridentate fashion in the inner sphere and then loosely complexes with the anions in the inner or outer sphere, depending on polarity of the diluent, resulting in the formation of a neutral species.[43] Therefore, as nitric acid concentrations increase and as $HTcO_4$ starts to form, an order of magnitude decline in the k' values occurs. This is expected since the diglycolamide active site tends to prefer cations with an ionic radius between ~72-120 pm.[38]

Since Arisaka, et al. determined how DGA typically complexes cations, at low nitric acid concentrations it is likely that the ammonium is the complexed cation in the inner sphere and the TcO_4^- is the complexed anion in the outer sphere.[43] Due to the wide range of adsorption values for Tc-99 in nitric acid, there may be potential to separate Tc from other metal analytes', where Tc would be adsorbed at low nitric acid concentrations and eluted at high concentrations. The lowest k'_{Tc} value in nitric acid is however ~60, which is not low enough to

ensure complete elution from the column within a practical elution volume. Reducing agents may be able to lower this to an acceptable level by taking advantage of Tc's lower oxidations states but further studies are needed to fully assess DGA's potential for Tc(VII) separation.

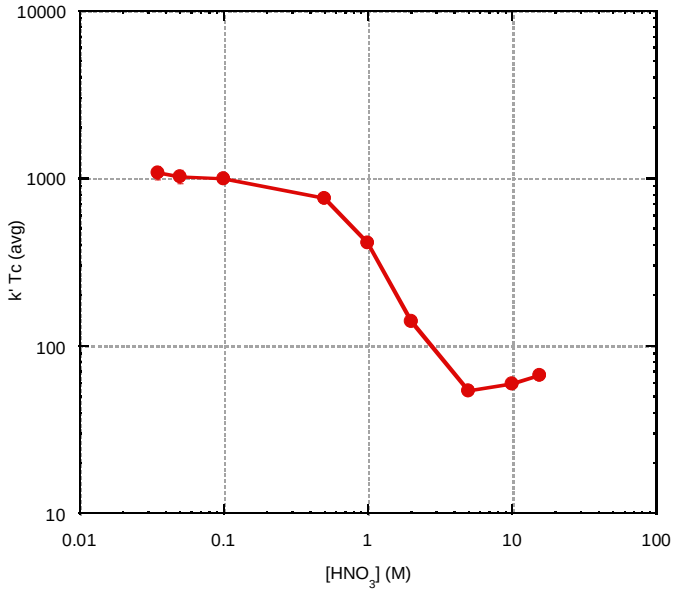

Figure 23. Technetium Adsorption to DGA resin in 1 M HNO_3

Technetium adsorption was also studied in varying concentrations of hydrochloric acid and the results can be seen in Figure 24. Over all the concentrations examined the adsorption is high. The lowest k' value is ~1000, which is not low enough to ensure complete elution from the column within a reasonable elution volume. Since the k' values are so high across all hydrochloric acid concentrations studied, separations of Tc in hydrochloric matrices would not be practical. Depending on the affinity of Tc's other oxidation states to DGA

resin, reducing agents may be able to lower this to an acceptable level or provide a useful separation scheme. The speciation of Tc in hydrochloric acid has been previously studied and found to form varying technetium chloride complexes based off of the hydrochloric acid concentrations. As the hydrochloric acid concentrations increases, the Tc(VII) changes to Tc(IV).[109] Above ~1 M HCl, $TcCl_5^-$ and $TcCl_6^{2-}$ are formed.[109] Since Tc tends to complex which oxygens, Tc may be directly complexing with the oxygens in the diglycolamide. At higher hydrochloric concentrations, there appears to be indication of a further increase in k', but due to the large error bars for the data in consideration it is inconclusive if the chlorides have an effect on the Tc affinity. Further studies would need to be performed to identify and confirm the complex in hydrochloric and nitric acid.

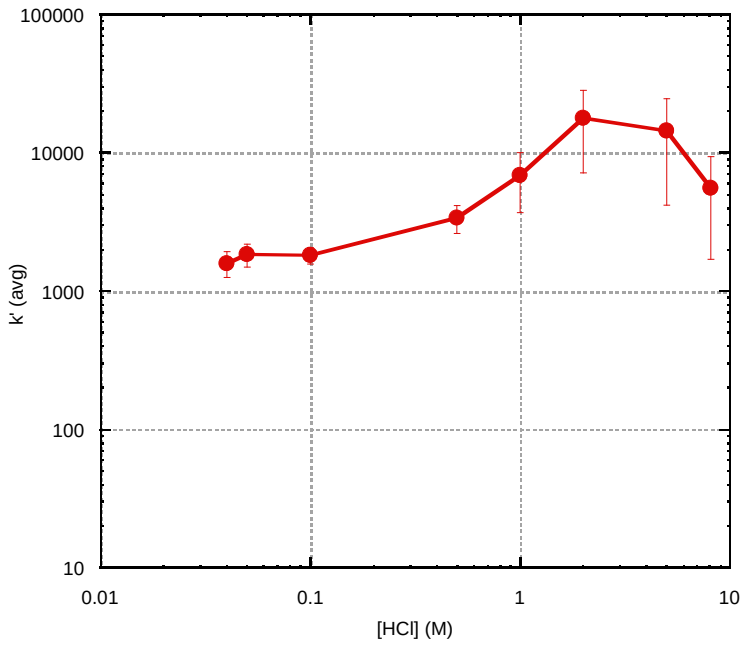

Figure 24. Technetium adsorption to DGA resin in varying concentrations of HCl

Section 3.5 Nitric Acid Results and Discussion

The effects of additional components in solution were studied and at an acid concentration of 1 M HNO_3. This condition was chosen since the k' values, although high, are not too close to the detection limits of the LSC to see changes in the adsorption. This allows for synergistic, interference, or competitive effects to be identified. In 1 M HNO_3, the k' value for Am is near 10^4 and for Pu near 200. In the following graphs (Figure 25 and 26) the Am and Pu sorption in 1 M HNO_3 without addition of impurities is represented by the solid line. The dotted lines represent the adsorption of Am and Pu in the presence of the metal analyte listed. The concentration ranges for metal analytes vary from 1-20 mM M^{+x} for Zr, Er, Nd, Cs, and Sr to ensure that the capacity of the metal analytes on the resin is not exceeded over the entire range. Tc will be reported separately since it was analyzed under different concentrations. In all the following graphs, the analyte being graphed is represented by an asterisk (*) next to its abbreviation. In the case of Am*-Zr, the k' values would be only for Am, but Zr was present in the solution. Error bars are reported on all of the graphs and represent the standard deviation between the five replicates performed.

In Figure 25, the greatest effects on Am adsorption are seen in the presence of Zr, Nd, and Er at high concentrations of each of these metals. This is expected as DGA has been found to have a high affinity for those metals with a +3 or +4 charge. The details of these effects will be described later following their individual interference graphs. Based on these results it is safe to assume that all +3 and +4 charged metals are going to interfere with Am adsorption, especially

when column capacity is exceeded. To maintain an efficient separation, it will be essential to mediate this interference or divert the interfering metals prior to reaching DGA. Another interesting characteristic of this graph is the plateau reached for Am adsorption above 10 mM M^{+x}, where it would be expected to see a continued decrease with the increase of the metal concentrations.

At low concentrations of Zr there is an increase in Am adsorption which may be due to a synergistic effect which could be caused by a Zr-Am co-complex. This possibility will be further discussed after the Zr interference graph, Figure 29, where more detail in the behavior of Zr's adsorption on DGA is supplied. Cs and Sr show the least effect on the adsorption of Am. This is also expected as DGA has been found to have a low affinity for those metals with a +1 or +2 charge.

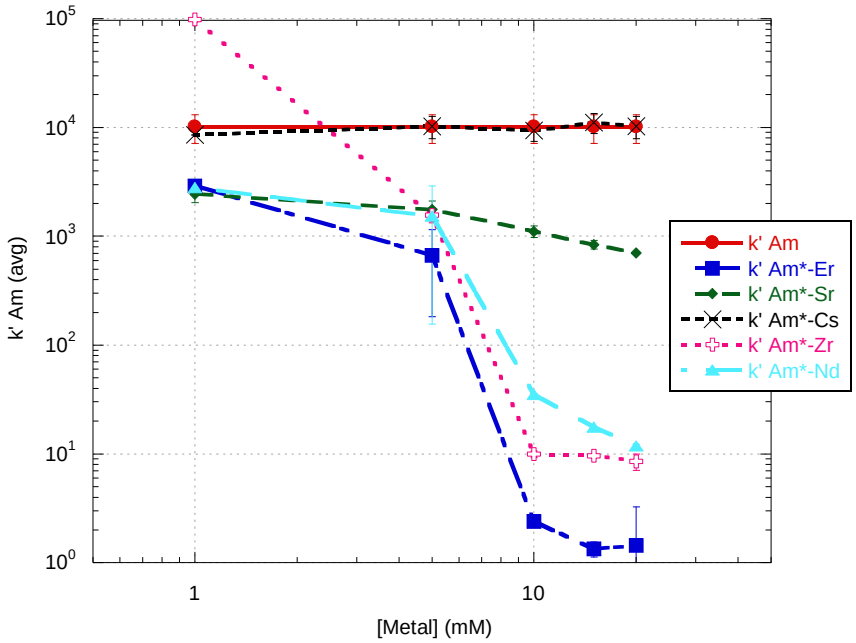

Figure 25. Used Fuel Component Effects on Am Adsorption to DGA resin in 1 M HNO_3

The individual component graphs and detailed discussion will be provided in the following section. Due to the similarities between Am and Cm characteristics on DGA resin, only Am adsorption values are reported and can be assumed to be the same as Cm; any differences will be reported. At about 1 mM Metal, there seems to be little to no effects on Am. Since the largest effects on Am adsorption is after the capacity of the resin is exceeded, which is slightly above 5 mM, the concentration of the metals will need to be taken into account either when deciding on the size of the column or the volume/concentration of the aliquot that can be added to the column. Since Am will not be eluted off in 1 M HNO_3, due to its high affinity, the synergistic effect seen in the presence of Zr will not be of great concern.

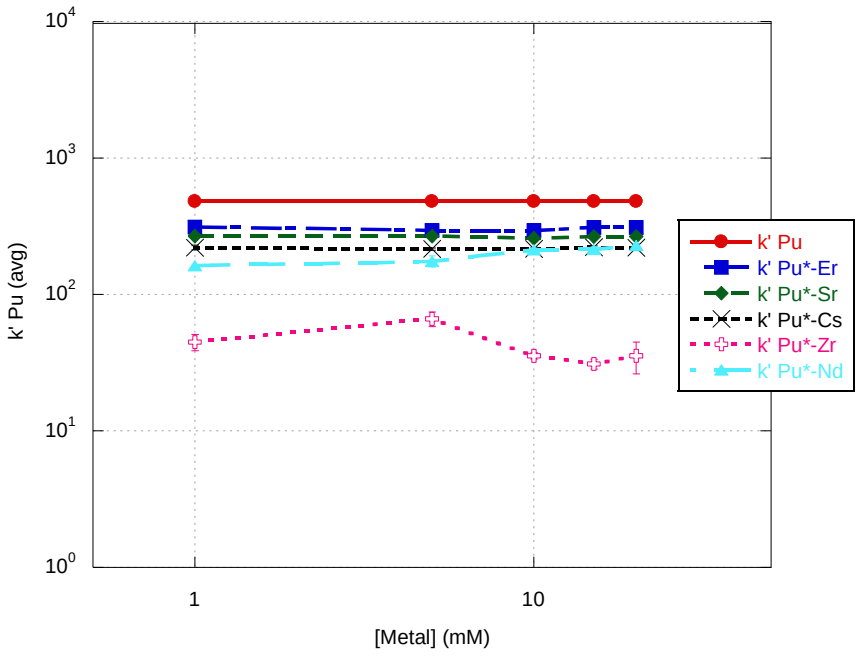

Figure 26. Used Fuel Component Effects on Pu Adsorption to DGA resin in 1 M HNO_3

Most of the used fuel components had little to no effect on the Pu adsorption across all metal concentrations, as seen in Figure 26. The only component which shows some interference effects is Zr, showing an order of magnitude decrease across all concentrations of $Zr(NO_3)_4$. Since there is no decrease in k' values with the increased amount of interference, it is necessary to see how Zr sorbs to fully understand the role it plays in this scenario, as seen in Figure 29. From the data seen in Figure 26, we can ascertain that $Pu(NO_3)_4$ has a very large affinity for DGA in comparison to most of the components in fuel, even when they are considerably in excess. This is good for loading conditions, as the adsorption of Pu will not be affected, but may lead to difficulties in elution if Pu is too strongly adsorbed. This is another reason investigation of possible reducing/oxidizing and complexing agents will be useful.

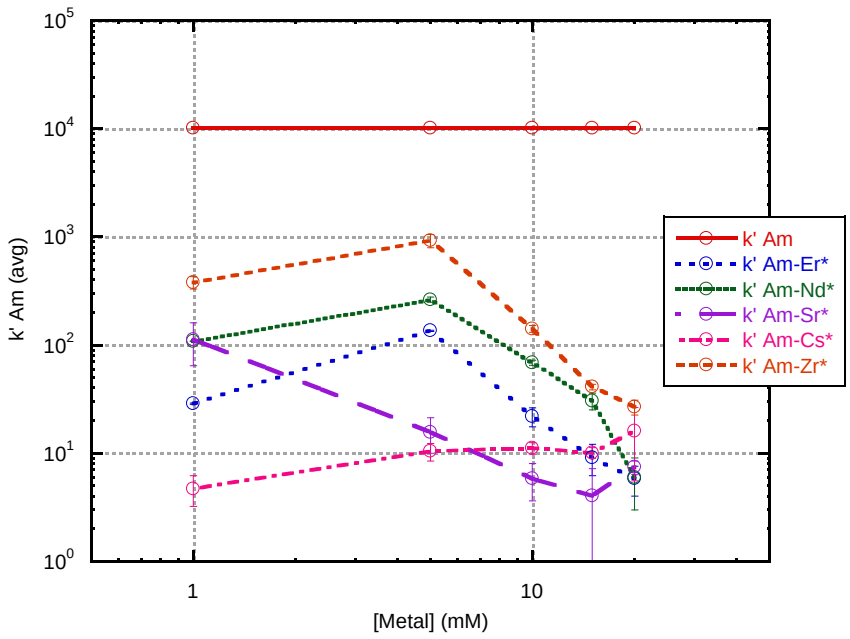

Figure 27. Used Fuel Component Adsorption in presence of Am to DGA resin in 1 M HNO_3

In the above graph, Figure 23, the k' values of the components mixed with Am are graphed versus the metal concentration in solution. The k' Am represents the adsorption of Am individually. This graph allows us to compare the various component affinities to one another. As expected, tri- and tetravalent metals have similar adsorption trends. In contrast, the mono- and divalent metals have different trends with increasing metal concentration. It seems there are multiple factors which influence the affinity trends seen. For instance, DGA's affinity for metals with an ionic radii between 80-120 pm is apparent since Cs has an ionic radii larger than 120 pm and has little to no affinity for the resin. Although, this is seen the ionic radii do not describe the rest of the affinity trends. If DGA preferred

a metals with smaller ionic radii the trend expected would be: Cs(I) (167 pm) < Sr(II) (118 pm) < Nd(III) (98.3 pm) < Am(III) (97.5 pm) < Er(III) (89 pm) < Pu(IV) (86 pm) < U(VI) (73 pm) < Zr(IV) (72 pm) < Mo(VI) (59 pm).[110,111]

Adsorption trends may also depend on charge density of the metals. If DGA preferred a metal with a larger charge density the trend expected would be: Mo(VI) > U(VI) > Zr(IV) > Pu(IV) > Er(III) > Am(III) > Nd(III) > Sr(II) > Cs(I).This order is also not seen; therefore, it is possible that the trend is due to a combination of the two factors.

Similar trends are seen in Figure 28 for the used fuel components in the presence of Pu as in the presence of Am. The only exception is that Zr affinity rises above the Pu affinity at 5 mM metal concentrations which would agree with the trend based on the charge density of the metal. Overall, due to the high k' values for tri- and tetravalent metals it is expected that out of the components studied they may have an effect on the actinide adsorption trends.

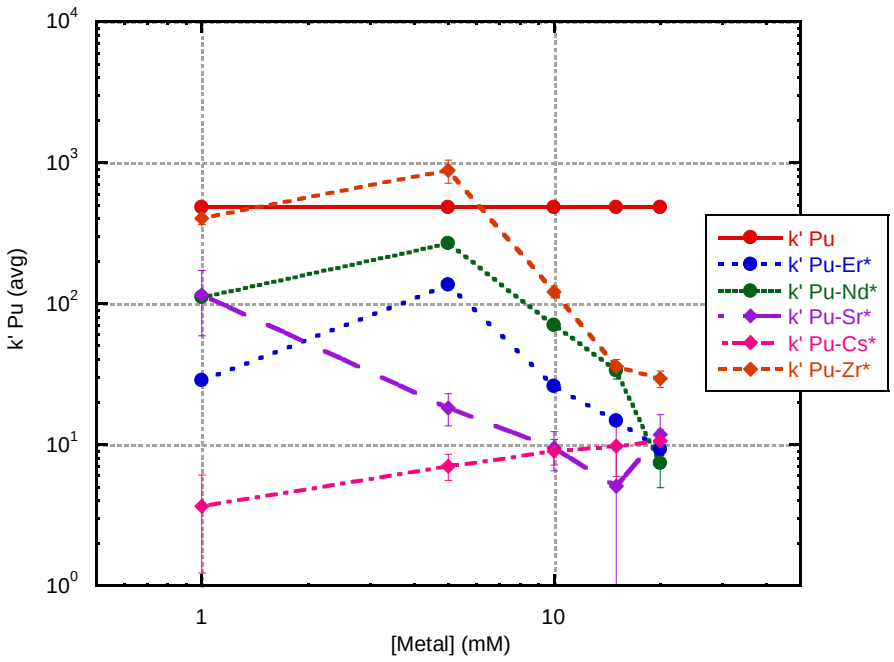

Figure 28. Used Fuel Component Adsorption in presence of Pu to DGA resin in 1 M HNO_3

Zirconium Effects

Even though in the fuel cycle the fuel is decladded prior to dissolution, which will decrease the amount of Zr found in the sample matrix, it is still necessary to consider Zr's effects on the adsorption, since it is a fairly abundant fission product. In Figure 29, the maximum capacity is reached around 5 mM Zr, k' = 10^3, after which there is a gradual decline of Zr adsorption. This decline is due to the amount of Zr increasing in the solution but the maximum capacity of the resin staying constant, giving a lower k' value. Therefore, it can be assumed that Zr has filled all the adsorption sites on the resin which explains the sharp

decrease in Am k' values. Zr seems to be adsorbing to the resin with similar trends independent of the various actinides present in solution. This is most likely due to the fact that the concentration of the actinides are below the detectable limit of the ICP-AES, which means that if the actinides do have an effect on Zr adsorption, it would not be detected. Therefore, $Pu(NO_3)_4$ most likely is having a stronger affinity for DGA than $Zr(NO_3)_4$ and is slightly decreasing Zr's k' values, but this is not detected due to the ICP-AES detection limit. The detection limit for Zr on the ICP-AES is typically ~1 ppm and the concentration of Pu(IV) less than 1 ppm therefore and changes on Zr adsorption due to Pu(IV) would not be detected.

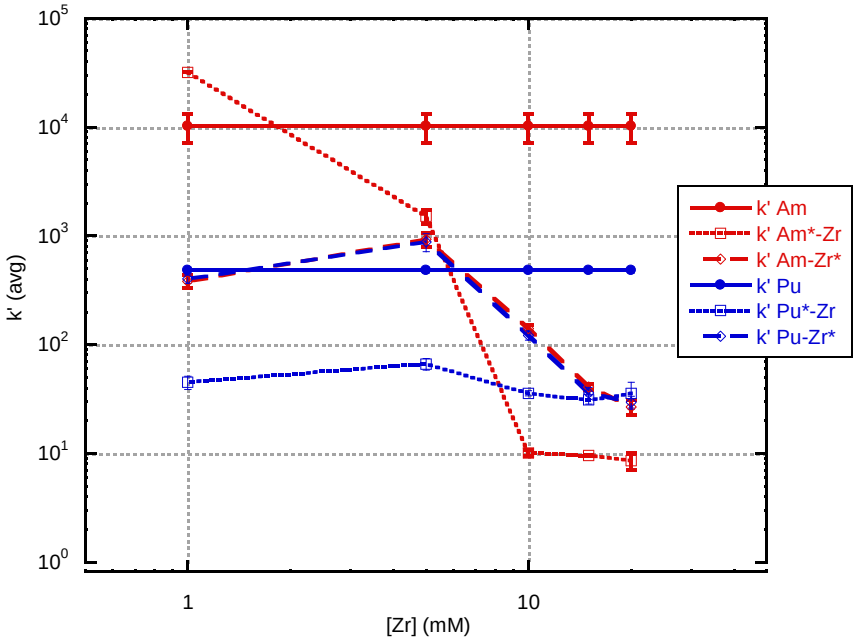

Figure 29. Zirconium Effects in 1 M HNO_3
The solid line represents Am or Pu k' values with no additional analyte in solution, the dotted line represents Am or Pu k' values with $Zr(NO_3)_4$ in solution, and the dashed line represents Zr k' values with Am or Pu nitrate in solution.

There appears to be a slight synergistic effect on Am for 1 mM Zr(IV) concentrations. It is still unclear why this may occur. It could be due to a salting out effect, where once capacity is exceeded, a Zr chemistry trend, such as formation of polyatomic species, that dominates the affinity trends but masks the typical salting out trends at higher Zr concentrations. In order to identify the increased Am adsorption more detailed studies below the resin capacity are needed.

For solutions with $[Zr]_{tot}$ = 1 mM, Zr hydrolysis occurs at molar acidity generating a Zr complex that is primarily the tetramer $Zr_4(OH)_8^{8+}$.[112, 113, 114, 115, 116, 117] It is also possible that these tetramers are complexing with Am at the 1 mM Zr(IV) concentration which either being retained on the resin or is caught in the filter. This seems unlikely since the tetramers are typically cations themselves and instead would typically complex with anions in order to neutralize. It is possible that the polymerized Zr is creating a salting out effect. The reason the effects of Zr changes with the changed Zr concentrations may due to the extent of aggregation which increases with the Zr concentrations.[117] These larger molecules may be causing different interactions

The sorption of these polymers would not be a typical complex of 1:3 $M^{+x}(NO_3)_x$:DGA since polymerized Zr usually forms complex polynuclear polymers.[112] Therefore, if Zr is polymerizing it would not be to the complexing with the adsorption sites. To fully explain the effects seen from Zr further investigation is still needed.

Even though the exact speciation in solution is unknown, it can be seen from these results that Am and Pu with Zr(IV) in 1 M HNO_3 should still efficiently load onto a column. It is also unclear where Zr(IV) will elute off the column in the presence of actinides.

Neodymium Effects

The lanthanides can be used as chemical analogs for the trivalent actinides due to the similar characteristics between them.[110] Therefore it is generally expected for the trivalent actinides and lanthanides to have similar adsorption trends. Lanthanide adsorption trends have been previously reported by Horwitz and Pourmand where the k' values exceed 10^3 for the entire nitric acid range.[29, 31] Therefore, it was expected that lanthanides would cause a large competition effect on Am due to their similar affinity for active sites on DGA resin. Even though the most abundant lanthanides in spent fuel are the lighter lanthanides, it can be assumed that they will have very similar chemistry with one another; whereas, the difference between light and heavy lanthanides may give rise to a different effect on actinide adsorption. For instance, a light lanthanide may have a higher affinity for DGA than Am but a heavy lanthanide may not. This difference would change the effect where a light lanthanide would cause a decrease in Am adsorption reaching near the capacity of the resin, whereas, there would be no seen effect on Am from the heavy lanthanide. For this reason, Nd was selected to represent the light lanthanides, Figure 30, and Er for the heavy lanthanides, Figure 31.

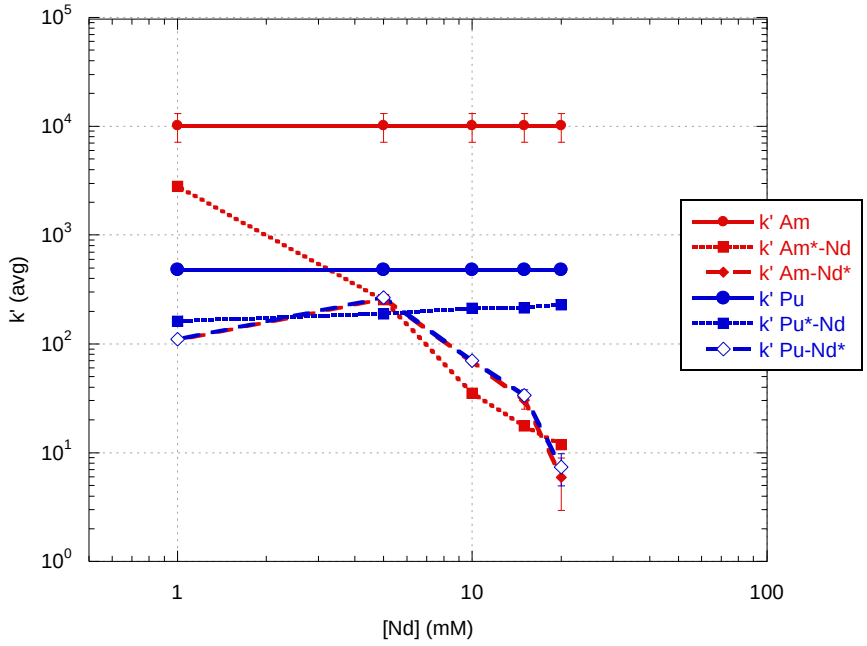

Figure 30. Neodymium Interference in 1 M HNO_3
The solid line represents Am or Pu k' values with no additional analyte in solution, the dotted line represents Am or Pu k' values with $Nd(NO_3)_3$ in solution, and the dashed line represents Nd k' values with Am or Pu nitrate in solution.

As seen in Figure 30, the capacity of the resin for Nd was determined to be close to 5 mM Nd; which is denoted by the sharp decrease in k' values after 5 mM. Since the actinides effects would be below the detectable limits of the ICP-AES, this Nd lines only represents the Nd characteristics. In the above graph, the four order of magnitude decrease in Am uptake is due to the competition for adsorption sites with Nd. It is clear that there is a competition occurring between Nd and Am/Cm because k' values for Nd are also suppressed from the previously reported value of 10^3. This also implies the affinity for Nd and Am/Cm is close to one another in 1 M HNO_3. Before the maximum capacity of the resin is

reached, it appears that Am has a higher affinity for DGA than Nd, with Am and Cm having a k' value 1.5 times larger than Nd.

As seen in Figure 30, across all the ranges of Nd there is no effect on Pu adsorption which is probably due to the higher affinity for Pu nitrate complex compared to the Nd nitrate complex. The loading characteristics of Am and Pu on DGA will not be affected as long as the sum of the lighter lanthanides and actinides is below the capacity of the column. Since the actinides and lighter lanthanides have similar characteristics on DGA, they will most likely elute off the column at similar times.

Erbium Effects

Similar interference trends are seen with the addition of Er, in Figure 31, but it does not have such a large effect on Am and Pu adsorption at lower Er concentrations. This was surprising due to the previously reported k' $>10^4$ in 1 M HNO_3 which is an order of magnitude greater than Nd.[29] Therefore, since it has higher affinity, it was expected to have a greater competition effect on the actinides. These results show a competition reaction between Er and Am, where the Am k' values decrease as the Er k' values increase proportionally to each other.

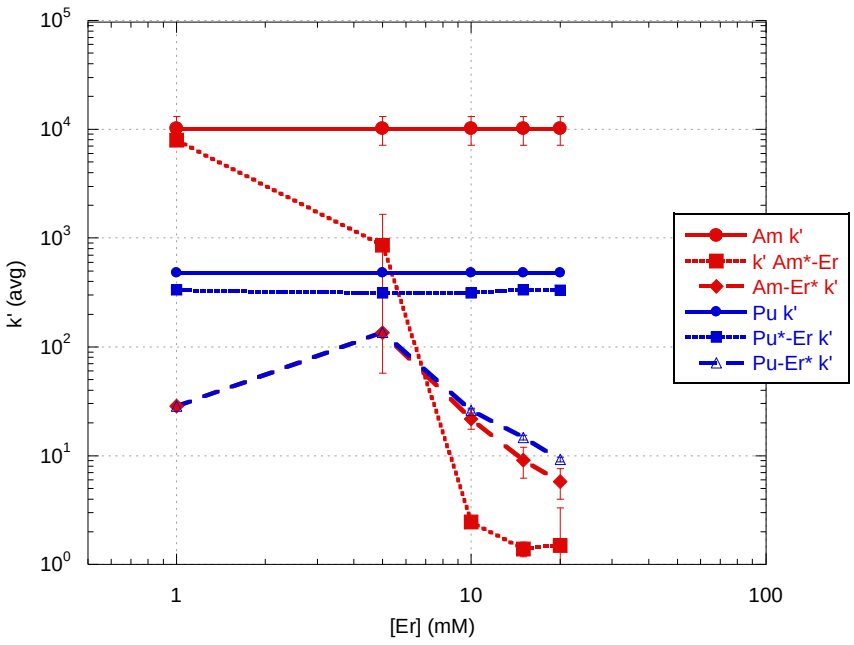

Figure 31. Erbium Interference in 1 M HNO_3
The solid line represents Am or Pu k' values with no additional analyte in solution, the dotted line represents Am or Pu k' values with $Er(NO_3)_3$ in solution, and the dashed line represents Er k' values with Am or Pu nitrate in solution.

The maximum capacity of DGA for Er is also apparent in this graph it is close to 5 mM Er. Once the maximum capacity of DGA is reached, the neutral Er nitrate complex is exceeding the capacity, and therefore it's k' values are decreasing due to the excess complex in solution. In comparing the trends for Er and Nd, it is apparent that they are very similar, implying that the same effects are occurring in both cases.

Strontium Effects

Sr adsorption in the presence of actinides and its effects on actinide adsorption in presented in Figure 32. The $k'_{Am\text{-}Sr^*}$ and $k'_{Pu\text{-}Sr^*}$ start out very high and reach a maximum capacity at 5 mM Sr. After the capacity is exceeded, the k' values for Sr gradually decrease. The high k' values for Sr were not unexpected, since Horwitz et al. reported Sr had shown high adsorption (k'~100) for nitric acid concentrations above 0.2 M.[29] The adsorption of Am and Pu does not seem to be affected, because the $k'_{Am^*\text{-}Sr}$ and $k'_{Pu^*\text{-}Sr}$ do not change in comparison to the k'_{Am} and k'_{Pu}. Since the actinide k' values are unaffected, it is probable that $Am(NO_3)_3$ and $Pu(NO_3)_4$ form a more favorable neutral complex with DGA than $Sr(NO_3)_2$.

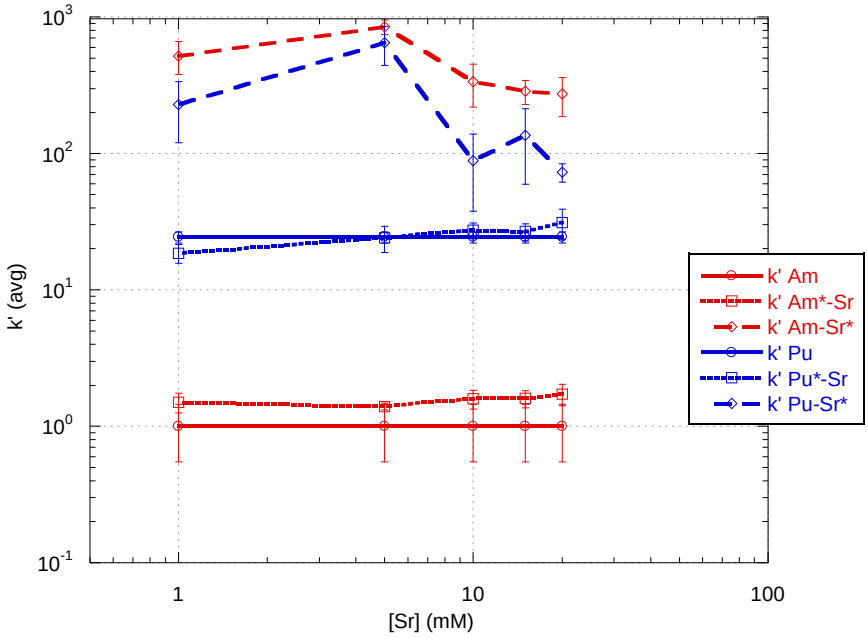

Figure 32. Strontium Effects on Am and Pu Adsorption on DGA resin in 1 M HNO_3
The solid line represents Am or Pu k' values with no additional analyte in solution, the dotted line represents Am or Pu k' values with $Sr(NO_3)_2$ in solution, and the dashed line represents Sr k' values with Am or Pu nitrate in solution.

Cesium Effects

Cesium nitrate was not expected to adsorb to the resin due to its monovalent state since Pourmand et al. reported no adsorption of Cs to DGA resin in nitric acid.[31] Since this study analyzed all metals in one study it is not a good representation for a more simple sample matrix, as studied here. Although in Figure 33, Cs unexpectedly has a k' value ~10 for all concentrations of Cs it does not show an effect on Am and Pu k' values. This means that Cs will not have any effect on Am or Pu adsorption, elution or stripping characteristics.

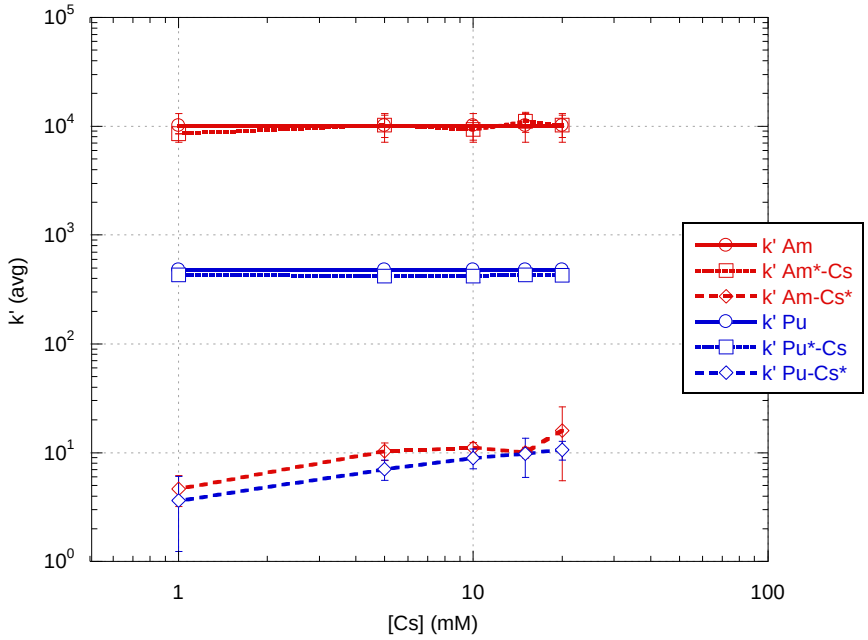

Figure 33. Cesium Effects on Am and Pu Adsorption on DGA resin in 1 M HNO_3
The solid line represents Am or Pu k' values with no additional analyte in solution, the dotted line represents Am or Pu k' values with $CsNO_3$ in solution, and the dashed line represents Cs k' values with Am or Pu nitrate in solution.

Technetium Effects

To study Tc interference on Am and Pu adsorption, it was essential to perform an alpha/beta discrimination on the LSC. This interference study was performed in 1 M HNO_3, where Tc has a k' value ~400. This provided plenty of room to detect a change in Tc adsorption. The adsorption of Tc in these systems, $k'_{Am\text{-}Tc^*}$ and $k'_{Pu\text{-}Tc^*}$, shows a lower k' value than found for pure Tc, see Figure 23, where the k' value was ~400. In Figure 34 the k' values ~150 for Am-Tc* and ~80 for Am-Pu*. The Am and Pu adsorption trends seem to be independent of Tc concentration, since they all stay constant across all activities of Tc. There

seems to be a slight increase of Am adsorption across all Tc activities. This may be due to the loss of alpha counts, based on the discrimination set point, from the alpha/beta discrimination which may exhibit a false synergism and further studies will be needed to identify the cause of these trends.

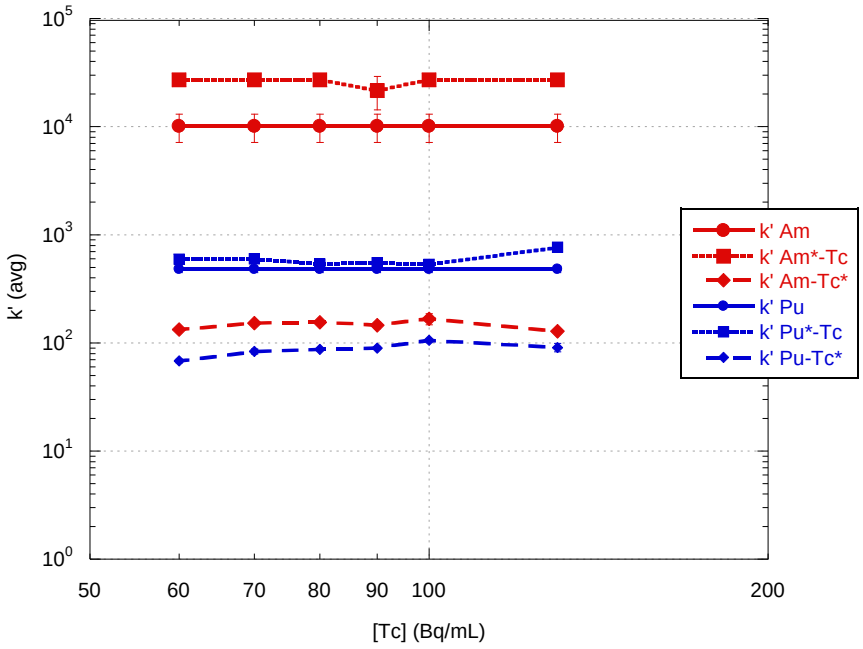

Figure 34. Technetium Effects on Am and Pu Adsorption to DGA in 1 M HNO_3
The solid line represents Am or Pu k' values with no additional analyte in solution, the dotted line represents Am or Pu k' values with NH_4TcO_4 in solution, and the dashed line represents Tc k' values with Am or Pu nitrate in solution.

Section 3.6 Hydrochloric Acid Results and Discussion

For the following studies on the possible effects of used fuel components the adsorption of Am and Pu was studied at 1 M HCl, because any synergistic, interference, or competition effects can still be easily distinguished since their k' values are not too close to detection limits The formatting of the graphs follows the same as previously described in Section 3.5.

In Figure 35, the largest effects on Am adsorption are seen in the presence of Zr, Nd, and Er in 1 M HCl. This was expected since DGA has been found to have a high affinity for those metals with a +3 or +4 charge and metals with an ionic radius between 80~120 pm in chloride matrixes.[31] Therefore, it was expected that Zr(IV), Nd(III), Er(III) would have some type of effect on the actinide adsorption. The lanthanides show similar trends in hydrochloric acid as was seen in nitric acid matrices, where the Am adsorption is suppressed with an increased concentration of lanthanide. Above 10 mM Er, the k' values for Am were below detectable limits and therefore not reported in Figure 35. The reasoning behind these results is further discussed in the following sections.

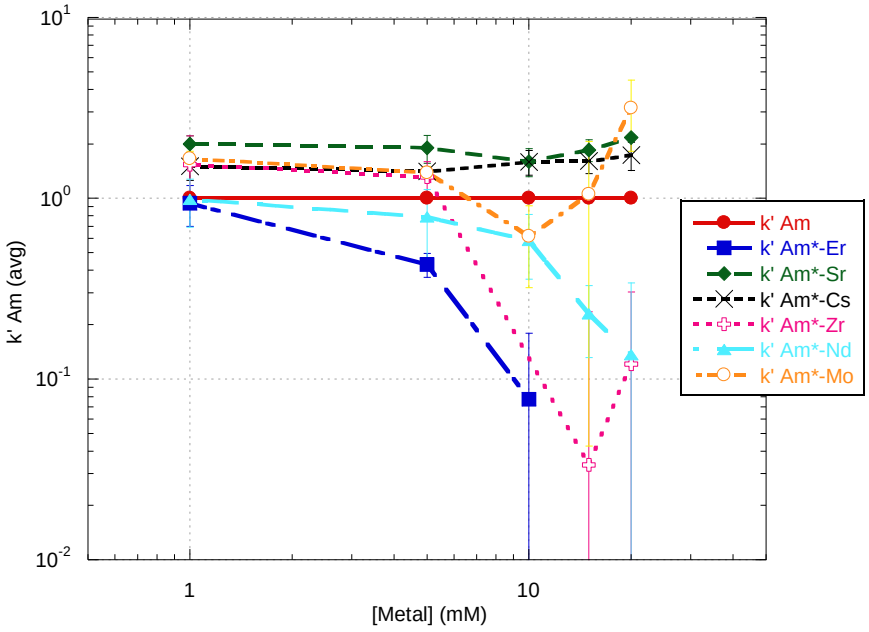

Figure 35. Spent Fuel Component Effects on Am Adsorption in 1 M HCl

In Figure 35, Cs, Sr, and Mo show the least effect on the adsorption of Am. The minimal affects from the addition of Cs and Sr was expected since DGA has been found to have a low affinity for those metals with a +1 or +2 charge.[29] At about 1 mM metal, there seems to be little to no interference effects seen on both Am and Cm. So, as long as the capacity of the resin is not exceeded for metals of similar oxidation states the loading characteristics of DGA should not be affected.

In Figure 36, the majority of the components show little to no effect on Pu adsorption. This is especially the case for metals with the oxidations states +1, +2, +3 in 1 M HCl, since there was no change on Pu k' values observed in comparison with the k' values of pure Pu solution's. There is an effect from the presence of the Mo(VI) metal ion which evenly decreases the Pu adsorption over all concentrations of Mo but this effect does not change with the increased concentrations of Mo, as would be expected. These effects seen will be explained in further detail later after the graphs for the component effects on Am and Pu, Figure 39-45.

The results seen in the below Figure 36 imply that in the presence of Mo there will be a change in the loading characteristics for Pu in 1 M HCl. Therefore, it will be important to understand how to adapt the matrix to reduce these effects, if a hydrochloric loading matrix is desired. The effects on implementation into a reprocessing stream are discussed following the individual Mo component graph.

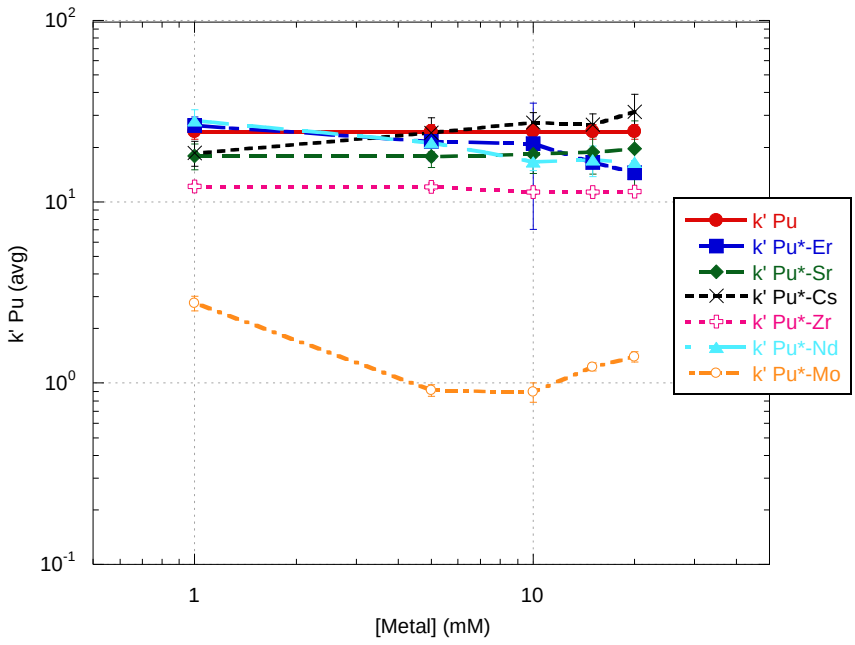

Figure 36. Used Fuel Component Effects on Pu Adsorption to DGA resin in 1 M HCl

The adsorption of used fuel components in the presence of Am or Pu are graphed against the concentration of the metal concentration. The solid line in the following two graphs, Figure 37 and 34, represents the k' value for Am or Pu individually in 1 M HNO_3 or HCl. Zr has the highest affinity for DGA below capacity. Above capacity, especially in great excess, all k' values start to converge. Cs has no detectable adsorption to DGA in 1 M HCl.

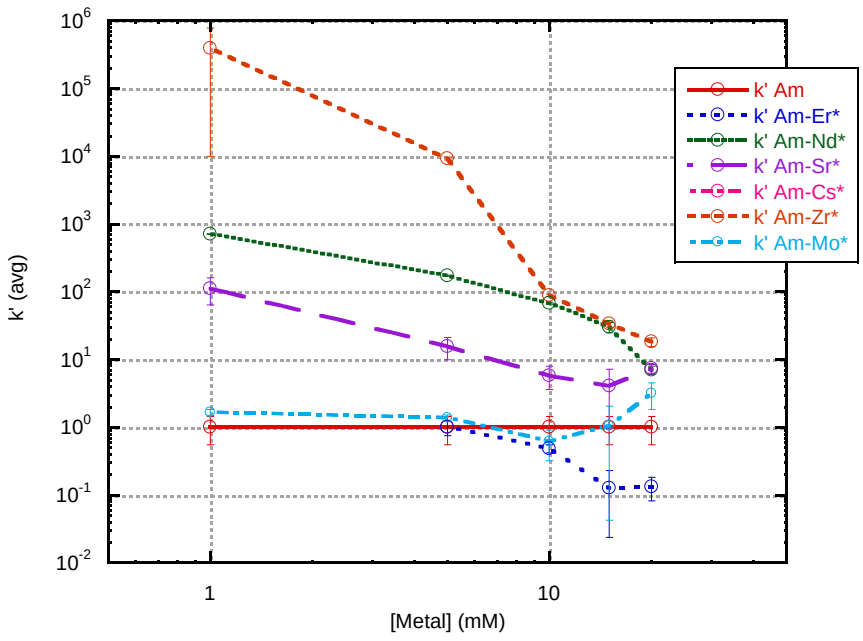

Figure 37. Used Fuel Component Adsorption in presence of Am to DGA resin in 1 M HCl

There does not seem to be any discernable relation between the used fuel components adsorptions and their various factors, such as ionic radii, charge density, ionic strength, and activity of the ions. There may be a combination of these factors influencing the effects seen in hydrochloric matrices. Similar adsorption trends, with the exception of $k'_{Pu\text{-}Sr*}$, are seen between the components in presence of Am and Pu. Therefore, it is expected that Am and Pu have little to no effect on the components' adsorption.

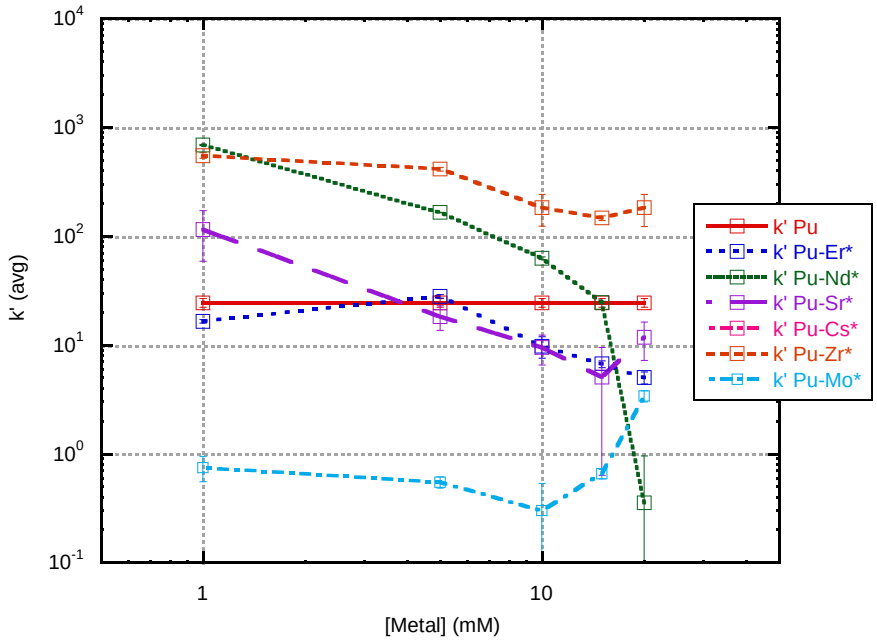

Figure 38. Used Fuel Component Adsorption in presence of Am to DGA resin in 1 M HCl

Zirconium Effects

In Figure 39, the k' values of Am and Pu with Zr in their presence and Zr in the presence of Am and Pu are graphed in respect to the concentration of Zr in solution. The adsorption of a pure Am and Pu solution is graphed in order to have an easy comparison and identification of the effects of Zr. As Zr concentration increases, the k'_{Zr} decreases sharply for Am until 10 mM and then it levels off. For the analysis of Pu and Zr, the maximum capacity of Zr is noted by the $k'_{Pu\text{-}Zr^*}$ peak at 5 mM Zr. Above 5 mM Zr, as the Zr concentration increases in the presence of Pu, the $k'_{Pu\text{-}Zr^*}$ gradually decreases as well which is most likely due to exceeding the capacity of the resin. The difference in $k_{Am\text{-}Zr^*}$ and $k'_{Pu\text{-}Zr^*}$

may be due to the different interactions based on the oxidation states, this difference was also seen for $k'_{Am\text{-}Zr^*}$ verus $k'_{Pu\text{-}Zr^*}$ in 1 M HNO_3. Therefore, this supports the possibility of Am and Zr interacting in a manner which changes the Zr adsorption to DGA. The adsorption of Am and Pu will most likely not be effected by the presence of Zr in 1 M HCl unless the capacity of the resin is exceeded.

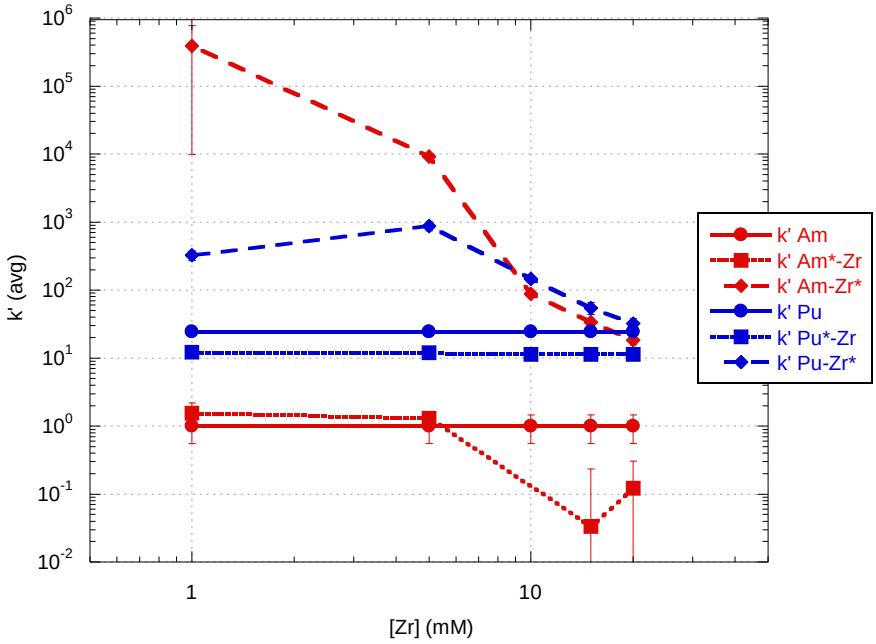

Figure 39. Zirconium Effects on Am and Pu Adsorption to DGA resin in 1 M HCl
The solid line represents Am or Pu k' values with no additional analyte in solution, the dotted line represents Am or Pu k' values with $Zr(Cl)_4$ in solution, and the dashed line represents Zr k' values with Am or Pu chloride in solution.

For Am adsorption in presence of 1 and 5 mM Zr, the $k'_{Am^*\text{-}Zr}$ are very close to k'_{Am} values but above 5 mM Zr there is a decrease in Am adsorption, which nears the limit of detection. The decrease seems to correlate to Zr concentrations since the suppression of Am sorption occurs once Zr's maximum

capacity for the resin is exceeded. The effect is not seen for 1 and 5 mM Zr and it is therefore not proportional to the amount of $ZrCl_4$ added, this means it is unlikely due to salting out or a more advantageous Am-Zr co-complex. The change in k'_{Am^*-Zr} values may be due to a competition reaction between Am and Zr where $ZrCl_4$ has a higher affinity for DGA than $AmCl_3$. Further evidence of this occurring is that the Am decrease only occurs after Zr's maximum capacity is reached; hence, limiting the sites for Am to adsorb to and lowering its k'_{Am^*-Zr} values. In 1 M HCl, the presence of Zr will affect the adsorption of Am if the maximum capacity of the column is exceeded, but its effect on the elution characteristics is still unclear. Since k'_{Am-Zr^*} is much higher than k'_{Am^*-Zr}, Zr should elute off after Am in 1 M HCl.

Neodymium Effects

The following graph, Figure 40, shows that Nd has high adsorption at low concentrations, but as the concentrations of Nd increases, the k' values for Nd decrease. The decrease of k' values at higher concentrations of Nd are most likely due to the fact that the capacity of the resin has been exceeded. No effect is seen on Nd from the adsorption of Pu or Am due to the fact that the amounts of Pu and Am that could impact Nd concentrations in the eluent was below the ICP-AES detection limit.

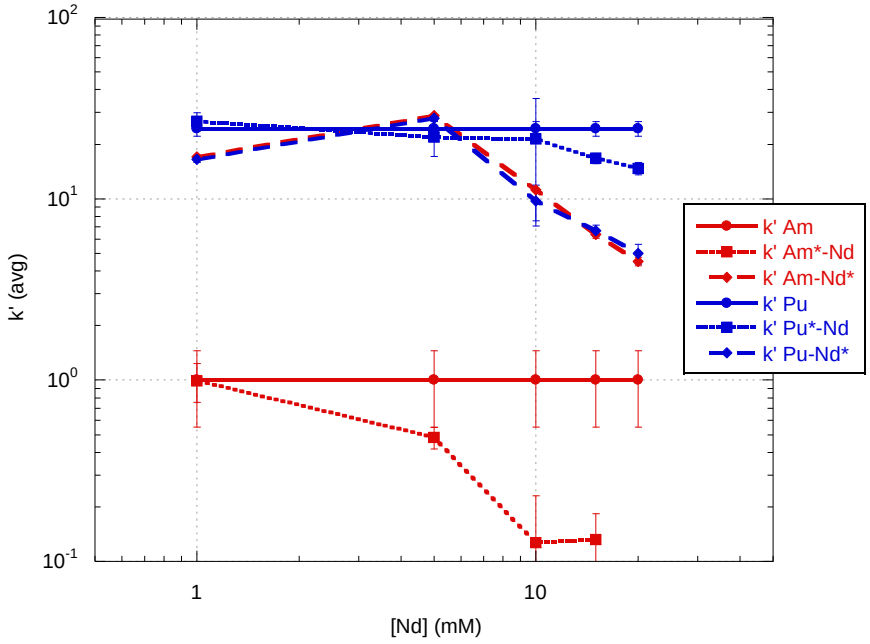

Figure 40. Neodymium Effects on Am and Pu Adsorption to DGA resin in 1 M HCl
The solid line represents Am or Pu k' values with no additional analyte in solution, the dotted line represents Am or Pu k' values with $Nd(NO_3)_3$ in solution, and the dashed line represents Nd k' values with Am or Pu chloride in solution.

Nd has little to no effect on Pu adsorption, but the adsorption of Am is suppressed to the point of being either close to the detection limit for most $k'_{Am^*\text{-}Nd}$ values or below the detection limit for 20 mM Nd and therefore not reported. The suppression of Am was expected due to Nd's and Am's similar charge density. Unexpectedly, there is a fair difference, above an order of magnitude, in the k' values for Nd compared to Am, this shows the preference towards Nd over Am exhibited by the resin in 1 M HCl. A higher adsorption of heavy lanthanides over Am adsorption has been previously reported for heavy lanthanides in hydrochloric matrices by Pourmand et al., but not for lighter lanthanides such as

Nd.[31] This difference may lead to the ability to separately elute off the lanthanides from Am and Cm.

Erbium Effects

The Er interference curves are very similar to those seen above for Nd. This was expected, since their chemical characteristics are very similar. The main difference between these two graphs is in the magnitude of the k' values for Er in comparison to Nd. Neodymium has a k' value range from ~8 to 20, while Er has a range of ~1 to 1000. Since there is a difference in affinity for light lanthanides in comparison to heavy lanthanides they may elute off in different fractions. As stated in the Nd discussion, a higher adsorption of heavy lanthanides was expected since Pourmand et al. studied them in hydrochloric matrices.[31] This difference may be due to the difference in charge density and being in a chloride matrix.

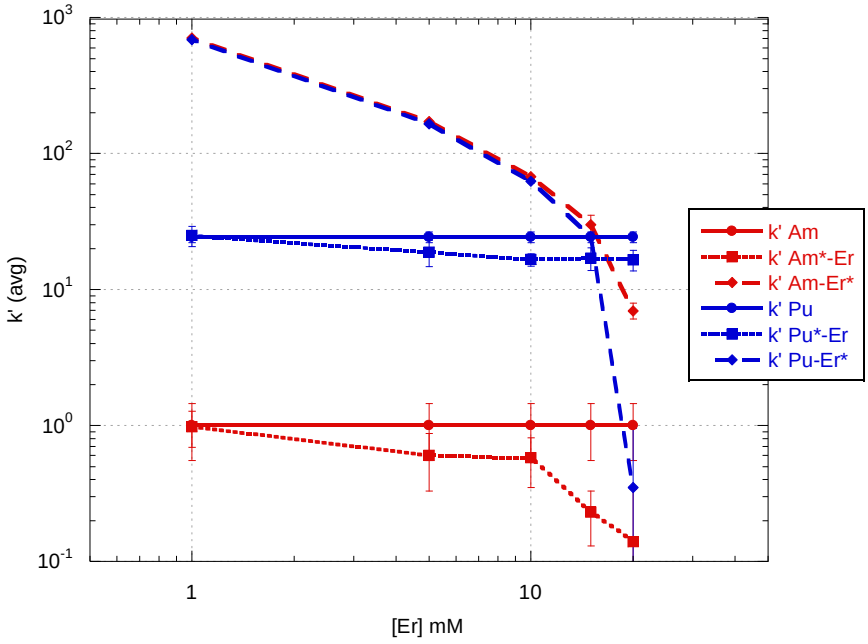

Figure 41. Erbium Effects on Am and Pu Adsorption to DGA resin in 1 M HCl
The solid line represents Am or Pu k' values with no additional analyte in solution, the dotted line represents Am or Pu k' values with $Er(NO_3)_3$ in solution, and the dashed line represents Er k' values with Am or Pu chloride in solution.

The Pu uptake is once again unaffected by the presence of Er, but the Am uptake declines up to an order of magnitude with the increased concentrations of Er, as seen in Figure 41. At 1 mM Nd and Er, the $k'_{Am\text{-}Er^*}$ and $k'_{Pu\text{-}Er^*}$ is about two orders of magnitude larger than $k'_{Am\text{-}Nd^*}$ and $k'_{Pu\text{-}Nd^*}$. This supports Horwitz et al.'s results showing Er having a higher affinity for DGA than Nd.[29]

There may be a salting out effect which counteracts DGA's attraction with the addition of $ErCl_3$ salt which keeps it in the mobile phase rather than extracting with the ligand and therefore decreases the adsorption with its increased concentration. Another interesting feature of Figure 41 is that Er seems to reach

maximum capacity prior to 5 mM which was not expected. This may be simply due to an error in the weight of the resin used.

Molybdenum Effects

In Figure 42, the adsorption of Mo with actinide and adsorption of actinide with Mo(VI) is graphed to see the relationship between them. As expected, the Mo adsorption doesn't show any change with respect to the actinides. The adsorption of Mo is not high enough to typically cause much competition effects. Therefore, the depressed Pu k' values by an order of magnitude across all Mo concentrations and the seemingly slight increase in the Am k' values were unexpected. The k' values for Am and Pu are very similar in trend and magnitude.

Recently Lee et al. studied the adsorption of Mo(VI) complexes formed in hydrochloric acid to ion exchange columns.[118] In these studies, concentrations of 1 to 9 M HCl solutions were loaded onto AG 1-X8 and Diphonix resin the amount of Mo complexes loaded on these columns gave information on the charge of the species formed. At 1 M HCl, which pertains to the studies in Figure 42, near 100% of the Mo species loaded onto Diphonix, supporting the formation of cationic Mo species $H_6Mo_2O_8^{2+}$ $(Mo_2O_2H(OH)_6^{2+})$ and $H_3MoO_4^+$ and anionic species were not formed until 3 M HCl.[119] The changes with the addition of $AmCl_3$ and $PuCl_4$ may be causing the change in Mo species or due to Mo being in large excess in comparison to Am and Pu the smallest amount of anion species forming may be creating a co-complex. Although it seems unlikely, it is

possible that Am and Pu may be forming a co-complex with Mo. Since the k'_{Am^*-Mo} and k'_{Pu^*-Mo} are very close to the k'_{Am-Mo^*} and k'_{Pu-Mo^*}, including the error bars, it is possible that this commonality is showing the co-complex. If the formation of the co-complex is preferred over complexation with DGA, it would be expected that both the actinide and Mo k' values would be close to one another which is seen. Further studies will be necessary to fully identify the complexes occurring in these systems.

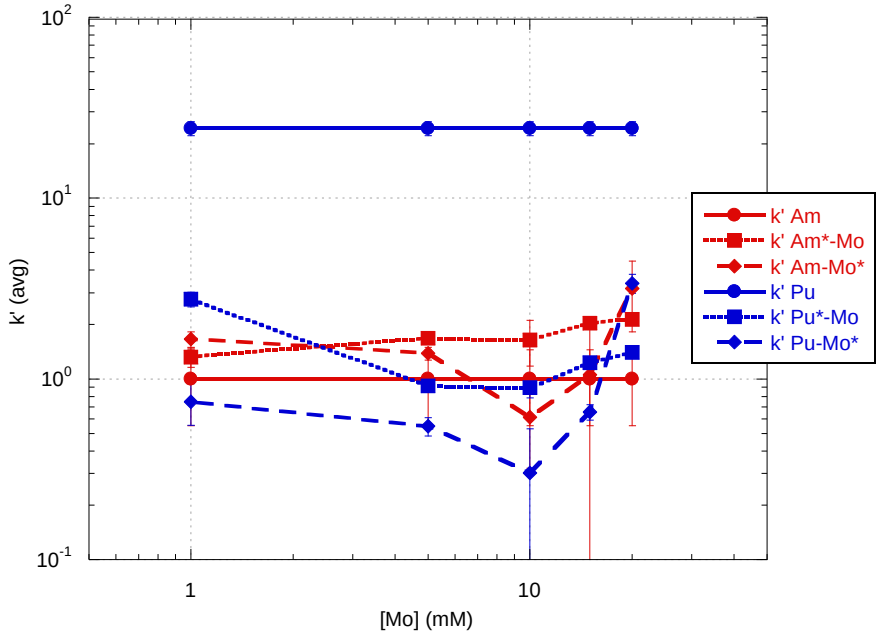

Figure 42. Molybenum Effects on Am and Pu Adsorption to DGA resin in 1 M HCl
The solid line represents Am or Pu k' values with no additional analyte in solution,
the dotted line represents Am or Pu k' values with $MoCl_6$ in solution,
and the dashed line represents Mo k' values with Am or Pu chloride in solution.

There is some variance in the Mo k' values which may be due to variations in the complexes formed. Overall, it is expected that Mo will have an effect on

actinide adsorption and elution in 1 M HCl, but since Mo has a much lower atomic mass than the actinides, it should not interfere with an ICP-MS analysis.

Strontium Effects

The adsorption of Sr has been previously studied to have k'_{Sr} ~1 in 1 M HCl.[29, 30] As can be seen in Figure 43, the Am-Sr* and Pu-Sr* adsorption reaches its highest k' value of ~100 at 1 mM Sr. This variance may be due to the presence of Am and Pu. As the Sr concentration increases, the k' values for Am-Sr* and Pu-Sr* both decrease. The Am adsorption is affected by the amount of Sr present in solution. With the increased concentration of Sr there is a gradual decrease of Am adsorption. The effect of Sr is not great enough to affect the Am loading when Sr is in excess, but may cause broader elution bands for Am. As long as Sr is below the capacity of the resin, little to no changes on Am's and Pu's adsorption, elution, and stripping characterization should be seen.

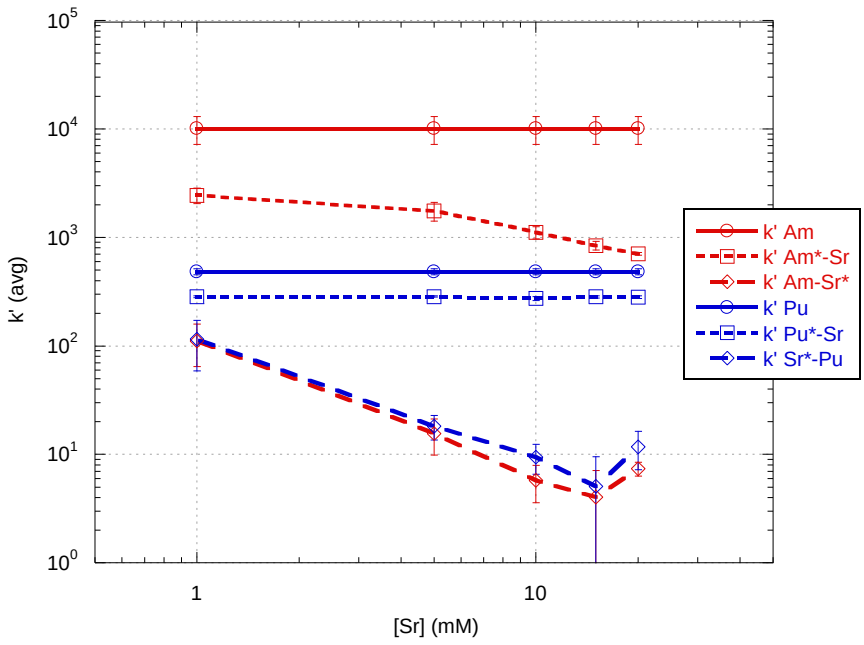

Figure 43. Strontium Effects on Am and Pu Adsorption to DGA resin in 1 M HCl
The solid line represents Am or Pu k' values with no additional analyte in solution, the dotted line represents Am or Pu k' values with $SrCl_2$ in solution, and the dashed line represents Sr k' values with Am or Pu chloride in solution.

Cesium Effects

Cesium was previously studied by Pourmand et al. and was determined to have no adsorption to DGA resin in any hydrochloric matrices.[31] There was no Cs adsorption detected in 1 M HCl and therefore, the $k'_{Am\text{-}Cs*}$ and $k'_{Pu\text{-}Cs*}$ was not reported in Figure 44 below. With the error bars in consideration between k'_{Am}, k'_{Pu} and $k'_{Am*\text{-}Cs}$, $k'_{Pu*\text{-}Cs}$ there is no change to the adsorption of Am and Pu with the increased concentration of $CsNO_3$; therefore, Cs will not affect actinide adsorption characteristics to DGA in chloride matrices.

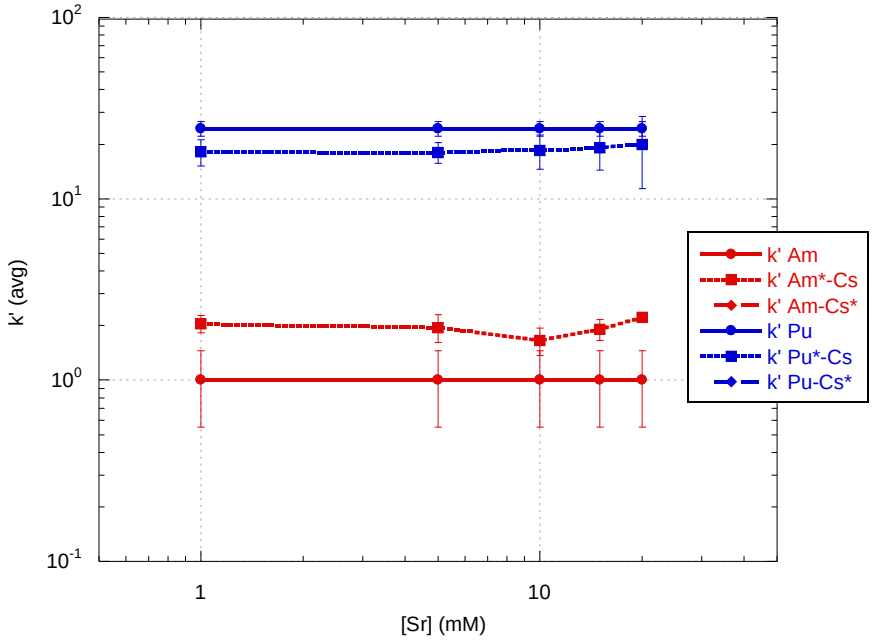

Figure 44 Cesium Effect on Am and Pu Adsorption to DGA resin in 1 M HCl
The solid line represents Am or Pu k' values with no additional analyte in solution,
the dotted line represents Am or Pu k' values with CsCl in solution,
and the dashed line represents Cs k' values with Am or Pu chloride in solution.

Technetium Effects

Technetium shows synergistic effects for Am, where the k' values have increased by an order of magnitude (~1 to ~10). This was expected due to the fact that Iron(III) Chloride formed a co-complex with Am, as reported by Horwitz et al., and has a higher affinity than Am alone on DGA.[29] Since Tc pertechnetate (TcO_4^-) tends to complex with a variety of cations, it was suspected to act similarly to $FeCl_4^-$. If there is a co-complex between Am and TcO_4^-, their k' values should show similar trends but not necessarily the same magnitude, since the ratio of Am and TcO_4^- may not be consistent for all Tc activities because the

amounts of Tc and actinides are very close to one another, it is possible that the ratio of Am and TcO_4- is 1:1 in these Tc concentrations. Also, with the increased amount of TcO_4^- there was an increase in the actinide adsorption, which supports the idea that the presence of TcO_4^- gives a synergistic effect and that the ratio may be 1:1. To thoroughly investigate this possibility, a study varying the amount of Am and keeping Tc the same would be useful in further identifying the ratio. Also, if there truly is a co-complex, the interaction between Am and TcO_4^- would slow down the kinetics of the reaction in comparison to $AmCl_3$; therefore a kinetic study would be able to clarify how TcO_4^- is causing this effect.

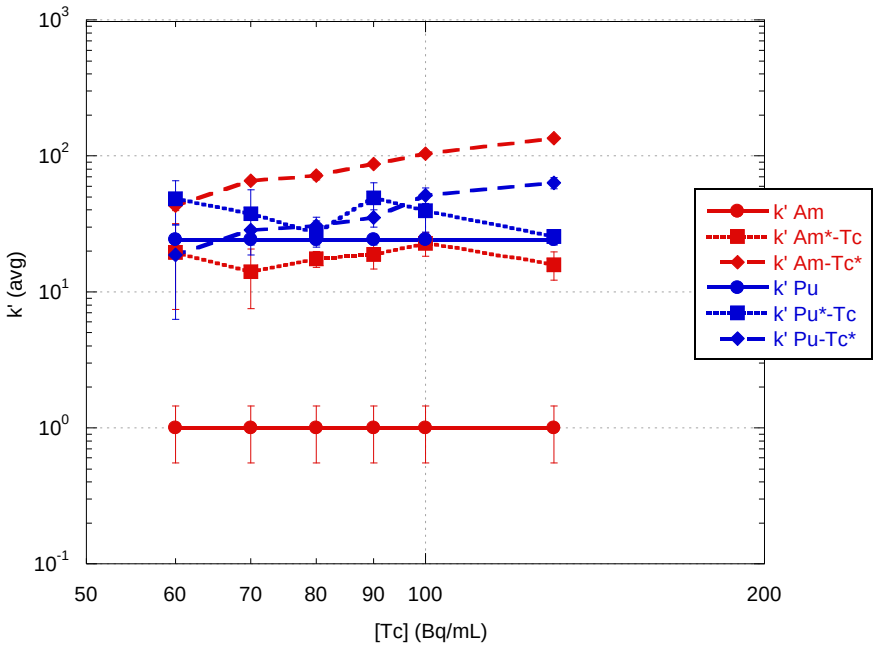

Figure 45. Technetium Effects on Am and Pu Adsorption to DGA resin in 1 M HCl
The solid line represents Am or Pu k' values with no additional analyte in solution, the dotted line represents Am or Pu k' values with NH_4TcO_4 in solution, and the dashed line represents Er k' values with Am or Pu chloride in solution.

The Pu adsorption is unaffected by the presence of Tc and is still found to have a k'~10. Since the synergistic effects seem to be exclusive to only trivalent actinides, this may represent the effects of steric hindrance imposed by DGA making a Pu and TcO_4^- co-complex unfavorable.

Section 3.7 Concluding Remarks

The largest effects seen on Am adsorption to DGA resin in nitric media are due to the presence of excess Zr, Nd, and Er. There is little to no effect on Pu adsorption across all concentrations of the metal components in nitric acid, with an exception of Zr which decreases the Pu adsorption by less than an order of magnitude. The Zr effects are possibly due to polymerization; whereas, the lanthanides have a competition reaction with Am and Cm for the adsorption sites on DGA. The same trends were seen for Am in hydrochloric acid, but for Pu the only metal component which effected the adsorption was Mo(VI). This may be due to the complex oxyanion clusters forming.

Tc has a synergistic effect on the adsorption of trivalent actinides in hydrochloric matrixes. Since an Am/Tc co-complex will have different kinetics and is most likely slower, elution band broadening may occur. This band broadening may cause the elution or stripping phase to increase in volume and hence increase separation time. Further studies, are needed to identify the Am/Tc ratio and kinetics.

Although there are effects seen on Am and Pu adsorption to DGA, they are typically only seen after the capacity of the resin has been exceeded.

Therefore, as long as separations are run under capacity, there should be little to no effects from the components studied, with the exception of Zr in nitric and Mo and Tc in hydrochloric acid. The loading characteristics of Am and Pu on DGA resin in nitric acid are not expected to change, but the elution characteristics may vary in either nitric or hydrochloric acid.

Chapter 4. EFFECTS OF USED FUEL COMPONENTS ON ACTINIDE ADSORPTION TO UTEVA RESIN

Section 4.1 Abstract

As seen in Table 1, in a dissolved used fuel the U concentration is going to largely exceed the concentrations of Am, Pu, and U. Therefore, it could be beneficial to implement an extraction chromatography column prior to DGA resin which is selective specifically towards U. This UTEVA column would allow smaller DGA column size and possibly lower total volumes needed for sufficient separations to be achieved. For these reasons, UTEVA resin is characterized in this thesis in order to develop rapid separations of Am, Pu, and U from used fuel from reprocessing waste streams. In this chapter, first the methodology utilized to ensure reliable and reproducible adsorption studies for Am, Pu, and U. All these studies are discussed in the following sections.

Due to the complexity of the matrices found in reprocessing waste streams the adsorption characteristics of the elements may not stay the same as previously determined. Thus, the main part of this chapter describes the effects that result from the addition of some of the more abundant used fuel consitutents, on Am, Pu, and U adsorption to UTEVA resin, in nitric and hydrochloric acid. Interference and synergistic effects are seen in in the presence of mg/L quantities of various metals in 1 M HNO_3 and HCl. The effects of Cs, Sr, Nd, Er,

Zr, and Mo on Am, Pu, and U adsorption and separation will be discussed in detail.

Section 4.2 Materials and Methods

Batch Contact Method

Batch contact studies were performed in separate M^+-Am, M^+-Pu, and M^+-U batches with five replicates to individually analyze the spent fuel components' interference on Am, Pu, and U uptake. To wet the resin, 50 mg of UTEVA resin was contacted with 0.5 mL of 1.45 M HNO_3 or HCl and placed on a shaking table for 1 hour, and allowed to sit. After the resin was wetted, 0.5 mL of 1.45 M HNO_3 solution containing either 3, 15, 30, 45, or 60 mM metal (Cs, Sr, Nd, Er, and Zr), and 0.5 mL of a standard consisting of 0.1 M HNO_3 or HCl with 75-100 Bq/mL of Am-241, Cm-244, Pu-239, or U-233 were added. These samples were agitated for 1 hour to ensure equilibrium was reached. Separation of the liquid from the resin beads was achieved by transferring the liquid to a PTFE filtered 3 mL syringe. Volume, radioisotope and acid concentrations were kept constant and only the metal analyte concentrations were varied.

Reagents

The extraction chromatography resin UTEVA was obtained from Eichrom Technologies, Inc. Nitric and hydrochloric acid stock solutions, listed in the previous chapter in Table 7, were prepared from ACS reagent grade acid (Sigma-Aldrich) using deionized water with a resistivity of 18.2 Megaohms from a

Cascada system manufactured by Pall Corporation. These stock solution concentrations were chosen based off of the desired final concentrations, seen in Table 7, after the addition of the 0.5 mL of 0.1 M acid radionuclide standard.

The Am-241, Cm-244, and Pu-239 stock solutions of activities between 75 – 100 Bq/mL in 0.1 M nitric or hydrochloric acid were obtained from Isotope Products Laboratories. Metal solutions of 3 – 60 mM and 1 – 100 ppm ICPAES standards were prepared from $Sr(NO_3)_2$ (Alfa Aesar, ACS, 99%), $CsNO_3$ (Sigma-Aldrich, 99%), $Nd(NO_3)_3$ (Sigma-Aldrich, trace metal basis, 99.9%), $Er(NO_3)_3{\cdot}6H_2O$ (Sigma-Aldrich, 99.9%), and $Zr(NO_3)_4$. For the nitric acid matrices, the nitrate salts were dissolved directly in 1.45 M HNO_3. For the hydrochloric acid matrices, these metals salts were converted to the chloride system by dissolving the salts in concentrated hydrochloric acid, brought to dryness, which was repeated three times and finally reconstituted in 1.45 M HCl.

Measurements

Samples of Am-241, Cm-244, and Pu-239 were measured either on a Tri-Carb 2800TR or a Tri-Carb 3100TR scintillation counter in polypropylene vials by taking a 0.9 mL aliquot of the filtrate and added 15 mL of Ultima Gold AB cocktail. The radiotracers were measured for up to an hour or until the one sigma counting error (10,000 counts) was reached. Non-radioactive metal concentrations were determined on an iCAP 6500 ICP-AES Spectrometer (Thermo Scientific). The Elan DRC II Inductively Coupled Plasma-Mass

Spectroscopy was used to analyze for Cs and any metals or replicates with concentrations below the ICP-AES detection limit.

Section 4.3 Methodology

In order to ensure the batch contact study method is offering an accurate representation of the analyte's adsorption, the amount of liquid adsorbed by the resin needs to be taken into account to give the proper volume correction factor. Certain resins have a specific affinity for acid which can result in a preferential adsorption of the acid in comparison to the water, just as DGA adsorbed nitric acid found in the previous chapter. Therefore it was essential to investigate the amount of nitric and hydrochloric adsorbing to UTEVA in varying concentrations in order to determine the proper density to use. In the studies below, each data point represents the average of three replicates and the error bars is the deviation between those replicates.

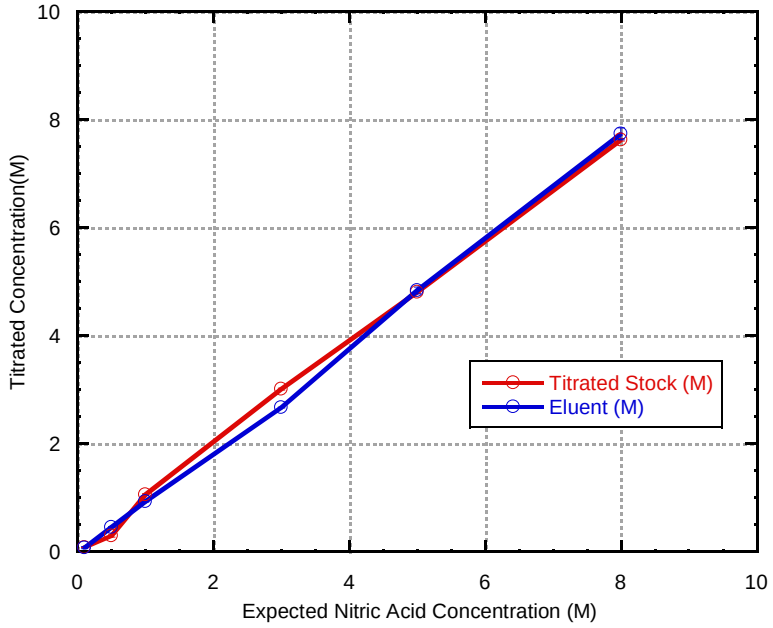

Figure 46. Nitric Acid Concentrations in Stock vs Eluent Solutions

Based on Figure 46 (above) and 47 (below), there does not appear to be any change in the nitric or hydrochloric acid concentrations after contact with UTEVA resin. The rinses were titrated as well and showed no signs of acid. Therefore, it can be assumed that UTEVA does not adsorb nitric or hydrochloric acid and the stock solution density can be used to determine the volume correction factor.

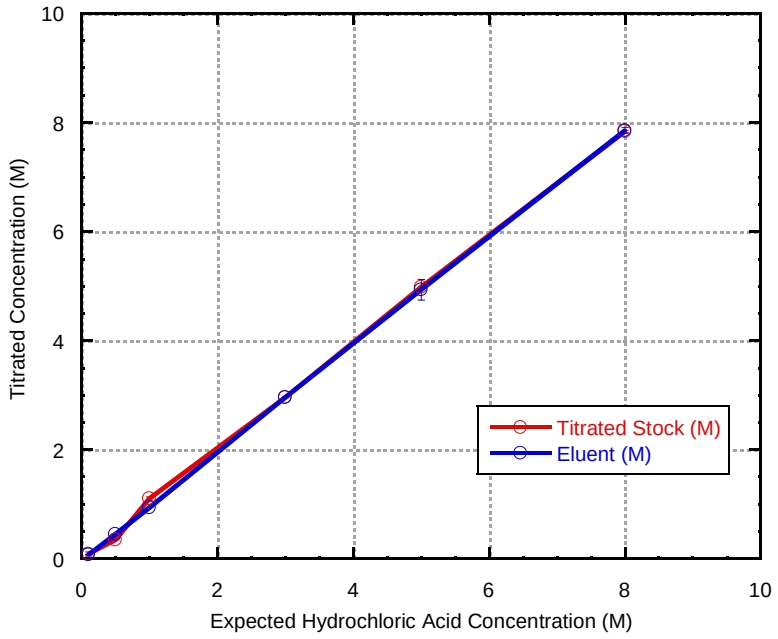

Figure 47. Hydrochloric Acid Concentrations in Stock vs Eluent Solutions

Since it is possible that with varying concentrations of acid the amount of liquid being retained by the resin could change, the mass percentages of retained acid solutions retained were calculated and are presented in Figure 48. Considering the error present, there seems to be no change in the amount of acid retained with the change of acid concentration. Therefore, the same mass percent of acid is retained for all acids and concentrations and the average of all the values was used to determine the volume eluted.

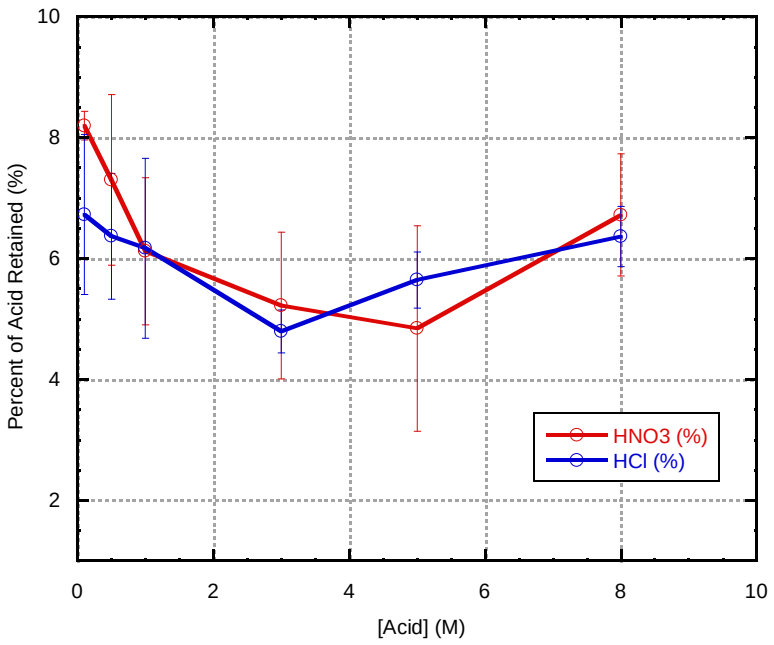

Figure 48. Percentage of the Mass of Acid Retained on UTEVA

The adsorption of Am, Cm, Pu, and U from varying concentrations of nitric and hydrochloric acid were analyzed using the batch contact methodology. In Figure 49, Am and Cm adsorption are very similar over all nitric acid concentrations with k' values around 1. Even though, the trends found for actinides are the same as those published by Horwitz et al., the magnitude of the Am k' values was found to be an order of magnitude higher, ~3, where a range between 0.1 and 0.4 was previously published.[32] In contrast with Horwitz et al., it was also found, as seen in Figure 49, that Pu(IV) has a higher k' values with UTEVA than U(VI) except for concentrations ≥1 M.[32] Horwitz et al. found a larger difference between Pu(IV) and U(VI) k' values across all concentrations

than those shown in Figure 49 but also reported Pu having a higher affinity than U.[32] Even though the absolute magnitude of the k' values are varying, reported in Figure 49, the trends are the same. Therefore we can assume that methodology described here, but the slightly lower values may be due to differences in analyte concentrations or amount of resin utilized between this research and Horwitz's research.

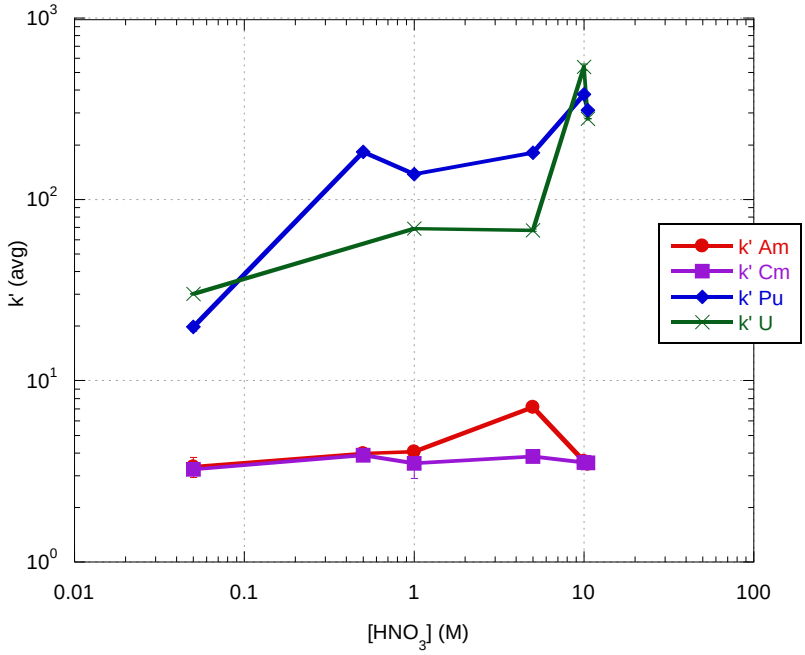

Figure 49. Actinide Adsorption to UTEVA in Varying Nitric Acid Concentrations

The k' values for Pu and U do not drop below 20 for all nitric acid concentrations, so if a solution containing Am, Cm, Pu and U is loaded on to a column in a nitric matrix, Pu and U will be adsorbed while Am and Cm will be eluted from the column. This separation is desirable for a sequential separation scheme with UTEVA preceding DGA, where Pu and U would adsorb onto

UTEVA and Am and Cm would adsorb onto DGA. Since the k'_{Am} values are so low, the Am elution volume needed should be fairly low which is highly desirable as it will help keep the overall mobile phase volume low.

The actinide adsorption to UTEVA in hydrochloric acid, Figure 50, is similar to the adsorption in nitric acid matrices, where the k' values for Pu and U are retained much stronger than Am. Surprisingly the k'_{Am} values were below $k'_{Cm,}$ but there is not enough of a difference in k' values to achieve an individual elution. The Pu k' values range from ~2 to ~100 and the U k' values are from ~3 to ~300; both increase as the concentration of HCl increases. Since there is such a wide variety of k' values for Pu and U in HCl matrices, elution and separation may be possible without a change in matrix. The increase below 0.1 M HCl is possibly due to polymerization or formation of colloids since it is known that Pu can polymerize in low chloride concentrations.[120] The increased k' values may also be due to the Pu adhering to the plastic tubes used in the methodology.

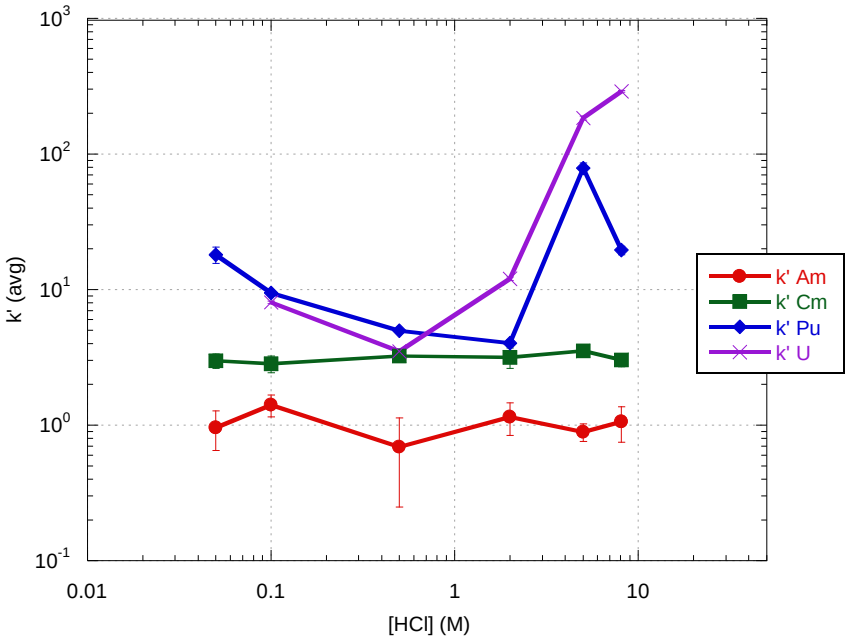

Figure 50. Actinide Adsorption to UTEVA in Varying Hydrochloric Concentrations

The kinetics for the actinide adsorption to UTEVA and varying UTEVA mass were also analyzed using the batch contact study methodology. Since these results match well with Horwitz et al.'s, reaching equilibrium in under an hour, it can be assumed that the batch contact study's methodology is reliable and reproducible.[29]

Section 4.4 Nitric Acid Results and Discussion

The possible effects of used fuel components on Am, Pu, and U adsorption were studied in 1 M HNO_3. Use of this acid concentration allows an increase or decrease in the k' values to be detected for all the actinides since the

original values are not near detection limits. In the following graphs, the solid lines represent the actinide adsorption without any additional components. The dotted lines represent the adsorption of an actinide in the presence of the metal analyte labelled on the x-axis. The ranges of metal analytes vary from 1-20 mM M^{+x} for Zr, Er, Nd, Cs, Mo, and Sr. In all the following graphs, the analyte being graphed is represented by an asterisk(*) next to its abbreviation such as Am*-Zr, where the k' values graphed would only be for Am, but Zr was present in the solution. Error bars only take into account the deviation of the five replicates and are reported on all of the graphs. Any unreported data was due to the values being below detectable limits.

The Am adsorption to UTEVA in 1 M HNO_3 in the presence of varying concentrations of Cs, Sr, Er, Nd, and Zr is graphed in Figure 51. Since UTEVA is highly selective towards tetra-, penta-, and hexavalent metals most of the used fuel components were not expected to cause any interference. The main component to give rise to potential interference was Zr(IV), which did not have an effect as can be seen in the figure below. Also, since Am shows little to no adsorption to UTEVA, it was probable that other trivalent metals would have similar adsorption characteristics. Due to the similarity in oxidation states between the lanthanides and Am, a competition effect may be seen but since Am has such low k' values and lanthanides are expected to be the same little effect is expected from the addition of lanthanides, as seen. Therefore, it is expected that the adsorption of Am in nitric acid should not be affected by these additional components.

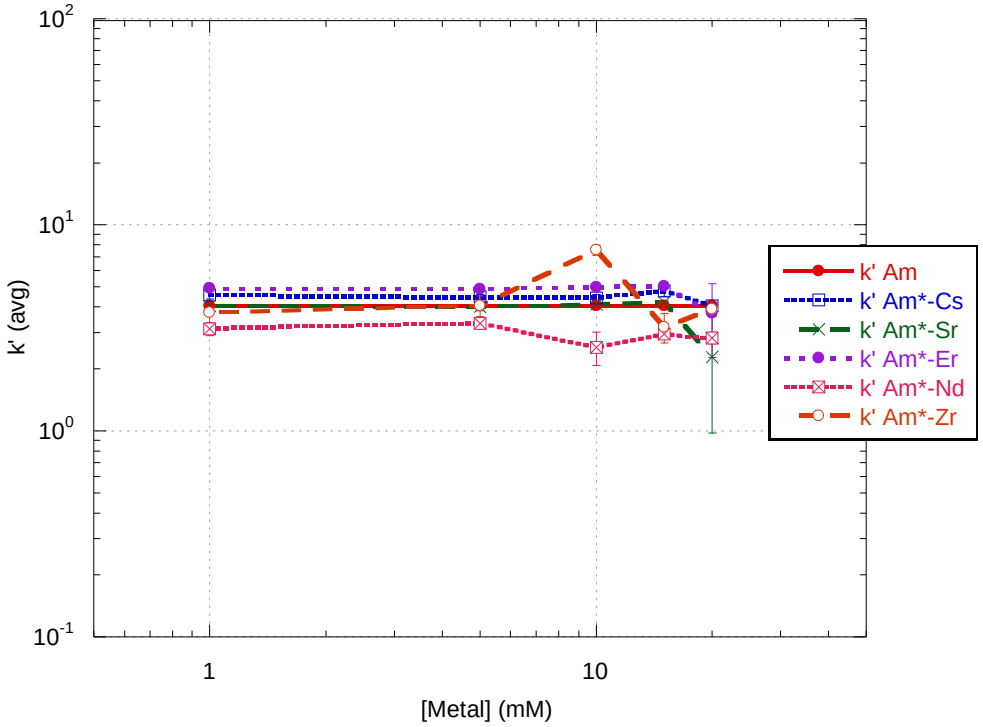

Figure 51. Used Fuel Component Effects on Am Adsorption to UTEVA resin in 1 M HNO_3

The Pu was studied in combination with some of the used fuel components and the results are presented in Figure 52. There are no effects of the used fuel components on Pu adsorption, even when they are in excess. Also, because the metals added were in the form of a nitrate salt, the nitrate concentration increases as the metal concentration increases. This means that UTEVA has a higher affinity for $Pu(NO_3)_4$ than the components studied. Therefore the Pu loading and eluting characteristics on UTEVA resin will not change based on the components studied in Figure 52.

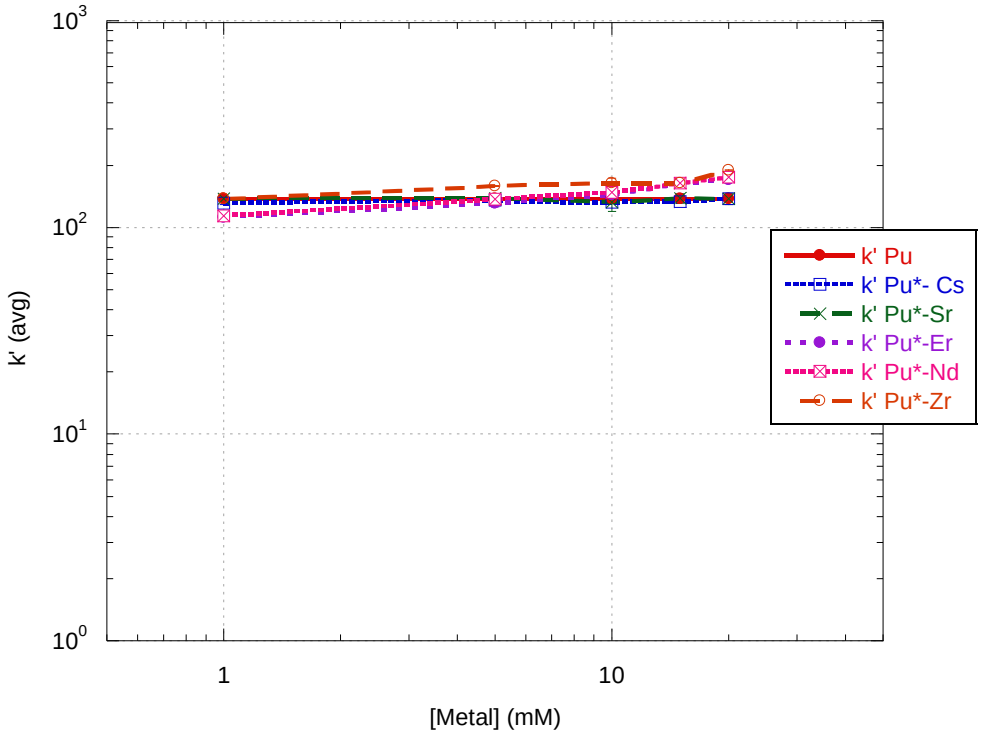

Figure 52. Used Fuel Component Effects on Pu Adsorption to UTEVA resin in 1 M HNO_3

When studying U adsorption characteristics with used fuel components, little to no changes were detected, as seen in Figure 53. Since UTEVA has such a selective extraction of U, not many effects were expected from the components. Further discussion of the adsorption of the individual used fuel component will be in the following sections. No changes in the loading or eluting characteristics would be expected from the presence of any of the components studied.

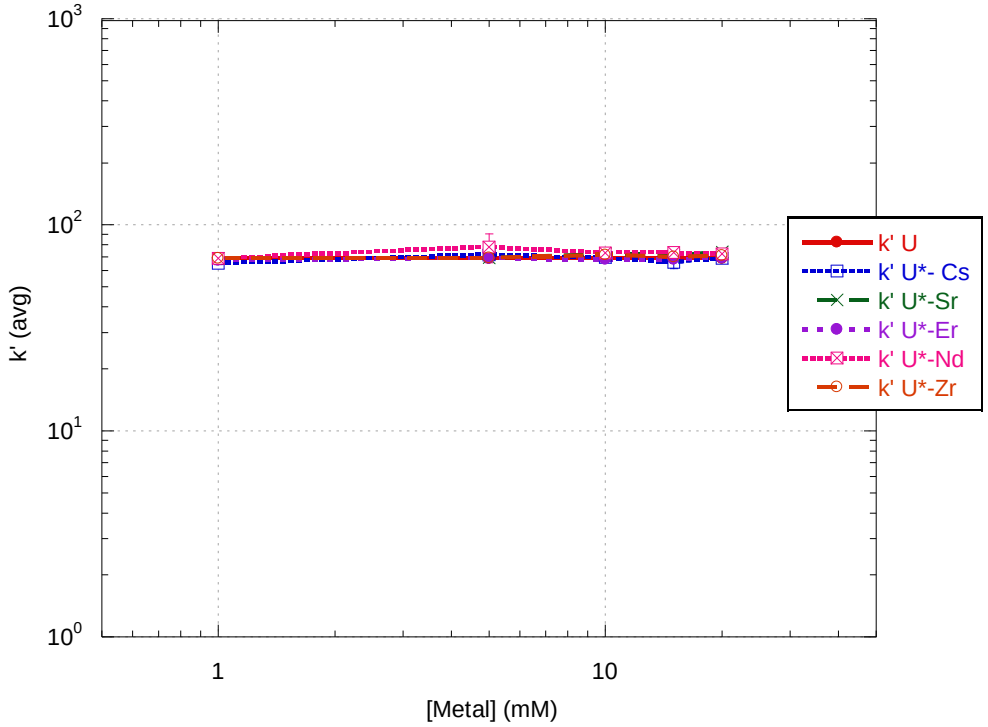

Figure 53. Used Fuel Component Effects on U Adsorption to UTEVA resin in 1 M HNO_3

In Figure 54, 51 and 52, the adsorption of the used fuel components in the presence of an individual actinide is graphed with respect to the metal's concentration in 1 M HNO_3. Sr has the highest affinity for UTEVA in 1 M HNO_3 across all concentrations of Sr nitrate. Nd has no detectable adsorption and therefore is not graphed. In this matrix, only Sr and Er have high enough adsorption to have potential effects on Am adsorption. The rest of the components have such a low adsorption that no effects should be due to their presence.

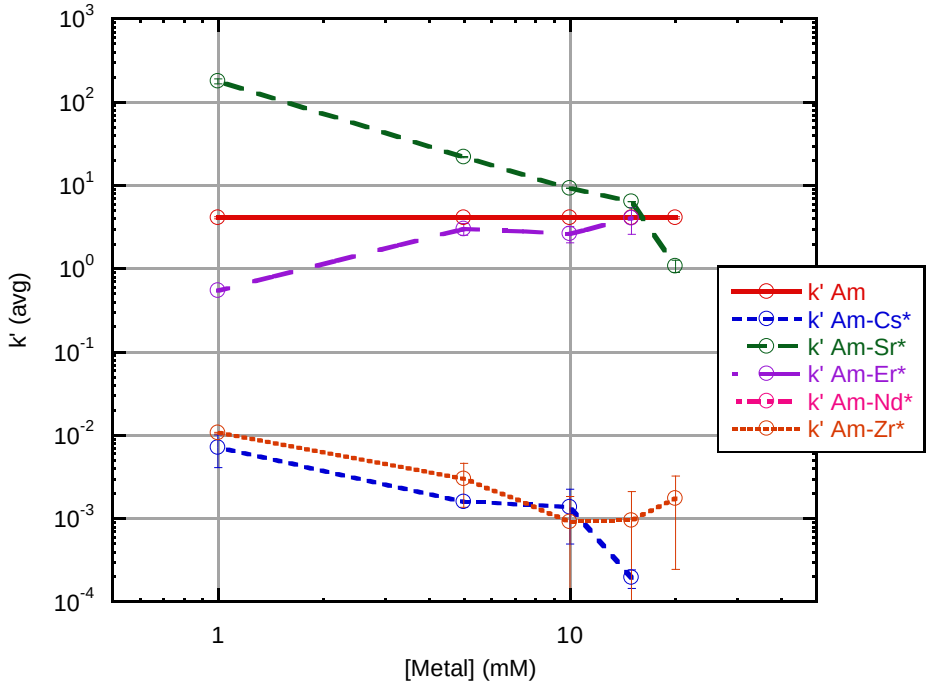

Figure 54. Used Fuel Component Adsorption in presence of Am to UTEVA resin in 1 M HNO_3

Upon comparing the adsorption trends of the used fuel components in the presence of Am versus Pu, in Figure 55, there are very similar magnitudes and trends. Therefore, it seems unlikely that the adsorption of these elements are affected by the presence of Am or Pu. Since all the components have lower affinity than Pu, then any effect from the components would most likely not be due to their adsorption but their chemical effects on the Pu complex.

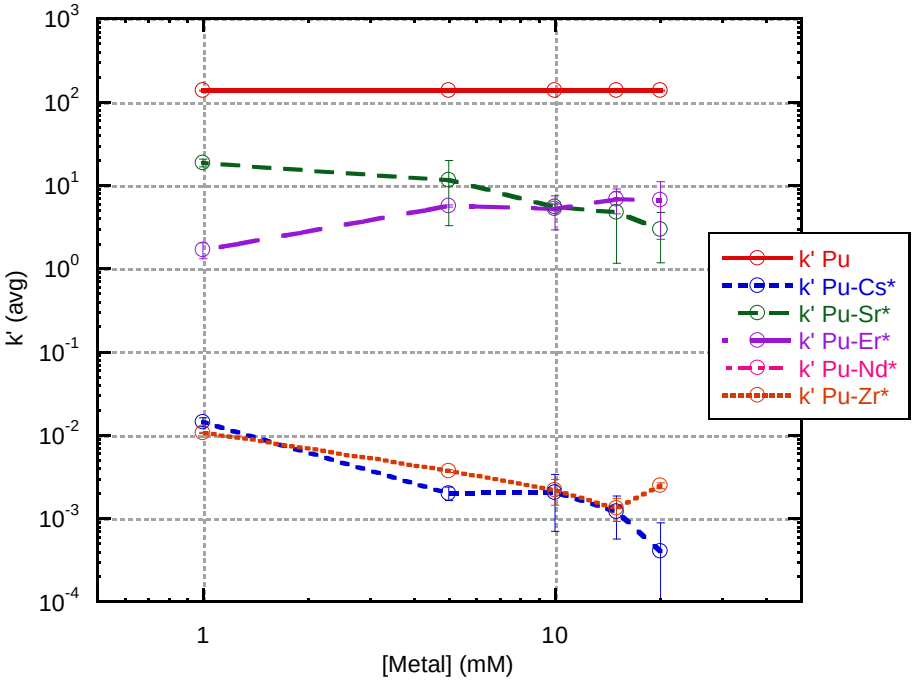

Figure 55. Used Fuel Component Adsorption in presence of Pu to UTEVA resin in 1 M HNO_3

In Figure 52, the majority of the used fuel components have little to no detectable adsorption on UTEVA from 1 M HNO_3 in the presence of uranium. Strontium and zirconium do have some measureable adsorption, but it is so low for both elements that no effect from their presence on U adsorption would be expected. In comparing the Sr and Zr trends in the presence of all the actinides, they seem to be similar and independent of the actinides. Whereas Er, Nd, and Cs showed no detectable adsorption in the presence of U. Due to the difference in concentration of U and the additional components this effect was not expected.

Overall, no effect is expected on Pu and U adsorption or elution, but there may be an effect on Am adsorption using UTEVA in 1 M HNO_3.

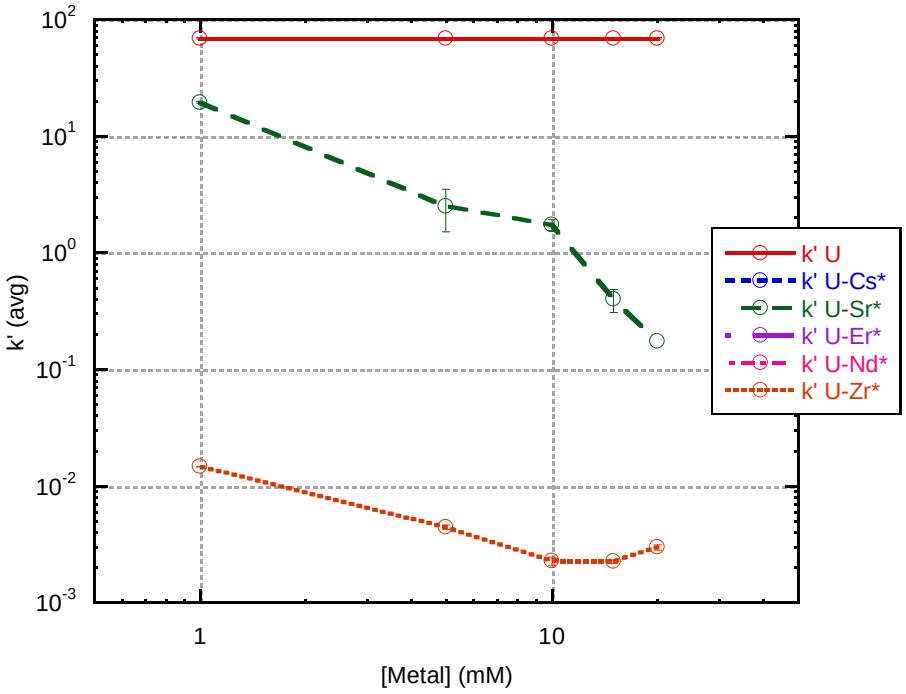

Figure 56. Used Fuel Component Adsorption in presence of U to UTEVA resin in 1 M HNO_3

Zirconium Effects

Horwitz et al. studied the elution behavior or Zr in 2 M HNO_3 where it took roughly 10 free column volumes to elute the majority of Zr from the column which would suggest that Zr would have a k' value ~5.[32, 33] Therefore, Zr was expected to have an effect on U adsorption since they are both tetravalent but that was not seen in Figure 57. Overall, the adsorption of actinides to UTEVA

characteristics seems unaffected by the presence of $Zr(NO_3)_4$. Also, Zr was found to have little to no adsorption, where the k' ≤ 0.01, to UTEVA resin for all Zr concentrations in 1 M HNO_3.

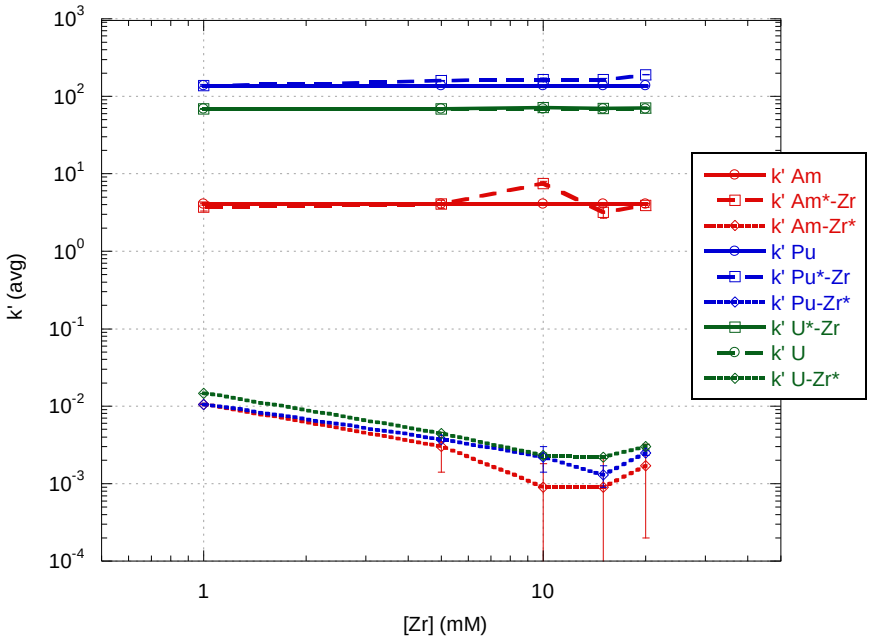

Figure 57. Zirconium Effects on Am, Pu, and U Adsorption to UTEVA resin in 1 M HNO_3
The solid line represents Am, Pu, or U k' values with no additional analyte in solution, the dotted line represents Am, Pu or U k' values with $Zr(NO_3)_4$ in solution, and the dashed line represents Zr k' values with Am, Pu or U nitrate in solution.

Neodymium Effects

Since Nd is trivalent and has a similar radius as Am, it was expected that it would have similar adsorption characteristics. However, it can be seen in Figure 58, that there was no Nd adsorption to UTEVA detected across any of the Nd concentrations studied which means that UTEVA has a lower affinity for Nd than

Am. Horwitz et al. has also studied the elution profile of Nd in 2 M HNO_3 from UTEVA with k' values below 5.[32, 33] Overall, all adsorption data seem independent of one another. There is little to no change to Am, Pu or U adsorption in the presence of Nd. No effects on Am, Pu or U loading, eluting, or stripping characteristics will be due to the presence of Nd.

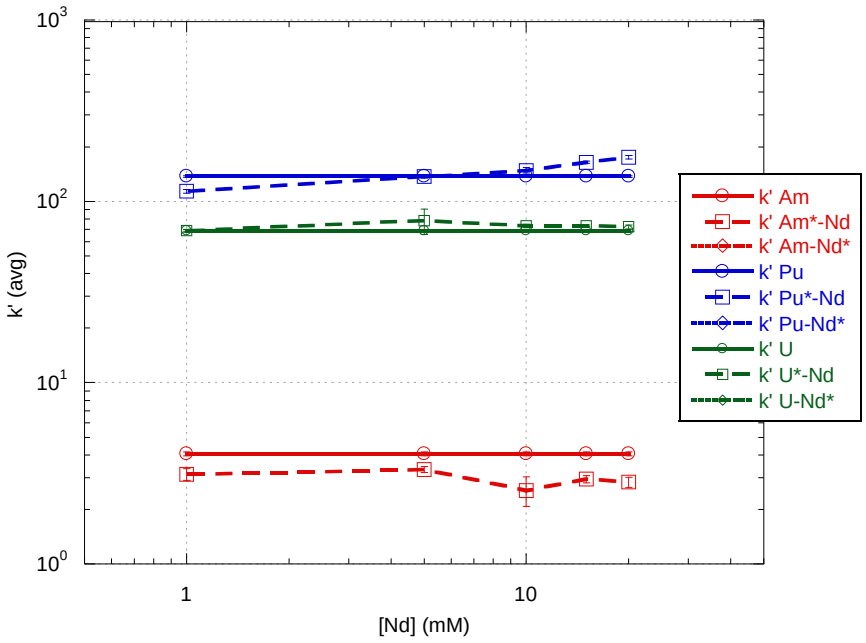

Figure 58. Neodymium Effects on Am, Pu, and U Adsorption to UTEVA in 1 M HNO_3
The solid line represents Am, Pu, or U k' values with no additional analyte in solution, the dotted line represents Am, Pu or U k' values with $Nd(NO_3)_3$ in solution, and the dashed line represents Nd k' values with Am, Pu or U nitrate in solution.

Erbium Effects

The lanthanides are generally expected to have the same adsorption characteristics as one another, since they are so similar in chemical and physical

characteristics. Therefore, it was expected that Nd and Er would have similar k' values but Er in Figure 59 seems to have a high enough affinity to UTEVA that the adsorption is above the detection limit. Surprisingly, $k'_{U\text{-}Er^*}$ is very different from $k'_{Am\text{-}Er^*}$ and $k'_{Pu\text{-}Er^*}$ where $k'_{U\text{-}Er^*}$ are below detectable limits and therefore not graphed. Er has no effect on Am, Pu, and U adsorption characteristics.

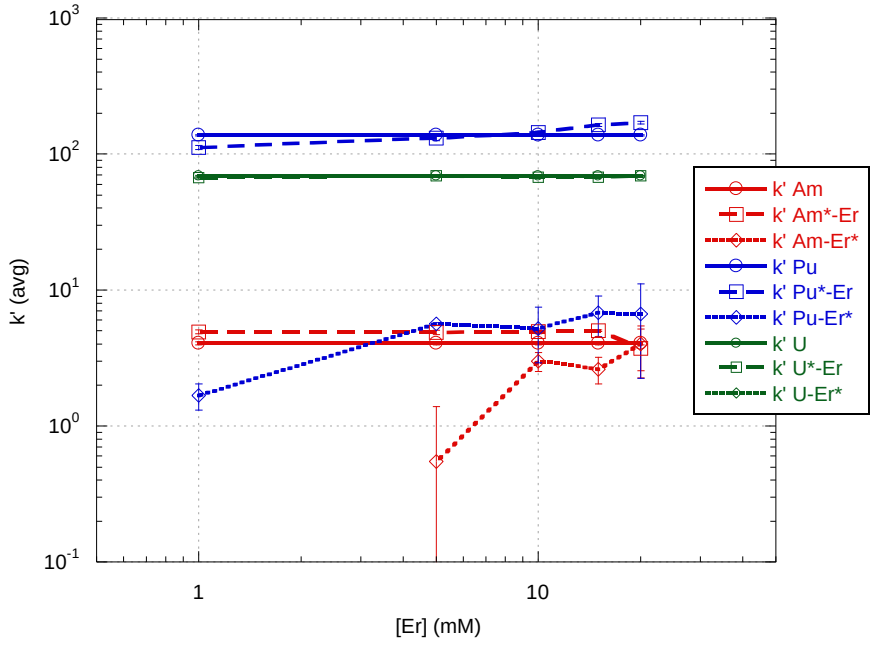

Figure 59. Erbium Effects on Am, Pu, and U Adsorption to UTEVA in 1 M HNO_3
The solid line represents Am, Pu or U k' values with no additional analyte in solution, the dotted line represents Am, Pu or U k' values with $Er(NO_3)_3$ in solution, and the dashed line represents Er k' values with Am, Pu or U nitrate in solution.

Strontium Effects

In Figure 60, Sr effects on Am, Pu, and U adsorption on UTEVA resin are graphed with respect to the Sr concentration. The elution behavior of Sr was

studied by Horwitz et al. in 2 M HNO_3 where the k' value was found to be below 5.[32, 33] As stated earlier, the actinides are unaffected by all concentrations of Sr. However, the k' values for Sr are affected by the presence of those actinides which is shown in the inverse proportional trends where [U] > [Pu] > [Am] and $k'_{Am\text{-}Sr^*} > k'_{Pu\text{-}Sr^*} > k'_{U\text{-}Sr^*}$. It was expected that if the presence of the actinides affected Sr it would be in equal amounts and most likely in a competition reaction, where one neutral Sr complex would compete with one neutral actinide complex. At the actinide concentrations studied, which around 0.1-100 nM, they are below the ICP-AES detectable limit and would therefore not detect any changes in the Sr adsorption due to the actinides. Since Sr adsorption does seem to change with the presence of the actinides, it appears that Sr adsorption is affected at a larger ratio than 1:1 (mol Sr: mol Actinide).

Overall, the Am, Pu and U adsorption and elution characteristics are not affected by the addition of $Sr(NO_3)_2$, but the Sr adsorption on UTEVA did change in the presence of the actinides. Therefore, if Sr is of interest in a separation, then negative effects may be seen even when a column separation is performed under capacity for samples containing actinides. Since Sr is not of interest in this work, this should not affect the separation scheme envisioned here.

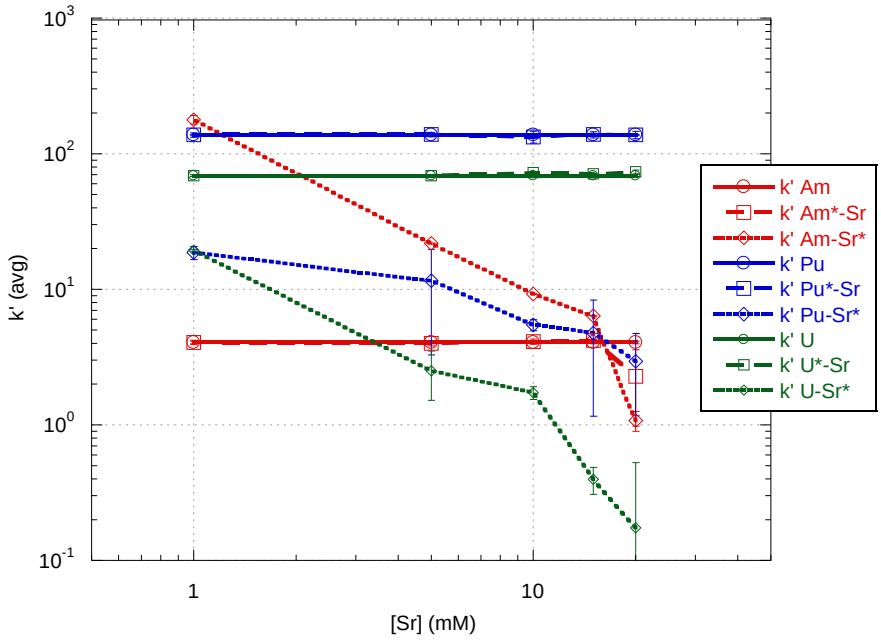

Figure 60. Strontium Effects on Am, Pu, and U Adsorption to UTEVA in 1 M HNO_3
The solid line represents Am, Pu or U k' values with no additional analyte in solution, the dotted line represents Am, Pu or U k' values with $Sr(NO_3)_2$ in solution, and the dashed line represents Sr k' values with Am, Pu or U nitrate in solution.

Cesium Effects

It was expected that Cs would not show any effects on actinide adsorption due to the low k' value reported by Horwitz et al. in 2 M HNO_3.[32] The Cs adsportion shows low k' values in Figure 61, as expected. Cesium shows no effects on the actinide adsorption in 1 M HNO_3 on UTEVA resin. The actinides do not seem to affect the Cs adsorption since all the Cs-Actinide k' values are consistent with one another.

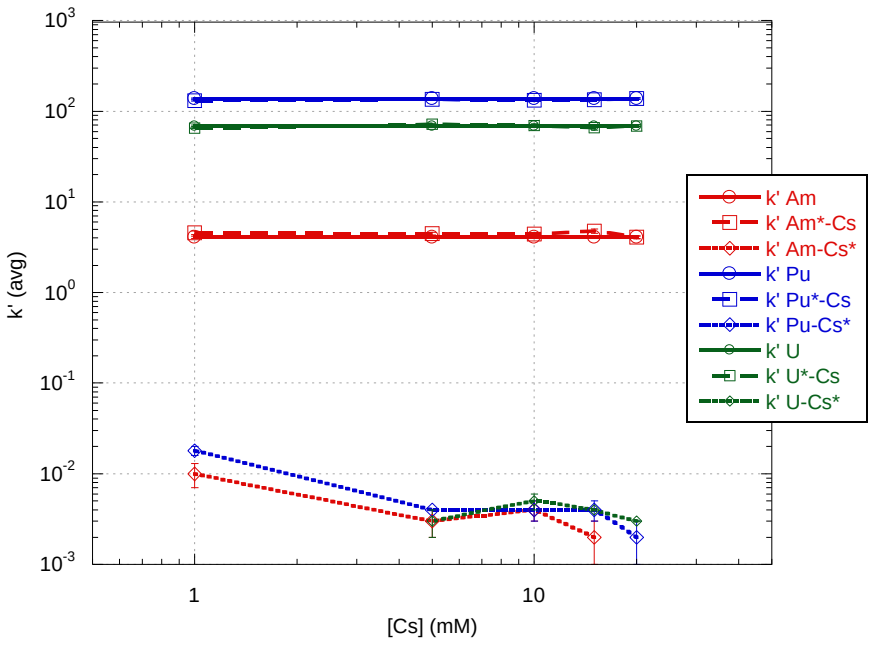

Figure 61. Cesium Effects on Am, Pu, and U Adsorption to UTEVA resin in 1 M HNO_3

The solid line represents Am, Pu or U k' values with no additional analyte in solution,
the dotted line represents Am, Pu or U k' values with $CsNO_3$ in solution,
and the dashed line represents Cs k' values with Am, Pu or U nitrate in solution.

Section 4.5 Hydrochloric Results and Discussion

The possible effects of used fuel components on Am, Pu, and U adsorption were also studied from 1 M HCl. Use of this acid concentration allows an increase or decrease in the k' values to be detected for all the actinides, since the original values are not too close to the detection limits. In the following graphs, the solid lines represent the actinide adsorption without any additional components present. The dotted lines represent the adsorption of an actinide in the presence of the metal analyte labelled on the x-axis. The ranges of metal

analytes vary from 1-20mM M^{+x} for Zr, Er, Nd, Cs, Mo, and Sr. In all the following graphs, the analyte being graphed is represented by an asterisk (*) next to its abbreviation such as Am*-Zr, where the k' values graphed would only be for Am, but Zr was present in the solution. Error bars only take into account the deviation of the five replicates and are reported on all of the graphs and any unreported data was due to the values being below detectable limits.

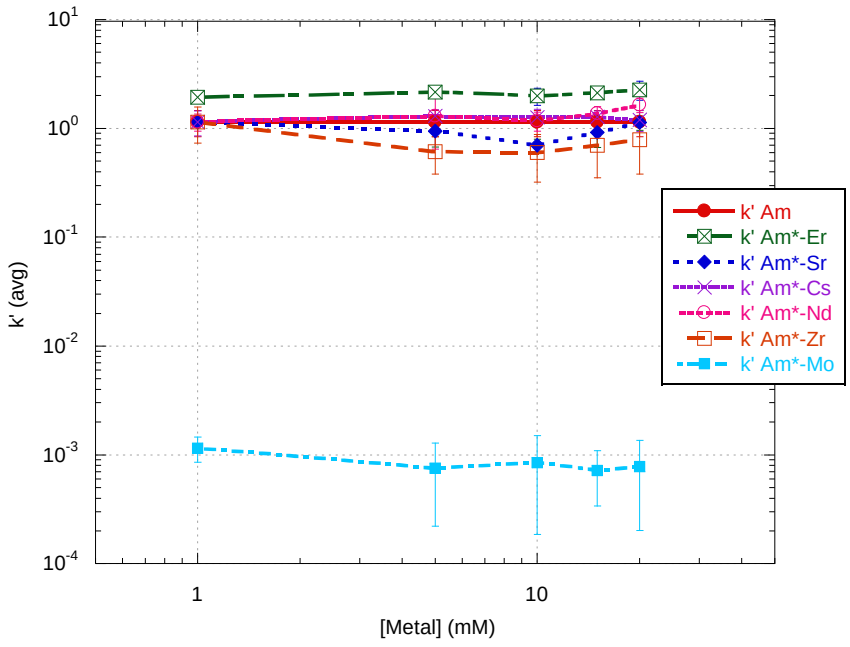

Figure 62. Effects of Used Fuel Components on Am Adsorption to UTEVA in 1 M HCl

Since Am will not be loaded onto the UTEVA column, it would be necessary to identify any component that may increase the adsorption of Am onto UTEVA resin. Therefore, Am adsorption in combination with the most common used fuel components was studied and is graphed in Figure 62. Most of

the components have no effect on Am adsorption except for Mo(VI), which decreases from k'_{Am} ~1 to k'_{Am^*-Mo} ~ 0.001. A more detailed discussion of the effects on Am adsorption in the presence of Mo will precede Figure 73.

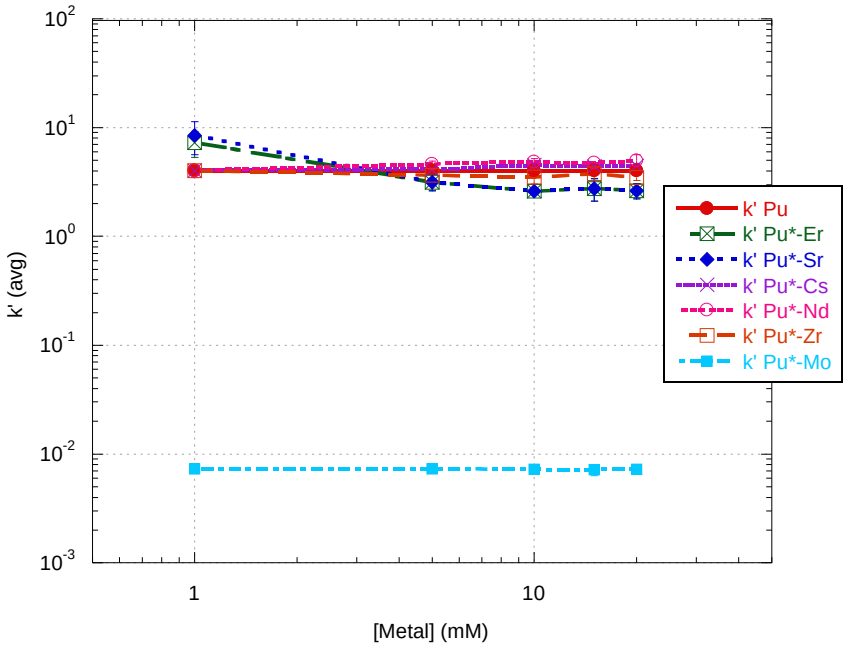

Figure 63. Used Fuel Component Effects on Pu Adsorption to UTEVA in 1 M HCl

The Pu adsorption in combination with the used fuel components, in Figure 63, are similar to those seen for Am, where the majority of the components do not have an effect with the exception of Mo(VI). The addition of Mo(VI) results in a very large and constant suppression of the Pu(IV) adsorption by three orders of magnitude.

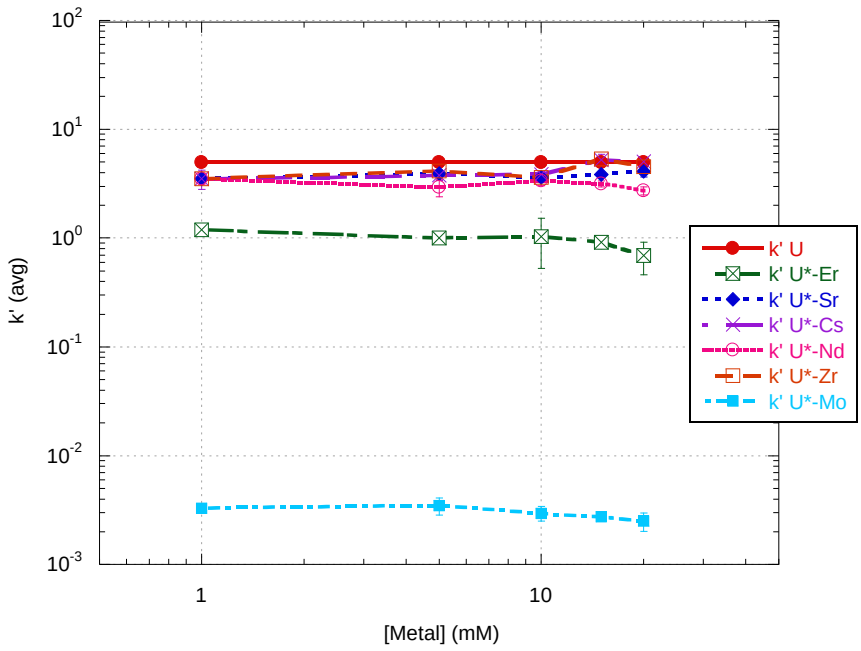

Figure 64. Used Fuel Component Effects on U Adsorption to UTEVA in 1 M HCl

The adsorption of U, in Figure 64, is affected by the presence of Er and Mo. They result in a constant effect that does not increase with the increased concentrations of each metal. The effect of Er was unexpected, since it is trivalent and therefore not expected to show much affinity for UTEVA, or cause a competition reaction. Since Mo is hexavalent an effect was thought to be possible. However the degree to which it lowers U adsorption is unexpected. The large suppression caused by Mo is seen for all the actinides studied. These effects will be discussed in more detail later in this section.

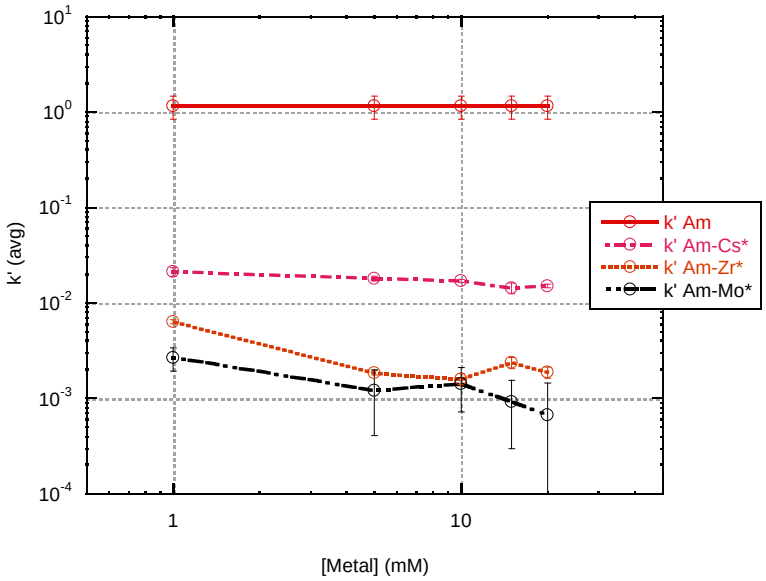

Figure 65. Used Fuel Components Adsorption in presence of Am to UTEVA in 1 M HCl

In Figures 61 through 63, the used fuel components' k' values in the presence of Am, Pu, and U are graphed with respect to the metal concentration. In all three graphs, the majority of the components had no detectable adsorption and the rest had such low adsorption that no effects should occur due to their adsorption to UTEVA in 1 M HCl. There are similar trends and magnitudes detected for these Cs, Zr, and Mo, which most likely means these trends are independent of the actinide adsorption.

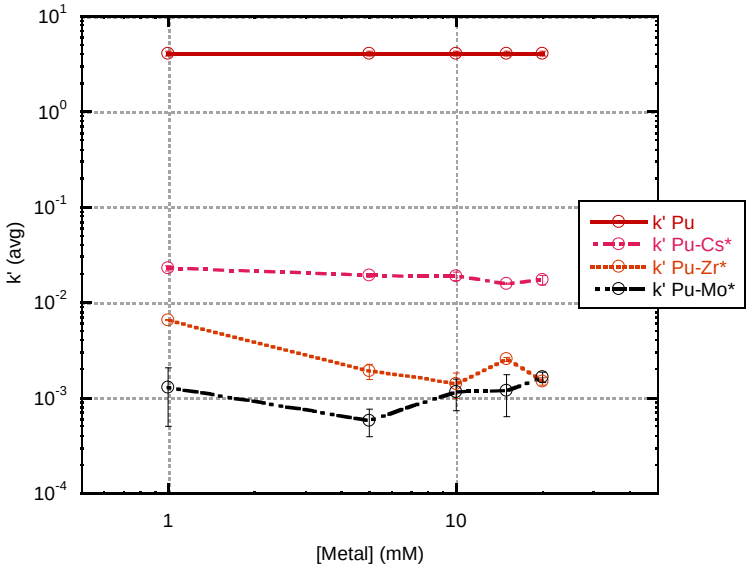

Figure 66. Used Fuel Component Adsorption in presence of Pu to UTEVA resin in 1 M HCl

Overall, the adsorption and elution of Am, Pu and U should be unaffected by any of the used components studied on UTEVA resin in 1 M HCl. Therefore, this would be a good mobile phase since UTEVA exhibits a very selective affinity for Pu and U.

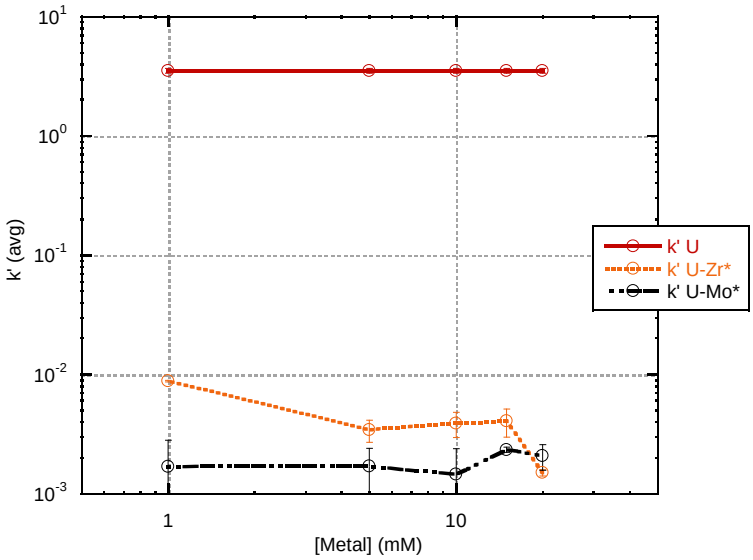

Figure 67. Used Fuel Component Adsorption in presence of U to UTEVA resin in 1 M HCl

Zirconium Effects

A mixture of Zr and the actinides was studied and the results are presented in Figure 68. Since the $k'_{Am\text{-}Zr*}$, $k'_{Pu\text{-}Zr*}$, and $k'_{U\text{-}Zr*}$ are ~0.003 and similar to one another, Zr will not adsorb to UTEVA in 1 M HCl. After taking into consideration the error bars, there seems to be no effect on the Am, Pu, and U adsorption to UTEVA across all Zr concentrations. Since there is such a large difference between the actinide k' values and Zr k' values, they are expected to elute off separately where Zr would elute off first and the actinides second.

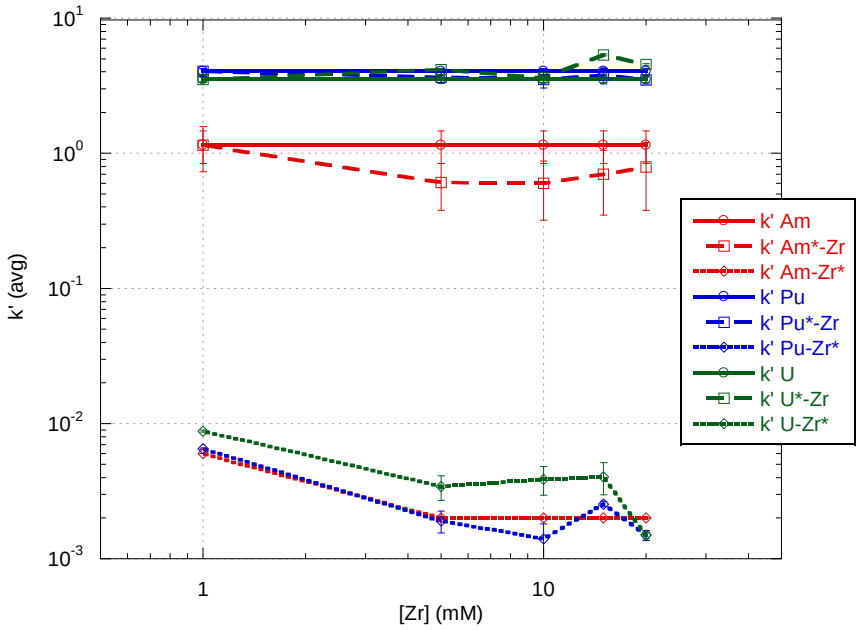

Figure 68. Zirconium Effects on Am, Pu, and U Adsorption to UTEVA in 1 M HCl
The solid line represents Am, Pu, or U k' values with no additional analyte in solution, the dotted line represents Am, Pu or U k' values with $Zr(Cl)_4$ in solution, and the dashed line represents Zr k' values with Am, Pu or U chloride in solution.

Neodymium Effects

As seen in Figure 69, there is no Nd adsorption detected for any of the Nd concentrations studied in 1 M HCl. This was expected since other trivalent metals, such as Am and Cm studied earlier in this chapter, typically have little to no adsorption to UTEVA. There is no literature found on Nd adsorption in 1 M HCl for UTEVA resin. Even though Nd has exceeded the UTEVA capacity, there is no effect on Am, Pu, and U adsorption across all Nd concentrations.

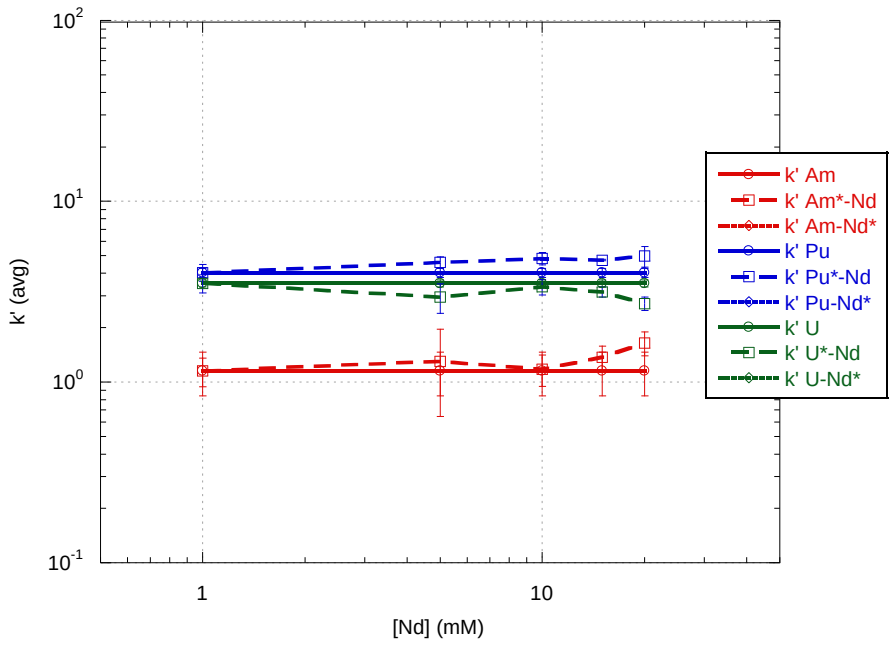

Figure 69. Neodymium Effects on Am, Pu, and U Adsorption to UTEVA in 1 M HCl
The solid line represents Am, Pu, or U k' values with no additional analyte in solution, the dotted line represents Am, Pu or U k' values with $Nd(Cl)_3$ in solution, and the dashed line represents Nd k' values with Am, Pu or U chloride in solution.

Erbium Effects

Erbium and neodymium were found to have similar characteristics with UTEVA, since no Er adsorption was detected in 1 M HCl, as seen in Figure 70. As expected for a metal which has little to no affinity for UTEVA, it does not affect the Am, Pu, and U adsorption. No studies of Er adsorption to UTEVA resin in 1 M HCl are reported in literature.

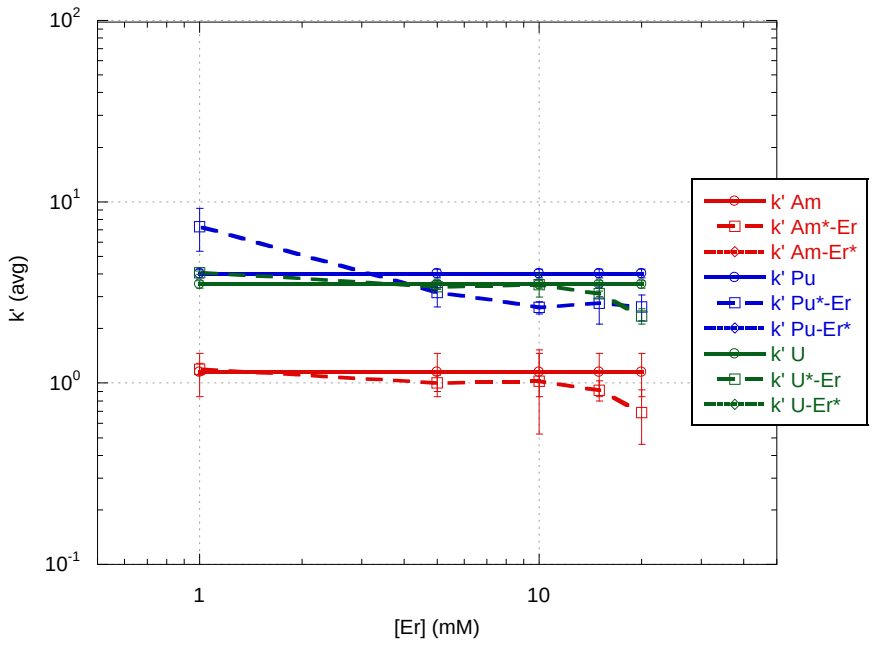

Figure 70. Erbium Effects on Am, Pu, and U Adsorption to UTEVA in 1 M HCl
The solid line represents Am, Pu, or U k' values with no additional analyte in solution, the dotted line represents Am, Pu or U k' values with $Er(Cl)_3$ in solution, and the dashed line represents Er k' values with Am, Pu or U chloride in solution.

Strontium Effects

Strontium adsorption in 1 M HCl has not been previously reported in literature. The effect of Sr on Am, Pu, and U adsorption to UTEVA resin in 1 M HCl was investigated and the results are presented in Figure 71. Sr adsorption to UTEVA above the below detectable limits of the ICP-AES used was not detected.

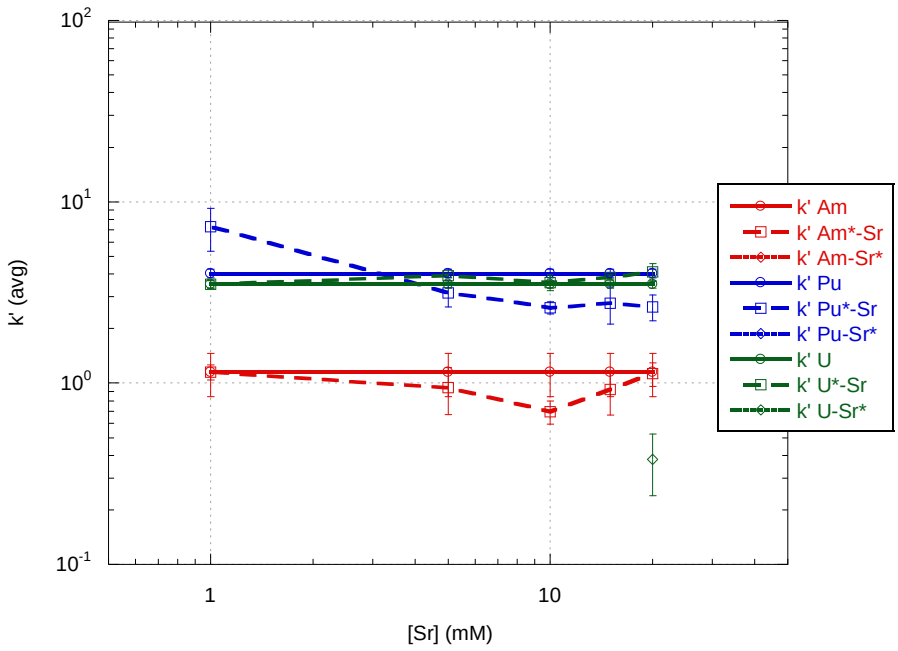

Figure 71. Strontium Effects on Am, Pu, and U Adsorption to UTEVA in 1 M HCl
The solid line represents Am, Pu, or U k' values with no additional analyte in solution, the dotted line represents Am, Pu or U k' values with $Sr(Cl)_2$ in solution, and the dashed line represents Sr k' values with Am, Pu or U chloride in solution.

Cesium Effects

There is no published data on Cs or monovalent metals adsorption to UTEVA's in hydrochloric matrices. The adsorption of Cs, as seen in Figure 72, is fairly low. The $k'_{Am\text{-}Cs^*}$, $k'_{Pu\text{-}Cs^*}$, and $k'_{U\text{-}Cs^*}$ have k' values ~0.1 to 0.3 which would result in elution off the UTEVA column prior to the actinides since there is such a large separation factor (SF) for $k'_{Am^*\text{-}Cs}$, $k'_{Pu^*\text{-}Cs}$, and $k'_{U\text{-}Cs^*}$.

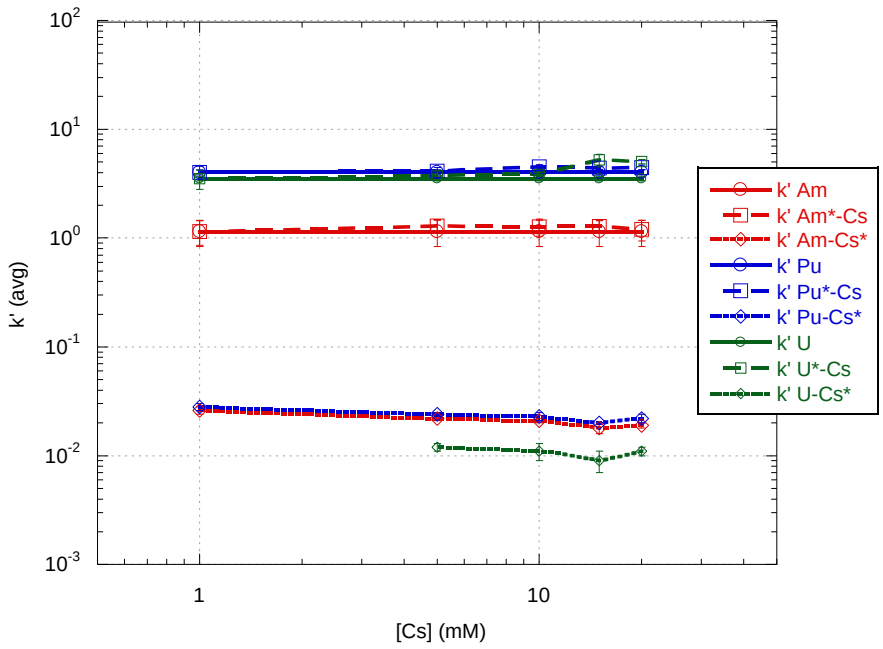

Figure 72. Cs Effects on Am, Pu, and U Adsorption to UTEVA in 1 M HCl
The solid line represents Am, Pu, or U k' values with no additional analyte in solution, the dotted line represents Am, Pu or U k' values with CsCl in solution, and the dashed line represents Cs k' values with Am, Pu or U chloride in solution.

Molybdenum Effects

The adsorption of Mo in 1 M HCl to UTEVA resin has yet to be reported in literature to date. The adsorption of Mo with actinide elements present and adsorption of actinide with Mo are presented in Figure 73. The Mo adsorption is consistently low, with k' values ranging from 0.009 to 0.01, and shows no difference between those solutions with Am, Pu, or U in them. This implies that the actinides do not affect Mo adsorption.

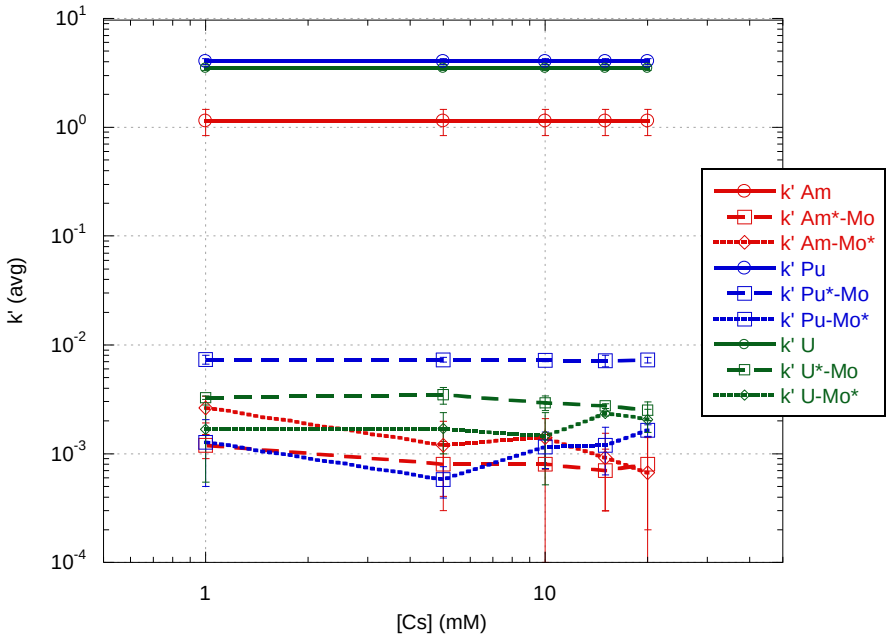

Figure 73. Mo Effects on Am, Pu, and U Adsorption to UTEVA in 1 M HCl
The solid line represents Am, Pu, or U k' values with no additional analyte in solution, the dotted line represents Am, Pu or U k' values with $Mo(Cl)_6$ in solution, and the dashed line represents Mo k' values with Am, Pu or U chloride in solution.

As mentioned in the previous chapter, Lee et al. studied the adsorption of Mo(VI) complexes formed in hydrochloric acid to ion exchange columns.[118] The $H_6Mo_2O_8^{2+}$ ($Mo_2O_2H(OH)_6^{2+}$) and $H_3MoO_4^+$ were the dominate species in 1 M HCl and anionic Mo species were not formed until 3 M HCl.[118] The changes with the addition of $AmCl_3$ and $PuCl_4$ may be causing the change in Mo species or due to Mo being in large excess in comparison to Am and Pu the smallest amount of anion species forming may be creating a co-complex. Although it seems unlikely, it is possible that Am and Pu may be forming a co-complex with Mo. Since the $k'_{Am^*\text{-}Mo}$ and $k'_{Pu^*\text{-}Mo}$ are very close to the $k'_{Am\text{-}Mo^*}$ and $k'_{Pu\text{-}Mo^*}$,

including the error bars, it is possible that this commonality is showing the co-complex. If the formation of the co-complex is preferred over complexation with DGA, it would be expected that both the actinide and Mo k' values would be close to one another which is seen. Further studies will be necessary to fully identify the complexes occurring in these systems.

Although the k'_{Am^*-Mo}, k'_{Pu^*-Mo}, and k'_{U^*-Mo} have significant variance between one another this may be due to the amount of activity in each sample where the larger activity is able to obtain a lower k' value when the minimum detection of the LSC is reached. Therefore, the difference between the actinide adsorption in presence of Mo and the Mo adsorption in the presence of actinides may not be masked and no conclusions can be formed.

Section 4.6 Concluding Remarks

Upon studying the effects of used fuel components on Am, Pu, and U adsorption to UTEVA from 1 M HNO_3, no effects were seen on the actinide's adsorption characteristics. Since no significant effects were detected it is safe to assume that Am, Pu, and U will load and elute from the column as dictated by their own affinities. Out of the used fuel components analyzed Sr had the highest k' values for UTEVA, which was unexpected and could potentially cause effects on other elements in a separation scheme but should not greatly affect separation or detection in a material accountancy system. It is possible that other

divalent metals will have the similar trends but further investigation would be necessary to determine which ones and the extent of their affinity.

For 1 M HCl, Mo(VI) showed large interference effects on Am, Pu, and U k' values for all Mo concentrations. A co-complex is thought to be forming since the $k'_{actinides}$ and k'_{Mo} are close to one another. So if Mo is in large excess in solution with the actinides, loading and eluting characteristics will not be maintained in 1 M HCl. The effect may be able to be manipulated by use of redox and oxidation reagents. Further studies are necessary to identify the complexes occurring between Mo and the actinides. Since Mo does not dissolve in nitric acid, Mo is not expected to be in the loading of Am, Pu, and U in nitric acid. The separation scheme should operate as expected for used fuel samples for the PUREX process.

Chapter 5. EFFECTS OF VARIOUS MATRICES ON ACTINIDE ADSORPTION CHARACTERISTICS

Section 5.1 Abstract

In order to understand the effects a matrix and in particular the counter ion can have on actinide adsorption, the adsorption of actinides in various acid matrixes and in the presence of additional anions were investigated. The results are discussed in this chapter. The Am, Cm, Pu, and U adsorption characteristics on DGA and UTEVA resin were studied in various concentrations of nitric, hydrochloric, sulfuric, hydrobromic, and hydroiodic acid. The comparison of these acids may allow for trends to be identified based on characteristics of the matrices such as: ionic radii, charge density, and/or ionic strength of the solution. Also, investigations of these acids' effect on Am, Cm, Pu, and U adsorption may provide novel separation schemes. Since the nitric and hydrochloric results were already presented in Chapter 3. they will not be presented individually in this chapter, but comparisons between all acids and matrices studied in this thesis will be made and discussed.

Also in this chapter, sodium sulfate, sodium bromide, acetic acid, oxalic acid, and sodium nitrite to HNO_3 and HCl matrices was investigated. Sodium sulfate and sodium bromide were investigated in nitric and hydrochloric matrices in order to identify the effect of purely the sulfate and bromide anion on the

system. Acetic acid, oxalic acid and sodium nitrite were studied in order to assess the potential for reducing agents in a separation scheme.

The potential application of the various matrices in a separation of the actinides and the advantages and disadvantages for each matrix for an efficient separation scheme will be discussed. Since the matrices with high separation factors between Am and Pu are necessary for material accountancy application, a comparison is made and discussed to identify the optimal matrix for a rapid separation.

Section 5.2 Materials and Methods

Batch Contact Method

Batch contact studies were performed using the same methodology that was presented earlier in Chapter 2, and applied in Chapters 3 and 4. The adsorption of Am-241, Cm-244, and Pu-239 was studied in various concentrations of sulfuric, hydroiodic, hydrobromic, hydrochloric, and nitric acid matrices. In all of these cases, the resin was preconditioned with 0.5 mL of the desired acid concentration and then 0.5 mL of the same concentration of acid and 0.5 mL of the respective radionuclide in 0.1 M of acid was added. The concentrations of the stock acid solutions used were selected based on the fact that the 0.1 M acid radionuclide spike would either dilute or concentrate the acid with its addition. For the studies of mixed matrices, sodium nitrite, sodium sulfate, sodium bromide, acetic, and ascorbic acid were added to either 1 M

HNO_3 or HCl. In these studies, the resin was preconditioned with 0.5 mL of the mixed matrix solution, and during the spiking step another 0.5 mL of the same matrix and 0.5 mL of radioisotope stock solution 0.1 M HNO_3 or HCl was added. The matrices consisted only of either pure nitrates or chlorides; there were no mixtures of nitrate and chlorides were studied. All studies were performed with five replicates.

Reagents

The DGA and UTEVA extraction chromatography resin was obtained from Eichrom Technologies, Inc. All acid solutions were prepared from using deionized water from a water purification Cascada from Pall Corporation. ^{241}Am, ^{239}Pu, and ^{233}U were obtained from Isotope Products Laboratories. Hydrobromic acid (48%, Sigma-Aldrich) and hydroiodic acid (57%, stabilized, Sigma-Aldrich) were used. Sulfuric, nitric, and hydrochloric acid solutions were prepared from ACS grade acid (Sigma-Aldrich). To prepare the mixed solutions, sodium sulfate decahydrate (ACS reagent, ≥99.0%, Sigma-Aldrich), sodium bromide (BioEtra, ≥99.0%, Sigma-Aldrich), sodium nitrite (Baker Analyzed ACS Reagent, Mallinckrodt Baker), acetic acid (>99%, Columbus Chemical Industries, Inc.), and oxalic acid (>99%, Mallinckrodt Baker) were used.

Measurements

All acids were titrated before use using a Thermo Electron Corporation Orion 940/960 connected to an Orion AutoTitration-500 in order to assure that the actual concentrations were known. Am-241, Cm-244 , Pu-239 , and U-233 were measured on a Tri-Carb 2800TR or Tri-Carb 3100TR liquid scintillation counter in polypropylene vials and taking 0.9 mL aliquot of the filtrate and adding 15 mL of Ultima Gold AB cocktail. The radiotracers were measured for up to an hour or until the one sigma counting error (10,000 counts) was reached. In order to account for any affects due to the matrix, the blanks and standards prepared included an aliquot of the acid/solution matrix.

Section 5.3 Effects of Various Acid on Actinide Adsorption

In order to better characterize DGA and its ability to efficiently separate the actinides, the actinide k' values were determined in various concentrations of sulfuric, hydroiodic, and hydrobromic acid. The comparison of nitric, hydrochloric, sulfuric, hydroiodic, and hydrobromic acid k' values for actinides allows selection of the most optimal loading and eluting matrix for an Am and Pu separation. The best separation would be defined by the largest separation factor. The separation factor is determined by taking the ratio of two metal's k' values such as:[94]

$$SF_{Am:Pu} = \frac{k'_{Am}}{k'_{Pu}} \qquad \textbf{(5-1)}$$

The further from unity a separation factor is the further the elution peaks will be from one another in an elution profile curve. This is of great importance for achieving clean elution peaks of an individual analyte.

Sulfuric Acid

There is no published data on the uptake of Am, Cm, and Pu with respect to the concentration of sulfuric acid for DGA resin. Therefore, investigating the adsorption of actinides from sulfuric acid could lead to new separation schemes for the tri- and tetravalent metals. As seen in Figure 74, the Pu uptake is fairly high at k' ~ 70 and increases to k' ~110 near 4 M. Since Pu's concentration equilibrium constant for disproportionation of Pu(IV) in H_2SO_4 is so low, appreciable amounts of Pu(III), Pu(IV) and Pu(VI) should not exist together in solution.[120] Therefore, Pu oxidation state is not expected to change with increased sulfuric acid concentrations. The constant k'_{Pu} values show that Pu adsorption is independent of the changing [SO_4^-] and [H^+] concentrations.

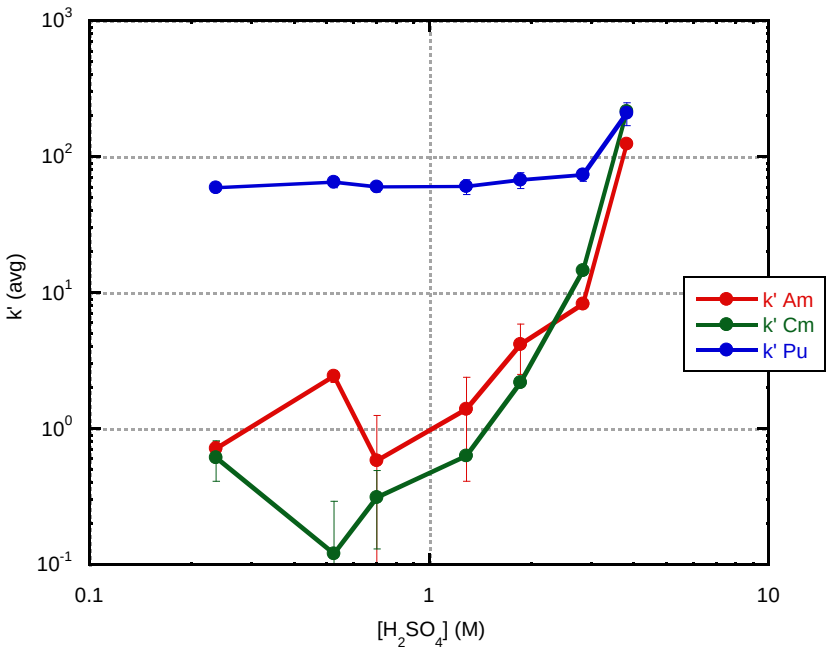

Figure 74. Actinide Adsorption in Varying Concentrations of Sulfuric Acid on DGA resin

The Am and Cm uptake trends and magnitudes match well with one another. As the concentration of sulfuric acid increases above 1 M, the Am and Cm k' values increase as well. The adsorption of Am and Cm are therefore dependent on the concentration of sulfates in the system and the increased concentration drives the formation of the desired adsorption complex. Their highest k' value matches well with Pu's k' value near 4 M. Due to the large separation factor between Pu and Am ($SF_{Pu:Am}$), ~100 at 0.7 M H_2SO_4, a sufficient separation of Am and Pu would be achievable where Pu would stay retained on a column while Am is eluted.

Hydrobromic Acid

The adsorption of Am and Cm to DGA has been previously studied in HBr acid but Pu adsorption on DGA resin in HBr has not been previously reported.[97] Due to HBr's corrosive and fuming nature its use is not practical at higher acid concentrations for full scale application and were therefore not studied beyond 0.3 M HBr.[121] An investigation of the trends in HBr matrices was of interest for Pu on DGA resin. The Am k' value trends and magnitudes seen from 0.01 to 0.1 M, in Figure 75, match well the previous study by Gharibyan.[97] It appears that at higher HBr concentrations, the Pu adsorption is dropping. This may be due to the reduction in Pu's oxidation state.

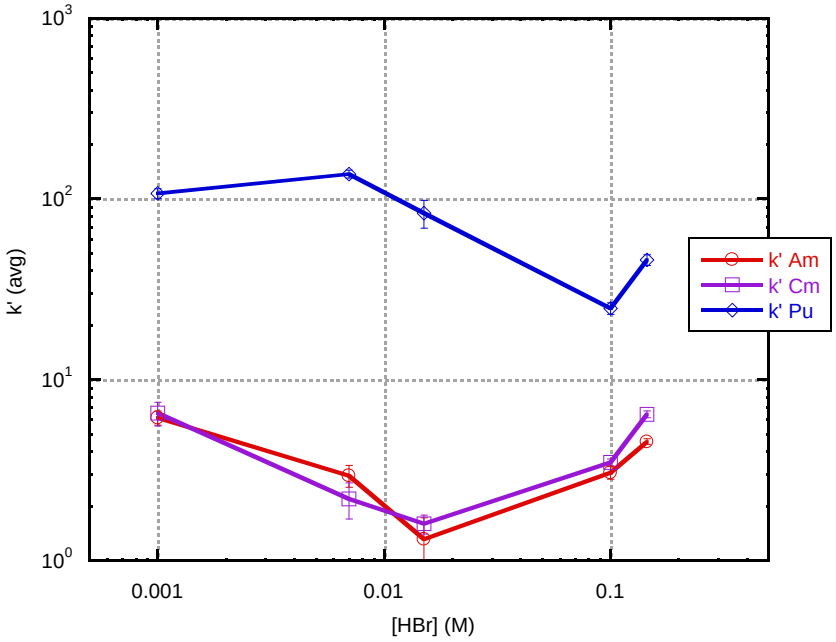

Figure 75. Actinide Adsorption to DGA in Varying Concentrations of Hydrobromic Acid

The separation factor for Pu:Am, range from 10-60. The highest $SF_{Pu:Am}$ could achieve a sufficient separation between Pu and Am. However, since the k' value for Am is still >1, the volume needed for this separation would not be desirable. Therefore in these conditions, hydrobromic acid would not be an advantageous eluent phase.

Hydroiodic Acid

Hydroiodic acid may have more of an effect on actinide adsorption to DGA since it most prone to dissociation in comparison with the other hydrogen halides and is composed one of the largest halides.[119] No data has been published on actinide adsorption in varying concentrations of HI solutions. The concentration ranges studied for HI is much more limited than other acids due to the limited amount available at the time of the study. The adsorption trends of the actinides in HI to DGA resin are graphed in Figure 76. The largest uptake is for Am and Cm, where the limit of detection is reached for both.

There appears to be a variance between k'_{Am} and k'_{Cm} which would be highly desirable since Am and Cm have such a similar chemical characteristics and are thus very hard to separate. However, since the k'_{Am} values reached the upper limit of detection in all concentrations, it is not possible to see the trends of Am would follow those of Cm. The reason the limit of detection is reached for all Am k' values but not for all Cm k' values is due to the difference in the activity of the stock solution used. Due to the differences in the activities in the Am and Cm

stock solutions, the detection limits vary. The Am detection limit is reach at 0.001 M HI, and the Cm detection limit is not reached until 0.1M HI. Therefore no definitive conclusions can be made from this study. In order to fully investigate the effects of HI on Am adsorption trends, higher activity of Am would be needed to reach higher k' value limits or a column elution profile would also provide details on the potential separation of k'_{Am} and k'_{Cm}.

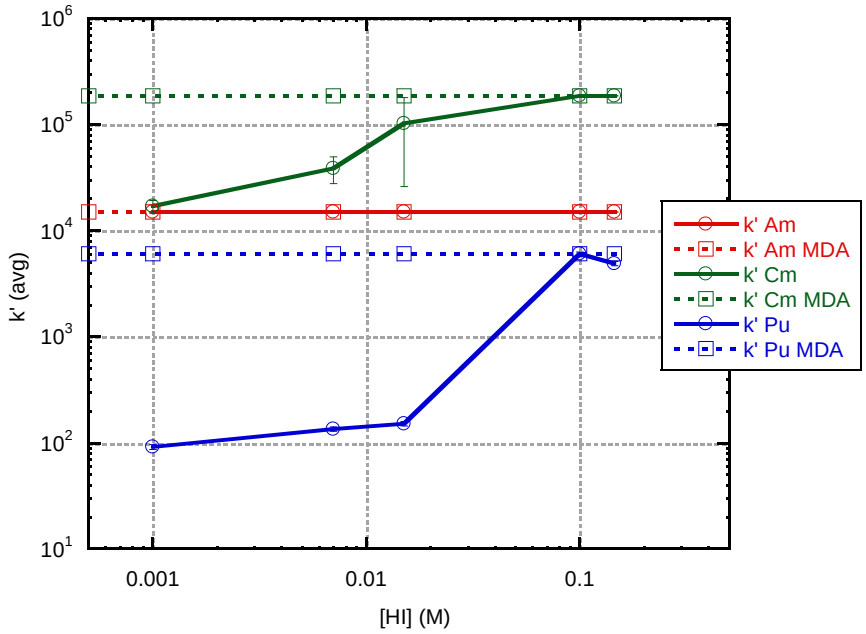

Figure 76. Actinide Adsorption to DGA in Varying Concentrations of Hydroiodic Acid

Even though the k'_{Pu} is below k'_{Am} and k'_{Cm}, the magnitude of Pu adsorption is high, k' ~ 100, between 0.001 and 0.015 M HI, at 0.1 M HI and above the k'_{Pu} values increase about 1.5 orders of magnitude. This increase

brings k'_{Pu} close to k'_{Am}, and is likely caused by reduction of Pu(IV) to Pu(III) by the HI. This would cause Pu to have similar adsorption values to Am(III). Further investigation of the higher HI concentrations could be of value. The $SF_{Pu:Am}$ is significantly high, ~160, but since the k' values are so large for all the actinides, this would not produce a viable separation scheme due to the volumes of mobile phase that would be needed.

Section 5.4 Addition of Complexants and Reducing Agents

The addition of reducing agents can play an important role in tailoring the selectivity of a specific resin. To determine the optimal loading and elution matrices for a column separation, varying concentrations of sodium nitrite, sodium sulfate, sodium bromide, oxalic and ascorbic acid were added to 1 M HNO_3 or HCl and then mixed with solutions contain the radionuclides Am, Cm, and Pu. The sodium sulfate and sodium bromide salts were used to investigate the combination of nitrates and chlorides with sulfates and bromides without changing the acidity. By adding additional anions in this manner the preferred actinide complex is thought to adsorb to DGA in 1 M HNO_3 or HCl. Sodium salts were used since sodium was previously found to have no affinity for DGA resin and therefore should not affect any of the adsorption.[29]

Bromide Effects

The effect of bromide on Am and Pu adsorption to DGA resin is graphed in comparison to Am and Pu adsorption in nitric and hydrochloric acid matrices in Figures 77 and 78. The HBr k' values are plotted as a reference to determine the change due to the mixed matrices. The bromide/chloride mixed matrix has the lowest k' values for Am and Pu at all bromide concentrations. In Figure 77, the Am k' values are close together for HBr, NaBr + 1 M HNO_3, and for 1 M HNO_3. Therefore, the addition of bromides into the nitrate system do not supply any benefits. For Am adsorption in the NaBr + 1 M HCl matrices, it appears that Am adsorption is being controlled by the presence of bromide since the $k'_{Am\ (NaBr + 1\ M\ HCl)}$ is closer to $k'_{Am\ (HBr)}$ than $k'_{Am\ (1\ M\ HCl)}$ for all concentrations. The addition of Br may be useful if the increased k' value is selective to only Am since it may allow for the retention of Am in hydrochloric acid concentrations where it would usually elute off a column.

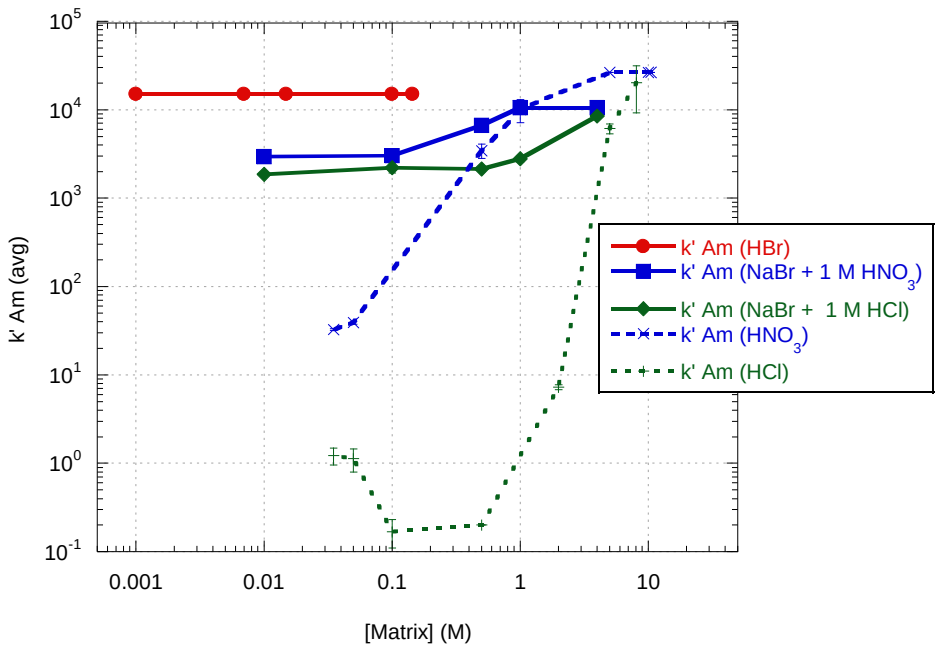

Figure 77. Americium Adsorption Trends with respect to Matrices Concentration

In Figure, the effect of bromides on Pu adsorption is graphed in comparison to the Pu adsorption in nitric and hydrochloric matrices. The largest change is seen on Pu adsorption at low concentrations of NaBr in 1 M HCl, but as the bromide concentration increases, the k' values start to approach the other k' values for Pu. This increase is thought to be due to the fact that at low bromide concentrations, the chlorides are in excess; therefore driving the trends. Since the Pu adsorption in the mixed matrices is close to the Pu adsorption in 1 M HNO_3 and HCl, the largest separation factor is still achieved in pure HBr matrices. Therefore these mixed matrices do not supply any benefit.

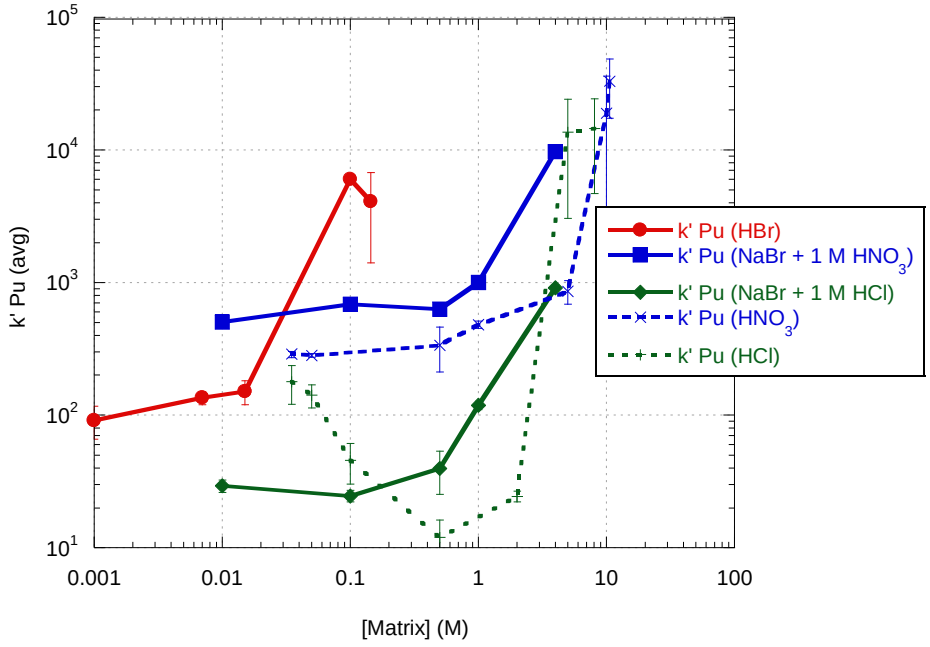

Figure 78. Plutonium Adsorption Trends with respect to Matrices Concentration

Sulfate Effects

The effects of sulfate on the adsorption of Am and Pu were studied in various concentrations and matrices. In order to do this, various amounts of sodium sulfate were added to either 1 M HNO_3 or HCl solutions containing a constant amount of Am or Pu, in Figure 79 and 80.

In Figure 79, the Am adsorptions in sulfate matrices are graphed in comparison to Am adsorption in nitric and hydrochloric acid matrices. Even though the magnitudes for k'_{Am} in sulfate/hydrochloride matrices matches fairly well with the k'_{Am} sulfate matrices, the trends do not match those seen in sulfate

matrices. The k'_{Am} in 1 M HCl is approximately one, which matches closely with k'_{Am} in the sulfate/chloride matrices. Since the hydrochloric acid concentration stays constant in the mixed matrices, the $k'_{Am\ (Na_2SO_4 + 1\ M\ HCl)}$ is most likely driven by the hydrochloric acid concentration and not the sodium sulfate concentration. For the mixed sulfuric/nitric matrices, the k' Am values are fairly constant and correlate well with $k'_{Am\ (HNO_3)}$ at 1 M in comparison to the $k'_{Am\ (H_2SO_4)}$ concentrations. Therefore, it is suspected that the nitric acid concentrations drive the Am adsorption trends in the mixed matrices.

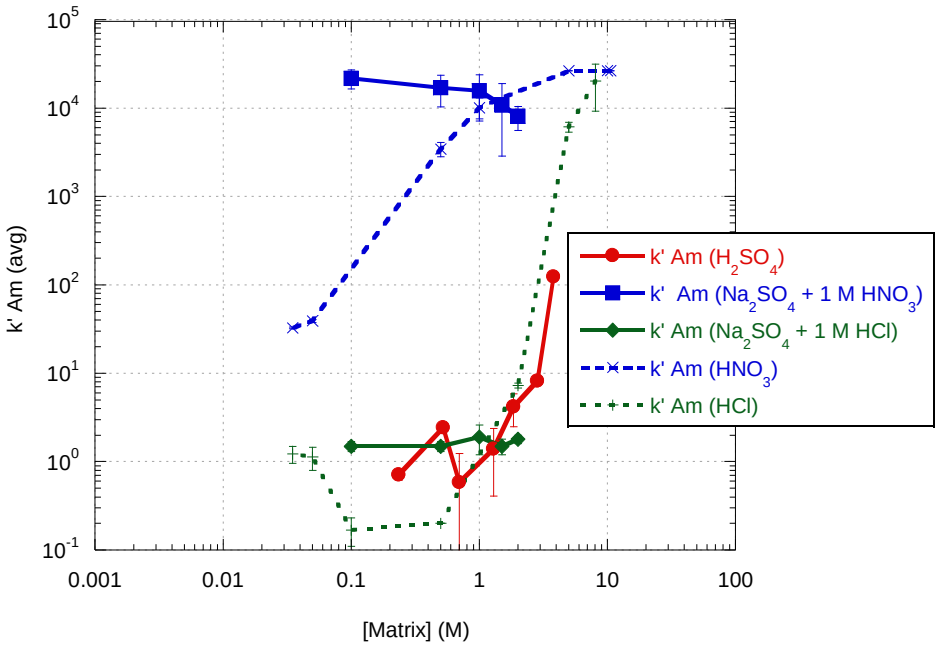

Figure 79. Americium Adsorption Trends with respect to Sulfate Concentration

In the case of Pu adsorption, the k'_{Pu} in sulfate/chloride matrix also matches most closely with the k'_{Pu} in 1 M HCl which is ~10. There is a slight decrease in k'_{Pu} as the sulfate concentration increases in the matrix. This trend is most likely not due to the formation of a Pu sulfate complex, since the k'_{Pu} would be expected to increase to reach near k'_{Pu} in H_2SO_4. Although unlikely, this trend could be due to the presence of sodium or due to a combined complex between Pu, sulfates, and chlorides. The $k'_{Pu\ (Na_2SO_4\ +\ 1\ M\ HNO_3)}$ stays fairly constant with the change in sodium sulfate and are similar to the k'_{Pu} in 1 M HNO_3. Therefore, it is expected that the nitric acid concentrations are driving the Pu adsorption to DGA.

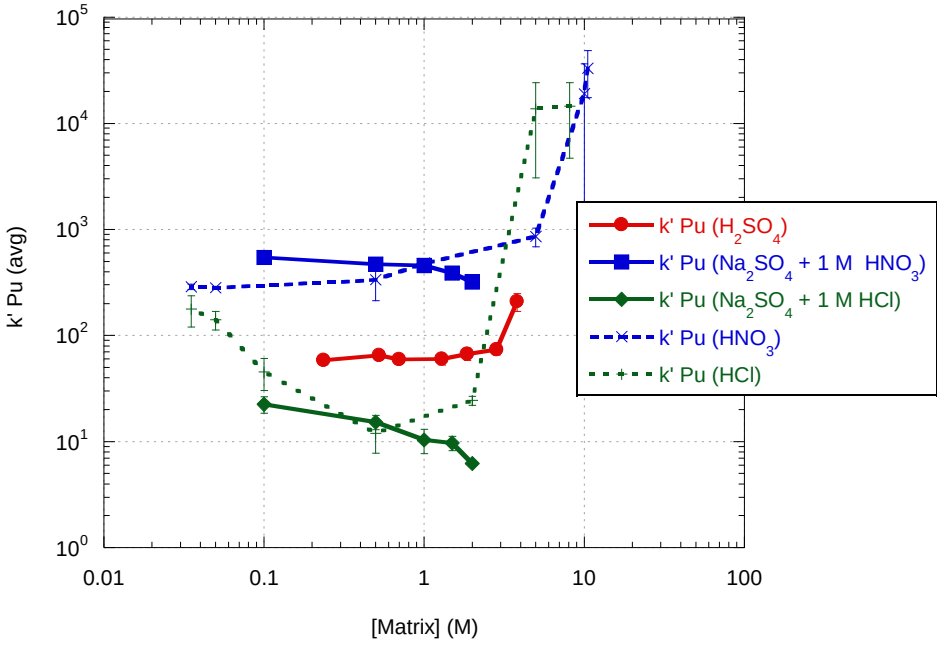

Figure 80. Plutonium Adsorption Trends with respect to Sulfate Concentration

Since there are no changes in the Am or Pu adsorption with the addition of sulfates, there is no advantage to using mixed matrices in the proposed separation. Overall, the nitric and hydrochloric systems prove the most useful separation schemes for separating Am and Pu on DGA resin.

Ascorbic Acid with DGA resin

The addition of various amounts of ascorbic acid to nitric and hydrochloric matrices were studied and the results for Am and Pu adsorption to DGA resin are presented in Figure 81 and 82. The $k'_{Am\ (Ascorbic\ Acid + 1\ M\ HNO_3)}$, ~$10^4$, is unaffected by the addition of ascorbic and oxalic acid in nitric matrices since they are at the same magnitude of k'_{Am}, ~10^4, in 1 M HNO_3. The same trends are seen for the hydrochloride matrices where the $k'_{Am\ (Ascorbic\ Acid + 1\ M\ HCl)}$ values are ~0.4 and the k'_{Am} is ~1 in 1 M HCl. This is most likely due to the fact that ascorbic is a reducing agent and there is no lower oxidation state of Am achievable in this system and therefore does not change the adsorption characteristics on DGA.

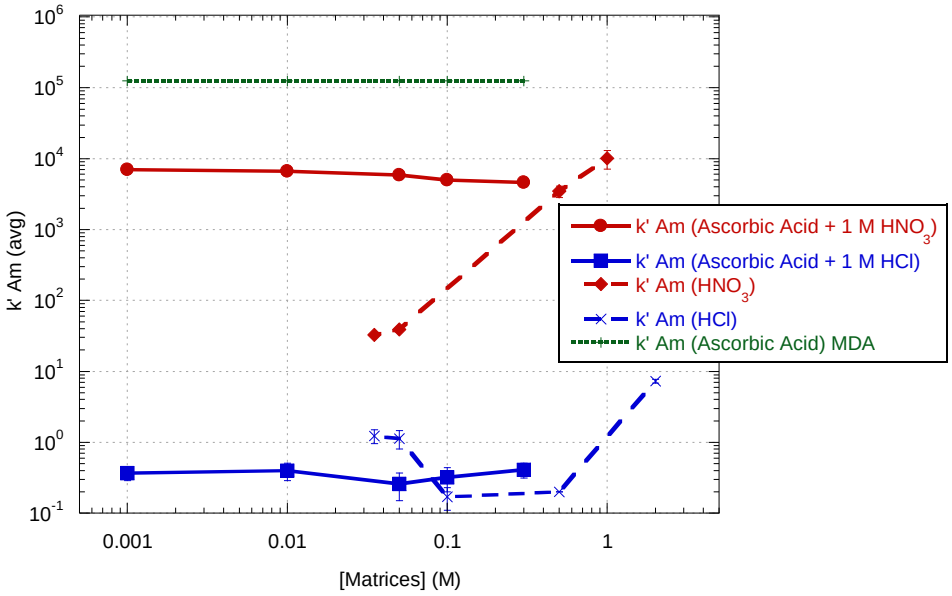

Figure 81. Americium Adsorption on DGA with Ascorbic Acid

For Pu adsorption, as ascorbic concentrations increase in the nitric matrix the $k'_{Pu\ (Ascorbic\ Acid\ +\ 1\ M\ HNO3)}$ decreases which may be due to an ascorbic reducing Pu(IV) to Pu(III) but an increased k'_{Pu} value would be expected for a Pu(III) since it would be expected to be similar to k'_{Am} which is higher. Since ascorbic acid is a reducing agent and nitric acid is an oxidizing agent, it is very likely that we are seeing the effects of the oxidation and reduction of ascorbic and nitric acid on Pu adsorption. For instance, after the HNO_3 is reduced, NO, NO_2 and H^+ are produced and the oxidized ascorbic acid is produced.[122] These products and their concentrations would increase with the increased concentration of ascorbic acid added. For k'_{Pu} mixed matrices with hydrochloric acid and ascorbic acid, at

any concentration, the k' values are ~8 which is near k'_{Pu} in only 1 M HCl matrices which is ~10. Therefore, we can assume that ascorbic acid will not affect the adsorption or elution of Pu in hydrochloric matrices.

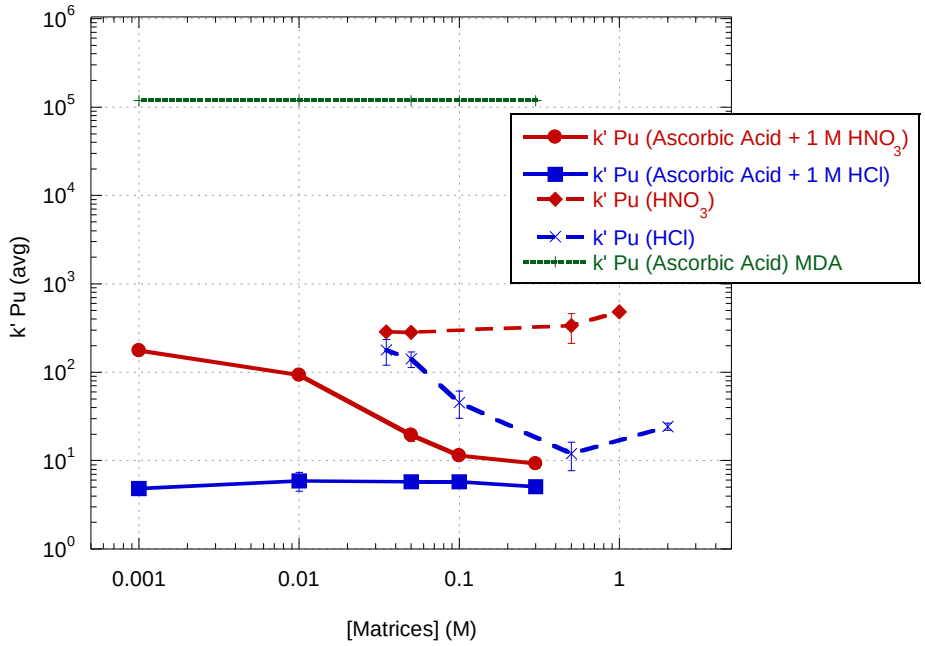

Figure 82. Plutonium Adsorption on DGA with Ascorbic Acid

Overall, the addition of ascorbic acid to 1 M HNO_3 and HCl matrices do not change the adsorption of Am greatly but do change the Pu adsorption with increased ascorbic acid concentrations. The $SF_{Am:Pu}$ is near 500 in 0.3 M ascorbic acid, 1.0 M HNO_3 mobile phases. Although, this matrix would give a very efficient separation due to the magnitude of the SF, the k'_{Pu} in this matrix is

unfortunately not low enough to achieve such a separation in a low elution volume.

Oxalic Acid with DGA resin

The addition of various amounts of oxalic acid to nitric and hydrochloric matrices were studied and the results for Am and Pu adsorption to DGA resin are presented in Figure 83. The k'_{Am}, ~10^4, is unaffected by the addition of oxalic acid in nitric matrices since they are at the same magnitude of k'_{Am}, ~10^4, in 1 M HNO_3. At the concentrations studied the nitrate complex is most likely the dominant adsorbing species and therefore driving the trend. For k'_{Am} in oxalic acid/hydrochloric acid matrix, the k' values are close to k'_{Am} in 1 M HCl, ~1 with the exception to 0.3 M ascorbic acid where $k'_{Am\ (Ascorbic\ Acid\ +\ 1\ M\ HCl)}$ increases to 10. Therefore, oxalic acid will not be a useful addition to 1 M nitric or hydrochloric matrices to enhance the Am adsorption or elution for DGA.

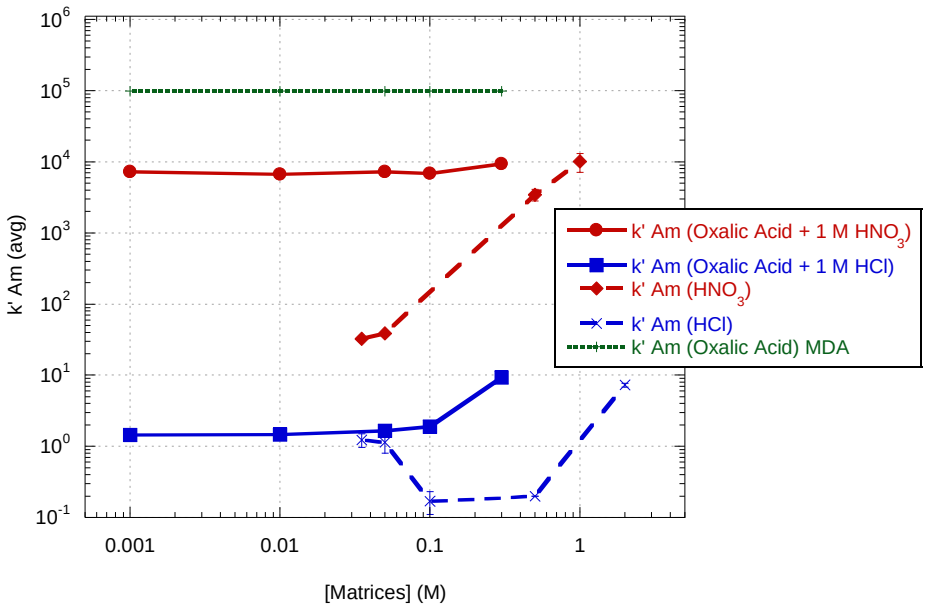

Figure 83. Americium Adsorption on DGA with Oxalic Acid

The k'_{Pu} in mixed oxalic acid/nitric acid matrices is consistently ~300 and correlates to the k'_{Pu} in 1 M HNO_3. At the concentrations studied the nitrate complex is most likely dominant and therefore driving the trend. For k'_{Pu} mixed matrices with hydrochloric acid, for both oxalic acid at any concentration, the k' values are ~8 which is near k'_{Pu} in 1 M HCl matrices. Therefore, we can assume that oxalic acid will not affect the adsorption or elution of Pu in 1 M hydrochloric or nitric acid matrices for DGA resin.

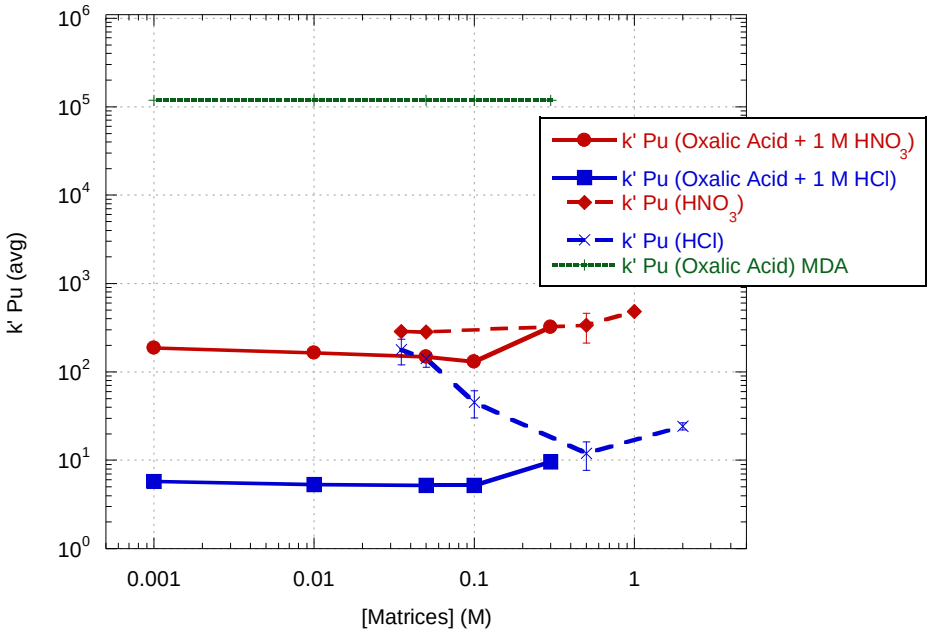

Figure 84. Plutonium Adsorption on DGA with Oxalic Acid

Overall, oxalic acid was not found to enhance the separation of Am from Pu for DGA resin in comparison to that provided by ascorbic acid. Therefore, it would not be an advantageous reagent.

Ascorbic Acid with UTEVA resin

The same ascorbic acid conditions used for DGA were investigated on UTEVA for Pu and U adsorption. As ascorbic acid is added into the nitric acid matrices, there appears to be a change in the Pu and U oxidation states. This is exemplified by the fact that trivalent metals tend to have little to no adsorption; k'

≤ 0.1, and tetravalent metals tend to have k' values ~100 in 1 M HNO_3. The reduction of Pu(IV) to Pu(III) is noticeable by its $k'_{Pu\ (Ascorbic\ Acid\ +\ 1\ M\ HNO3)}$ in all concentrations of ascorbic acid.

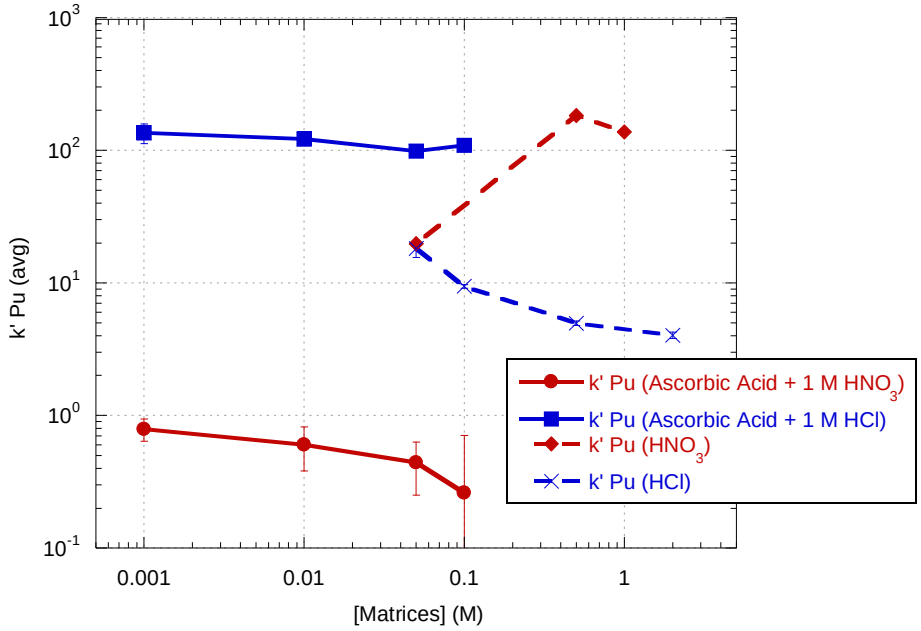

Figure 85. Plutonium Adsorption on UTEVA with respect to Ascorbic Acid

In Figure 86, the reduction of U(VI) to U(IV) is seen in its increased k' values up to ~100. For ascorbic acid in hydrochloric matrices, there seems to be a reduction in U's oxidation state, due to its increased k' values, but Pu seems unaffected, since its k' values stay the same. This selective reduction of U may be due to their difference in their reduction/oxidation potentials in acid, seen

below. Since U has a larger redox potential than Pu, the reduction of U is accomplished more easily than the reduction of Pu.[120, 123]

$$U(VI) \underset{-0.334}{\longleftrightarrow} U(IV)$$

$$Pu(IV) \underset{-0.97}{\longleftrightarrow} Pu(III)$$

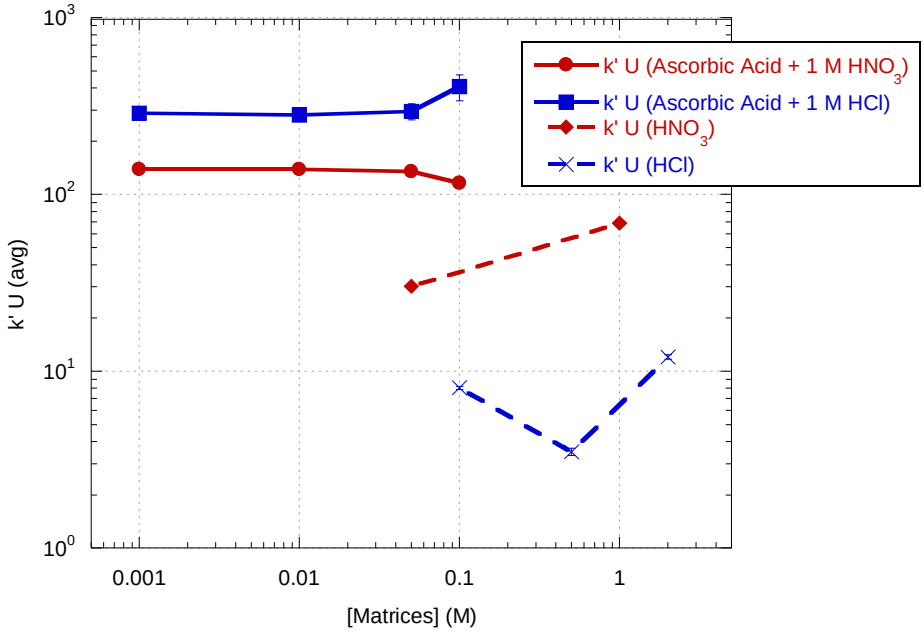

Figure 86. Uranium Adsorption on UTEVA with respect to Ascorbic Acid

In Figure 87, the hydrochloric/oxalic acid and nitric/oxalic mixed matrices the k'_U values are increased up to ~100. It is known that uranyl reacts with oxalate forming complexes such as $[UO_2(C_2O_4)_n]^{2-2n}$ (n = 1 – 3) in aqueous solutions.[124] Since UTEVA tends to form nitrato complexes with the actinides it

is possible that the uranyl oxalate complex is charged as well.[32] The Pu uptake is so low in the hydrochloric/oxalic acid and nitric/oxalic acid matrices that no adsorption was detected and therefore not reported. It is known that Pu(IV) oxalate is insoluble in aqueous solutions 1 M H^+ and therefore was expected to have little to no adsorption to UTEVA.[125] This large decrease in Pu adsorption is probably dictated by the formation of the insoluble plutonium oxalate complex. This large decrease in Pu adsorption will greatly increase the ability to separate Pu from U on UTEVA resin since Pu has no adsorption and U has an increased adsorption the elution of Pu should be achievable in low elution volumes and in high purity. Therefore, the use of oxalic acids could prove very beneficial for U and Pu separations from UTEVA.

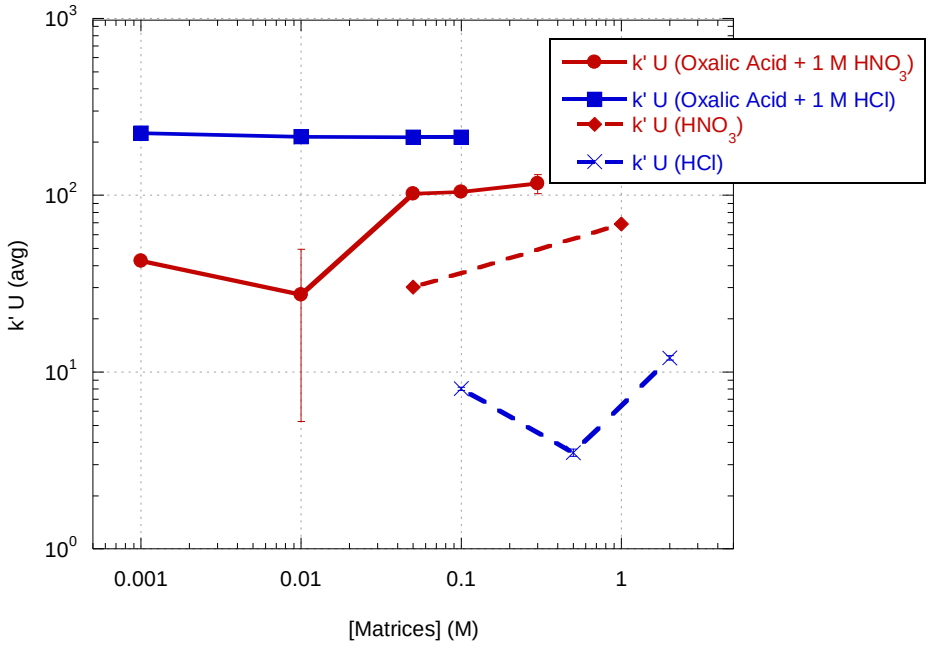

Figure 87. Uranium Adsorption on UTEVA with respect to Oxalic Acid

Sodium Nitrite with DGA resin

Sodium nitrite is often used to manipulate the oxidation states of Pu in order to keep it in its tetravalent state.[125] In Figure 88 and 89, the adsorption of Am and Pu in varying concentrations of sodium nitrate in 1 M HNO_3 or HCl is graphed with respect to the sodium nitrite concentrations for DGA resin. The adsorption of Am and Pu in varying concentrations of nitric and hydrochloric acid is also included in the graph for comparison purposes.

For the sodium nitrite/nitric acid matrices, Am and Pu have similar adsorption which was unexpected since Pu is expected to be in it tetravalent state and therefore would typically have different adsorption than the trivalent Am. For k'_{Am} in sodium nitrite/nitric acid, the $k'_{Am\ (NaNO_2 + 1\ M\ HNO_3)}$ values are close to $k'_{Am\ (HCl)}$, but the k' values gradually increase with the increase in sodium nitrite. The same increase is seen for $k'_{Pu\ (NaNO_2 + 1\ M\ HNO_3)}$, but below 0.05 M $NaNO_2$ no adsorption was detected. Even though $NaNO_2$ was a successful in changing the Pu adsorption, it did not result in a large enough separation factor, but could potentially be used as a Pu stripping agent.

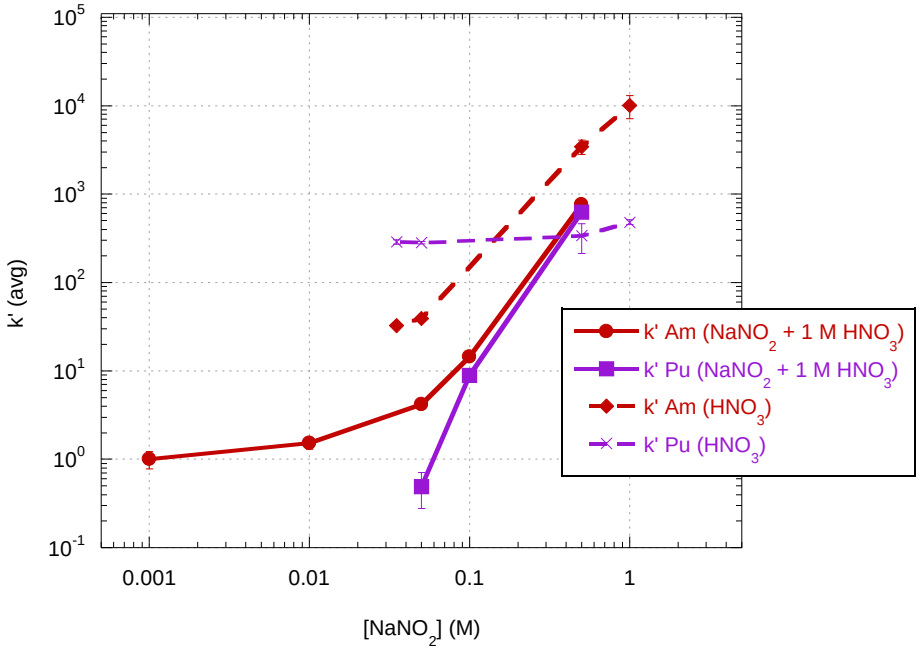

Figure 88. Actinide Adsorption on DGA with varying Sodium Nitrite Concentrations and 1 M HNO_3

In Figure 89, for $k'_{Am\ (NaNO_2 + 1\ M\ HCl)}$, the k' values are consistently ~1000 and $k'_{Pu\ (NaNO_2 + 1\ M\ HCl)}$ varies between 100 and 500. These values greatly differ for those in only nitric and hydrochloric acid and therefore are possibly driven by the sodium nitrite rather than the hydrochloric acid. These mixed matrices do not have a large Am and Pu separation factor on DGA resin and therefore are not advantageous to use for that purpose.

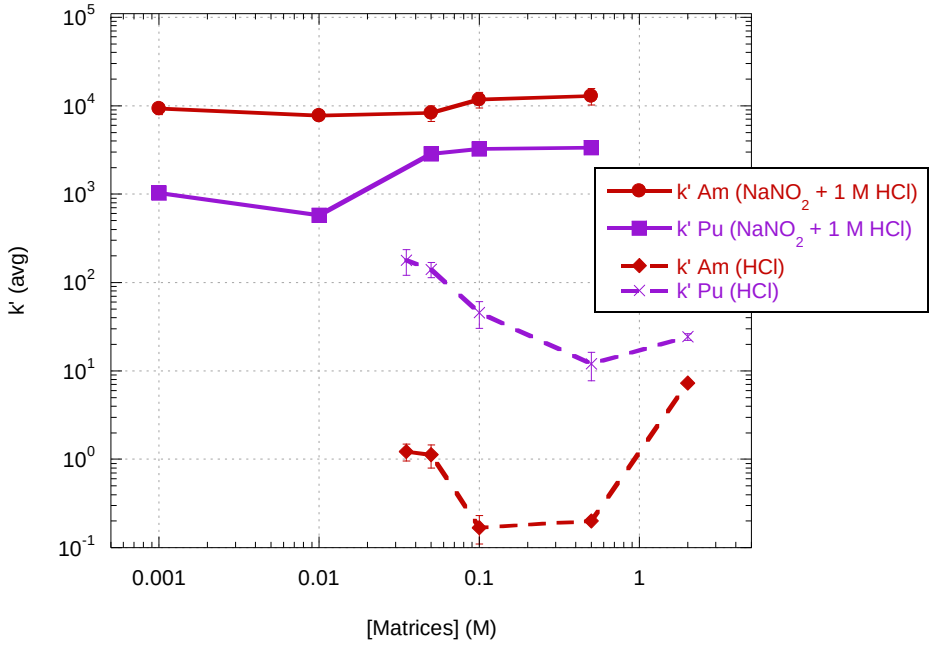

Figure 89. Actinide Adsorption on DGA with varying Sodium Nitrite Concentrations and 1 M HCl

Sodium Nitrite with UTEVA resin

Since it could be very beneficial to separate Pu and U on UTEVA resin, the effects of $NaNO_2$ were also investigated with UTEVA, as seen in Figure 90 and 91. In sodium nitrite/nitric acid matrices, the adsorption for U is higher than $k'_{U\ (HNO3)}$ in 1 M HNO_3. At lower nitrite concentrations, it appears that Pu and U are both in the tetravalent state since they have similar adsorption. As the concentration of sodium nitrite increases the Pu appears to be reduced to its trivalent state, causing its decrease in k'_{Pu} while U stays in the tetravalent state

and maintains generally the same k values. This large decrease in $k'_{Pu\ (NaNO_2 + 1\ M\ HCl)}$ would provide an advantageous separation scheme for Pu and U on UTEVA resin.

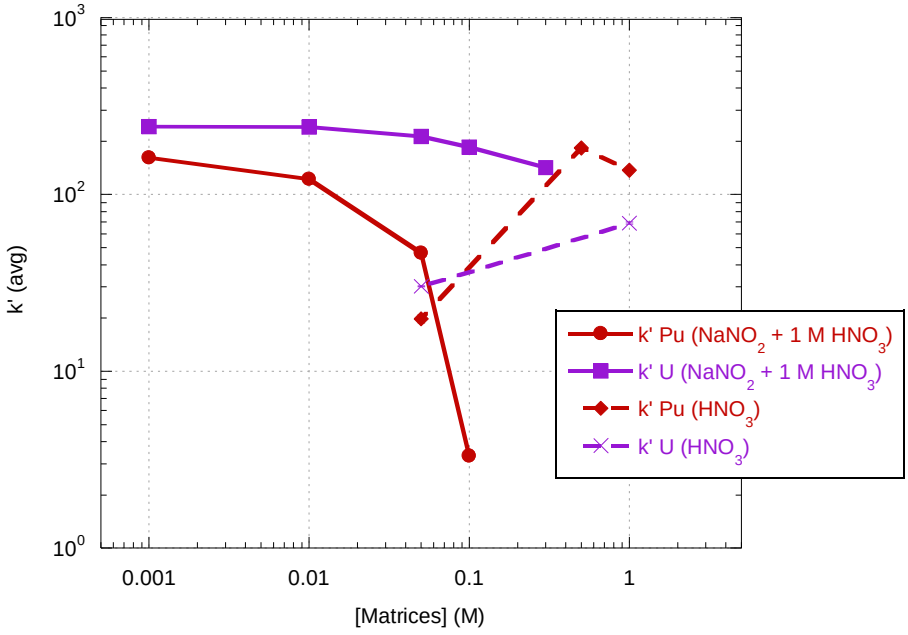

Figure 90. Actinide Adsorption on UTEVA with varying Sodium Nitrite Concentrations in 1 M HNO_3

In Figure 91 sodium nitrite/hydrochloric acid matrices, the $k'_{Pu\ (NaNO_2 + 1\ M\ HCl)}$ matches well with k'_{Am} in 1 M HCl. Therefore, it may be possible that Pu was reduced to its trivalent state in these matrices. Since $k'_{U\ (NaNO_2 + 1\ M\ HCl)}$ is unchanged with the addition of $NaNO_2$, it's unclear if it has been reduced since tetra and hexavalent metals generally absorb about the same amount as seen previously in Figure 49 and 50. Overall, sodium nitrite could be used to separate

Pu from U on UTEVA resin since Pu has little to no adsorption in HCl while U still has considerable adsorption.

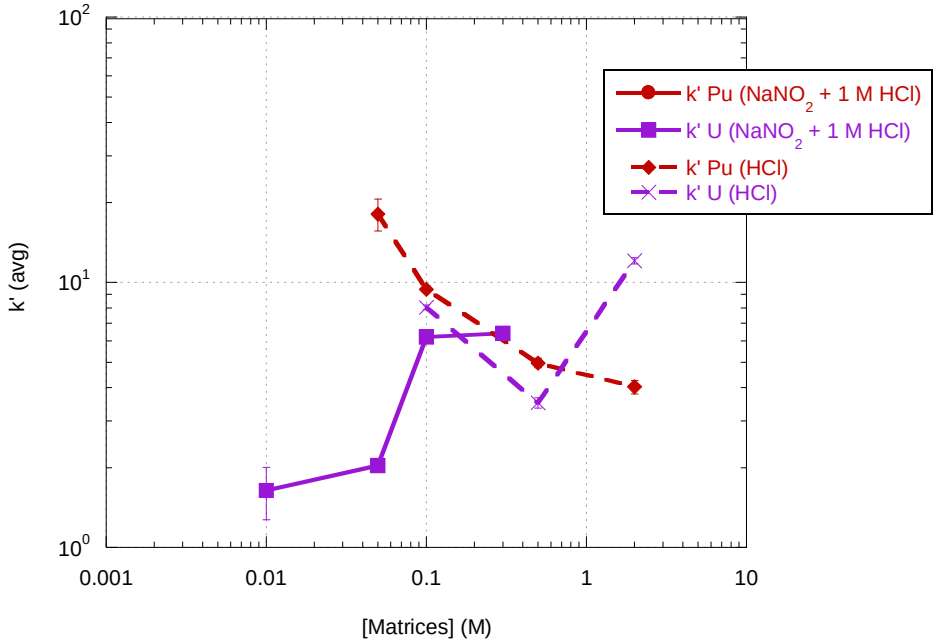

Figure 91. Actinide Adsorption on UTEVA with varying Sodium Nitrite Concentrations in 1 M HCl

Comparison of Complexants and Redox Reagents

In comparing the complexants, it is apparent that many of them achieve the same results even though they are fairly different compounds. As seen in Figure 92, oxalic acid, ascorbic acid, sodium sulfate, and sodium bromide achieve similar k'_{Am} values in 1 M HNO_3. Bromide and sulfate would not be expected to cause any chemical difference, but would be expected to cause a change in adsorption due to differing complex affinities for DGA resin. The

largest effect on k'_{Am} is seen from the addition of sodium nitrite in 1 M HNO_3, where k'_{Am} values drop below those for only nitric acid. The lower sodium nitrite matrices could be beneficial for eluting Am off DGA in a more efficient manner.

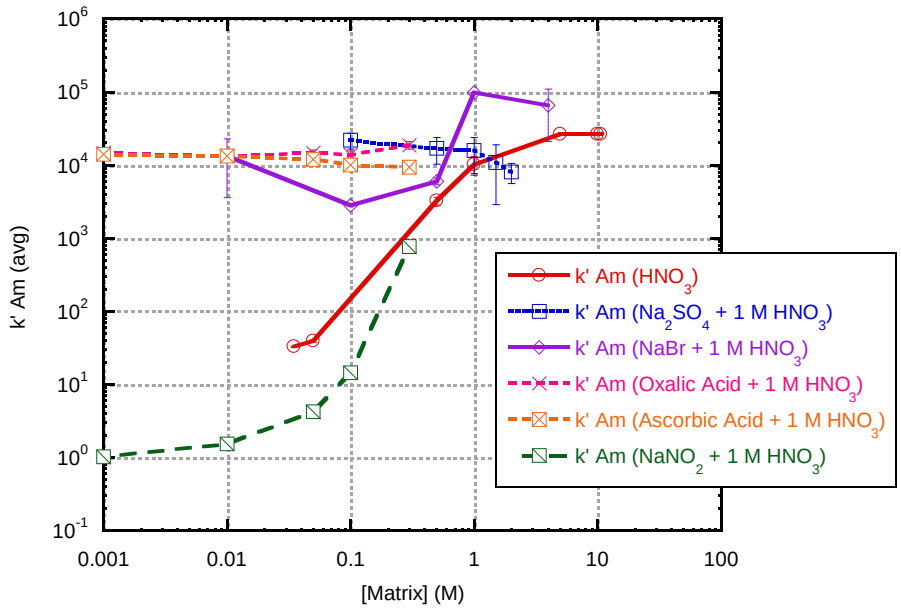

Figure 92. Effects of Added Reagents on Am Adsorption to DGA in 1 M HNO_3

The k'_{Am} values in 1 M HCl are more widely affected than in 1 M HNO_3, as seen in Figure 93, where the k' values for the complexants are more widely separated. It appears that the sodium sulfate is most likely dominated by the Am chloride complex forming with DGA, since the k' values match well with k'_{Am} for pure 1 M HCl. Sodium nitrite gives the highest Am adsorption in 1 M HCl, which is comparable to the highest k'_{Am} value achieved in ~10 M HCl. Sodium bromide also give high k'_{Am} values, but they are below the highest values for $NaNO_2$ and

HCl matrices. For loading and eluting matrices, there does not seem to be any advantage to adding any of the complexants studied as they do not exceed or drop below the values determined for Am adsorption in 1 M HCl.

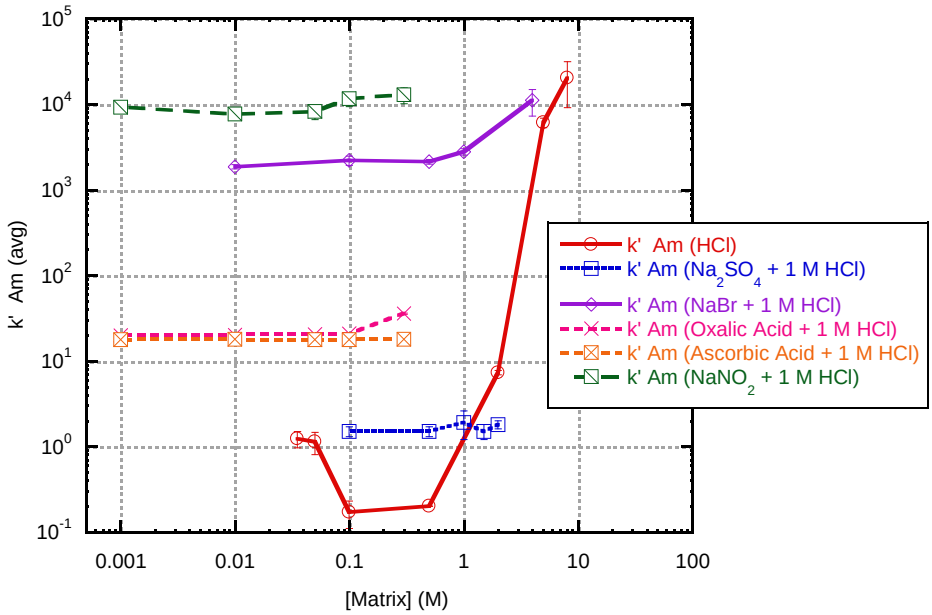

Figure 93. Effects of Added Complexants on Am Adsorption to DGA in 1 M HCl

Manipulating the multiple oxidation states of Pu can be a useful factor to provide additional separation schemes. Therefore, the reducing agents which can take most advantage of that factor can be very beneficial. In Figure 94, the complexants in 1 M HNO_3 are graphed with their effect on Pu adsorption to DGA resin. The only matrix which seems to have much of any effect on Pu adsorption in 1 M HNO_3 is sodium nitrite. In comparing Pu to Am adsorption in the same matrices, they have similar k' value magnitudes and trends, which most likely is

due to Pu being in its trivalent oxidation state. Another matrix which may be of interest for future studies is ascorbic acid because of the decrease at >0.1 M ascorbic acid, but higher concentrations would have to be explored to fully understand the influence of ascorbic acid. Overall for loading purposes, none of the matrices studied show any advantage but sodium nitrite could be a beneficial addition to an elution matrix to elute Pu in 1 M HNO_3.

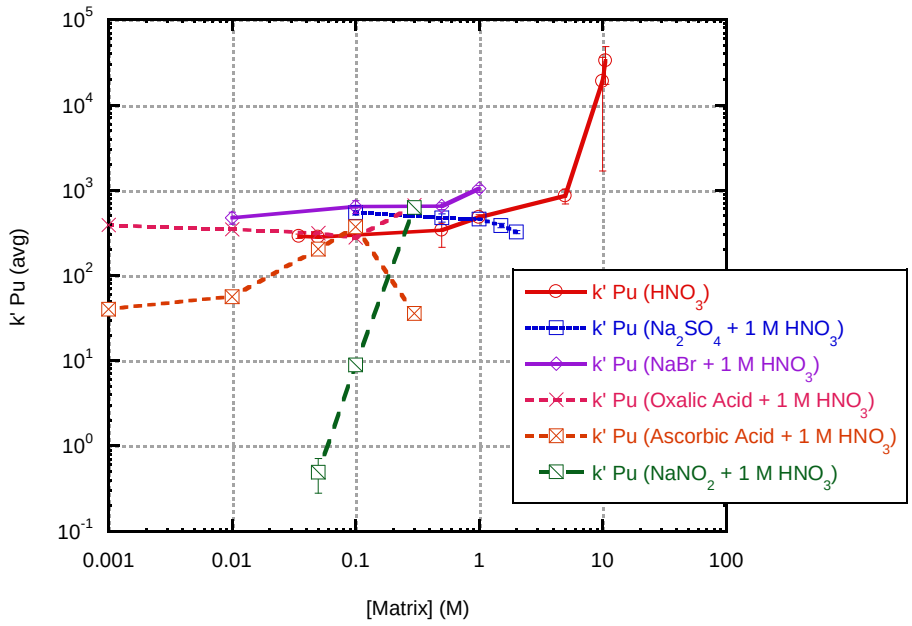

Figure 94. Effects of Added Complexants on Pu Adsorption to DGA in 1 M HNO_3

For Pu adsorption in 1 M HCl with the addition of complexants, in Figure 95, there is a little more variance in the k' values across the concentrations, but the majority of the complexants do not greatly change k'_{Pu} in 1 M HCl, with the exception of $NaNO_2$ and NaBr. The k'_{Pu} value for $NaNO_2$ varies between 100 and

400. Therefore, if the mobile phase is 1 M HCl, the Pu adsorption can be increased by the addition of $NaNO_2$. For NaBr, the increased Pu adsorption is only seen at 1 M NaBr and above. With the addition of sodium sulfate, the k'_{Pu} values decrease and may provide a better elution phase than for HCl matrices alone.

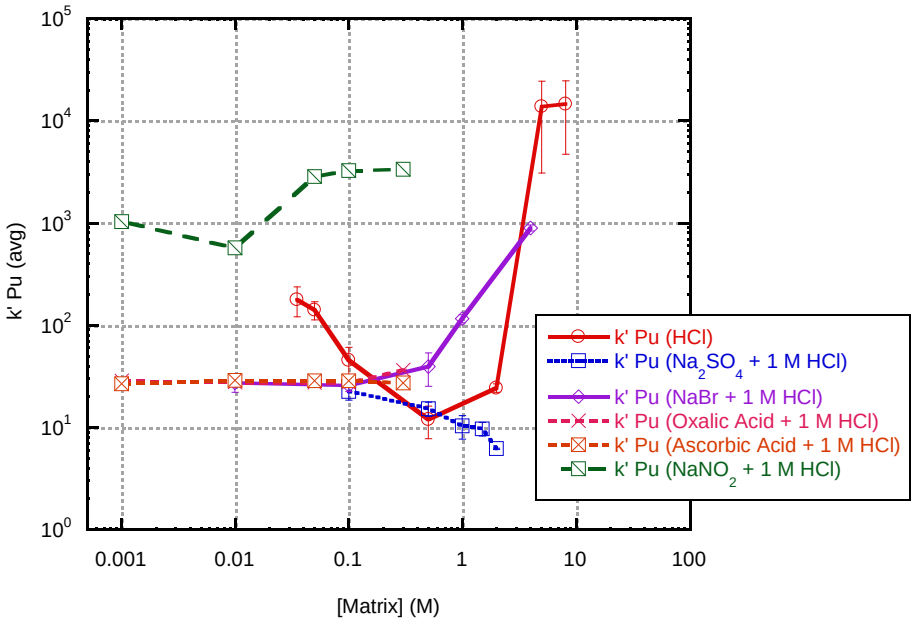

Figure 95. Effects of Added Complexants on Pu Adsorption to DGA in 1 M HCl

Comparison of all Matrices Studied

Since the purpose of this chapter was to identify the optimal separation scheme for potentially separating Am and Pu on a DGA column, the separation of the k' values are of great importance. Therefore the separation factor for Am and Pu in all the matrices studied in this chapter is graphed in Figure 96. The

highest Am and Pu separation factor was achieved on DGA resin in 0.3 M ascorbic acid and 1.0 M HNO_3. This matrix would be the best separation phase in order to elute Pu from DGA while Am is still retained. Due to Am's adsorption properties with DGA, other mobile phases will be needed for stripping Am off the column, such as a mixed hydrochloric matrix with small concentrations of HF.

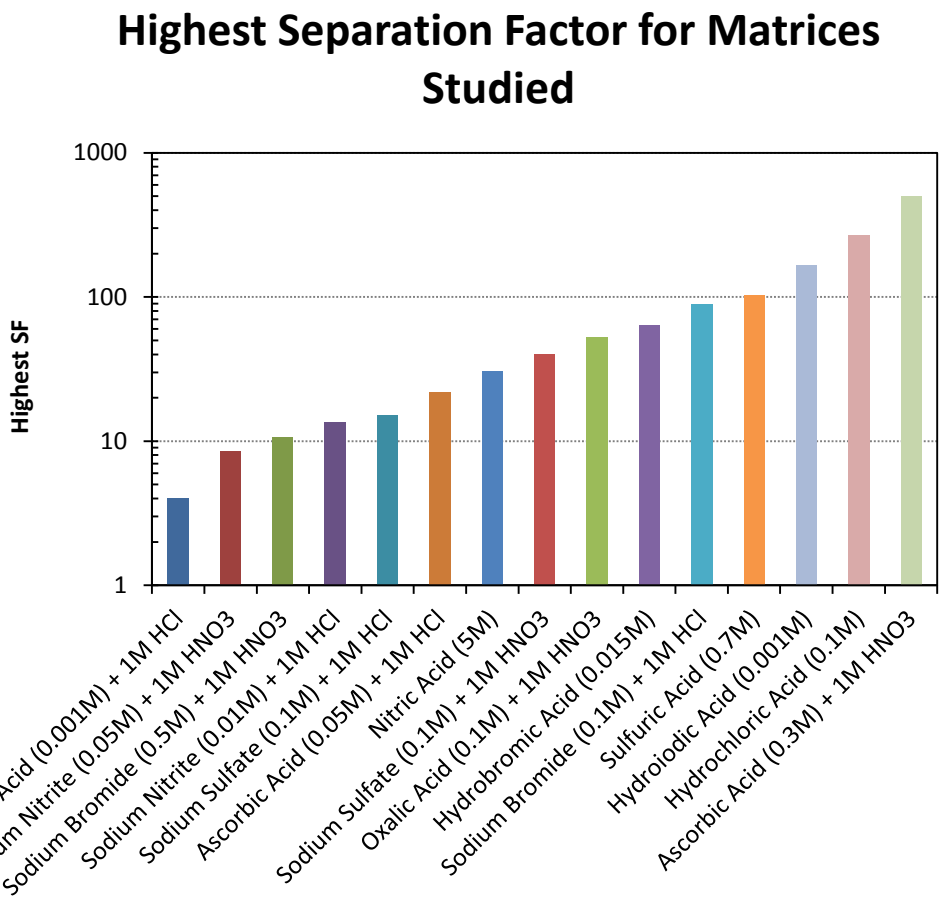

Figure 96. Highest Am and Pu Separation Factor for the Matrices Studied

Section 5.5 Concluding Remarks

For DGA's potential application to the nuclear fuel cycle material accountancy there are multiple separation schemes which could be used. Under the assumption that DGA will be sequentially added to UTEVA resin, it is ideal to separate Pu and Am individually from the DGA column. In this case, it would be important to have a separation scheme which does not take too much volume to separate one from another. Ideally, the Pu and Am would have totally separate, sharp elution peaks which would minimize the elution volume needed.

In the studies performed and discussed in this chapter, the best Pu and Am separation factor was provided by 0.3 M ascorbic acid and 1.0 M HNO_3 matrices, since it enhanced the separation of the k' values better than any other matrix. In this case, it will not be beneficial to elute Am and Pu off DGA since Am's k' values are so high that large elution volumes would be needed. Therefore, instead of focusing only on separation factors, the combination of a reasonable separation factor and the lowering of both the k'_{Pu} and k'_{Am} may prove useful to elute Am and Pu in the same mobile phase. In this scenario, the closest matrixes to meet these requirements are the lower concentrations of HCl.

UTEVA resin was investigated for separating Pu and U using various concentrations of sodium nitrite, ascorbic, and oxalic acid in 1 M HNO_3 and HCl. In these studies, the hydrochloric/sodium nitrite matrices gave the optimal separation scheme where k'_{Pu} was so low it was not detected and k'_{U} was ~1-8. This makes the separation of Pu and U possible on the same mobile phase without too large of elution volumes necessary.

Chapter 6. CHARACTERIZATION OF RESINS FOR NUCLEAR FORENSIC PURPOSES

Section 6.1 Abstract

Federal and international agencies rely on quickly obtained and highly accurate technical data for nuclear forensic investigations. This requires rapid and accurate analysis of a variety of samples and matrices. To advance the analytical timeline of samples, the more rapid and efficient a separation can be made, the shorter the total time from sample acquisition to data analysis. Therefore, in this chapter various studies of DGA and UTEVA resin geared towards their application for separation schemes for post detonation samples are described. In order to ascertain the potential application of separations using DGA and UTEVA for these scenarios, these resins have been characterized for constituents found in soil and urban samples.

Actinide adsorption has been studied widely for UTEVA and DGA resins.[29, 30, 32, 33] Most of the studies in this chapter do not directly involve actinide adsorption, but rather focus on defining the general trends of mono-, di-, and tri- valent metals, which are commonly found in these samples, to identify potential effects, such as competition, synergistic, and antagonistic effects which are explained in Chapter 2. There have been extensive studies performed previously on both DGA and UTEVA resins, as described in Chapter 1 and 2.

The trends and implications of the various metals analyzed in this chapter will be discussed.

Also, a separation scheme was developed and investigated for the separation of stable and activated first row transition metals and actinides of interest from a glass bead, prepared as a simulate for post detonation melt glass. These metals are of interest due to the prompt fast neutron activation occurring after a detonation which can provide information about the device. This separation's efficiency and recoveries will be discussed in this chapter.

Section 6.2 Materials and Methods

Batch Contact Method

Batch contact studies were generally performed as presented earlier but instead of 50 mg of resin, 100 mg samples were used and any variance will be denoted below the figure. For the combined analyte studies, the batch contact study method was previously described in Chapter 2. The resin was preconditioned with 0.5 mL of a desired acid concentration in a 2mL Biospin column which was drained prior to sample addition. Then 1.0 mL of the same concentration of acid and 0.5 mL of radionuclide or metal analyte in 0.1 M of acid was added. The concentrations of the stock acid solutions used were decided based of the fact that the 0.1 M acid metal spike could dilute or concentrate the

acid with its addition, as discussed in Chapter 2. All error bars represent the deviation between replicates. Three replicates were performed for all studies discussed in this chapter.

Column Separation

The columns used for the separation described in this chapter were packed using the slurry packing technique as described in Chapter 2. The 20 mL Evergreen column contained 10 mL of DGA resin preconditioned with 11 M HCl and topped with glass wool and was gravity fed. The total mass of the dissolved glass bead solution was determined and a 5 mL aliquot, was determined by weighing, was analyzed by gamma spectrometry. The total volume of the dissolved glass bead was loaded onto the column. All fractions, 25 mL per fraction, were dried to completeness and reconstituted in 5 mL of acid to retain common geometry for gamma analysis. All samples were placed in LSC vials for gamma analysis. The column was gravity fed.

Due to the high concentrations of calcium relative to the rest of the matrix components, the assumed Ca concentration and the DGA column's working capacity, 7.23 mg Sr/mL resin, was used to determine the volume of the resin needed.[29] It was assumed that Sr and Ca would have the same working capacity. The glass/cement bead was created with equal parts soda lime and Quikrete cement, 1 g each. Quickrete cement consists of an unspecified mixture of hydrate lime, cement and white sands. Since the exact composition of the

cement was proprietary, it was assumed to be composed of 50% Portland cement, the most common cement which also has the highest amount of Ca.[127] Since the Portland cement is known to contain up to 67% CaO and the soda lime is 11.2% $CaCO_3$, it was assumed that roughly 14.2% of the 2 g bead was Ca.[127] Based on the working capacity of DGA, this would necessitate a ~40 mL volume column. Since Horwitz has previously successfully run a column with Sr exceeding the capacity of the column by a factor of 30, 10 mL volume of resin was used.[29]

Reagents

The DGA and UTEVA extraction chromatography resins were obtained from Eichrom Technologies, Inc. All solutions were prepared using deionized water with a resistivity of 18.1 MegaOhm and all reagents used were of reagent grade or better.

Measurements

All radionuclides studied in the batch contact studies in this chapter were analyzed on the assembled gamma spectrometer described in Chapter 2. All samples were counted until 10,000 counts above background were achieved. All stable elements studied using the batch contact method were analyzed by ICP-AES. The column separation fractions were analyzed on HPGe detectors where

peak area analysis and nuclide identification were performed using the in-house program SPECANL. These samples were counted for 2,000 minutes each.

Section 6.3 Batch Contact Studies for Nuclear Forensic Characterization of DGA and UTEVA resin

Nuclear forensic analysis is based around obtaining information from samples which can consist of a wide array of isotopes and matrices in order to provide technical data for attribution. These samples can also originate from a wide variety of sources, such as: smoke detectors, medical isotopes, or post detonation samples. This chapter primarily focuses on separations for post detonation samples. For nuclear forensic analysis, most of the sampling, especially in relation to post-detonation, will be taken near the point of detonation and will potentially consist of soil, vegetation, or urban rubble.

Soil is commonly used nuclear forensic sample due to its simple and easy sampling. As a result it would be highly desirable to create novel separations which could achieve higher recoveries and better purities for a wide variety of nuclear forensic signatures from soil samples. Therefore, the main focus is surrounding soil samples and more specifically the adsorption of some of the elements found in higher abundance. Fully characterizing resins for a variety of metals in the sample will ensure the separation’s trends being unaffected for true samples and may lead to novel partitioning methods.

For post detonation samples, the analytes of interest are signatures which are often used to determine information regarding the initial design and material used in the device. Depending on the desired results, some selective activation and fission products are the preferred analytes for attribution in a post detonation scenario. In this chapter, the column separation performed was focused on activiation products possibly found due to the prompt neutron activation of material used in the initial device. This is elaborated further later in this chapter.

Sodium Adsorption

Sodium is of interest since it is commonly found in many environmental samples and will most likely be a large component of soil samples. The US Geological Survey found on average 12,000 ppm Na in soil for the conterminous US.[128] The adsorption of Na has been previously investigated on DGA and UTEVA. Pourmand reported no adsorption of Na to DGA in nitric and hydrochloric acids.[31] The elution behavior of Na was studied in 2 M HNO_3 for UTEVA resin by Horwitz which showed some retention, but not a highly significant amount.[29]

Initially, Na adsorption was studied on DGA resin by contacting cold 5mM $NaNO_3$ with DGA resin in varying nitric acid concentrations. These samples were analyzed on the ICP-AES. Approximately 1.5 ppm was found in the method blanks that were contacted with the resin, which complicated the data analysis. Since the resin was used as received and not rinsed prior to the batch study, it is

possible that the sodium was adsorbed onto the resin from its synthesis. The extraction phase of TODGA ligand used during the synthesis of DGA resin consisted of $NaHCO_3$ and NaCl solutions, which were directly added into a rotovap together with the inert support.[29] In this evaporation step, the Na may have adsorbed and is therefore contributing to the Na being removed from the resin upon contact with the acid.

In order to investigate the possibility of Na being sorbed to DGA from its synthesis, 100 mg of DGA resin was contacted with 1.5 mL of various concentrations of nitric and hydrochloric acid. The eluted acid was then analyzed on the ICP-AES to determine the Na concentration. The results from this study are presented in Figure 97. The eluted acid had >1 ppm Na.

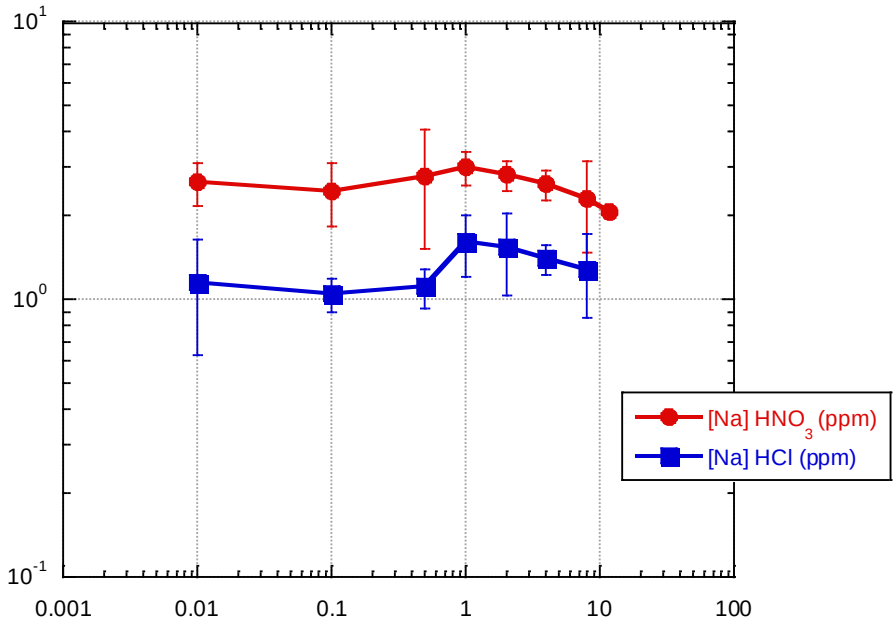

Figure 97. Sodium Detected in Rinses of DGA Resin from Nitric and Hydrochloric Acid

More sodium was detected in the nitric acid rinses than the hydrochloric rinses, with the exception of 8 M concentrations. The amount of sodium eluting from the resin seems independent of the acid concentration, since it is consistent across all concentrations, which may be due to the fact that the Na is present in such a low concentration on the resin. The volume of rinses and replicates needed to fully remove Na was studied; it was found that 3 rinses of 1.5 mL in each rinse were necessary.

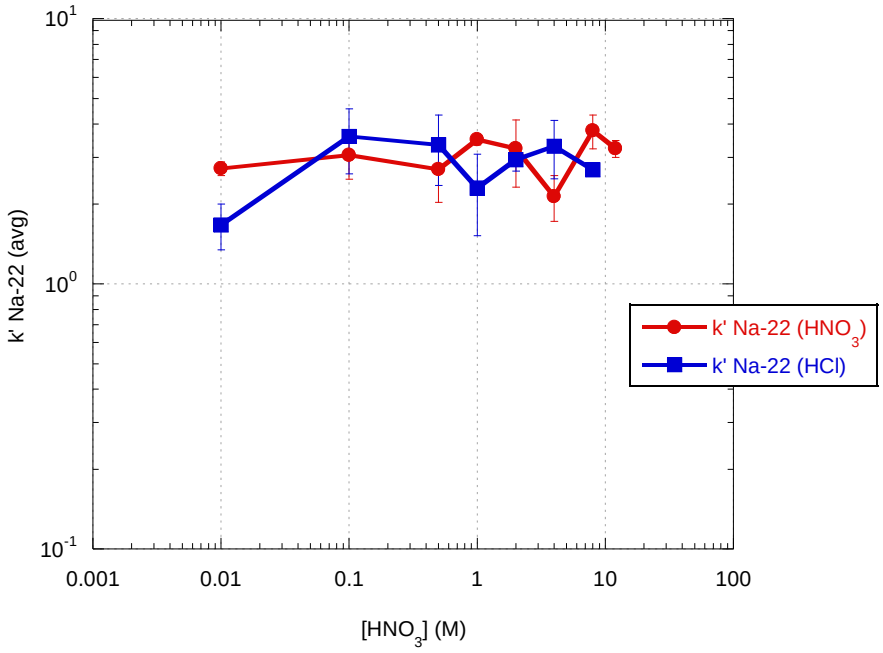

Figure 98. Na-22 Adsorption to DGA Resin in Various Nitric and Hydrochloric Acid Concentrations

Since DGA has sodium adsorbed to the resin, as discussed in the previous paragraph, complicating the ICP-AES analysis, the determination of k'_{Na} was performed using Na-22. In order to remove the sodium found in the DGA resin, the resin was preconditioned with 1.5 mL of the desired acid three times. The acid was filtered off after each rinse and prior to the addition of Na-22. The data is represented in Figure 98 and shows $K'_{Na\text{-}22}$ ~3 for both nitric and hydrochloric matrices. This k' value represents some adsorption of sodium to DGA. It is surprising that these results do not show any difference in adsorption between nitric and hydrochloric acid, even though a difference was previously seen in the rinses. This discrepancy may be due to the error not representing the total error of the procedure. This variance may also be due to the detection limits of the instruments utilized. The rinses were analyzed by ICP-AES and the Na-22 batch contact studies were analyzed on a NaI detector. This k'_{Na} is higher than any sodium adsorption values for DGA previously published. The difference of Na adsorption is most likely due to the extensive rinses prior to the studies and the use of Na-22. The use of a radionuclide allows for lower detection limits. Also, even though Pourmand et al. preconditioned the DGA, they may not have used enough volume in order to fully rinse off the Na and therefore giving no adsorption.[31] Even though these values are higher than previously published, they are most likely not high enough to cause considerable effects on other analytes' adsorptions.

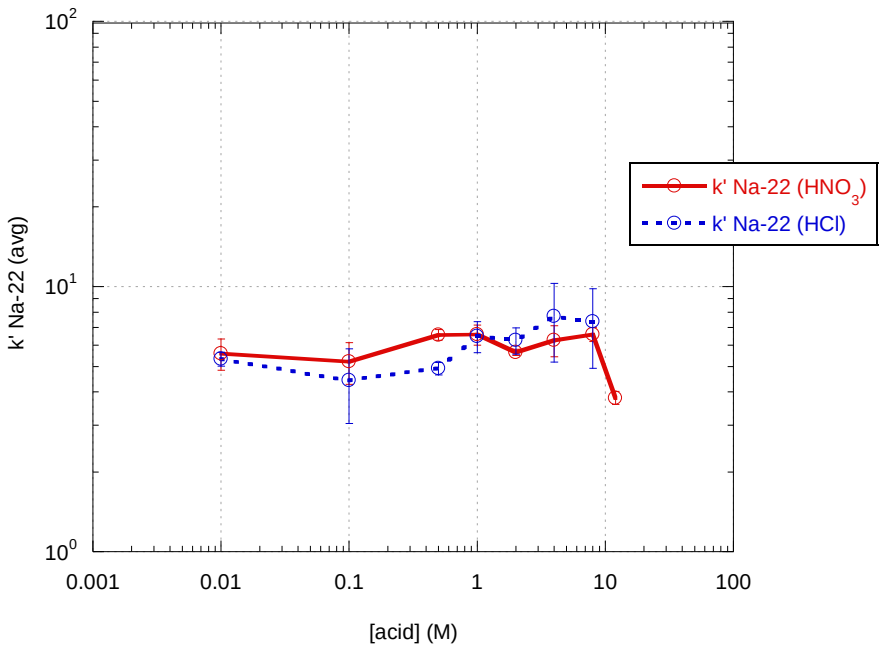

Figure 99. Adsorption of Na-22 to UTEVA in Various Nitric and Hydrochloric Acid Concentrations

The adsorption of sodium using Na-22 was also studied on UTEVA resin from nitric and hydrochloric acids. There is no data available in the literature for the adsorption of sodium to UTEVA resin. The $k'_{Na\text{-}22}$ values are ~4-8 which may cause some interference if it is present in excess and/or is competing with other metals of the same affinity. This result is not completely unexpected, since in Horwitz' study of Na on UTEVA in 2 M HNO_3, the elution trends did show some retention with k' ~4, which matches well with the results in Figure 99.[29] For those metals with higher affinities band broadening could occur if Na is largely in excess, but no large interference effects are expected for columns operated

under its working capacity. Therefore, separations of samples with high sodium concentrations should not greatly veer from expected trends.

Aluminum Adsorption and Effects

The adsorption of aluminum is of interest since aluminum is often found in soils and aluminum clays in fairly high concentrations. An average concentration of 72,000 ppm Al(III) has been reported by the U.S. Geological Survey.[116]. Even though Al is found in a variety of forms in soil, after digestion and dissolution the aluminum will be converted to its trivalent state, which is more readily dissolved. Therefore, the amount of aluminum dissolved could greatly exceed the quantity of any analyte of interest for nuclear forensic analysis.

Even though ionic aluminum is trivalent, like Am, the ion is below the preferred ionic radii for DGA adsorption, discussed earlier, which therefore decreases its adsorption to DGA. Horwitz found aluminum to have k' <2 for all concentrations of nitric and hydrochloric acids on DGA resin.[29] The same trends are seen in Figure 100, where $k'_{Am\text{-}Al^*}$ or $k'_{Pu\text{-}Al^*}$ in 1M HNO_3 does not exceed 4. At 1mM Al^{3+}, the $k'_{Am\text{-}Al^*}$ and $k'_{Pu\text{-}Al^*}$ was below detectable limits and consequently not reported. There was no affect seen on Am or Pu adsorption across all aluminum concentrations, which was expected due to the low k'_{Al} values. No effects on a separation performed in nitric acid would be expected due to the presence of Al(III).

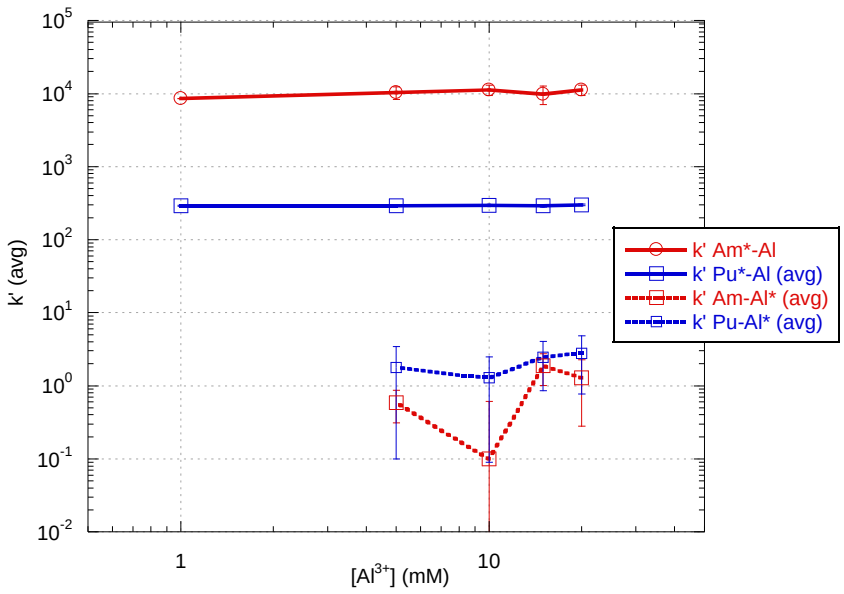

Figure 100. Effects of Al on Actinide Adsorption to DGA in 1 M HNO_3

In Figure 101, the adsorption of trivalent Al has similar magnitudes as Am. It appears that at 5 mM Al^{3+}, the maximum capacity is reached and therefore the k' for Al decreases with increasing aluminum concentration. No aluminum adsorption is reported for 1 mM Al^{3+} since there was no detectable adsorption. The k'_{Am} is generally unaffected by the addition of $AlCl_3$. The $k'_{Pu^*\text{-}Al}$ seems to be increased above 5 mM Al^{3+} concentrations, this may be due to a salting out effect caused by the $AlCl_3$ salt, but no direct correlation was found. An additional study at higher concentrations of $AlCl_3$ salt would be beneficial to elucidate the effects.

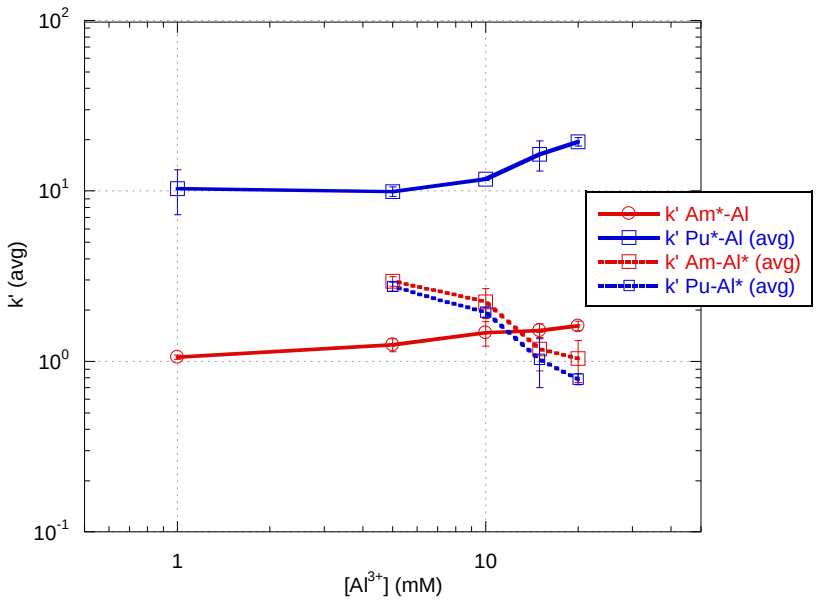

Figure 101. Effects of Aluminum on Actinide Adsorption to DGA in 1 M HCl

Calcium Adsorption and Effects

Calcium is one of the largest components of soil, with average concentrations ~24,000 ppm, and could therefore cause large changes in adsorption characteristics for various analytes.[128] Adsorption characteristics of Sr on Sr extraction chromatography resin is suppressed in the presence of 0.5 M Ca concentrations or higher.[129] This was surprising, since Ca was determined to have a lower affinity for the resin than Sr. Even though calcium is divalent and its adsorption to DGA is expected to be fairly low, there could still be effects caused by the excess Ca present in the samples.

In Figure 102, the maximum $k'_{Am\text{-}Ca^*}$ and $k'_{Pu\text{-}Ca^*}$ values in 1 M HNO_3 were an order of magnitude lower than those previously reported for Ca alone by Horwitz et al. where k'_{Ca} ~100.[29] The observed difference may be due to the presence of the actinides, but that due to the low relative concentration. It is also possible that the difference between the amount of Calcium used in comparison to the amount of DGA in these studies versus Horwitz et al.'s may be responsible for the difference of the k'_{Ca} values. The maximum capacity for Ca is reached at 5 mM Ca^{2+} followed by a decrease in k'_{Ca} values at higher concentrations.

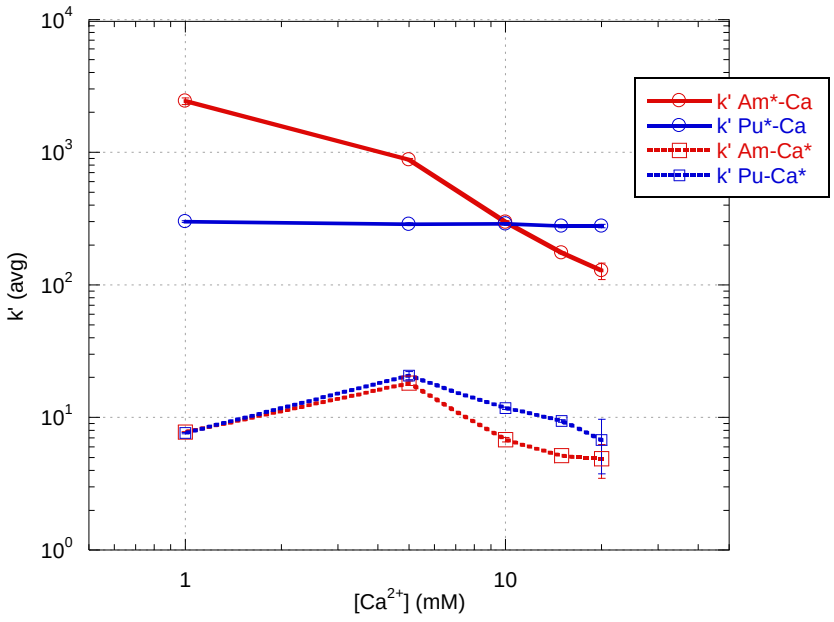

Figure 102. Calcium Effects on Actinide Adsorption to DGA in 1 M HNO_3

The Pu adsorption characteristics are unchanged in the presence of calcium, which most likely means that the Pu nitrate complex offers the more energetically stable complex than calcium nitrate. In contrast, the k'_{Am} values are effected by the addition of $Ca(NO_3)_2$. As the calcium nitrate concentration increases, the k'_{Am} values decrease. Even at the 1 mM Ca^{2+} concentration, the $k'_{Am^*\text{-}Ca}$, ~2,000, is noticeably lower than k'_{Am} in only 1 M HNO_3, ~10,000; so, even smaller amounts of Ca^{2+} seem to affect trivalent actinide adsorption. There is possibly a competition reaction between Ca and Am where $Ca(NO_3)_2$ has the more favorable complex with DGA. It is more likely is due to the large amount of Ca^{2+} in relation to the amount of Am^{3+} where DGA's preference is overwhelmed by the amount of Ca present. Therefore, it would be expected that Am adsorption to DGA resin in nitric acid would be considerably affected if Ca exceeded the capacity of the column, but only moderately if the capacity is maintained.

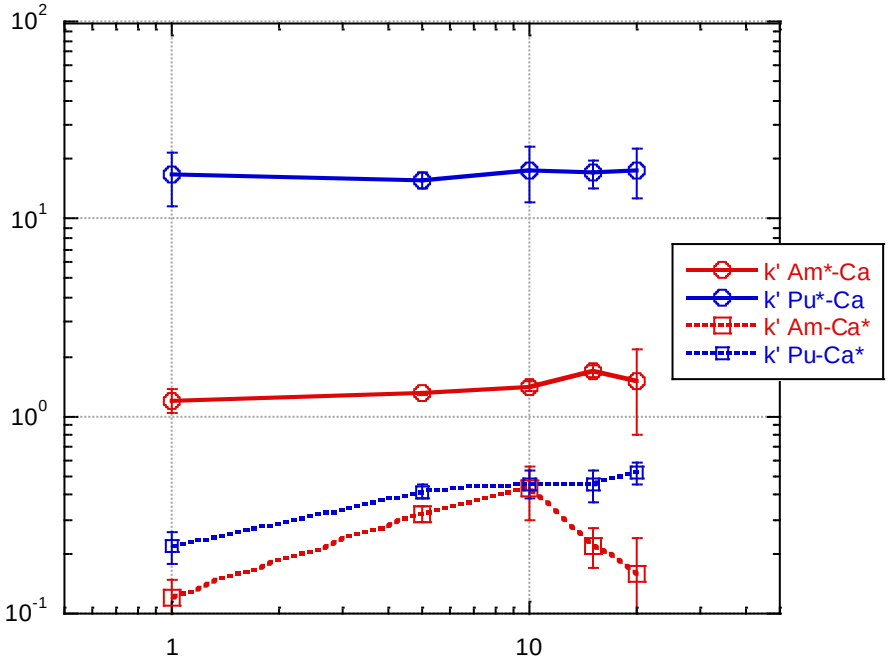

Figure 103. Calcium Effects on Actinide Adsorption to DGA in 1 M HCl

The calcium adsorption, k' ~0.3, in hydrochloric acid determined by Horwitz et al., matches well with the $k'_{Actinide\text{-}Ca^*}$ values of 0.2-0.4. It appears that the maximum capacity is not well defined for Ca in hydrochloric matrices, since $k'_{Pu\text{-}Ca^*}$ does not decrease with increasing Ca^{2+} concentrations. It seems unlikely that there is additional calcium chloride complexed in the inner sphere but it may be loosely in the outer sphere. To define the calcium maximum capacity for DGA in hydrochloric matrices, elution profiles could provide more detailed information. The adsorption of the actinides are unaffected by the addition of calcium.

Scandium Adsorption

Although Sc is not commonly found in soils, it may be found in post detonation samples due to prompt fast neutron activation of metals found in a nuclear bomb. There has been no published data on scandium adsorption to DGA or UTEVA resins. It is expected that scandium may act similarly to the lanthanides and trivalent actinides. Since scandium has much smaller ionic radii than the lanthanides and actinides, it may not have a different affinity to DGA or UTEVA.[110, 111]

In Figure 104, the adsorption of scandium to DGA resin in varying concentrations of nitric and hydrochloric acid is illustrated. The scandium adsorption is highly dependent on nitric and hydrochloric acid concentrations. For nitric acid matrices, scandium has k' > 2,000 and reaches the minimum detectable limit at 10^6. Scandium would readily adsorb to DGA resin in nitric acid matrices, but it would prove difficult with such high adsorption to desorb scandium in nitric acid. In hydrochloric acid, the lowest k' value is ~30 and reaches the maximum k' value, based on the MDL of the IPC-AES, ~10,000. Since Sc tends to hydrolyze in low pH solutions, the raised adsorption at 0.01 and 0.1 M HCl may be due to partial hydrolysis of Sc.[130, 131] For Sc^{3+} in 1 M $NaClO_4$ solutions the pKa is 5.15 for the formation of $ScOH^{2+}$.[132] Further studies are needed to confirm the reason for such a trend.

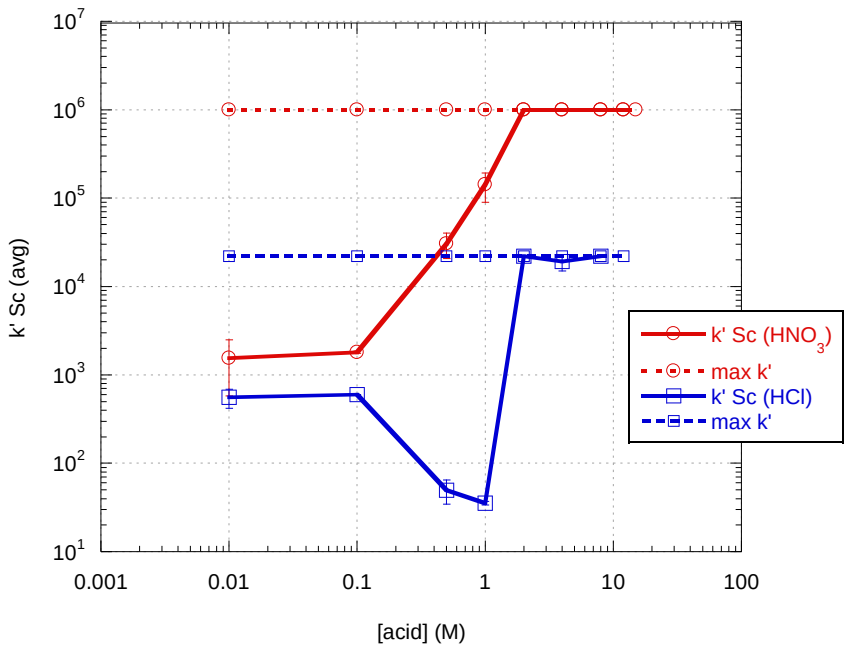

Figure 104. Scandium Adsorption to DGA in Nitric and Hydrochloric Acid

max k' is the highest k' value achievable due to the detection limit of the ICP-AES

Even with the lower k' values, in comparison with the nitric matrix, it may not be possible to remove Sc from the resin using hydrochloric acid. Therefore, other complexants or acids would most likely need to be employed to create low enough k'_{Sc} values to achieve an efficient elution of Sc. In a separation, scandium would most likely elute off with the lanthanides and/or possibly the actinides due to their adsorption similarities in nitric and hydrochloric acid concentrations, seen in the below figure.

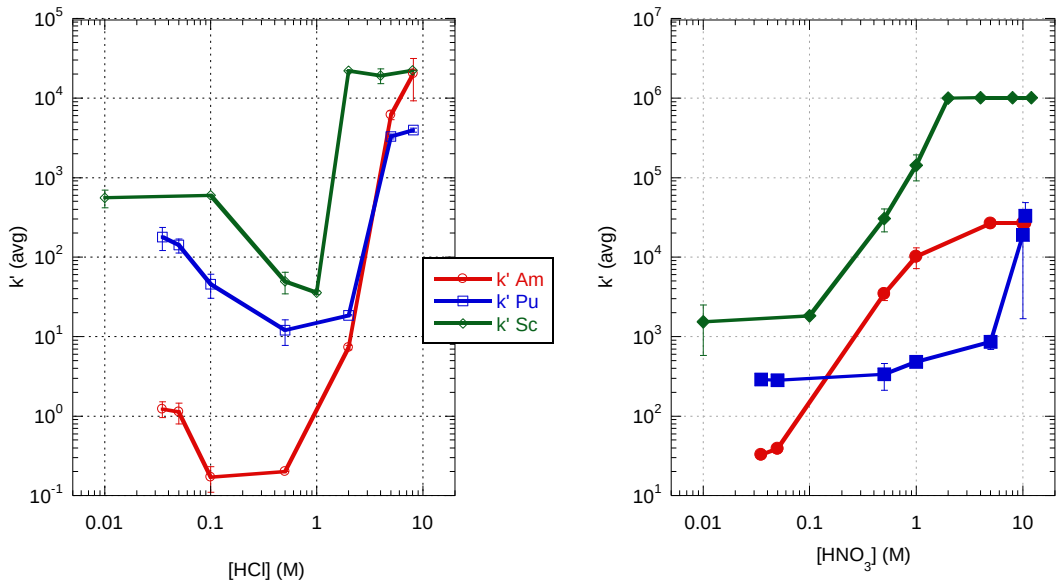

Figure 105. Comparison of Scandium to Americium and Plutonium Adsorption to DGA resin

Scandium adsorption to UTEVA resin was studied in various nitric and hydrochloric acid concentrations and the results are shown in Figure 106. Due to the similarity in charge density, yttrium and scandium are expected to have the same adsorption characteristics. Horwitz et al. studied the elution characteristics of yttrium on UTEVA in 2 M HNO_3, which showed little to no retention on a column.[30] This yttrium adsorption data matches well with those seen for 1 M HNO_3, where k'_{Sc} ~2; although, the scandium adsorption does increase with the increased nitric acid concentration > 5 M HNO_3. There is large a variability of the k'_{Sc} in hydrochloric acid, ~0.8 to 200. Even though these k' values have different magnitudes, they have similar trends to those seen for Sc in hydrochloric acid on DGA. This may mean that this trend is more due to the chemical form of Sc in

HCl than the chemistry between the scandium complex and the resin. The range of the k' values would allow for scandium adsorption in high acid concentrations, > 5 M, and elution at lower concentrations, < 5 M HNO_3 and between 0.1 M and 5 M HCl.

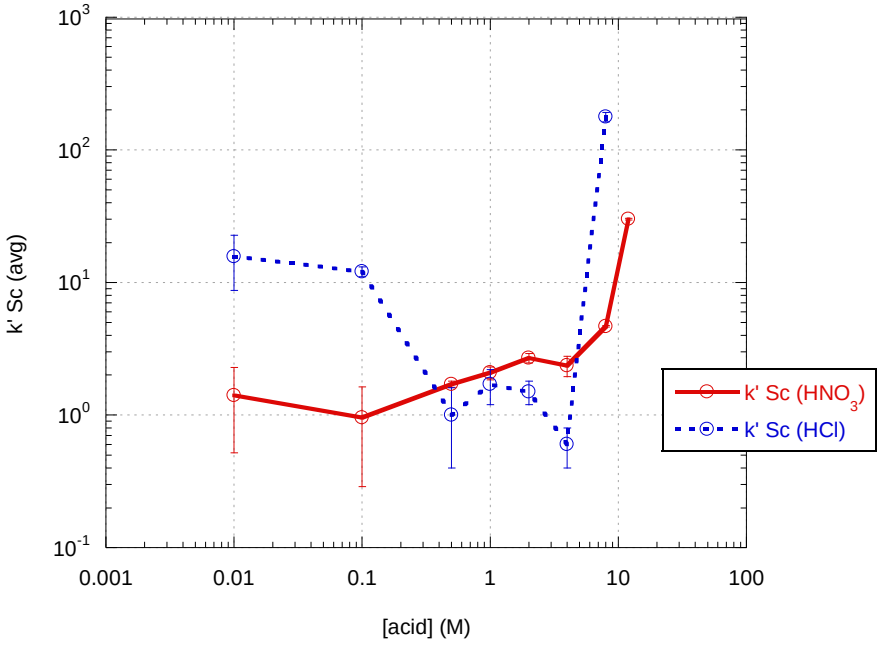

Figure 106. Scandium Adsorption to UTEVA in Nitric and Hydrochloric Acid

Cobalt Adsorption

Cobalt adsorption is also of interest due to prompt fast neutron. Also, there has been no published literature on cobalt's adsorption to UTEVA resin. As a result, the radiotracer Co-60 was used to study cobalt's adsorption to UTEVA in

nitric and hydrochloric acid. DGA was not investigated since data has been previously published by Horwitz et al.[29]

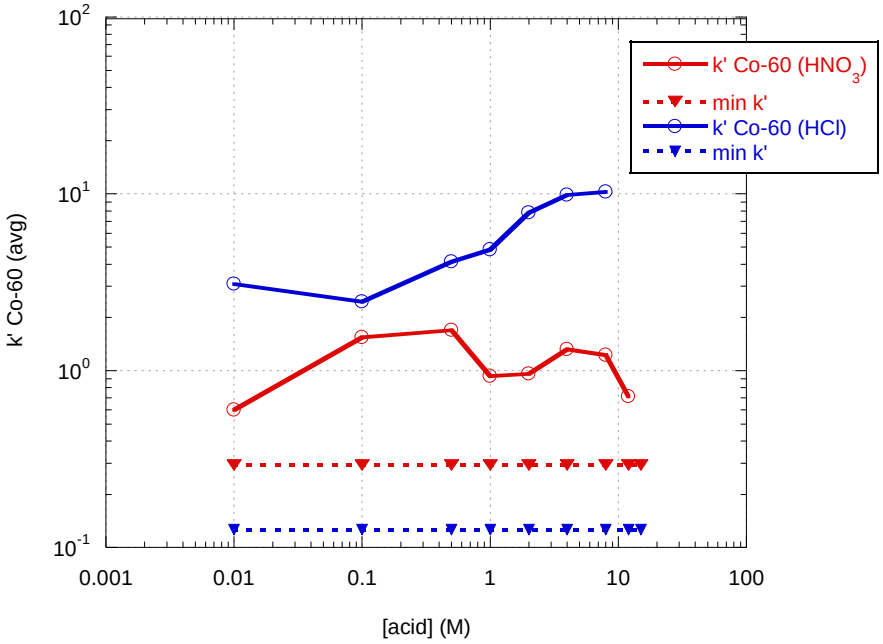

Figure 107. Co-60 Adsorption to UTEVA in Nitric and Hydrochloric Acid

k' min is the lowest k' value achievable based on the instrument detection limits

As seen in Figure 107, cobalt has very little affinity for UTEVA resin in nitric acid matrices where $k'_{Co\text{-}60}$ ~1. These low k' values were not a surprise, since other divalent metals have similar k' values in nitric acid.[29] The adsorption of $k'_{Co\text{-}60}$ is slightly higher in hydrochloric acid where a peak is reached at 5 M, with k' ~ 10. Based on these results it may be possible to adsorb cobalt onto UTEVA in 5 M HCl and elute the cobalt off at lower concentrations of

HCl. Due to the lower cobalt k' values it unlikely that Co has an effect on the adsorption of other metal's with high k' values in nitric acid, but possibly in hydrochloric acid.

Lutetium Adsorption

Lanthanides are of interest since they are a part of the spectrum of fission products from a nuclear device, which could be seen in a post detonation scenario. Even though Horwitz studied lanthanide elution behavior from UTEVA, in 2 M HNO_3, there is no detailed information for the total trends across varying concentrations of nitric and hydrochloric acid.[33] Although other lanthanides have been characterized for their effects on actinide adsorption to UTEVA in Chapter 4, the trends based on the acid concentrations were not investigated. Therefore, Lu-173 was used to identify the adsorption characteristics, as seen in Figure 108.

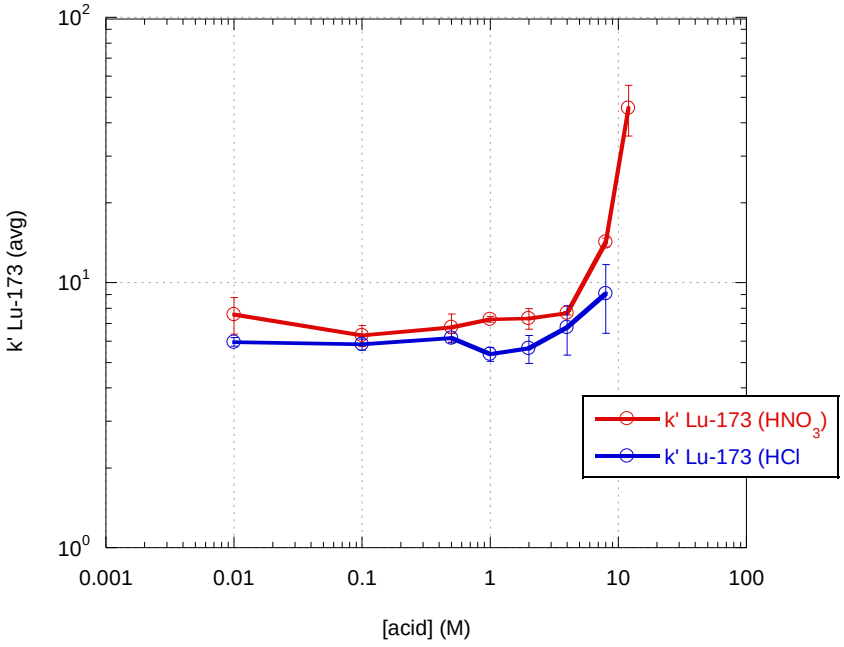

Figure 108. Adsorption of Lu-173 to UTEVA in Nitric and Hydrochloric Acid

Since lanthanides have similar chemistry to Am, Lu was expected to have similar adsorption to UTEVA.[110] As shown in the below figure, the k'_{Am} in 1 M nitric acid was ~ 0.1 and in 1 M hydrochloric acids was ~1. Up to 5 M HNO_3, k'_{Lu-173} was determined to be ~ 8 and increased up to 50 above 5 M HNO_3. This Lu affinity is higher than Am's. This result was not completely unexpected since the same trends are seen on DGA. This higher preference for Lu is most likely due to the larger charge density of Lu compared to Am which forms more stable complexes with UTEVA. No other lanthanides have been studied for their adsorption in varying nitric and hydrochloric acid concentrations therefore a comparison across the lanthanide series is not possible. For all hydrochloric

concentrations, the $k'_{Lu\text{-}173}$ stays fairly constant and is independent, up to 8M HCl, of the increased hydrochloric acid concentration. It is possible and likely that higher concentrations of HCl would lead to higher adsorption as the increased Cl^- concentrations will drive the formation of $LuCl_3$. Overall at these concentrations and matrices studied, UTEVA would not be a useful resin for separation of lutetium from a complex samples since the affinity of Lu will match many other metals and a pure separation would prove difficult.

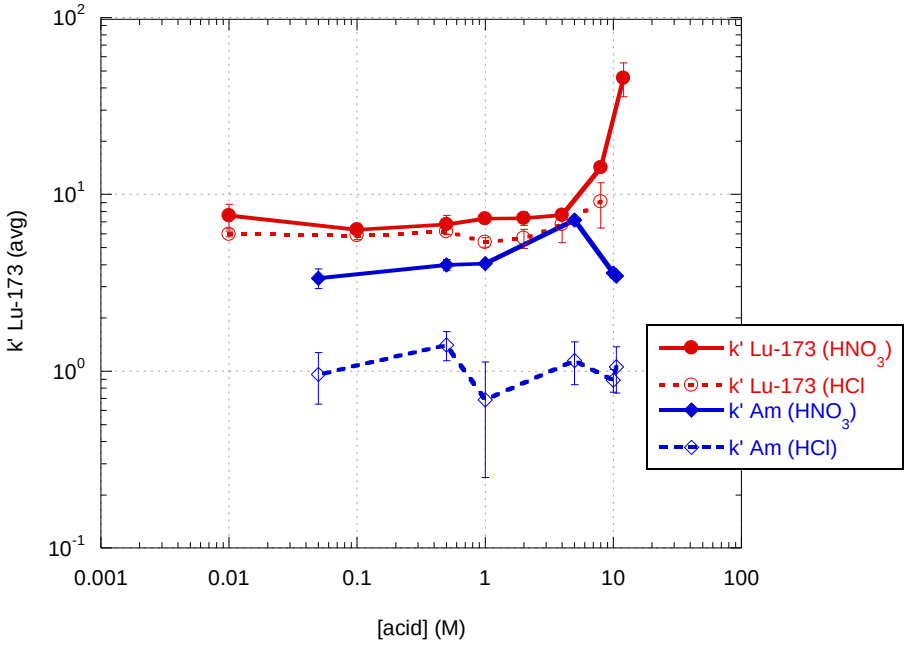

Figure 109. Comparison of Lutetium and Americium Adsorption to UTEVA resin

Bismuth Adsorption

Bismuth is of interest for post detonation scenarios because information regarding a nuclear device's original material can be deduced from its isotopic ratios.[6] These isotopic ratios are often determined by analysis on ICP-MS. In order to identify these ratios with high certainty, due to the isobaric overlaps the sample matrix introduced into the ICP-MS will need to be simple, or bismuth be separated from the rest of the sample prior to instrument introduction. Bi is trivalent and has a fairly large ionic radius in comparison to the lanthanides and actinides. [110, 112] Since UTEVA has not shown any significant preference for trivalent metals, such as previously discussed Lu and Am, Bi is not expected to have strong adsorption characteristics to UTEVA resin in nitric and hydrochloric acids.

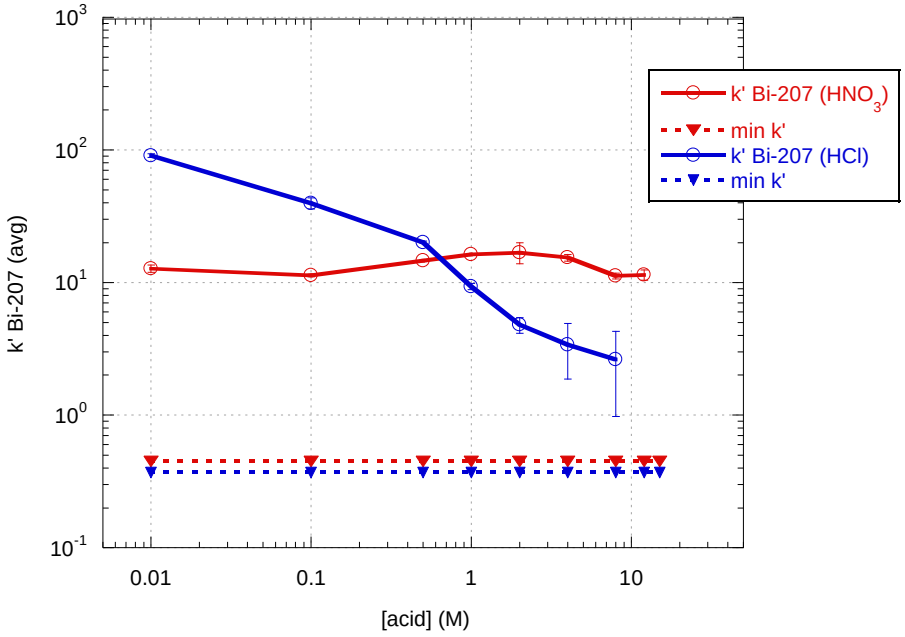

Figure 110. Adsorption of Bi-207 to UTEVA in Nitric and Hydrochloric Acid

k' min is the lowest k' value achievable based on the instrument detection limits

In Figure 110, the trends for bismuth adsorption in nitric acid correlate well with the magnitude seen for lutetium adsorption. The k'_{Bi} varies between 3 and 100 where the highest adsorption is seen at the lowest acid concentration and gradually decreases with the increasing acid concentration. This may be due to polymerization of bismuth found in low acid concentrations.[132] The H^+ concentrations changes the degrees of aggregation where the lower concentrations have higher polynuclear species.[132] Hydrolysis occurs more readily in strong acids or in higher pH solutions.[132] Therefore, hydrolysis would most likely occur in nitric acid over hydrochloric acid due to the difference in

strength where hydrochloric acid, pKa ~$1.3 \cdot 10^6$, and nitric acid pKa ~24.[133] Bismuth hydrolysis was studied in perchloric acid, which is stronger than both nitric and hydrochloric acid, and below 1 M 50% of the 0.5 M Bi was found to be hydrolyzed.[134] Therefore, it can be assumed that in nitric acid the majority of the Bi would be hydrolyzed, and the decreased adsorption of Bi at increased HCl concentrations may be due to the suppression of hydrolysis. The decrease in Bi k' values as the acid HCl concentrations increases, which may be due to suppression of bismuth hydrolysis and the production of ionic Bi. A less favorable neutral complex may be formed with the ionic Bi than the hydrolyzed form with UTEVA which then results in lower k'_{Bi} values. Further research is needed to confirm the formation of hydrolysis.

Section 6.4 Column Separations for Nuclear Forensic Purposes

The separation described in this section is directed towards glass/cement hybrid beads which were made to model melt glass beads possibly found in post detonation scenarios in an urban environment. Since these beads have very complex matrices, the most abundant components were taken into consideration for the separation and are listed in Table 8.

Table 8. Materials Added into the Glass Beads and their Main Compounds [127]

Material	Main Compounds
Glass	SiO_2, Na_2O, CaO, MgO, Al_2O_3
Cement	CaO, SiO_2, Al_2O_3, Fe_2O_3, $CaSO_4 \bullet H_2O$

The activation products incorporated in the glass beads were created by irradiating four metal foil targets, titanium, iron, nickel, and gold. These foils were irradiated by various collaborators from LLNL and LANL using fast neutrons and the (n,p) nuclear reaction created various isotopes of scandium, manganese, cobalt, and platinum isotopes, respectively. The isotopes expected to form were based off of the natural abundance of the stable isotopes of the original metal targets, listed in Table 9. Not all starting isotopes, such as ^{59}Co, ^{197}Au, ^{198}Au, had (n,p) reactions as their dominant reaction, but instead underwent (n,2n) reactions, an example is listed below.

$$^{197}Au \xrightarrow{(n,2n),\ \sigma=2.132} {}^{196}Au \xrightarrow{(n,2n),\ \sigma=1.976} {}^{195}Au \xrightarrow{(n,2n),\ \sigma=0.8849} {}^{194}Au$$

In this case, the change in isotopes of gold and not platinum will be the telling sign of neutron flux. Since platinum is not a potential activation product, it will not be of importance for the separation. Due to the half-lives, and time that passed prior to separation and analysis, Sc-46, Mn-54, Co-58, and Co-60 are the isotopes of interest in the separation. It is important to note that the concentrations of Ti(IV), Sc(III), Fe(III), Ni(II), Co(II), and Gold(III) were not selected to represent true concentrations found in field samples. Therefore, this separation will only give a general idea of the possible separations schemes.

Table 9. Foil Composition and 14.1 MeV (n,p) Reaction Products

Element	Isotope	Natural Abundance (%)[135]	Neutron Cross Section (barns)[136]*	(n,p) Product	Product $T_{1/2}$ (unless noted otherwise)
Titanium	48	73.72	0.05927	^{48}Sc	43.67 h
	46	8.25	0.2893	^{46}Sc	83.79 d
	47	7.44	0.14503	^{47}Sc	3.349 d
	49	5.41	0.0512	^{49}Sc	57.18 m
	50	5.18	0.0113	^{50}Sc	102.50 m
Iron	56	91.75	0.11436	^{56}Mn	2.58 h
	54	5.8	0.33447	^{54}Mn	312.12 d
	57	2.12	0.05705	^{57}Mn	85.40 s
Nickel	58	68.07	0.36358	^{58}Co	70.86 d
	60	26.22	0.1456	^{60}Co	1925.28 d
	62	3.63	0.03117	^{62}Co	1.50 m
	61	1.14	0.09473	^{61}Co	1.65 h
Gold**	197	100	0.00188	^{197}Pt	19.89 h
	196	n/a	0.0056	$^{196}Pt_{(stable)}$	^{196}Au, 6.17 d
	195	n/a	0.003083	$^{195}Pt_{(stable)}$	^{195}Au, 186.09 d

*14.1 MeV neutron energy, for n,p reactions

**^{197}Au, elastic scattering σ=2.6354b and n,2n σ=2.1323b

^{196}Au, inl=0.193b and n,2n=1.975578b

^{195}Au, n-2n=0.8849b or n,p=0.003083b

The foils were dissolved after irradiation and small aliquots were transferred into a glass/cement matrix and formed in a furnace by Maryline Ferrier at UNLV. Once the glass/cement bead was received at LANL, it was then dissolved in nitric, hydrochloric, sulfuric, and hydrofluoric acid just below the acid's boiling point to avoid splattering and sample loss. To start, nitric and hydrochloric acids were used for digestion but very little of the sample dissolved.

Then mixtures of nitric and hydrochloric acids were added to no avail. Then the addition of HF and sulfuric acid followed, which increased the dissolution of the sample but was very time consuming. The entire dissolution procedure took approximately 3-4 weeks. Once the bead was dissolved completely, it was taken to complete dryness and reconstituted in aqua regia. All of the precipitate could not be redissolved in a moderate volume. Therefore, some of the glass bead residue was filtered off and analyzed by gamma spectroscopy. No radioisotopes were found on the filter.

The matrix of this sample was so complicated that it was essential to consider multiple ways to separate the sample. This matrix has never been studied previously; the separation scheme therefore had to be devised using published k' values for UTEVA and DGA resins. A separation based on DGA resin was chosen because of its potential to separate activated products from one another. In this separation scheme, illustrated in Figure 102, the elution of Am and Pu was considered, even though they were not present in the glass bead, they likely would be present in a post detonation sample.

Studies performed by Horwitz et al. and Pourmand et al. analyzed the adsorption of a large variety of metals to DGA resin in nitric and hydrochloric matrices.[29, 31] Hydrochloric acid had the largest range of adsorption for multiple analytes of interest and was therefore used as the matrix used for separation. A summary of literature adsorption values to DGA resin at 8 M, 2 M, and 0.1 M HCl are presented in Table 10.

Table 10. Summary of published adsorption values to DGA resin in 8 M, 2 M, and 0.1 M HCl[29, 30]

Analyte	8M HCl		2M HCl		0.1M HCl	
	Horwitz k'	Pourmand Kd	Horwitz k'	Pourmand Kd	Horwitz k'	Pourmand Kd
Na(I)		none		none		none
Al(III)	<2	0.1	<2	none	<2	none
Ni(I)	<2	0.1	<2	none	<2	none
Mg(II)	<1	none	<1	none	<1	none
Mn(II)		0.1		<0.1		<0.1
Ca(II)	2	0.1	0.6	10	0.3	0.1
Co(II)	<2	~30	<2	1	<2	0.1
Ti(IV)	<2	~80	<2	1	<2	0.1
Fe(III)	2,500	>10,000	300	1000	0.3	10
Au(III)		1000		1000		1000

The loading solution consisted of 11 M HCl in order to increase the chances of Co(II), Ti(IV), Fe(III), and Au(III) adsorbing to the resin. The next mobile phase was 2 M HCl, in order to elute off Co(II) and Ti(IV), since the k' values dropped near 1, but Fe(III) and Gold(III) adsorption is still high enough to stay retained. In the next step 2.0 M HCl and 0.3 M ascorbic acid was used to reduce Fe(III) to Fe(II), since divalent metals do not have any particular affinity for DGA. In this phase, it is expected that Pu(IV) would be reduced to Pu(III), but since DGA still has a large preference for trivalent actinides, Pu(III) would not be expected to be eluted in this phase. At the time of planning this separation, the Sc batch studies had not been analyzed yet. Therefore, the elution was based off of a presentation provided by TrisKem, concerning their DGA resin and its Sc adsorption where the k' values were found to drop around 1 below 1 M HCl concentrations, which would allow for Sc elution within a small volume.[137] Due

to gold's overall large adsorption to DGA, it was not expected to elute off in any hydrochloric matrices. Therefore, gold was thought to elute off in either 0.1 M HCl + 0.01 M HF or 0.01 M HNO_3. Hydrofluoric acid is often used to strip metals off a column due to the strong complexes F^- makes with metals are not typically compatible with resin.

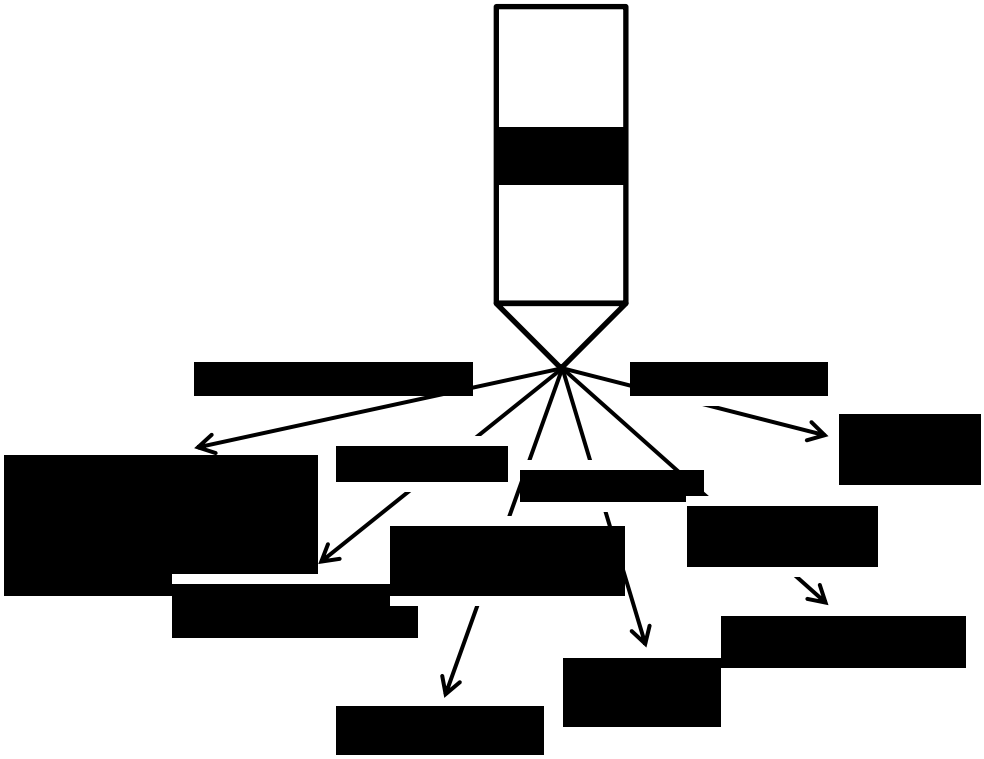

Figure 111. Proposed Separation Scheme of the Glass/Cement Bead

There are no reported separations of the first row of transition metals with glass matrices utilizing DGA resin. Horwitz et al. performed a separation of Mg, Ba, Sr, and Ca in nitric matrices with the intent of separating Sr and Ca from the mixture. Mg, and Ba were eluted off in 4 M HNO_3, Sr in 0.25 M HNO_3 and Ca in 0.1 M HCl.[30] There have been separations of soil, cement, and brick samples,

which would have similar compositions but only with the intent of separating the actinides. Therefore, this separation of a glass cement bead with the intent to separate some of the first row transition metals using DGA is unique.

By the time the separation was started only Co-58, Co-58, Co-60, Mn-54, and Sc-46 were detectable in the dissolved glass bead solution by gamma spectroscopy. The reason limited radioisotopes present in the sample were mainly due to shipping, onsite approval for the material, and the lengthy dissolution procedure. This resulted in the majority of the activated products already decaying by ~7-8 half-lives. Also, since there was so much material, it could not be completely dissolved in 5 mL. This volume is necessary since the gamma spectrometers used did not allow for an efficient counting geometry for larger volumes. As a result, only a fraction of the total activity was analyzed. Therefore, even those radionuclides present but in low activities may not have been detected. The cold constituents could be analyzed by ICP-AES or ICP-MS, but such analysis could not be performed due to the time constraint at LANL. The elution of cobalt, manganese and scandium from the DGA column are presented in Figure 112. The elution profile of Mn bleeds into the theorized Co and Fe elution fractions. This may be due to the large amount of material from a glass/cement bead which needs larger rinse volumes with the load mobile phase, 10 M HCl. The larger mobile phase should provide then the possibility for pure Co and Fe elution fractions. It appears that the majority of Co is eluted from the column within the first 2 M HCl fraction. Some of Sc started to elute off in the expected Sc elution phase, 0.01 M HCl, but it did not elute off in the amount

expected based on the TrisKem values and bled into the Pu elution fraction. This elution profile does match with the Sc batch studies performed on DGA, provided by Eichrom, which were discussed earlier in this chapter. Therefore based off of those Sc batch contact studies, a slightly higher hydrochloric concentration, maybe around 0.5 M, may provide a sharper elution.

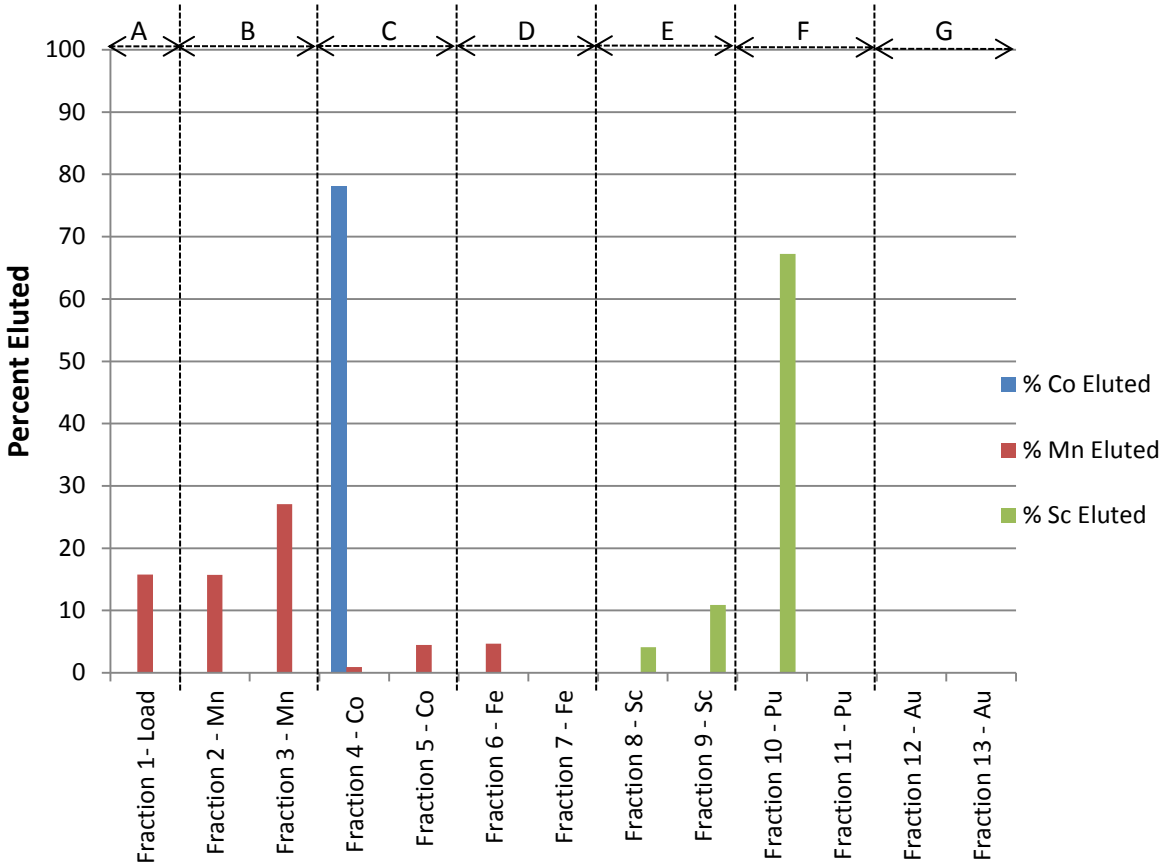

Figure 112. Glass/Cement Bead Separation Co, Mn, and Sc Elute Profiles
All fractions are in 25 mL volumes. Mobile phases are as follows: A: 11 M HCl, B: 10 M HCl, C: 2 M HCl, D: 2 M HCl + 0.3 M Ascorbic Acid, E: 0.1 M HCl, F: 0.1 M HCl + 0.01 M HF, G: 0.01 M HNO_3

The total percent recoveries are listed in Table 11 and are fairly small. These recoveries are possibly due to the radionuclides sticking to the column, but this seems unlikely since the column should have been well stripped after the 0.1 M HCl + 0.01 M HF mobile phase. Instead, the lower recoveries are most likely due to counting errors and efficiency. About a month passed from the time the separation started until the last vial underwent analysis. Therefore, isotopes in the vials which already had low activities to begin with would most likely have decayed to a point that no activity was detectable; hence, the unaccounted for Sc, Co, and Mn.

Table 11. Glass/Cement Bead Percent Recoveries

Radionuclide	% Recovery
Co-57	78.05
Mn-54	68.70
Sc-46	82.25

This separation still needs further investigation to fully characterize its potential. First of all, characterization with only cold material could prove very valuable. The load solution could be tailored closer to the concentrations that would be expected in real world post detonation samples where majority of the transition metals would be in tracer levels. Working with smaller concentrations of analytes would then give potentially smaller elution volumes for each mobile phase. This would simplify sample analysis, lower the separation time, and reduce waste produced. It also would be beneficial to separate each metal

individually on the sample column to determine where each metal would elute off and then perform a separation of the mixture to determine the effects of the additional components on one another. Understanding these relationships may provide extra details and information to allow for further adaption and optimization.

Section 6.5 Concluding Remarks

In this chapter, Na was found to have a higher adsorption to DGA in nitric acid than previously found. Even though the affinity is higher, it is still not high enough to cause a large effect on other metal adsorption. Aluminum was found to have k' values ~1 but when in excess has no effect on actinide adsorption in both 1 M nitric and hydrochloric acid. Calcium has little to no affinity for DGA resin in 1 M HCl and also has no effect on Am adsorption, but in 1 M HNO_3 calcium has higher k' values and decreases k'_{Am} as Ca concentrations increase. Therefore, of these possible sample components calcium may cause decrease Am adsorption in nitric loading matrices but will still work well in hydrochloric.

Also a few metals potentially found in nuclear forensic soil samples were studied for their adsorption to DGA and UTEVA. The adsorption of Sc, Co, Lu, and Bi were studied at varying concentrations and of those metals the highest k' values were found for Sc and Lu at high acid concentrations and Bi at low hydrochloric acid concentrations. Overall, the maximum k' value found was ~200 for Sc in high hydrochloric acid concentrations. The metals which may cause the

largest effects on a column separation are Sc at high HCl concentrations and Bi at low HCl concentrations.

The chromatography separation of the glass/cement bead solution was performed and moderate recoveries of Sc, Co, and Mn were achieved. This separation needs further research is needed to fully characterize its separation potential. At this time, this separation may not be suitable for vacuum box application since the Mn and Sc elution peaks were so broad. Further optimization of mobile phase composition and volumes are needed to reduce the separation time frame.

Chapter 7. INVESTIGATION OF EXTRACTION CHROMATOGRAPHY COLUMN SEPARATIONS FOR ACTINIDES

Section 7.1 Abstract

The work described in this chapter focuses on actinide separations and the determination of elution profiles on DGA and UTEVA columns. The capacity of DGA resin for uranium was initially studied by batch experiments, and completed by obtaining column elution profiles with varying U loading concentrations. Actinide separations and elution profiles on columns operated by gravity are useful precursors to vacuum box separations, since the fine details of separation schemes and elution profiles can be used to optimize the mobile phase volume needed. The lower the mobile phase volume, the faster the separation and the less waste will be generated. A comparison of the k' values determined by batch contact studies and those determined by the free column volume to peak maximum in the elution profiles are discussed. Application and discussion of various elution conditions for DGA and UTEVA resin is discussed. An optimal separation scheme is investigated, identified, and discussed in this chapter for Am, Pu, and U separation using both DGA and UTEVA resin.

Section 7.2 Materials and Methods

Elution and Batch Studies Method

The DGA and UTEVA columns were packed by slurry technique, as previously described in Chapter 2. The loading solution volumes were consistently kept at 1 mL, but concentrations may have varied depending on the purpose and the column bed volume, 1 to 2 mL. All separations were gravity fed and 1 mL fractions of all mobile phases were collected and analyzed on the LSC. The batch experiments were performed as described earlier. All separations and batch studies were run at room temperature, 20-23 ^{o}C. For column elution profiles consisting of Am, Pu, and U together, each radionuclide was passed through the same column individually. After each radionuclide was run, the columns were thoroughly flushed until no further activity was detectable. Therefore, it was assumed the columns had been thoroughly stripped. Each column was reconditioned with 20 mL of the loading matrix.

Reagents

The DGA and UTEVA extraction chromatography resins were obtained from Eichrom Technologies, Inc. All solutions were prepared from using deionized water with a resistivity of 18.2 Megaohm from a Cascada water purification system manufactured by Pall Corporation. For the majority of the separations, the loading phase was 5 M HNO_3, the elution mobile phases studied consisted of hydrochloric acid, and the stripping mobile phase were mixed matrices of hydrochloric/hydrofluoric acids. These acids were acquired from

Sigma-Aldrich and are ACS grade. Sodium Nitrite (Baker Analyzed ACS Reagent, Mallinckrodt Baker) was used for the Pu and U separation on UTEVA.

Measurements

All fractions potentially consisting of Am-241 were detected on the automatic gamma spectrometer described in Chapter 2 where counting was terminated once a predetermined one sigma error was reached or up to 1 hour counting time. All fractions from all mobile phases were analyzed by LSC, using the same method described in Chapter 2. To account for quenching due to matrix composition, blanks and standards were added with a similar matrix as fractions collected. For combined radioisotopic samples, equal aliquots of a single fraction were taken to be analyzed on the LSC and the automated gamma counter.

Section 7.3 Column Elutions and Separations utilizing DGA and UTEVA Resin

Uranium Capacity on DGA Resin

Knowledge of the capacity of DGA resin for uranium would be of great importance for samples with high U concentrations, such as nuclear fuel. Initially U capacity studies were carried out using the batch contact method since this is a quicker and easier technique to employ. The capacity is indicated by a drop in

k’ values once capacity is exceeded, as determined for most other metals’ capacity in Chapters 3 and 4.

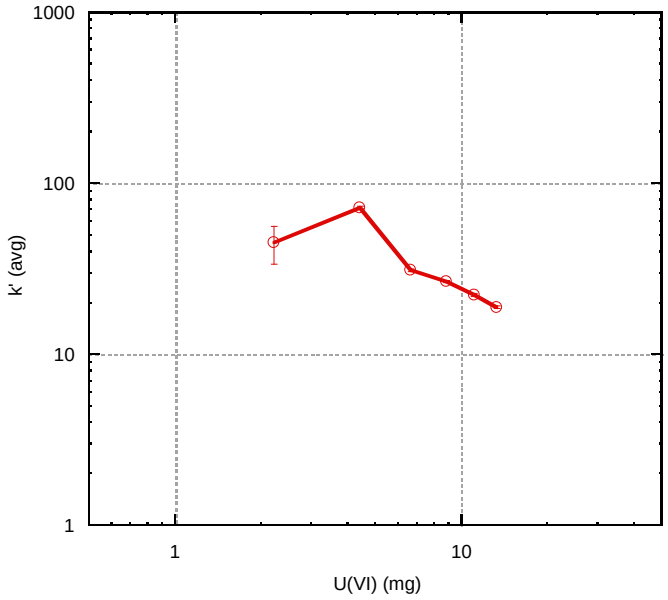

Figure 113. Uranium Capacity Determination on DGA resin by Batch Studies in 1 M HCl

Horwitz et al. theorized the europium capacity to be 0.52 mmol Eu(III)/g DGA resin and, using this value, the U(VI) capacity should be exceeded around 6.298 mg U(VI) per 50 mg DGA resin.[29] Therefore, it was expected to see a decrease in k’ values once 6.6 mg U(VI) was contacted with the resin, in Figure 113 and Figure 114. A drop in k'_U values was only seen in 1 M HCl, but in 1 M HNO_3 a constant increase in k’ values occurred even after the theoretical capacity was exceeded.

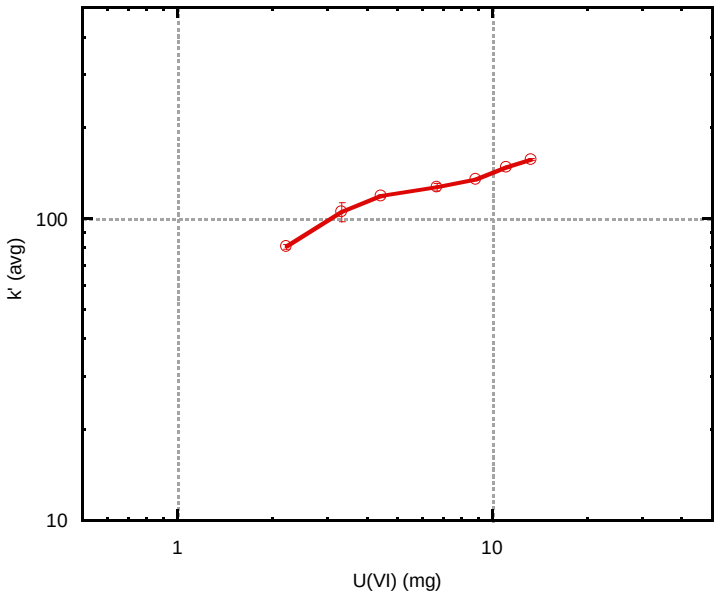

Figure 114. U Capacity Determination on DGA resin by Batch Studies in 1 M HNO_3

The seemingly higher U(VI) capacity in nitric acid may be due to additional U nitrate complexes loosely retained with DGA in the outer coordination sphere. Due to the flow dynamics, in the case of a U(VI) column separation, there would still be a change in the elution characteristics. If those additional U nitrate complexes are loosely retained on the resin, they will have different transfer kinetics than those tightly complexed; meaning that the elution profile curve, on a column, would not hold its symmetrical properties and would most likely become asymmetrical. For this reason, DGA's U(VI) capacity was then investigated for a slurry packed column.

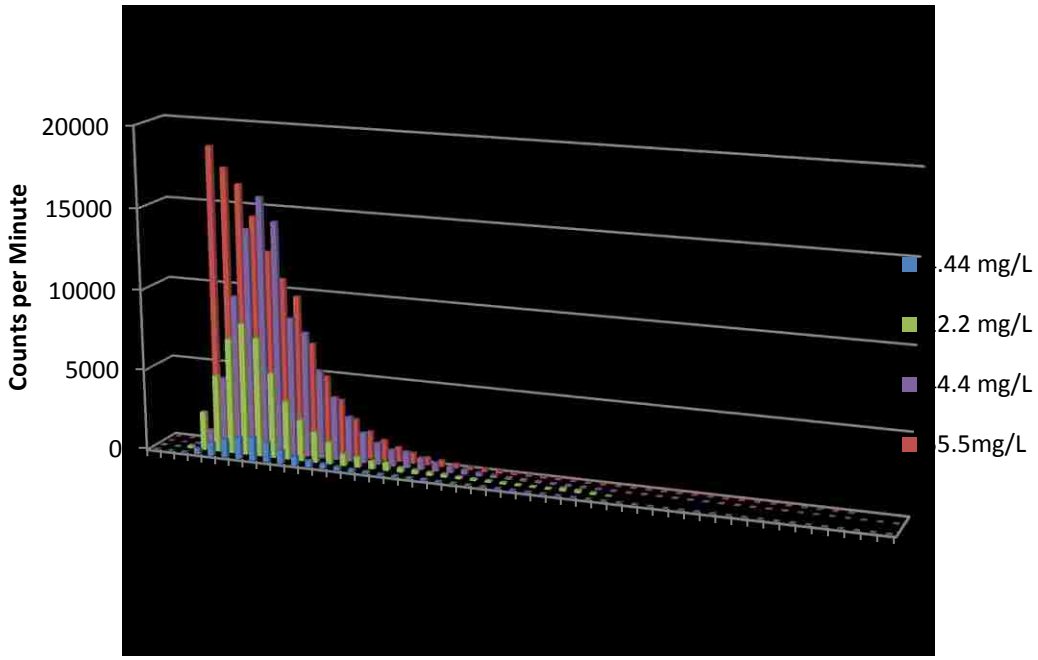

Figure 115. U Capacity on DGA in 0.1 M HNO_3

To determine the U capacity on DGA resin in the nitric matrices, column elution profiles of U(VI) were analyzed in varying U loading concentrations to identify the point of breakthrough. The loading solutions used were 1 mL of 4.44, 22.2, 44.4 and 55.5 mg U(VI)/mL in 0.1 M HNO_3. As seen in Figure 115, there is no breakthrough in the elution curves up to 44.4 mg U(VI)/mL since the symmetry is retained. There is breakthrough in the 55.5 mg U(VI)/mL elution profile. The theoretical capacity for the DGA column studied is at a loading solution of 51.15 mg U(VI)/mL, so these results help to support the theoretical capacity of DGA U(VI) in nitric acid matrices.

Optimization of Mobile Phase Conditions for Actinide Separations

Considering all the batch studies' results for DGA and UTEVA, a two column separation scheme would provide the most worthwhile and efficient separation for material accountancy of the used fuel. To identify the optimal conditions for separation, Am, Pu, and U loading, eluting, and separation characteristics need to be investigated. The separation schemes in Figure 116, are the most advantageous loading scenarios for a sequential separation. The separation of Pu and U separation from UTEVA, Scheme A, is compared to the Am, and Pu from DGA, Scheme B. The separation which gives the most efficient separation is identified and applied to a vacuum box separation, which is discussed in the following chapter.

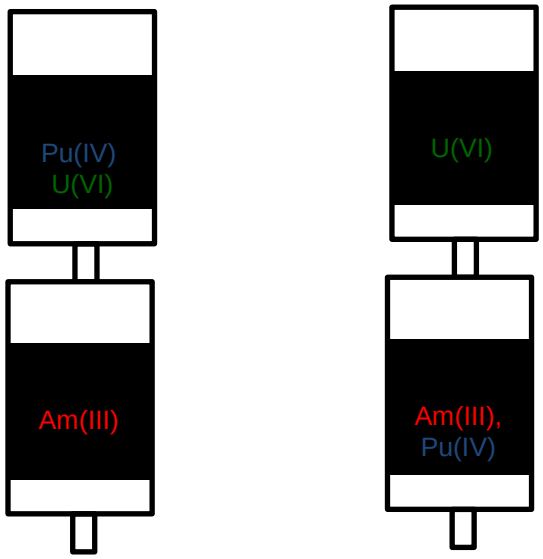

Figure 116. Loading Scheme A (left) and Scheme B (right)

In Scheme B, an efficient separation of Am and Pu on DGA resin is necessary. This separation was performed, and the elution profiles related to it

are in Figure 117. In order to distinguish the counts from Am-241 against those from Pu, all samples were counted on both the LSC and the automatic gamma counter. The differences of these counts were assumed to be due to Pu.

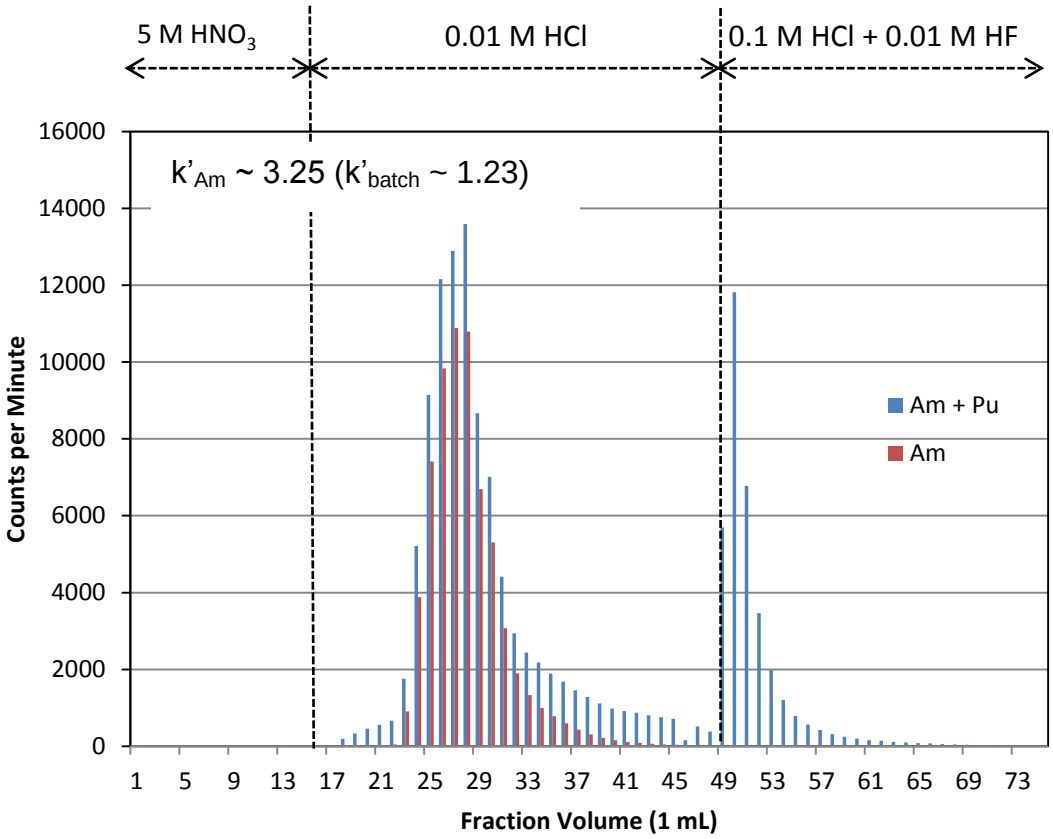

Figure 117. Am and Pu Elution Profiles from DGA resin

Load/Rinse: 5 M HNO_3, 14 mL

As seen in the above elution profile, some of Pu eluted off along with Am. This may be due to the disproportionation of Pu, where some of the Pu may be in its trivalent state. In this case the Pu(III) would be expected to have the same elution characteristics as Am. Plutonium's trivalent oxidation state is not totally

unexpected in lower concentrations of acid, such as the 0.01 M HCl used for the elution mobile phase, therefore an oxidation state adjustment would be needed prior to elution in 0.01 M HCl, which is not ideal. Further support of Pu following Am, is the percent recovery for each mobile phase. Upon looking at only the LSC counts, in which the Am and Pu counts are indiscernible, and upon comparing to total Am activity added onto the column 166% recovery is found. Therefore, more than just Am is eluted in this mobile phase. Since a portion of the elution fractions were analyzed on the autogamma detector it allowed for the subtraction of Am and Pu activity from one another. This allowed for us to determine that the partitioning of Am and Pu from one another was not achieved in this separation scheme. Since the combined elution of Am and Pu is due to their common oxidation state, control of Pu's oxidation state by an oxidizing agent could increase the purities of the elution fractions. The overall recoveries for Am and Pu were fairly high, as seen in Table 12.

Table 12. Percent Recoveries of Americium and Plutonium Separation on DGA

Mobile Phase	Am %	Pu %
Load	0.56	0.47
Elution	97.2	61.7
Strip	0.09	46.5
Total Recovery	97.9	109

Even though the Am recovery is high, the elution peak is considerably broad and would not be an optimal elution. A sharper Am elution peak would

enable a more efficient separation. Since it is possible that the broad elution is due to the combination of Am and Pu together, the Am elution individually would be of importance. Therefore, other elution schemes or mobile phases would be important to improve Am elution from DGA. For this reason, a comparison of 0.1 and 0.01 M HCl mobile phases is presented in Figure 118. The most notable change between the mobile phases is the shape of the elution peak. In 0.1 M HCl, the elution peak is very sharp, where 90% of the Am elutes off in 10 mL. For this reason, 0.1 M HCl elution phase is a more advantageous matrix for Am elution from DGA and will be applied in the vacuum box separation.

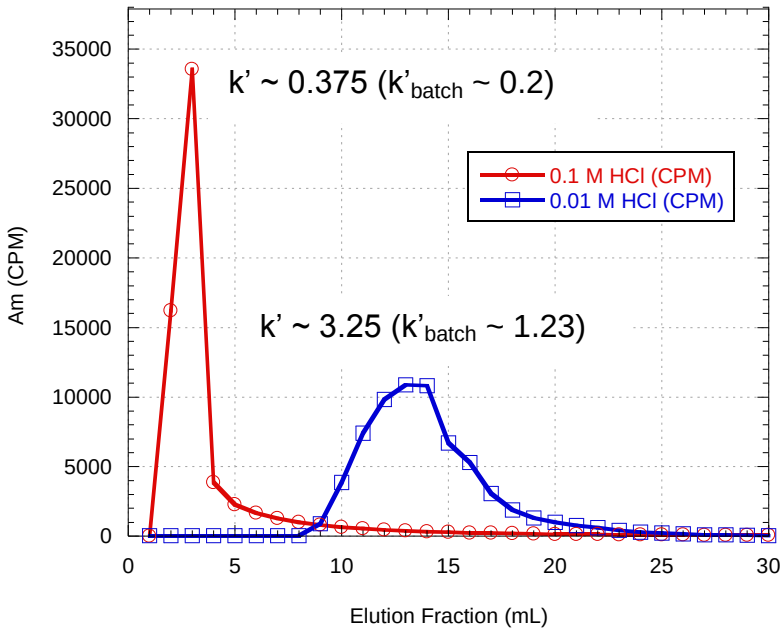

Figure 118. Comparison of Am Elution in 0.1 and 0.01 M HCl

Upon comparison, the batch studies' free column volume to peak maximum, k' value, with those obtained by the elution profiles show fairly close correlation. Smaller elution fractions may have helped to narrow down the variance between the two k' values for each matrix studied, since the finer the fractions, the closer to the elution peak's true volume to reach the maximum.

In separation Scheme A, it is important to know at what volume Am will completely elute from UTEVA, and which mobile phase conditions give the optimal Pu and U separation. Since the k' values determined by batch studies matched well with those determined by column elution profiles, it allows for those values to be used to estimate the metals' behavior on a column. Based on Am k' values in 5 M HNO_3 for UTEVA, it was expected that Am would elute off of the column with very little volume. For the initial separation, Pu and U separation was attempted in 2.0 M HCl because their k' values at this concentration have about an order of magnitude variance between them. These elution profiles are illustrated in Figure 119.

Americium eluted cleanly off UTEVA resin within 10 mL of 5 M HNO_3 with 97.9% recovery. This low elution volume is important for the use of UTEVA in combination with DGA, since the lower the volume, the less waste generated and less time will be needed. The 5 M HNO_3 loading phase is advantageous since it will give simple implementation into the fuel cycle because the current process uses similar nitric acid concentrations.

For the Pu and U separation on UTEVA in 2 M HCl, the separation was not ideal. Even though the Pu-239 eluted off quickly, the Pu-239 elution peak overlapped with the U-233 peak which does not give a clean sample for instrumental analysis. The U-233 elution peak is very broad and takes over 30 mL to complete elution in 2 M HCl. This elution volume is not desirable for a rapid separation. Also, the recoveries of Pu-239 and U-233 were both low, 80% and 82%. Overall, the separation of Pu and U in 2 M HCl is not optimal for a vacuum box separation.

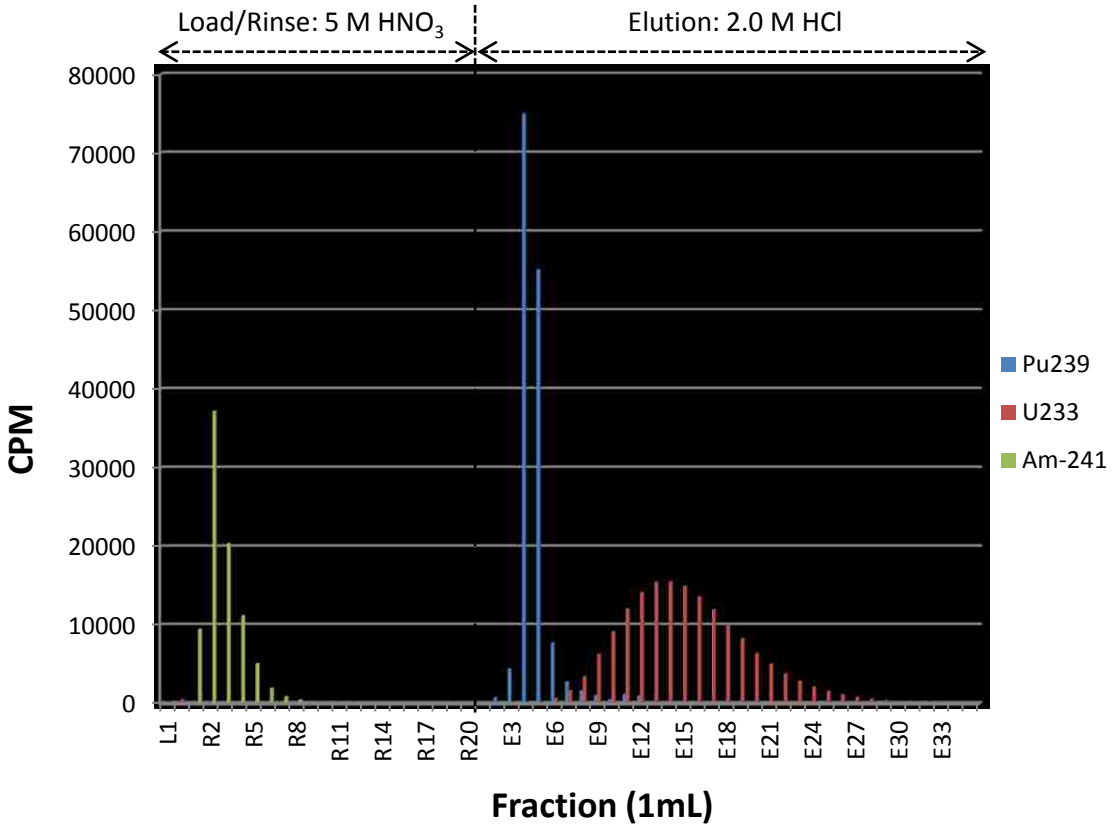

Figure 119. Am, Pu, and U Individual Isotope Elution Profiles from UTEVA resin

Further research was needed to find a more strategic separation for Pu and U. Therefore, sodium nitrite was investigated due to the k' values determined in Chapter 5, which would result in a low elution volume and sharp peaks for Pu(III) and U(IV). This separation is presented in Figure 120, where Pu(III) elutes off with 98.7% recovery, and U(IV) elutes off with 95.5% recovery. This scenario gives sufficient recoveries and elution volumes to be advantageously applied to a vacuum box.

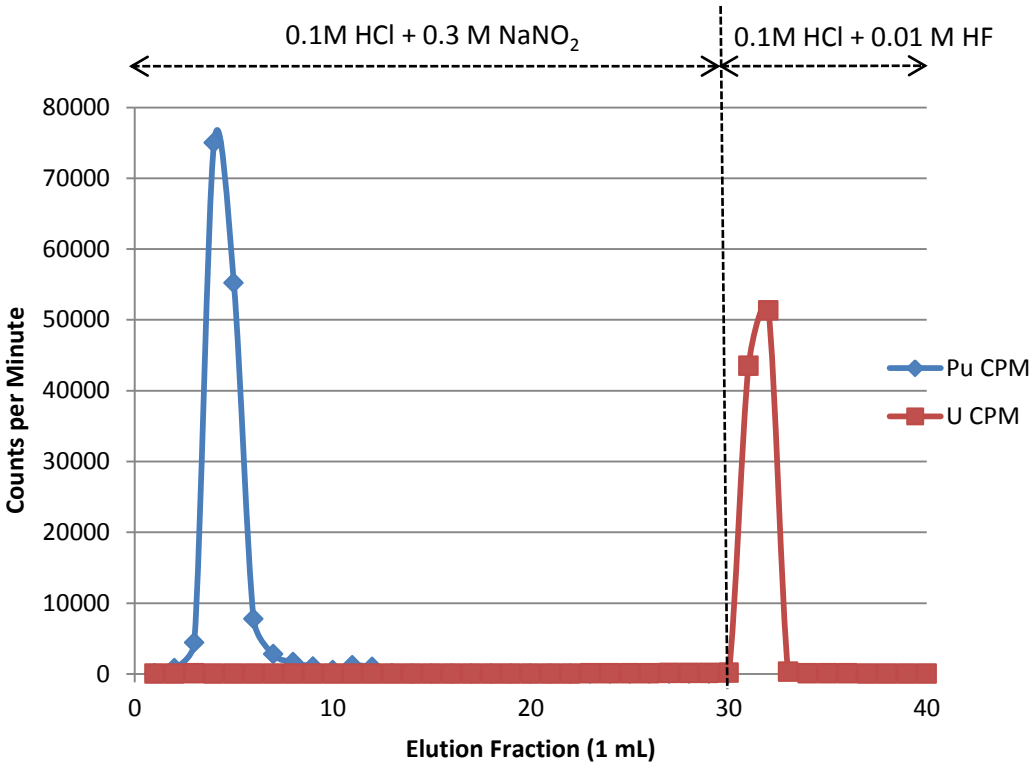

Figure 120. Pu(III) and U(IV) Elution from UTEVA using $NaNO_2$

Load/Rinse: 5 M HNO_3, 20 mL

Section 7.4 Concluding Remarks

Two elution scenarios were investigated for the potential separation of Am, Pu, and U on a vacuum box. Scenario A, described in Figure 116, was found to be the more effective and efficient separation. Based off the elution profiles for this scenario, the optimal mobile phase volume could be identified to ensure that majority of the actinides are recovered. With this knowledge, the proposed separation in Figure 121 is expected to provide a novel and beneficial separation which will need to be applied to a vacuum box to determine its true potential.

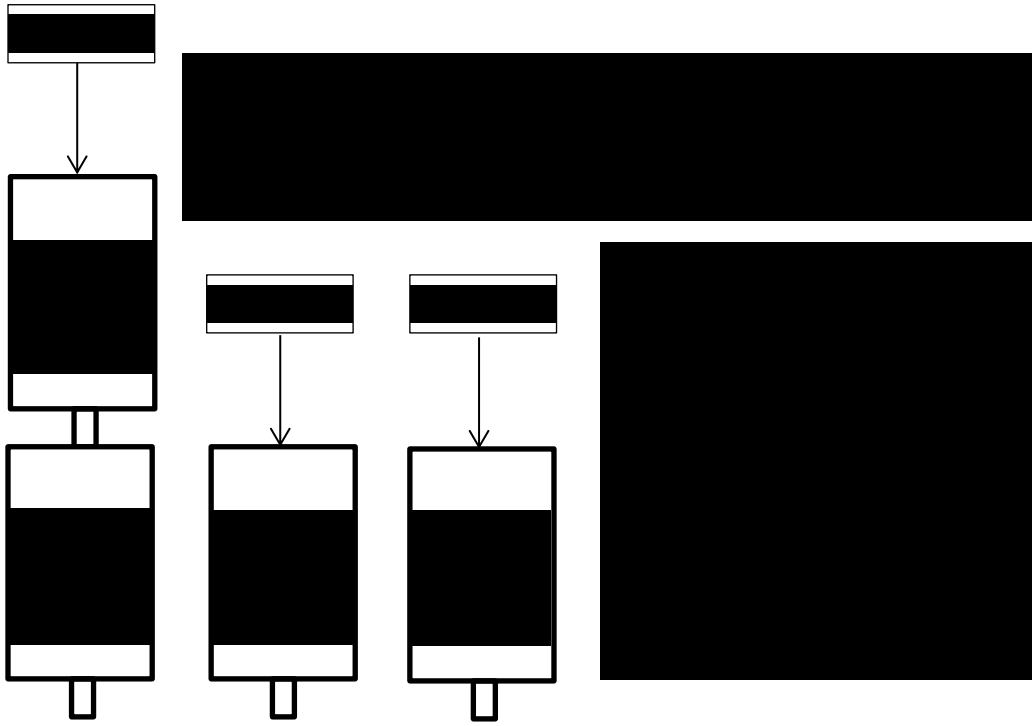

Figure 121. Proposed Used Fuel Separation utilizing UTEVA and DGA resin

Chapter 8. INVESTIGATION OF A RAPID SEQUENTIAL SEPARATION OF ACTINIDES UTILIZING A VACUUM BOX

Section 8.1 Abstract

To decrease the time a separation procedure takes the application of pressure or a vacuum is often used. Doing so can change the efficiency of a previously characterized gravity fed separation by broadening elution bands. The effects of such changes on extraction chromatography resins have previously been studied.[98] It was found that resins which have high transfer kinetics, like DGA and UTEVA, are not considerably affected by the change in flow rate and therefore, are well suited for application of increased flow rates.[98]

In this chapter, the separation of Am, Pu, and U is investigated by sequentially stacking prepacked UTEVA and DGA resin cartridges on a vacuum box. Acid concentrations, and flow rates were varied in order to achieve optimal separation. Once this separation was proven to be efficient at higher flow rates for just Am, Pu, and U alone, then a mock used fuel was added. This mock used fuel included the non-radioactive components studied in Chapters 3 and 4 at concentrations matching those presented in Table 1. The efficiency and percent recoveries for this separation are discussed. The effects of the additional components on the elution and separation of Am, Pu, and U are discussed as well.

Section 8.2 Materials and Methods

Vacuum Box Separation Method

The 2 mL DGA and UTEVA prepacked cartridges were used on the in-house designed vacuum box system described in Chapter 2. In this chapter all vacuum box separations were run in triplicate, side by side, and the graphs are the representation of their average. The flow rate for mobile phase elution used was based off of previous characterization by J. Gostic on the same system, where little to no effects on actinide elution properties were seen with flow rates varying between 1 and 9 mL/min.[98] For these studies the vacuum was set at 575 torr, corresponding to a flow rate of ~2 mL/min for preconditioning and loading steps and at 500 torr, corresponding to a flow rate of ~5 mL/min for rinsing, eluting and stripping phases.

All separations were carried out at room temperature, 20-23^{o}C. For all vacuum box separations, 5 mL fractions of all mobile phases were collected and 1 mL aliquots analyzed on the LSC. Another aliquot of varying size, depending on activity, was taken for electrodeposition and analysis by alpha spectrometry. The method used is as described in Chapter 2.

Reagents

The 2 mL DGA and UTEVA extraction chromatography prepacked cartridges were obtained from Eichrom Technologies, Inc. All solutions were

prepared from ACS reagent grade acid (Sigma-Aldrich) using deionized water with a resistivity of 18.2 Megaohms from a Cascada system manufactured by Pall Corporation. For the majority of the separations, the loading phase was 5 M HNO_3, the elution mobile phases studied consisted of hydrochloric acid, and the stripping mobile phase were mixed matrices of hydrochloric/hydrofluoric acids. These acids were acquired from Sigma-Aldrich and are ACS grade. Sodium nitrite (Baker Analyzed ACS Reagent, Mallinckrodt Baker) was used for the Pu and U separation on UTEVA.

Measurements

Aliquots of 1 mL were taken from all fractions from all mobile phases and were analyzed by LSC, using the same method described in Chapter 2. To account for quenching due to matrix composition, blanks and standards were prepared with a similar matrix as the fractions collected. All mobile phases were also electrodeposited and counted for 12 hours on the Alpha Analyst system described in Chapter 2. All of these samples were counted for 12 hours.

Section 8.3 Rapid Separations for Material Accountancy Purposes

Prior to investigating Am, Pu, and U adsorption and elution from UTEVA and DGA following the scheme presented in Figure 121, the vacuum box system needed to be tested to confirm that the last characterization still applied since it had not been used for several years. The vacuum pressure setting versus flow

rate, and variability at a certain setting were investigated and found to match those results previously obtained.

Upon applying a gravity fed separation onto a vacuum box, the separation is generally expected to keep the same overall trends but will often have a decrease in its separation efficiency and percent recoveries. Therefore, initially, only Am, Pu, and U were added to the stacked UTEVA and DGA prepacked cartridges for separation. Once the effects of the vacuum box were determined, then separation of a mock used fuel occurred. Since each sample had the potential to have all three radionuclides in one fraction, each fraction was electrodeposited and analyzed on the alpha spectrometer. The results are graphed in Figure 122.

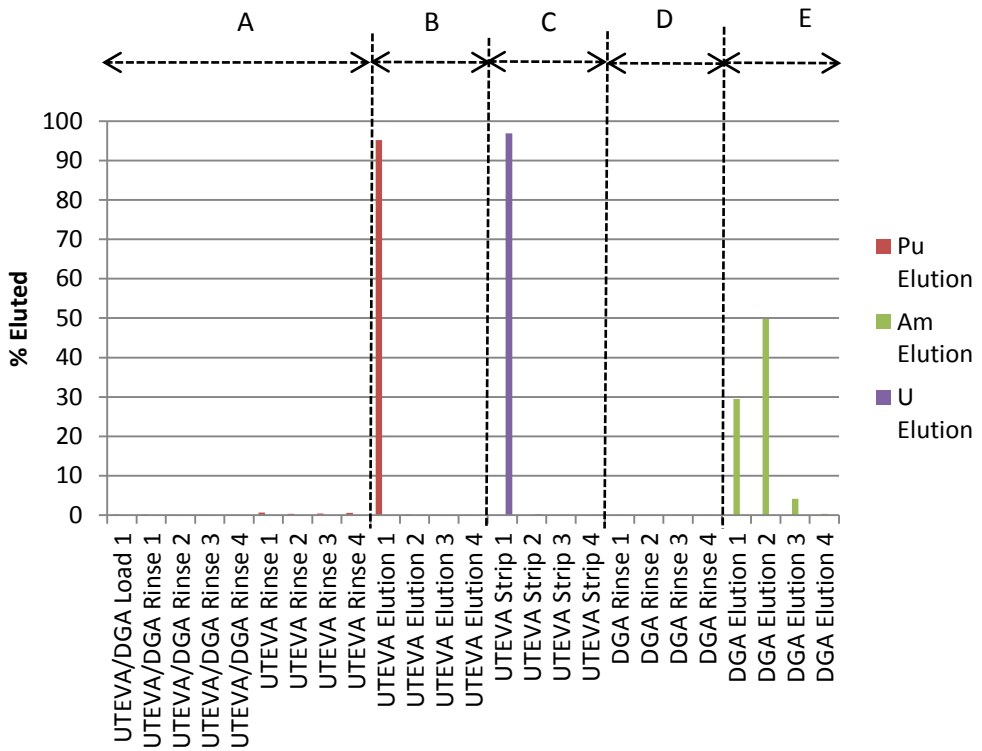

Figure 122. Am, Pu, and U Separation utilizing UTEVA and DGA Prepacked Cartridges on a Vacuum Box System

5 mL fractions were collected, Composition of labelled mobile phases are A – 5 M HNO_3, B – 0.1 M HCl + 0.3 M $NaNO_2$, C – 0.1 M HCl + 0.01 M HF, D – 5 M HNO_3, E – 0.1 M HCl

The separation of Pu and U on UTEVA resin matches well with the gravity fed separations described in the previous chapter. The elution peaks are sharp and elute >90% of the radionuclide in the first 5 mL fraction. This means that the mobile phase volume may be lowered, resulting in a decrease in the time the separation would take. The elution of Am from DGA is broader than determined for a gravity fed column. Even though the elution peak is broader, recovery is still high. The standard deviation for Am-241 elution is fairly high and would not be

sufficient for a reliable material accountancy system and therefore other elution matrices should be studied. All the recoveries for this separation are listed in Table 13.

Table 13. Percent Recoveries for Actinide Separation on Vacuum Box

	% Recovery	STD
Am-241	95.0	14.04
Pu-239	95.5	0.06
U-233	97.3	0.68

For more complicated samples, such as used fuel, further band broadening can occur due to various complexes forming which have slower transfer kinetics on the resins and recoveries can lower as well. Therefore, a mock used fuel was made based on the components previously studied at concentrations ratios similar to those calculated by origin, which was presented earlier. The relative concentrations of Am-241, Pu-239, and U-233 to one another were also made to match the mass percentages listed in Table 1. In order to identify the effects on elution from only the additional components, the same conditions were held for this separation as the one presented above, in Figure 122, and the mobile phase volumes were not decreased. Since no large interferences were detected below the capacity of the resin, in Chapters 3 and 4, and this separation is run below capacity no large changes are expected on the separation characteristics.

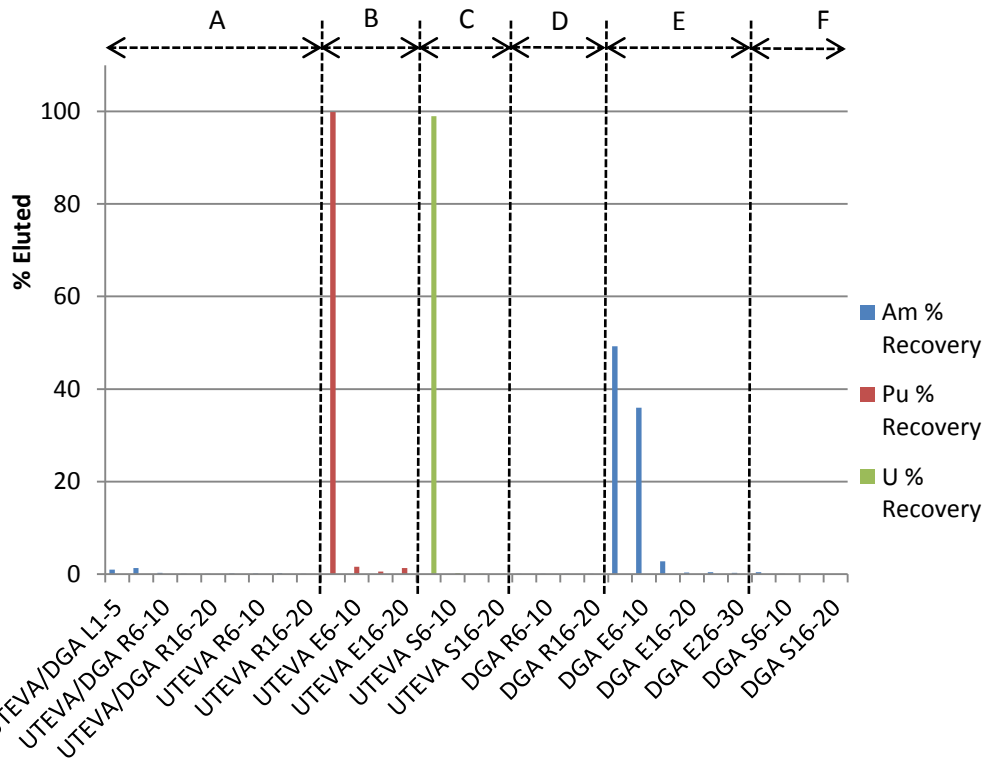

Figure 123. Rapid Mock Used Fuel Separation using UTEVA and DGA resins

Mobile phase compositions are A: 5 M HNO_3, B: 0.1 M HCl + 0.3 M $NaNO_2$,
C: 0.1 M HCl + 0.01 M HF, D: 5 M HNO_3, E: 0.1 M HCl, F: 0.1 M HCl + 0.01 M HF

Overall, the same elution trends were obtained for the mock used fuel separation as for the pure Am, Pu, and U separation. Even though the percent recoveries are high, the standard deviations have increased with the addition of the other components. This may be due to being too close to the maximum capacity of the resin cartridges. Therefore, investigation of larger resin volumes would be beneficial. To determine the potential of this system, it would be ideal to manipulate other parameters, such as flow rates, in order to try to decrease the deviation.

Table 14. Mock Used Fuel Separation Percent Recoveries

	% Recovery	STD
Am-241	92.68	39.60
Pu-239	99.18	1.65
U-233	103.29	5.27

Section 8.4 Concluding Remarks

Overall, the rapid separation shows potential for application in the fuel cycle for material accountancy purposes, but it still needs more work to lower the deviation of the separation. Although the recoveries are high, the deviation between each replicate was also very high which will not ensure the reproducibility necessary for material accountancy purposes. The UTEVA resin proved to be a very viable resin for vacuum box separation of Pu and U from used fuel. It may be necessary to replace DGA resin with another extraction chromatography resin or a new eluent which has lower deviations in Am elution. Investigations into the flow rate, resin volume, additional rinsing phases, and column dimensions could be useful to help in lowering the deviation. It would also be essential to investigate the separation of true used fuel, since there are most likely additional effects on the separation from high dose rates.

Chapter 9. CONCLUSIONS AND REFLECTIONS ON FUTURE RESEARCH

Section 9.1 Actinide Separations for Reprocessing Material Accountancy

Characterization of DGA and UTEVA resins were performed for some of the largest components found in used fuel at various metal ion concentrations in nitric and hydrochloric media. For the most part, little to no effect was seen on the actinide adsorption below the resin capacity with the exception of Zr and Tc. These effects have yet to be reported and may have significance for other samples separated on DGA or UTEVA. Although some of the driving forces behind the changes in actinide adsorption in the presence of Zr and Tc are still unclear and need further analysis, it can be assumed that the adsorption characteristics of Am, Pu, and U in the loading phase of 5 M HNO_3 would stay consistent with those determined in previous individual batch contact studies. This is of great importance for the application of DGA and UTEVA into the nuclear fuel cycle, since PUREX is performed in ~5 M nitric acid conditions and could allow for in-stream implementation. In-stream implementation is a crucial parameter to achieve rapid separations and measurements necessary for near-real time material accountancy.

The adsorption of metals to DGA was found to be highly dependent on the counter ion in the system, where their charge densities and hydration energies can define the trend. There may be multiple factors dictating the trends in other

conditions making it difficult to identify the driving factor. The effects of reducing agents and additional complexants were studied on DGA and UTEVA. Manipulation of the actinide oxidation states proved to give the largest separation factors for DGA and UTEVA resins. The analysis of actinides in these various matrices may aid in further development of novel separation schemes.

Based on the trends seen in the various matrices a novel separation scheme was investigated for potential use for rapid analysis of Am, Pu, and U from used fuel. The elution profiles were determined for Am, Pu, and U separately for the various resins and recoveries >96% of each actinide were achieved. Overall, there was good correlation between the k' values determined by batch contact studies and the elution profiles. Therefore, the k' values alone can be used to determine the appropriate mobile phase volumes necessary for an ideal separation scheme. Once the optimal mobile phase and volumes were determined for Am, Pu, and U. The separation was applied to a vacuum box. Initially the separation was performed only with the actinides present, giving similar recoveries >95% with fairly low standard deviation. A low standard deviation is of great importance for reproducibility of the material accountancy system. Upon separation of a mock used fuel, the recoveries were >92% but the standard deviation increased greatly. This was most likely due to the additional components affecting the elution characteristic, in particular Tc's effects on Am's adsorption to DGA. Due to this high deviation, it may be advantageous to investigate other extraction chromatography resins to replace DGA, such as TRU, for their potential to separate Am from used fuel.

Further optimization of this separation is possible, such as vacuum box operation conditions, varying mobile conditions to improve recoveries, and column parameters. Overall, due to the high recoveries, simple separation scheme, and vacuum box application, this separation shows great potential for its application into a reprocessing facility for material accountancy purposes.

Section 9.2 Separations for Nuclear Forensic Purposes

Characterization of UTEVA and DGA for nuclear forensic samples found that both resins keep great selectivity even in the presence of large amounts of other metals typically found in soil. For UTEVA, metals with +1, +2, or +3 oxidation states had consistently very little adsorption in nitric and hydrochloric matrices. For DGA, it is not as generally selective but still provides enough selectivity for advantageous use for soil and urban material based samples. Since DGA had more variability in its selectivity, it allows for more novel separations or a variety of analytes.

A novel separation of a glass/cement bead was performed on a DGA gravity fed column. Due to the time table available for this separation, it was only performed once and full characterization was not possible. Since the majority of the analytes had decayed prior to separation, the full potential of this separation was not identified. The separation recoveries were only >68.7%, and the separations were not pure. Further investigations into use of other reagents may be useful for obtaining pure separations. Since this separation could possibly

isolate the analytes of interest easily in one column, further characterization would be valuable. Ideally, analysis of all elution fractions would be necessary for full characterization. Also, obtaining elution profile curve would help optimize mobile phase volumes which could potentially decrease waste generated and the time the column separation would require. Overall, the studies performed for nuclear forensic samples supports the fact that extraction chromatography resin, especially UTEVA and DGA, are well suited for samples with complex matrices, and for separation of multiple analytes in one column.

REFERENCES

1. Maxwell, S. L., Culligan, B. K., Kelsey-Wall, A., Shaw, P. J. (2012). Rapid determination of actinides in emergency food samples, *Journal of Radioanalytical and Nuclear Chemistry*, 339-347.

2. Maxwell, S. L, Culligan, B. K., Kelsey-Wall, A., Shaw, P. J. (2011). Rapid radiochemical method for determination of actinides in emergency concrete and brick samples, *Analytica Chemica Acta*, 701, 112-118.

3. Maxwell, S. L., Culligan, B. K., Noyes, G. W. (2010). Rapid separation method for actinides in emergency soil samples, *Radiochemica Acta*, 793-800.

4. Maxwell, S. L. Culligan, B. K., Noyes, G. W. (2010) Rapid separation of actinides and radiostrontium in vegetation samples, *Journal of Radioanalytical and Nuclear Chemistry*, 286, 273-282.

5. Abernathey, R. M., Matlack, G. M., Rein, J. E. (1972). Sequential Ion Exchange Separation and Mass Spectrometric Determination of Neodymium, Uranium, and Plutonium in Mixed Oxide Fuels for Burn-up and Isotopic Distribution Measurements, *Analytical Methods in the Nuclear Fuel Cycle*, Vienna: IAEA, 513-521.

6. *Act of 1954*. Washington: United States Nuclear Regulatory Commission, n.d.

7. Moody, K. J., Hutcheon, I. K., Grant, P. M. (2005). *Nuclear Forensic Analysis*. Taylor and Francis.

8. IAEA Safeguards Glossary (2002). *International Nuclear Verification*, No. 3.

9. APS/AAAS (2008). *Nuclear Forensics – Role, State of the Art, and Program Needs*. Washington, DC: American Association for the Advancement of Science.

10. Safeguards Techniques and Equipment (2011 ed.). Vienna: IAEA.

11. "Special Nuclear Material Control and Counting Systems for Nuclear Power Plants." Regulatory Guide 5.29 Rev. 2. 2013.

12. Hou, X., Roos, P. (2007). *Critical Comparison of Radiometric and Mass Spectrometric Methods for the Determination of Radionuclides in Environmental, Biological and Nuclear Waste Samples*. Denmark: Elsevier.

13. Rosenberg, R. J. (1993). Non-conventional Measurement Techniques for the Determination of Some Long-lived Radionuclides Produced in Nuclear

Fuel a Literature Survey. *Journal of Radioanalytical and Nuclear Chemistry, Articles*, 171(2), 465-482.

14. Rollin, S. (1999). *On-line coupling of an ion chromatograph to the ICP-MS: Separations with a cation exchange chromatography column*. Stockholm: Swedish Nuclear Fuel and Waste Management Co.

15. Vajda, N., Kim, C.-K. (2011). Determination of Transuranium Isotopes (Pu, Np, Am) by Radiometric Techniques: A review of Analytical Methodology. *Analytical Chemistry*, 83, 4688-4719

16. Guenther, E. A. (n.d.). PNL-5109-105. Richland Washington: PNL.

17. Eikenberg, J., Jaggi, M., Beer, H., Ruthi, M., Zumsteg, I. (2009). Separation techniques for low level determination of actinides in soil samples. *Applied Radiation and Isotopes*, 67, 776-780

18. Grate, J. W., O'Hara, M. J., Farawila, A. F., Dougals, M., Haney, M. M., Petersen, S. L., Maiti, T. C., Aardahl, C. L. (2011). Extraction Chromatographic Methods in the Sample Preparation Sequence for Thermal Ionization Mass Spectrometric Analysis of Plutonium Isotopes. *Analytical Chemistry*, 83, 9086-9091.

19. Murali, M. S., Bhattacharayya, A., Raut, D. R., Kar, A. S., Tomar, B. S., Manchanda, V. K. (2012). Characterization of high level waste for minor actinides by chemical separation and alpha spectrometry. *Journal of Radioanalytical and Nuclear Chemistry*, 294, 149-153.

20. Venkatesan, K. A., Kumaresan, R., Antony, M. P., Kumar, T., Srinivasan, T. G., Vasudeva Rao, P. R. (2012). Characterization of high active waste (155 GWd/Te) arising from fast reactor fuel reprocessing. *Radiochimica Acta*, 100, 843-849.

21. Asai, S., Magara, M., Shinohara, N., Yamada, S., Nagai, M., Miyoshi, K., Saito, K. (2008). Separation of U and Pu in spent nuclear fuel sample using anion exchange group introduced porous polymer sheet for ICP-MS determination. Talanta, 77, 695-700.

22. Rundberg, R. S. (2013). *Post-Detonation Nuclear Forensics*. Lecture.

23. *Radiological Laboratory Sample Analysis Guide for Incident Response - Radionuclides in Soil*. EPA 402-R-12-006. Maryland: Environmental Management Support, INC., 2012.

24. Salminen, S. (2009). *Development of analytical methods for the separation of plutonium, americium, curium, and neptunium from environmental samples*. Helsinki: University of Helsinki, Academic Dissertation

25. Srncik, M., Hrnecek, E., Steier, P., Wallner, G. (2011). Determination of U, Pu and Am isotopes in Irish Sea sediment by a combination of AMS and radiometric methods. *Journal of Environmental Radioactivity*, 102, 331-335.

26. Thakur, P., Mulholland, G. P. (2011). Determination of Pu, Am, U and Cs in large soil samples in the vicinity of the USDOE Waste Isolation Pilot Plant. *Journal of Radioanalytical and Nuclear Chemistry*, 288, 499-506

27. Guerin, N, Nadeau, K., Potvin, S., Hardy, J.-M., Lariviere, D. (2013). Automated pressurized injection system for the separation of actinides by extraction chromatography. *Journal of Radioanalytical and Nuclear Chemistry*, 295, 1803-1811.

28. Lariviere, D., Benkhedda, K., Kiser, S., Johnson, S., Cornett, R. J. (2010). Rapid and automated sequential determination of ultra trace long lived actinides in air filters by inductively coupled plasma mass spectrometry. *Analytical Methods*, 2, 259-267.

29. Horwitz, E. P., et al. (2005). Novel Extraction of Chromatographic Resins Based on Tetraalkyldiglycolamides: Characterization and Potential Applications. *Solvent Extraction and Ion Exchange*, 23, 319-344.

30. Horwitz, E. P., McAlister, D. R., Thakkar, A. H. (2008). Synergistic Enhancement of the Extraction of Trivalent Lanthanides and Actinides by Tetra-(n-Octyl)Diglycolamide from Chloride Media. *Solvent Extraction and Ion Exchange*, 26, 12-24.

31. Pourmand, A., Nicolas, Dauphas (2010). Distribution coefficients of 60 elements on TODGA resin: Application to Ca, Lu, Hf, U and Th isotope geochemistry. *Talanta*, 81, 741-753.

32. Horwitz, E. P. et al. (1992). Separation and preconcentration of uranium from acidic media by extraction chromatography. *Analytica Chimica Acta*, 266, 25-34.

33. Horwitz, E. P. (1993). New Chromatographic Materials for Determinations of Actinides, Strontium, and Technetium in Environmental, Biosassay, and Nuclear Waste Samples. July, 1993, *www.eichrom.com.* document. 16 December 2013. http://www.eichrom.com/docs/bib/pdf/ZZ931-Determin%20of%20Actinides-Strontium-Technetium%20in%20Env-Bioassay-Nuc%20Wste.pdf

34. Siekierski, S. (1975). Theoretical Aspects of Extraction Chromatography. *Extraction Chromatography*, vol. 2, New York: Elsevier Scientific Publishing Company

35. Horwitz, E. P. (1998). Extraction Chromatography of actinides and selected fission products: principles and achievement of selectivity.

International Workshop on the Application of Extraction Chromatography in Radionuclide Measurement, Belgium: IRMM (HP199).

36. *Eichrom - DGA Resin*. 2013. Eichrom Technologies. March 2014. <http://www.eichrom.com/products/info/dga_resin.aspx>.

37. Lehritani, M., Mantero, J., Casacuberta, N., Masque, P., Garcia-Tenorio, R. (2012). Comparision of two sequential separation methods for U and Th determination in environment samples by alpha particle spectrometry. *Radiochimica Acta*, 100, 431-438.

38. Sasaki, Y., Masaki, T., Saeki, M. (2007). Selective Extraction of N,N,N',N'-Tetraoctyldiglycolamide and the Structure of its Divalent Metal Complex. *Chemistry Letters*, 36(4), 488-489.

39. Ansari, S. A., Pathak, P., Mohapatra, P. K., Manchanda, V. K. (2011). Chemistry of Diglycolamides: Promising Extractants for Actinide Partitioning. *Chemical Reviews*, 112, 1751-1772.

40. Jensen, M. P., Yaita, T., Chiarizia, R. (2007). Micelle Formation in the Partitioning of Trivalent f-Element Cations by Biphasic Systems Containing a Tetraalkyldiglycolamide. *Lanmuir*, 23, 4765-4774.

41. Sasaki, U., Rapold, R., Arisaka, M., et. al. (2007). An Additional Insight into the Correlation between the distribution ratios and the aqueous acidity of the TODGA system. *Solvent Extraction and Ion Exchange*, 25, 187-204.

42. Reilly, S. D., Gaunt, A. J., Scott, B. L., Modolo, G., Iqbal, M., Verboom, W., Sarsfield, M. J. (2012). Plutonium (IV) complexation by diglycolamide ligands – coordination chemistry insight into TODGA-based actinide separations. *Chemistry Communications*, 48, 9732-9734.

43. Arisaka, M., Kimura, T. (2011). Thermodynamic and Spectroscopic Studies on Am(III) and Eu(III) in the Extraction System of N,N,N',N'-Tetraoctyl-3-Oxapentane-1,5-Diamide in n-Dodecan/Nitric Acid. *Solvent Extraction and Ion Exchange*, 1, 72-85.

44. Ansari, S. A., Godbole, S. V., Dhobale, A. R., Manchanda, V. K. (2009). Interaction of Eu3+ with N,N,N',N'-tetraoctyl diglycolamide: A times resolved luminescence spectroscopy study. *Spectrochimica Acta Part A*, 348-352.

45. Sugo, Y., Izumi, Y., Yoshida, Y., Nishijima, S., et al. (2007). Influence of diluent on radiolysis of amides in organic solution. *Radiation Physics and Chemistry*, 76, 794-800.

46. Sugo, Y., Sasaki, Y., Tachimori, S. (2002) Studies on hydrolysis and radiolysis of N,N,N',N'-tetraoctyl-3-oxapentane-1,5-diamide, *Radiochemica Acta*, 90, 161-165.

47. Ansari, S. A., Prabhu, D. R., Gujar, R. B., Kanekar, A. S., et al. (2009). Counter current extraction of uranium and lanthanides from simulated high-level waste using N,N,N',N'-tetraoctyl diglycolamide. *Separation and Purification Technology*, 66, 118-124.

48. Modolo, G., Schreinemachers, C., Vijgen, H. (2007). Recovery of actinides and lanthanides from high-level liquid waste by extraction chromatography using TODGA + TBP impregnated resins. *Radiochemica Acta*, 95, 391-397.

49. Hoshi, H., Wei, Y.-Z., Kumagai, M., Asakura, T., Morita, Y. (2004). Separation of trivalent minor actinides and lanthanides by TODGA extraction chromatography for radioactive waste management. *Journal of Alloys and Compounds*, 374, 451-455.

50. Zhang, A., Wei, Y., Hoshi, H., Kumagai, M. (2005). Chromatographic Separation of Strontium(II) from a Nitric Acid Solution Containing some Typically Simulated Elements by a Novel Silica Based TODGA Impregnated Polymeric Composite in the MAREC Process. *Solvent Extraction and Ion Exchange*, 23, 231-247.

51. Zhang, A., Kuraoka, E., Kumagai, M. (2006). Removal of Pd(II), Zr(IV), Sr(II), Fe(III), and Mo(VI) from simulated high level liquid waste by extraction chromatography utilizing the macroporous silica-based polymeric materials. *Separation and Purification Technology*, 50, 35-44.

52. Shaibu, B. S., Reddy, M. L. P., Murali, M. S., Manchanda, V. K. (2007). N,N,N',N'-tetraoctyl-3-oxapentane-1,5-diamide impregnated magnetic particles for the uptake of lanthanides and actinides from nuclear waste streams. *Radiochemica Acta*, 95, 159-164.

53. Thakur, P. (2011). Sequential isotopic determination of plutonium, thorium, americium and uranium in the air filter and drinking water samples around the WIPP site. *Journal of Radioanalytical and Nuclear Chemistry*, 287, 311-321.

54. Luisier, F., Alvarado, J. A. C., Steinmann, P., Krachler, M., Froidevaux, P. (2009). A new method for the determination of plutonium and americium using high pressure microwave digestion and alpha spectrometry of ICP-MS. *Journal of Radioanalytical and Nuclear Chemistry*, 281, 425-432.

55. Maxwell III, S. L., Faison, D. M. (2008). Rapid column extraction method for actinides and strontium in fish and other animal tissue samples. *Journal of Radioanalytical and Nuclear Chemistry*. 275, 605-612.

56. Maxwell III, S. L., Culligan, B. K. (2006). Rapid column extraction method for actinides in soil. *Journal of Radioanalytical and Nuclear Chemistry*, 273(3), 699-704.

57. Maxwell III, S. L. (2008). Rapid method for determination of plutonium, americium and curium in large soil samples. *Journal of Radioanalytical and Nuclear Chemistry*, 275(2), 395-402.

58. Van Hecke, K., Modolo, G. (2004). Separation of actinide from Low Level Liquid Wastes (LLLW) by extraction chromatography using novel DMDOHEMA and TODGA impregnated resins. *Journal of Radioanalytical and Nuclear Chemistry*, 261(2), 269-275.

59. Esbelin, E., Buravand, E., Bejaoui, S., Lamontagne, J., Bonnerot, J. M. (2013). Americium, curium, and neodymium analysis in ECRIX-H irradiated pellet: sample preparation for TIMS measurement. *Radiochimica Acta*, 101, 293-300.

60. Bejaoui, S., Lamontagne, J., Esbelin, E., Bonnerot, J-M., Masson, M., Loubet, L., Brunon, E., Bourdot, P. "ECRIX-H Experiment: Post-Irradiation Examinations and Simulations." *Actinide and Fission Product Partiitoning and Transmutation*. San Francisco, Ca: Nuclear Energy Agency, 2012.

61. Zhang, A., Wei, Y., Kumagai, M. (2007). Separation of Minor Actinides and Rare Earths from a Simulated High Activity Liquid Waste by Two Macroporous Silica-based polymeric composites. *Separation Science and Technology*, 42(10), 2235-2253.

62. Li, C., Sadi, B., Benkhadda, K., St.-Amant, N., Moodie, G., Ko, R., DiNardo, A., Karmer, G. (2010). Method comparision for Am-241 emergency urine bioassay. *Radiation Protection Dosimetry*, 141(3), 228-232.

63. Mason, G. W., Griffin, H. E. (1980). Demonstration of the Potential for Designing Extractants with Preselected Extraction Properties Application to Reactor Fuel Reprocessing. *Actinide Separations*, Washington, DC: American Chemistry Society, Ch. 7.

64. Vajda, N., Torvenyi, A., Kis-Benedek, G., Kim, C. K. (2009). Development of extraction chromatographic separation procedure for the simultaneous determination of actinides. *Radiochimica Acta*, 97, 9-16.

65. *UTEVA Resin*. 2013. Eichrom Technologies. March 2014. http://www.eichrom.com/products/info/uteva_resin.aspx

66. Bond, E. M., Bredeweg, T. A., FitzPatrick, J. R., Jandel, M., Rundberg, R. S., Slemmons, A. K., Vieria, D. J. (2009). Preparation of targets for nuclear chemistry experiments at DANCE. *Journal of Radioanalytical and Nuclear Chemistry*, 282, 379-384

67. USEPA (2010). *Rapid Radiochemical Methods for Selected Radionuclides in Water for Environmental Restoration Following Homeland Security Events*. Cincinnati: National Homeland Security Research Center

68. Taddei, M. H. T., Vicente, R., Marumo, J. T., Sakata, S. K., Terremoto, L. A. A. (2013). Determination of long-lived radionuclides in radioactive wastes from the IEA-R1 nuclear research reactor. *Journal of Radioanalytical and Nuclear Chemistry*, 295, 951-957.

69. Fujikawa, Y., Sugahara, M., Ikeda, E., Fukui, M. (2002). Analysis of trace actinide elements in soil organic matter: optimization of sample processing to improve chemical separation of U and Pu. *Journal of Radioanalytical and Nuclear Chemistry*, 252(2), 399-405.

70. Gingell, T. (1997). The determination of uranium in environmental samples using extraction chromatography. *Journal of Radioanalytical and Nuclear Chemistry*. 266(1-2), 185-189.

71. Pilvio, R., Bickel, M. (1998). Separation of actinides from a bone ash matrix with extraction chromatography. *Journal of Alloys and Compounds*. 271-273, 49-53.

72. Warwick, P. E., Croudace, I. W., Dale, A. A. (1999). An optimised and robust method for the determination of uranium and plutonium in aqueous samples. *Applied Radiation and Isotopes*, 50, 579-583.

73. Lee, S.-H., La Rosa, J., Gastaud, J., Povinec, P. P. (2005). The development of sequential separation methods for the analysis of actinides in sediment and biological materials using anion-exchange resins and extraction chromatography. *Journal of Radioanalytical and Nuclear Chemistry*, 263(2), 419-425.

74. Lee, M. H., Park, T. H., Park, J., H., Song, K., Lee, M. S. (2013). Radiochemical separation fo Pu, U, Am and Sr isotopes in environmental samples using extraction chromatography resins. *Journal of Radioanalytical and Nuclear Chemistry*, 295, 1419-1422.

75. Kim, G., Burnett, W. C., Horwitz, E. P. (2000). Preconcentration and Separation of Actinide Elements from Large Soil and Sediment Samples. *Analytical Chemistry*, 72, 4882-4887.

76. Krachler, M., Alvarez-Sarandes, R., Carbol, P., Malmbeck, R., Van Winckel, S. (2013). Potential of high resolution ICP-OES for elemental and isotopic analysis of americium. *Microchemical Journal*, 110, 425-434.

77. Perna, L., Betti, M., Moreno, J. M. B., Fuoco, R. (2001). Investigation of the use of UTEVA as a stationary phase for chromatographic separation of actinides on-line to inductively coupled plasma mass spectrometry. *Journal of Analytical Atomic Spectrometry*, 16, 26-31.

78. Coleman, M. E., Bond, E. M., Moody, A., Tandon, L. (2013). The analysis of uranium-232: comparision of radiochemical techniques and an

improved method by alpha spectroscopy, *Journal of Radioanalytical and Nuclear Chemistry*, 296, 483-487.

79. Ohtsuka, Y., Takaka, Y., Nishimura, K., Kimura, J., Hisamatsu, S., Inaba, J. (2006). Rapid Method for the Analysis of Plutonium Isotopes in a Soil within 60 min. *Analytical Sciences*, 22, 309-311.

80. Milliard, A., Curand-Jezequel, M., Lariviere, D. (2011). Sequential automated fusion/extraction chromatography methodology for the dissolution of uranium in environmental samples for mass spectrometric determination. *Analytica Chimica Acta*, 684, 40-46.

81. Avivar, J., Ferrer, L., Casas, M., Cerda, V. (2012). Fully automated lab-on-valve-multisyringe flow injection analysis-ICP-MS system: an effective tool for fast, sensitive and selective determination of thorium and uranium at environmental levels exploiting solid phase extraction. Journal of analytical and atomic spectrometry, 27, 327-334.

82. Taguchi, S., Yamamoto, M., Surugaya, N., Kurosawa, A., Hiyama, T., Tanaka, T. (2011). Determination of trace amounts of plutonium in low-active liquid wastes from spent nuclear fuel reprocessing plants by flow injection-based solid-phase extraction/electrochemical detection system. *Journal of Radioanalytical and Nuclear Chemistry*, 288, 435-441.

83. Goodall, P., Lythgoe, C. (1999). Rapid Separation of uranium and plutonium by extraction chromatography for determination by thermal ionisation mass spectrometry. *The Analyst*, 124, 263-269.

84. Thakkar, A. H. (2001). Rapid sequential separation of actinides using Eichrom's extraction chromatography material. *Journal of Radioanalytical and Nuclear Chemistry*. 248(2), 453-456.

85. Grudpan, K., Kakmunee, J., Sooksamiti, P. (1998). Spectrophotometric determination of uranium by flow injection analysis using UTEVA Spec chromatographic resin, Journal of Radioanalytical and Nuclear Chemistry, 229(1-2), 179-181.

86. Horwitz, E. P., Dietz, M. L., Chiarizia, R., Diamond, H., Maxwell, S. L., Nelson, M. R. (1995). Separation and preconcentration of actinides by extraction chromatography using a supported liquid anion exchanger: application to the characterization of high-level nuclear waste solutions. *Analytica Chimica Acta*, 310, 63-78.

87. Maxwell, S. L. (1998). Rapid Actinide-Separation Methods, *Radioactivity and Radiochemistry*. 8(4), 36-44.

88. Osvath, Sz., Vajda, N., Stefanka, Zs., Szeles, E., Molnar, Zs. (2011). Determination of Zr-93 and Np-237 in nuclear power plant wastes. *Journal of Radioanalytical and Nuclear Chemistry*, 287, 459-463.

89. Solatie, D., Carbol, P., Peerani, P., Betti, M. (2001). Investigation of separation/purification methodologies for the determination of U-232 and Pu-236 in solution of spent nuclear fuel by alpha spectrometry. *Radiochimica Acta,* 89, 551-556.

90. Morgenstern, A., Apostolidis, C., Carlos-Marquez, R., Mayer, K., Molinet, R. (2002). Single-column extraction chromatographic separation of U, Pu, Np, and Am. *Radiochimica Acta,* 90, 81-85.

91. *Eichrom - Extraction Chromatography*. 2013. Eichrom Technologies. 6 March 2014. <http://www.eichrom.com/products/extraction.aspx>.

92. Glockner, G. *Polymer Characterization by Liquid Chromatography*. Vol. 34. Berlin: Elsevier Science Publishers, 1986.

93. Choppin, G. R., Bond, A. H., Hromada, P. M. (1997). Redox speciation of plutonium. *Journal of Radioanalytical and Nuclear Chemistry*, 219(2), 203-210.

94. Braun, T., Ghersini, G., ed. *Extraction Chromatography*. Vol. 2. Elsevier B.V., 1975.

95. Horwitz, E. P., Bloomquist, C. A. A. (1972). Separation, performance and factors effecting band spreading of high efficiency extraction chromatographic columns for actinide separations. *Journal of Inorganic and Nuclear Chemistry* 34, 3851-3871.

96. Markl, P., Schmid, E. R. (1975). Techniques in Column Extraction Chromatography. *Extraction Chromatography*. Vol. 2. New York: Elsevier Scientific Publishing Company.

97. Gharibyan, N., Dailey, A., McLain, D.R., Bond, E.M., Moody, W.A., Happel, S., Sudowe, R. "Extraction behavior of americium and curium on selected extraction chromatography resins from pure acidic matrices." *Solvent Extraction & Ion Exchange* (Accepted 2014).

98. Gostic, J. M. (2009). *Evaluation of Extraction Chromatography Resins for Rapid Actinide Analysis*. Las Vegas: University of Nevada, Las Vegas, PhD Thesis.

99. Skoog, D.A., Holler, F.J., Crouch, S.R. *Principles of Instrumental Analysis*. Cengage Learning, 2006.

100. CAP 6500 ICP Spectrometer (2005). Waltham, MA: Thermo Electron Corp.

101. Skoog, D. A., Holler, F.J., Crouch, S. R. (2006). *Principles of Instrumental Analysis*. Brooks Cole.

102. Knoll, G.F. (2000). *Radiation Detection and Measurement*. 3rd. Hoboken, NJ: John Wiley & Sons, Inc.

103. *Tri-Carb 3110TR Low Activity Liquid Scintillation Analyzer* (2009). Waltham, MA: Perkin Elmer Inc.

104. *Tri-Carb 2900TR Low Activity Low Scintillation Analyzer* (2004). Perkin Elmer Inc. Shelton, Ct: Perkin Elmer Life and Analytical Sciences.

105. *LSC in Practice: Counting Aqueous Samples by LSC* (2008). Waltham, MA: Perkin Elmer Inc.

106. *2470 and 2480 WIZARD2* (2011). Downers Grover, IL: PerkinElmer Life and Analytical Sciences.

107. Adolff, J.P., Guillaumont, R. (1993). Fundamentals of Radiochemistry.

108. Glover, S.E., Filby, R.H., Clark, S.B., Grytdal, S.P. (1998). Optimization and characterization of a sulfate based electrodeposition method for alpha-spectroscopy for actinide elements using chemometric analysis. *Journal of Radioanalytical and Nuclear Chemistry,* 234, 213-218.

109. Kanchiku, Y. "Separation and Identification of Chlorocomplexes of Technetium(IV) formed in Hydrochloric Acid Solutions." *Bulletin of the Chemical Society of Japan* 42 (1969): 2831-2835.

110. Edelstein, N.M., Fuger, J., Katz, J.J., Morss, L.R. "Summary and Comparison of Properties of the Actinide and Transactinide Elements." *The chemistry of the Actinide and Transactinide Elements*. New York: Springer, 2006.

111. Shannon, R.D. "Revised Effective Ionic Radii and Systematic Studies of Interatomic Distances in Halides and Chalcogenides." *Acta Crystallographica* 32 (1976): 751-767.

112. Aberg, M, Glaser, J. "O-17 and H-1 NMR study of the tetranuclear hydroxo zirconium complex in aqueous solution." *Inorganica Chimica Acta* 206 (1993): 53-61.

113. Hagfeldt, C., Kessler, V., Persson, I. "Structure of the hydrate, hydrolysed and solvated zirconium(IV) and hafnium(IV) ions in water and aprotic oxygen donor solvents: A crystallographic, EXAFS spectroscopic and large angle X-ray scattering study." *Dalton Transactions* (2004): 2142-2151.

114. Rose, J., De Bruin, T.J.M., Chauveteau, G., Tabary, R., Hazemann, J-L, Proux, O., Omari, A., Toulhoat, H., Bottero, J.-Y. "Aqueous Zirconium Complexes for Gelling Polymers. A Combined X-ray Absorption Spectroscopy and Quantum Mechanical Study." *Journal of Physical Chemistry, B* 107 (2003): 2910-2920.

115. Singhal, A., Toth, L.M., Lin, J.S., Affholter, K. "Zirconium(IV) Tetramer/Octamer Hydrolysis Equilibrium in Aqueous Hydrochloric Acid Solution." *Journal of American Chemical Society* 118 (1996): 11529-11534.

116. Walther, C. *From Hydrolysis to the Formation of Colloids - Polymerization of Tetravalent Actinide Ions*. Karlsruhe: Forschungszentrum Karlsruhe, 2008.

117. Zielen, A.J., Connick, R.E. "The Hydrolytic Polymerization of Zirconium in Perchloric Acid Solutions." *American Chemistry Society* 78 (1956): 5785-5792.

118. Lee, M., Sohn, S., Lee, M.,. "Ionic Equilibria and Ion Exchange of Molybdenum(VI) from Strong Acid Solution." *Bulletin of Korean Chemical Society* 32.10 (2011): 3687-3691.

119. Bell, R.P. *The Proton in Chemistry*. Ithaca: Cornell University Press, 1973.

120. Coleman, G.H. (1965). *The Radiochemistry of Plutonium*. Livermore, CA: National Academy of Sciences - National Research Council.

121. "Material Safety Data Sheet Hydrobromic Acid." n.d. *http://www.sciencelab.com/msds.php?msdsId=9924283.* 18 April 2014.

122. Laue, W., Thiemann, M., Scheibler, E., Wiegand, K.W. "Nitrates and Nitrites." *Ullmann's Encyclopedia of Industrial Chemistry*. 2000.

123. Gindler, J. E. (1962). The Radiochemistry of Uranium. Argonne, Illinois: National Academy of Sciences – National Research Council. *Radiological Laboratory Sample Analysis Guide for Incident Response - Radionuclides in Soil*. EPA 402-R-12-006. Maryland: Environmental Management Support, INC., 2012.

124. Havel, J., Soto-Guerrero, J., Lubal, P. "Spectrophotometric study of uranyl-oxalate complexation in solution." *Polyhedron* 21 (2002): 1411-1420.

125. Jarvinen, G. "Precipitation/Crystallization/Sorption ." n.d. *http://www.cresp.org/NuclearChemCourse/presentations/09_Jarvinen%20%20Precip-Cryst-Pres12-08v6REV_LSB.pdf.* Presentation. 18 April 2014.

126. Lehto, J., Hou, Z.,. *Chemistry and Analysis of Radionuclides: Laboratory Techniques and Methodology*. Wiley-VCH, 2011.

127. Kosmatka, S.H., Kerkhoff, B., Panarese, W.C. *Design and Control of Concrete Mixtures*. Skokie, IL: Portland Cement Association, 2002.

128. Shacklette, H.T., Boerngen, J.G. *Element Concentrations in Soils and Other Surficial Materials of the Counterminous United States*. US

Geological Survey Professional Paper 1270. Washington: United States Government Printing Office, 1984.

129. Horwitz, E.P., R. Chiarizia and M.L. Dietz. "A Novel Strontium-Selective Extraction Chromatographic Resin." *Solvent Extraction and Ion Exchange* 10.2 (1992): 313-336.

130. Aveston, J. "Hydrolysis of scandium(III): ultracentrifugation and acidity measurements." *Journal of the Chemical Society A: Inorganic, Physical, Theoretical* (1966): 1599-1601.

131. Melson, G.A., Olszanski, D.J., Rahimi, A.K. "Coordination chemistry of scandium. VIII[1] detection of complex formation in solution by Sc46 NMR spectroscopy." *Spectrochimica Acta* (1977): 301-309.

132. Baes, C.F., Mesmer, R.E. (1976). *The Hydrolysis of Cations*. Robert E. Krieger Publishing Co.

133. Cotton, F.A., Wilkinson, G. *Advanced Inorganic Chemistry*. New York: Wiley-Interscience, 1988.

134. Naslund, J., Persson, I., Sandstrom, M.,. "Solvation of the Bismuth(III) Ion by Water, Dimethyl Sulfoxide, N,N'=Dimethylpropyleneurea, and N,N-Dimethylthioformamide. An EXAFS, Large-Angle Xray Scattering, and Crystallographic Structural Study." *Inorganic Chemistry* 39 (2009): 4012-4021.

135. Lab, Knolls Atomic Power. *Nuclides and Isotopes: Chart of the Nuclides*. 17th. 2010.

136. *Evaluated Nuclear Data File*. n.d. 18 April 2014. <http://www.nndc.bnl.gov/exfor/endf00.jsp>.

137. Dirks, C., Happel, S., Jungclas, H. "http://www.triskem-international.com/iso_album/09_scandium_separation.pdf." n.d. Febuary 2014.

VITA

Graduate College
Univeristy of Nevada, Las Vegas

Audrey Roman

Degrees:

Bachelor of Science, Chemistry, 2009
University of Idaho

Special Honors and Awards:

Seaborg Institute Summer Research Fellow, 2011, 2012, 2013
Los Alamos National Laboratory, Los Alamos, NM

Dissertation Title:

Characterization and Optimization of Extraction Chromatography Resins for Rapid Separations for Safeguard and Nuclear Forensics Purposes

Dissertation Examination Committee:

Chairperson, Dr. Ralf Sudowe, Ph.D.
Committee Member, Dr. Kenneth Czerwinski, Ph.D.
Committee Member, Dr. Gary Cerefice, Ph.D.
Committee Member, Dr. Evelyn Bond, Ph.D.
Graduate Faculty Representative, Dr. William Culbreth, Ph.D.